UNIVERSITY OF OKLAHOMA

GRADUATE COLLEGE

CHARACTERIZATION AND BIOINFORMATIC ANALYSIS OF PSEUDOMONAS AERUGINOSA CONDENSINS

A DISSERTATION

SUBMITTED TO THE GRADUATE FACULTY

in partial fulfillment of the requirements for the

Degree of

DOCTOR OF PHILOSOPHY

By

APRIL LOUISA CLEVENGER
Norman, Oklahoma
2019

CHARACTERIZATION AND BIOINFORMATIC ANALYSIS OF PSEUDOMONAS AERUGINOSA CONDENSINS

A DISSERTATION APPROVED FOR THE
DEPARTMENT OF CHEMISTRY AND BIOCHEMISTRY

BY THE COMMITTEE CONSISTING OF

Dr. Valentin V. Rybenkov, Chair

Dr. Elena Zgurskaya, Co-Chair

Dr. Rakhi Rajan

Dr. Robert Cichewicz

Dr. Elizabeth Karr

Acknowledgements

I would like to express my deepest appreciation to all those who have made this dissertation possible. First, I am indebted to my committee chair, Dr. Valentin Rybenkov who has provided me with an enormous amount of help and guidance during my graduate studies. Without his help, this dissertation would not have been possible. His wisdom, knowledge and passion for scientific research has inspired and motivated me. I would also like to thank my co-chair Dr. Helen Zgurskaya for her tremendous encouragement and guidance.

I extend my gratitude to my committee members, Dr. Cichewicz, Dr. Rajan, and Dr. Karr for their valuable time and feedback. I would also like to thank Dr. Bartley and Dr. Najar for their help and recommendations. My thanks and appreciation to my lab members and friends, for sharing knowledge and experience as well as being a constant source of support. I would like to especially thank Dr. Zhao for all of his guidance and help.

Special thanks to my parents, family and friends for their continued support and patience. I owe an enormous debt of gratitude to my husband, Sameer, and my two children, Janna and Sumaiya. Through the struggles and trials of this dissertation, they have always been a constant source of joy.

Table of Contents

List of Tables

Appendix

List of Figures

List of Equations

Abstract

DNA is organized within chromosomes not only to permit a large amount of DNA to occupy a very small space, but also to serve essential functional roles. Varied levels of organization enable proper DNA replication, repair, transcription, segregation and cell division. A key player in maintaining proper global organization of the chromosome are condensins. Condensins dynamically interact with DNA and play critical roles in chromosomal duplication functions, including DNA segregation.

Pseudomonas aeruginosa (PA) is a virtually ubiquitous gram-negative bacterium capable of inhabiting a wide range of ecological niches, including the human host. A key to the survival and pathogenicity of PA in such diverse environments stems from its metabolic versatility, a large regulatory network including multiple virulence factors, and its dynamic ability to adapt via epigenetic factors and mutational plasticity. The evolution of PA during lung infections is of particular concern on account of its devastating impact on lung function for cystic fibrosis patients. PA has the ability to differentiate into different physiological states allowing it to adapt to different environments. This lifestyle switching is involved in the progression of infection as seen by the different growth morphologies during acute and chronic infection states. Therefore, a better understanding of how these genes are regulated and capable of switching into different physiological states could significantly help in preventing and treating PA progression during infection.

Typically, condensins are known for their roles as chromosomal organizers and maintainers. One of the key findings in this study showed that they are also global regulators of gene expression where phenotype is both context and strain dependent. Condensins can bind

DNA throughout the chromosome making it the ideal mediator between the control of gene expression and alterations in DNA structure. Here, we investigated the roles that PA condensins, SMC-ScpAB and MksBEF have on cell physiology and gene regulation in PA.

Transcriptomic analysis of PAO1 condensin deletion mutants revealed substantial changes in gene expression, in particular, for pathways involved in virulence. Many of these affected pathways were found to be oppositely regulated for Δ*mksB* and Δ*smc*, reminiscent of acute and chronic infection phases, respectively. Δ*mksB* revealed upregulated genes in the type 3 secretion system (T3SS), and downregulated type 6 secretion system (T6SS), iron uptake, biofilm and adhesion genes while Δ*smc* gene expression was opposite. Interestingly, the double deletion mutant (ΔΔ*)* revealed significant overlap with Δ*mksB* for T3SS and biofilm/adhesion genes however overlap was also seen with Δ*smc* for iron uptake genes related to siderophores. ΔΔ also revealed hundreds of uniquely upregulated genes including the pyochelin regulon, several virulence effectors, as well as quorum sensing and cell motility genes. Overall, each condensin deletion strain, showed a unique transcriptional profile (100+ uniquely regulated genes) implicating different regulatory pathways.

Physiological studies on condensin deletion strains in PAO1 were in line with transcriptional analysis, showing opposite differentiation states where deletion of *smc* produced sessile biofilm growing cells and deletion of *mksB* produced planktonic growing cells with reduced biofilm formation [1]. Physiologically, Δ*mksB* and ΔΔ look very similar for growth where phenotype of the double knockout was dominated by an absence of MksB [1] reflecting the prominent overlap seen in transcription for biofilm related genes.

Using biofilm formation as a reporter for *mksB* phenotype, complementation studies unexpectedly revealed that the link between MksB and biofilm is context dependent. Using the degron system and ATPase MksB point mutations, MksB was confirmed to be directly linked to biofilm formation while complementation of the *mksB* gene after a full *mksB* deletion, however, was not possible. These results indicate significant changes to cis effects in the *mksB* region of the chromosome or even secondary consequences resulting from the *mksB* deletion.

ATPase MksB point mutations also revealed that the link between MksB and biofilm is conformational dependent. ATPase point mutants have been previously shown to generate specific conformational intermediates of the MksB ATPase cycle [2, 3]. Two of the three generated ATPase MksB mutants, E864Q and S829R, reflected severe biofilm defects. Strikingly, a third mutant, D864A, was capable of full biofilm function. All of these mutations interfere in some aspect of dimerization of the SMC head domains. These results reveal that MksB intermediate conformations, rather than ATPase activity, is relevant for MksB regulatory function. Conformational dependence on phenotype was also seen for SMC [1].

Notably, physiological studies on PA14 condensins revealed that condensin phenotypes are largely strain dependent. Although slight deviations were seen for growth studies, condensin deletions revealed a much smaller effect than PAO1. Overall, this implicates significant differences in how condensins are integrated into the regulatory networks of the PAO1 and PA14 strains and highlights a possible fortuitous integration by condensins into the regulatory system of PAO1.

Strikingly, when *mksB* is removed in PAO1, a significant inversion in the chromosome occurs at two rRNA sites separated by 2.2 Mb [4]. This inversion altered the layout of key

markers in segregation (the chromosomal dimer resolution site, *dif*, found at the terminus of segregation) and replication (the origin of replication, *oriC*) illuminating asymmetry in the PAO1 chromosome. These markers are highly coordinated with nucleotide bias or (GC skew), which is an underlying signaling code in bacterial DNA where there is an abundance of guanines on the leading strand and cytosines on the lagging strand. Typically, the terminus of replication and *dif* align as most bacterial chromosomes are symmetric, making differentiation between their underlying processes difficult.

Therefore, we used the asymmetric PAO1 chromosome as a model to study the coordination between segregation, replication and nucleotide usage bias. Experimentally, replication was found to terminate opposite from *oriC* while segregation terminated at the asymmetric *dif* [5]. GC skew analysis showed switches in polarity at the *oriC* and *dif* sites, while the terminus of replication was almost 700 kbp away. Overall, this shows a lack of coordination between replication and segregation and that nucleotide bias is aligned with both processes. Using location markers for replication and segregation, we bioinformatically analyzed all complete sequenced bacterial chromosomes from NCBI [6]. Our findings show that nucleotide bias is correlated with *dif* but not the terminus of replication for all chromosome types, implicating the segregation process as a contributor to the nucleotide bias phenomenon.

Chapter 1: Introduction

Pseudomonas aeruginosa (PA) has reached a critical threat status after developing resistance to last line carbapenem antibiotics. "Superbugs" have increasingly emerged in the headlines as lethal outbreaks of bacterial strains completely resistant to antibiotics. These outbreaks are a grim realization that multi-drug resistant strains have inherent mechanisms in place for developing full resistance to currently available antibiotics. Over 2 million illnesses and 23,000 deaths occur annually from multi-drug resistant bacteria, a figure put forward by the US Centers for Disease Control and Prevention (CDC) in a 2013 report, and the figure is expected to rise as drug resistance develops [7]. Antibiotics which were once regarded as cures for infections are now understood to be a depleting treatment option. Combatting multi-drug resistant strains and the development of alternative antibiotic strategies is necessary for future generations.

PA is exceptionally difficult to treat being a highly robust gram-negative bacterium with low membrane permeability. PA has innate systems in place to survive in diverse environments including notable metabolic diversity and numerous virulence factors. Adaptive features include a significant regulatory network and mutational plasticity. One more intriguing aspect of PA adaptability is its ability to epigenetically control physiological lifestyle. Lifestyle switching is an essential component to the progression of infection, therefore understanding this process could lead to viable therapeutic targets.

Here we explore a novel pathway for epigenetic lifestyle switching and global regulation, PAO1 condensins. Condensins are conventionally known for their maintenance of the chromosome. They help with higher order structuring which is important for proper DNA

compaction and segregation. Therefore, global gene regulation is a newly reported function of condensins linking chromosomal organization with gene expression. In order to better understand this coordination, we introduce condensins and review PA lifestyle switching, infection phases, and known virulence systems.

In a separate study, we found that deletion of the *mksB* condensin gene triggers a large inversion in PAO1 [4]. This discovery reflected a poorly understood phenomenon of nucleotide bias and their coordination with chromosomal segregation and replication. This nucleotide skew is an inherent code in the DNA providing a global pattern which acts as markers for major location points for both replication and segregation. Here, we introduce concepts related to the phenomenon of nucleotide usage bias.

1.1 Chromosome organization

The PA chromosome is organized along with chromosomal associated proteins into the nucleoid of the cell. The chromosome of PA is roughly 1000 times longer than the cell. In addition to significant compaction, the chromosome must also be compatible with essential cellular processes including DNA replication, segregation and gene expression. Therefore, the overall process is highly dynamic, involving significant interplay between DNA binding proteins and processes occurring in the cell. The PA chromosome, and all prokaryotic DNA, is organized in hierarchical levels in order to achieve maximum compaction and compatibility with cell dynamics. These levels allow a higher order structuring for better control of the compaction process. Nucleoid associated protein mediated folding contributes to local organization and condensins contribute to global organization (Figure 1-1).

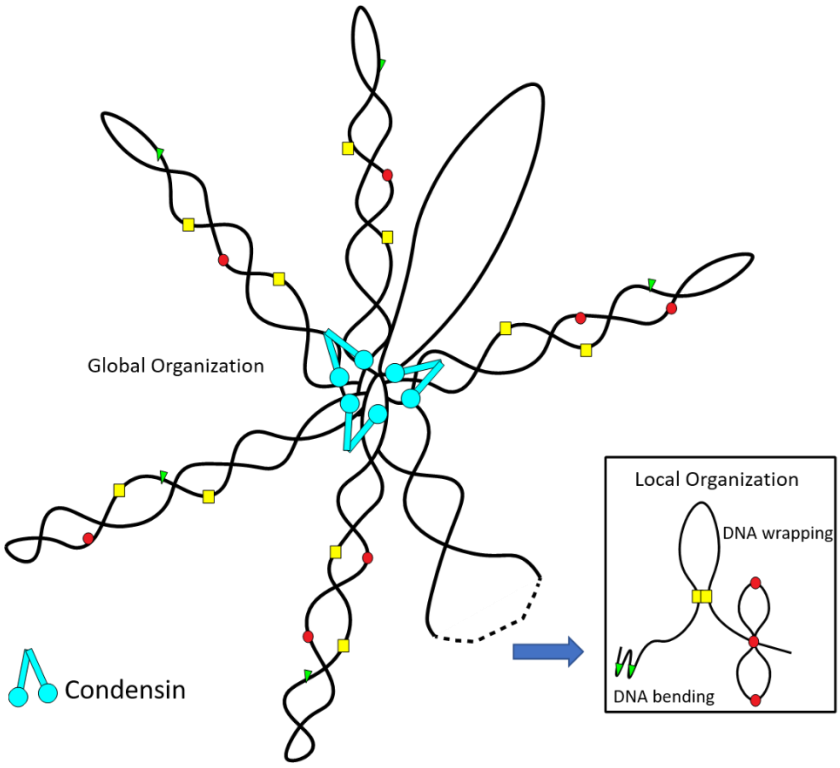

Figure 1- 1: Chromosome organization. Local level organization, by nucleoid associated proteins and global level of organization by condensins.

1.1.A Local organization, nucleoid associated proteins (NAP's)

In *Escherichia coli (E. coli)*, there are 12 major identified **nucleoid associated proteins (NAP's)**, NAP's including HU (Heat Unstable), IHF (Integration Host Factor), FIS (Factor for inversion stimulation), H-NS (Histone-like nucleoid-structuring), Lrp (Leucine-responsive regulatory protein), CbpA, CbpB, DnaA, Dps, Hfq, IciA and StpA [8, 9]. StpA is an H-NS paralogue that can functionally substitute for H-NS. H-NS paralogues also exist in other species of bacteria. *h-ns* and *stpA* are not present in PA Instead, PA uses its functional counterparts of

mvaT and mvaU [10]. Divergence is seen in other strains as well indicating that NAP's have evolved independently.

NAP's can be highly abundant (up to 55,000 molecules per cell in *E. coli* for some of them [11]) and play a diverse role as chromatin organizers, transcription factors, and as general accessory proteins for chromosomal maintenance, including replication[12]. The expression level of nucleoid-associated proteins is dependent on growth phase. Some NAPs are abundant during stationary growth but significantly reduced during planktonic growth or vice versa [13]. This variation in expression levels allows cells to modulate the compaction level of the chromosome based on growth conditions. Variations between different growth phases for the major NAP's are shown in Table 1-1.

Table 1- 1: Molecules /cell in both exponential and stationary phases for NAP's

Nucleotide Associated protein	Exponential phase Molecules/cell	Stationary Phase Molecules/cell	Reference
HU	30,000 – 55,000	< 18,000	[14] [13]
IHF	12,000	55,000	[13]
FIS	60,000	500	[13]
H-NS	20,000	8,000	[13]
Lrp	1,300 – 3,000	130	[15] [13]
Dps	6,000	180,000	[13]

Functions for the NAP's are quite diverse. These proteins occupy wide portions of genomic DNA [9,10] and are involved in a series of genome functions, such as transcription (Hu, IHF, H-NS, StpA, and Fis) [11–15], translation (Hu, HNS, StpA, and Hfq) [16–19], replication (HU, IHF, Fis, and Dps) [20–23], DNA protection (Dps) [24,25], and DNA packing (Hu, H-NS, Fis, and Dps) [16-20].

NAP's play an important role in chromosomal compaction. At the local level of organization, **NAP's**, induce bends and twists and lead to bridging of neighboring sections of the chromosome. These sections are approximately 10kb in length and form and dissolve based on processes occurring on the chromosome. Twisting and bending of the DNA induces curvature and folds, reducing the stiffness of the complex, making the chromosome thicker and shorter, helping with overall compaction.

Overall, NAP's play important and dynamic roles in governing global gene expression and local level organization of the chromosome in bacteria. This helps with the overall structuring of individual chromosomal loops which are organized at the global level.

1.1.B Global organization, condensins

At the global level of organization, the prokaryotic chromosome is organized into large loops which radiate from a central scaffold region. Evidence of this higher order structure of the prokaryotic chromosome has been seen in electron micrographs. These loops can range from 100 to 400 kbp long providing a means of compacting large portions of the chromosome and generating significant conformational changes to the DNA. These loops contribute to chromosomal organization as well as segregation and subsequently, the sub-cellular layout.

One of the major contributors to **large loop formation** in the prokaryotic chromosome are condensins. Condensins are chromosome maintenance proteins which have the ability to bind DNA and to cooperatively bind with one another. This provides condensins with the ability to form DNA bridges. Condensins form large stabilized chromosomal loops by acting as macromolecular clamps that bridge distant DNA's together [2].

Large chromosomal loops are further organized into higher order structures which cluster together in large regions (800 kb-1Mb) called **macrodomains**. These macrodomains are characteristically found within the same intracellular positions and impose specific dynamics and segregation patterns on the genes they carry. Due to their relative proximity, individual macrodomains show higher frequencies of recombination. Macrodomains have been identified in E. coli, but are speculated to be present in many bacterial chromosomes [21].

Domains which resemble those of *E. coli* were found by our group [5] in PA which were related by segregation patterns and cellular positioning. These macrodomains reflected segregation patterns, where large macrodomains segregated together in clusters of gene regions. Overall, macrodomains are an important component in chromosomal organization and an integral aspect in both segregation and subcellular layout.

Condensins have an intrinsic ability to aggregate and form clusters along the chromosome which allows them to provide a **scaffolding** element to the prokaryotic chromosome. Condensins have been obtained from the protein scaffold of isolated bacterial chromosomes indicating their involvement in chromosome structuring [22]. This scaffold structure, generally found in the center, gives added stability to the large chromosomal loops which emerge from it. [23]. Condensins, therefore, play pivotal structural roles in chromosomal organization.

One aspect which aids in DNA compaction is **supercoiling**. Supercoiling reduces the space that DNA takes up in the cell by twisting the DNA strands into a more compacted and energized form, which as described previously, can be formed into large loops. Supercoiling is particularly important during chromosomal division events in which greater compaction of the chromosome is needed.

Positive supercoils are induced by the byproduct of strand separation during replication and transcription. During these processes, the region ahead of the polymerase complex is unwound. The resulting stress is compensated with positive supercoils ahead of the complex. However, positive supercoiling results in global tension throughout the DNA strand. In order to relieve this stress, topoisomerases rewind DNA, generating negative supercoils behind the polymerase complex [24].

Additional contributors to supercoiling are **condensins.** The 13S condensin from frogs was reported to generate positive supercoils through DNA reshaping. Negative supercoils, which dominate bacteria the majority of the time, was also found to be induced by the prokaryotic MukBEF condensin [25].

Overall, condensins dynamically interact with DNA and play critical roles in chromosomal organization and duplication functions, including DNA segregation. This study also shows that condensins are global regulators of hundreds of genes, many of which are involved in PA virulence.

1.2 Condensins

1.2.A Structure of condensins

Three condensin complexes have been identified in prokaryotes, SMC-ScpAB, MukBEF, and MksBEF (SMC-ScpAB and MksBEF in PA). The main biochemically active component, the SMC subunit, belongs to the SMC family of ATPases which is highly conserved from bacteria to humans [26]. These include the SMC, MukB and MksB subunits [27].

The smc subunit is a homodimer. Each SMC monomer includes the following structural layout: The N-terminal region contains a Walker A site with the conserved sequence (G-X-S/T-G-X-G-K-S/T-S/T) [28]. The C terminal domain contains a Walker B site with the conserved sequence (h-h-h-h-D), where h represents hydrophobic amino acids. Also present on the C terminal domain is the signature C-motif and D-loop [28] [26]. In between these termini regions are two coiled coil regions which self fold through anti-parallel coiled coil interactions at a hinge domain. Two of these monomers interact through the hinge domain to form a homodimer and the SMC subunit [29] (Figure 1-2 A).

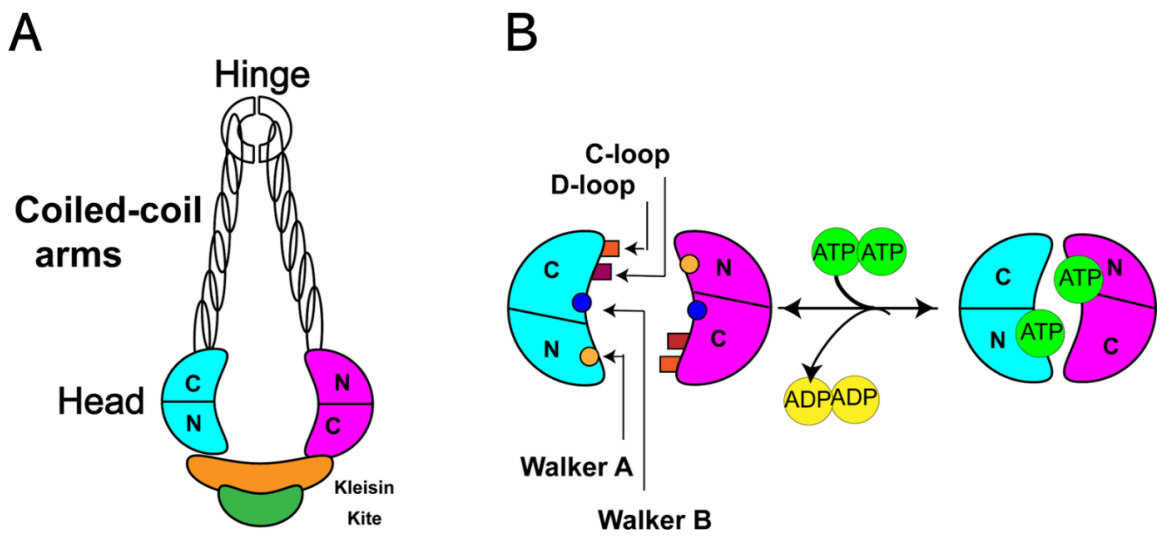

Figure 1- 2: Condensin structure. (A) Each SMC monomer in condensins consists of two globular domains at the N and C termini, two coiled α-helixes and a globular hinge domain between them. Each monomer self fold onto itself forming a functional ABC-type ATPase head domain. Association between two monomers occurs at the hinge domain for form a dimer. Non-SMC subunits which modulate activity (kleisin and kite subunits) bind to the head domain.

(B) Engagement of the two head domains for each monomer occurs through ATP binding. Each monomer head domain contains a Walker A motif from the N terminus and Walker B motif from the C terminus of the first monomer. The C-terminal domain of the second monomer contains the C-motif and D-loop. Disengagement of the head domains occurs though ATP hydrolysis.

The ATPase head domain in the overall SMC subunit contains two ATPases [30]. For each ATPases, the Walker A site functions in ATP binding. The Walker B site functions in ATP hydrolysis. The Signature C-motif and D-loop function in stabilizing the binding and hydrolysis of ATP [28] (Figure 1-2 B).

Overall, the main SMC subunit of the condensin complex binds DNA. The principle DNA binding site is located on the proximal hinge region of the SMC subunit head domain where there are positive patches of arginine and lysine which interact with negatively charged DNA. [31]. The location of this binding site implies that condensins likely embraces DNA within its V shaped structure .

Non-SMC subunits are essential for regulation of the complex and promoting inter-molecular interactions between condensins. These proteins positively affect DNA bridging activity [32] and negatively affect DNA binding activity when complexed with the SMC subunit [32-34]. The Kleisin family of non-SMC subunits includes ScpA, MukF, and MksF. The kleisin family of non-SMC subunits includes ScpB, MukE, and MksE [35]. Non-SMC subunits bind to the head domain of the main SMC subunit and can oligomerize with other SMC subunits, playing a major role in scaffold formation and DNA bridging.

ATP modulates the activity of condensins by altering its architecture and interaction with DNA [18, 24-26]. When bound to ATP, the complex dimerizes at the head domain and hydrolysis of ATP opens the condensin structure. For most condensins, binding of ATP also induces DNA binding while hydrolysis helps release it. Notably, DNA binding by the MksB condensin is negatively regulated by ATP which distinguishes it from other known SMC proteins. The different effect of ATP on DNA binding for MksB highlights the idea that several specialized condensins might be involved in organization of bacterial chromosomes. Overall, basic chromosome compaction through intermolecular interactions is enhanced by ATP.

1.3 Chromosome architecture

1.3.A Chromosome segregation

Precise DNA segregation is essential for proper inheritance of the chromosome. In bacteria, replication and segregation occur simultaneously (Figure 1-3). The ParABS partitioning system, condensins and topoisomerases all help to segregate most bacterial chromosomes, including PA.

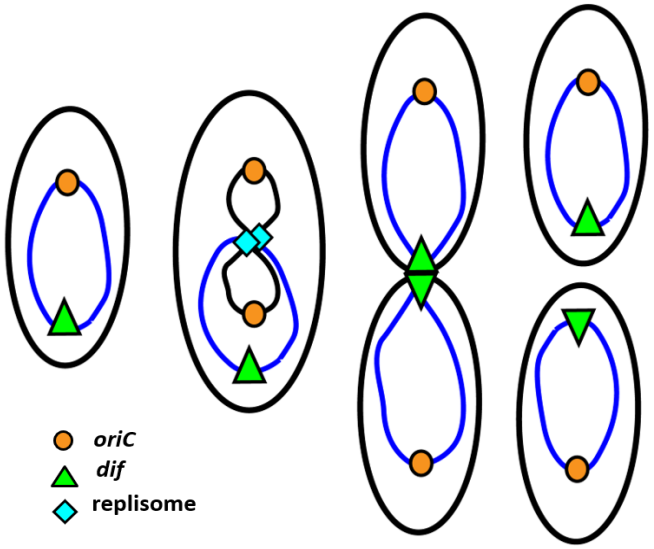

Figure 1- 3: Schematic for *Pseudomonas aeruginosa* (PA) chromosomal organization during replication and segregation. Fully replicated chromosomes are represented as blue lines and partially replicated by black lines. Replisomes are marked as green diamonds. Segregation starts at *parS*, proximal to *oriC* and ends at *dif*.

The **ParABS system** found in most proteo-gamma bacteria, involves three components. The first is the *parS* site which is a sequence located proximal to *oriC*. The second is the DNA binding protein, ParB, which binds to *parS* forming a nucleoprotein complex. The third component is the ATPase type protein, ParA, that provides the energy for segregation starting at the *parS* site.

The ParABS system utilizes these components to effectively segregate the chromosome. One proposed model this is accomplished by is through a **translocation mechanism**. Chromatin immunoprecipitation (ChIP) experiments have shown that ParB can not only bind with high

affinity to the *parS* site, but also to adjacent sites on the chromosome with less affinity, known as spreading [36]. In this model, the ParB/DNA complex is translocated by interaction with ParA which binds to DNA non-specifically [37]. When the ParB/DNA complex binds to ParA, the atpase activity is stimulated, followed by its dissociation from DNA. This allows the ParB-DNA complex to be translocated in waves of interactions [38].

In addition to the ParABS system, **condensin complexes** are also essential for faithful chromosome segregation [3]. Condensins provide chromosomal structuring and scaffolding stability which contribute to proper segregation. Deletion of condensins display chromosome segregation defects, including the formation of anucleate cells [27].

Condensins play a major role in segregation by their maintenance of the *oriC* position, where they are recruited to the *oriC* loci by ParB [39]. Deletions of condensins show defects in *oriC* localization. A complete loss of *oriC* localization, as seen in E. coli, results in disorganization of the entire chromosome and failure to locate proper loci to opposite halves of the cell [40, 41]. In other strains like PA, segregation of *oriC* localization was either delayed or accelerated, affecting overall segregation patterns [5]. Maintenance of the *oriC* position is therefore essential for proper segregation. These studies suggest an important link between chromosome organization and segregation where condensin localization on the *oriC* region dictates the organization and segregation of the remaining chromosome.

Topoisomerases also play an essential role in segregation. Topoisomerase II in particular is responsible for the decatenation of intertwined DNA molecules through the breaking and rejoining of double stranded DNA. The processes of decatenation performed by Topoisomerase

II is essential for the segregation of duplicated DNA. In many bacteria, Topoisomerases work in conjunction with condensins.

In *E. coli*, MukBEF recruits Topoisomerase IV to the *oriC* region by directly binding to the C-terminal domain of its ParC catalytic subunit [42, 43]. The formation of this complex was found to stimulate Topoisomerase IV activity. Topoisomerase IV promotes decatenation while MukBEF contributes to maintaining *oriC* positioning. Both of these actions play an important role for proper chromosome segregation [43].

Inactivation of MukBEF induces severe growth defects which affect segregation and renders cells hypersusceptible to novobiocin [32, 44]. Mutations in Topoisomerase I and DNA gyrase allow partial suppression of these MukBEF phenotypes [45]. These mutations increase DNA compaction, compensating for the chromosomal disorganization resulting from the deletion of *mukB.* More however, needs to be elucidated to better understand how these different mechanisms are coordinated.

The recruitment of condensins by ParB was found to be part of a larger coordinated pathway of segregation in PA. It was found that condensins are synthetically lethal with ParB while deletion of either condensin gene or *parB* by themselves was not. This revealed that condensins and the ParABS system make up essential and distinct components involved in PA segregation [5].

Deletion of condensins in PA was also coupled with significant alterations in macrodomains [5, 46]. Condensin are therefore involved in global organization of the chromosome which are directly involved with segregation. It is likely that their function as a

scaffold helps maintain the structure and integrity of varying DNA conformations, including maintenance of *oriC*, which plays a major role in segregation.

1.3.B Subcellular layout

Bacterial chromosomes are organized at the subcellular level. Fluorescence experiments have shown that different loci on the chromosome occupy specific regions inside the cell [46]. This organization has a distinct pattern which is maintained throughout the cell cycle. The PA chromosome organizes itself longitudinally within the cell [5, 46]. This configuration places the origin, *oriC*, at one pole (the new cell pole), and the *dif*, chromosome dimer resolution site, at the opposite pole (the new cell pole) (Figure 1-4). This organization is in contrast to a transverse organization in which both the *oriC* and *dif* region lie along the mid cell and the left and right arms of the chromosome are located at each cell pole (Figure 1-4).

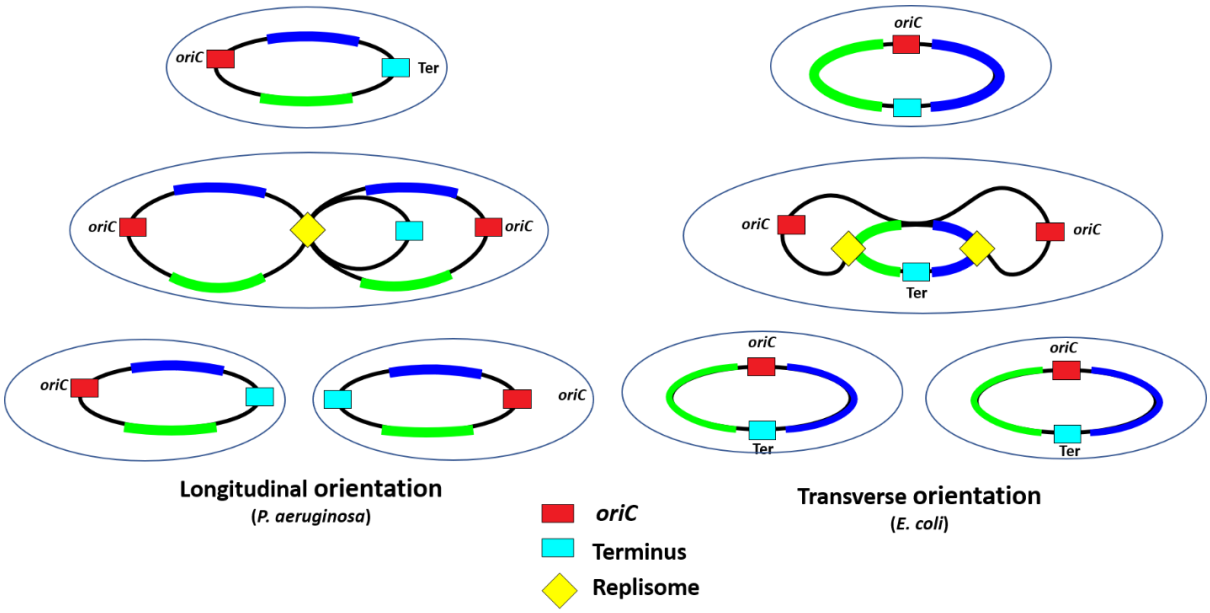

Figure 1- 4: Chromosomal orientation in bacteria, longitudinal and transverse. Chromosomes are organized between *oriC* and the Terminus of replication. Different species use different orientations. Growth factors can also alter orientation strategies. In the Longitudinal orientation, *oriC* and the Terminus are located at opposite cell-poles and the arms run parallel to each other along the. In the Transverse orientation, both *oriC* and the Terminus are located mid-cell and each arm are at opposite ends of the cell.

The starting sites for replication and segregation are proximal to each other on the chromosome, at the *oriC* and *parS* sites respectively. After replication is initiated in PA, segregation occurs concomitantly [46]. The newly replicated DNA is pulled away from the *oriC* locus starting site and moves to the opposite end of the cell while the un-replicated *dif* migrates to the mid-cell position. After replication and segregation is complete, the cells can fully divide. At this point, the newly replicated *oriC* occupies the old cell pole position and the newly

replicated *dif* region occupies the new cell pole position, in the longitudinal orientation (Figure 1-3).

Condensins were also found to contribute to chromosomal layout by way of their role in maintaining chromosome structure and integrity [5]. One of the main functions of condensins as mentioned previously, is their role in creating a chromosome scaffold structure which helps maintain and stabilize DNA conformations. Deletion of the PAO1-UW condensin, *mksB* results in an inversion at the ribosomal RNA sites, *rrnA* and *rrnB*, located on opposite chromosomal arms. This inversion reverted the asymmetric chromosomal layout, back to a symmetric organization [4].

This discovery helped illuminate a new and pivotal role that condensins have on overall chromosome structure. Further studies were performed here in order to determine the implications of these chromosomal changes and their coordination with replication, segregation and nucleotide bias, an inherent signaling code in most bacteria.

1.4 Pseudomonas aeruginosa

As of 2017, *Pseudomonas aeruginosa* (PA), a gram-negative multi drug resistant strain, was placed on a top three list of critical threats by the World Health Organization, WHO, in addition to *Acinetobacter baumannii* and *Enterobacteriaceae* [47]. PA is a virtually ubiquitous bacterium capable of inhabiting a wide range of habitats, including the human host [48]. This bacterium is an opportunistic pathogen commonly forming infections as skin rashes, and ear and urinary tract infections in healthy people. In immunocompromised individuals, PA can infect the airways and damaged tissues leading to severe blood infections and pneumonia . PA has also been designated

as one of the main perpetuators in chronic lung infections, particularly in patients with cystic fibrosis which affects 70,000 people worldwide [49]. PA infects approximately 75% of CF patients older than 25 years old making it one of the most prevalent gram-negative species during chronic lung infections. Therefore, understanding PA pathogenicity and its modes for adaptation is vital for the remediation of PA infections.

1.4.A. PA intrinsic fitness

PA is a highly robust bacterial strain which can occupy numerous ecological niches. PA is commonly found in soil and water. However, it can also occur on the surfaces of plants and animals. Currently, there are over 200 (as of 04-30-2019, 228) complete PA strains and clinical isolates that have been sequenced on the NCBI database [6]. The PA chromosome has a relatively large genome (between about 5-7 Mb). The larger size is due to gene complexity likely due to horizontal gene transfer from other bacteria and viruses (125, 126).

This complexity in the DNA allows PA to overcome varying environmental stressors not always tolerated by other organisms. PA encodes a number of different enzymes involved in various metabolic pathways. This gives PA high nutritional versatility where it can utilize several different organic compounds for growth, including fossil fuels. Cellular respiration of PA is also highly flexible. PA can grow in the absence of O_2 if an alternative terminal electron acceptor is available such as nitrate [50].

Another aspect which contributes to the overall robust fitness of PA is its decreased permeability. PA is a gram-negative bacterium. These bacteria have an extra outer membrane composed of mainly lipopolysaccharides, making it harder to penetrate. Adding to the

difficulty to permeate the membrane, PA has several different efflux pumps which shuttle toxins out of the cell.

A notable mode for bacterial fitness is the formation of biofilms. PA has multiple pathways which regulate biofilm formation, an essential lifestyle form which garners structure and protection to the growing PA community. These include quorum sensing mechanisms, two-component systems GacA/GacS, RetS/LadS, and intracellular messaging by c-di-GMP.

Lastly, PA has multiple virulence factors which help promote survival. These include various toxins which can break down material in its surrounding environment in order to obtain nutrients. The combination of inherent systems for metabolic versatility, virulence factors, and lowered permeability provide ample adaptation features for PA to exploit numerous environmental niches.

1.4.B. *Pseudomonas aeruginosa* biofilms

One aspect which makes PA so difficult to target is its ability to form biofilms. Biofilms are a community of cells that grow together on a surface, surrounded by a protective exopolysaccharide matrix that provides both a structure and protection to the community against harmful agents [51]. Biofilms can act as both liquid and solid often being described as a "slime". If they are in an environment where they can collect sediment, or where they can accumulate rust or calcium deposits, these biofilms can develop into a hard-solid state. Therefore, biofilms are found in a range of environments from the buildup in water pipes to chronic infections in human lungs.

Biofilms contain about 2-5% of microbial cells, 97 % water, and the remaining portion

comes from the extra-cellular matrix. The components of the matrix includes different types of extracellular polymeric substances (EPS), including extra-cellular DNA and RNA (<1%), proteins including enzymes(<1-2%) and exopolysacharides (1-2%) [52]. Exopolysacharides and DNA have been implicated in the stability of the overall biofilm matrix contributing to cell-cell adherence. [53, 54].

Biofilms have proven exceptionally difficult to eradicate. In the case of infections, antibiotics and white blood cells are less effective against established biofilms. A number of reasons contribute to this enhanced resistance. The first reason includes reduced penetration across biofilms. Exopolysacharides help in reducing diffusion of white blood cells and other large molecules. This is particularly the case for positive aminoglycosides, which are possibly bound by the negative charges from exopolysacharides [55]. The second factor is decreased growth rate as this is a phenotype associated with many cells growing in biofilms (section 1.4.C.1). Many antibiotics target replication machinery so slower growing cells can often avoid being targeted, or at least less effectively. The third reason is the expression of resistance genes. In PA, these include beta lactamase, and β-Galactosidase which becomes an issue when in combination with reduced permeability of the biofilm as certain drugs can be better targeted. Multi-drug efflux pumps, specific for drugs can also be upregulated contributing to overall drug resistance. Lastly, the presence of persister cells, a cell morphology that is dormant (section 1.4.C.2), helps make removal of biofilms extremely difficult. For the cases of antibiotics which can effectively permeate the biofilm matrix such as fluoroquinolones, persister cells can provide a means of survival and continuation of growth after removal of the drug [56].

1.4.B.1 Biofilm structure: pel, psl, alginate, and DNA

Biofilm development is a highly dynamic process which is constantly changing according to its environment. Overall, several different structures can be generated in a biofilm. The simple types include patchy monolayers or biomasses. When more organized, they can form mushroom type structures when grown in still liquid and filamentous streamers when grown in moving liquid. Biofilms can move together by rippling or rolling across the surface, or by detaching in clumps [57]. Biofilms can also change locations by dispersal, where cells in the inner portion of the biofilm modify to planktonic cells and swim out to new locations [58].

Advanced biofilms act as a city in which major resources including water, nutrients and oxygen, are brought throughout the community of cells via channels [59]. The overall structure then provides a scaffold engineered for the distribution of nutrients to all parts of the biofilm community, even deeply embedded cells within the biofilm.

It has been shown that the major constituents for biofilm matrix adhesion are exo-polysacharides and extra-cellular DNA. *P. aeruginosa* produces at least three exo-polysaccharides, psl, pel, and alginate. The psl exo-polysacchride has been identified as an important factor in the initiation and maintenance of biofilms [60]. The structure of psl was identified as repeating units of a neutral, branched pentasaccharide consisting of D-glucose, D-mannose and L-rhamnose monosaccharides [61] (Figure 1-5). In addition to its structural role in biofilm, Psl has also been linked to roles in pathogenesis and protection against the immune system [62], in antibiotic resistance [63] as well as a signaling molecule for diguanylate cyclase, SiaD and SadC, which acts on c-di-GMP. The role as a signaling molecule in essence allows psl

to form a positive feedback loop with c-di-GMP [64].

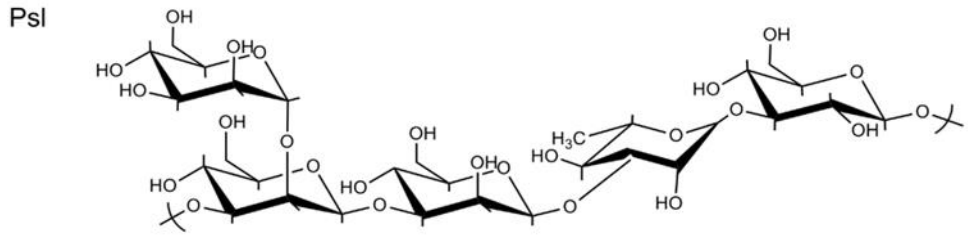

Figure 1- 5: Structure of the psl component of biofilms. Psl consists of repeating units of a neutral, branched pentasaccharide consisting of D-glucose, D-mannose and L-rhamnose monosaccharides The structure of Pel includes partially acetylated 1,4 linked *N*-acetylglucosamine and *N*-acetylgalactosamine, however, the structure has not been fully established [61].

The pel polysaccharide is a cationic polymer composed of partially acetylated 1,4 linked *N*-acetylglucosamine and *N*-acetylgalactosamine [65]. Currently, the chemical composition and structure of pel polysaccharide have not been fully established [66]. The cationic behavior of pel was reported to help facilitate its binding to extracellular DNA in the biofilm stalk. Like psl, it plays an important role in the structural maintenance of the biofilm.

Pel and psl are both important in the initial stages of biofilm growth where it maintains the integrity of biofilms by functioning as structural scaffolds [67]. Colvin et al 2012 found that psl and pel play redundant roles in the PA01 strain in which the deletion of either exopolysaccharide results in compensation by the other[68]. Depending on the strain studied, the role of pel and psl in biofilm formation can have variations [68]. The PA01 strain of PA is capable of expressing both psl and pel, however, it relies primarily on psl. PA14 in contrast uses

pel exclusively on account of it lacking three necessary genes in the pel operon [67].

Overall, both pel and psl have the characteristic of promoting cell-cell and cell-surface interactions [69] which explains why when overexpressed, they have also been linked to hyper-adherence and hyper-aggregation [70]. Together, pel and psl form the primary structure scaffold for biofilm development, providing the first line of defense as the biofilm begins to develop.

Alginate, a linear unbranched polymer composed of D-mannuronic acid and L-guluronic acid [71] (Figure 1-6). Alginate contributes to the structural stability and protection of mature biofilms by adding to the already established layers of pel and psl components. They also play an important role in water and nutrient retention [72]. Alginate acts as a porous material. This allows the establishment of gradients in the biofilm for nutrients, oxygen and other resources. Isolates that overproduce alginate are often found to be mucoidal variants, a marker for the last stages of chronic lung infection. It was found that when pel and psl are deleted, alginate is not able to form mature biofilms on its own.

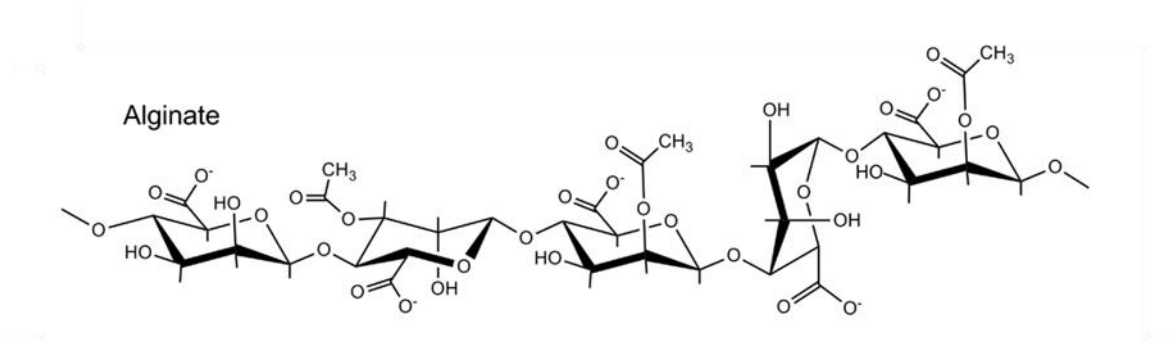

Figure 1- 6: Structure of the alginate component of biofilms. Alginate is a linear unbranched polymer composed of D-mannuronic acid and L-guluronic acid [61].

Extra-cellular DNA (E DNA) plays an important role in the overall adherence and formation of biofilms. E DNA can be produced by cell lysis or through the release of small vesicles from the outer membrane [73]. Using flow-chambers to monitor biofilm growth, Whitechurch et. al have shown that PA cell growth was diminished in the presence of DNase 1, while growing extensive colonies without [53]. They also showed that DNase I can dissolved already formed biofilms. This shows the importance of extracellular-DNA on biofilm growth. Therefore, the combination of at least pel or psl with alginate and extracellular-DNA is therefore essential in order to form fully mature biofilms in PA

1.4.C PA Morphotypes

1.4.C.1 Planktonic and sessile: major lifestyles

Basic regulatory mechanisms and mutational plasticity ensures survival against stressors in different environments. On account of these adaptive mechanisms, PA generates morphologies with particular phenotypes. One general morphotype incorporates the **planktonic lifestyle** in which cells grow as single cells and are actively motile using flagella [74]. Planktonic growth is geared for optimum mobility and acquisition of nutrients from its environment be it in soil or in a host organism. Typically, this lifestyle is found in environmental strains with enhanced toxin secretion of proteases that allow the breakdown of material around it for nutrient uptake. This particular morphotype acts as a scavenger seeking out new

environments while exploiting resources. Typically, this morphotype is more vulnerable to antibiotics and host immune system defenses.

Another major broad morphotype includes cells having a **sessile lifestyle** which is associated with biofilm growth. The sessile lifestyle slows down in growth rate as one of its prime objectives is survival and biofilm formation. Typically, downregulation is seen for genes involved in motility and protease toxins which are secreted in planktonic cells. Sessile cells often upregulate genes involved in adhesion, such as exopolysacharides, thereby enhancing stickiness during biofilm formation. Together, planktonic and sessile morphotypes make up the two major lifestyles of PA. From these modalities, additional morphotypes can show further divergence.

1.4.C.2 Additional morphotypes

An important morphotype which can emerge from either planktonic or sessile growth styles are **persister cells.** Two different types of persister cells have been postulated. The first type is thought to occur stochastically in a cell population by prior to the antibiotic treatment [75]. The second type occurs in response to to environmental stimuli such as a variety of antibiotics [76]. Persister cells are characterized by a dormant state, transient, lifestyle in which no growth occurs [77]. Therefore, persister cells have been reported to play an important role in surviving antibiotics as they are more difficult to target.

Another specific type of morphotype is **small colony variants (SCVs).** This particular cell variant has been shown to be derived directly from biofilms and is primarily associated with the sessile lifestyle. SCVs were discovered from isolates of chronic infections. These variants have

been reportedly associated with phenotypes predominate in the sessile lifestyle, including slower growth and enhanced biofilm formation. Prevalent in about 3% of cells in the chronic infection state, SCVs have been attributed to a sharp decline in CF patient prognoses. These variants are generated from a number of different ways, but the simplest way is directly from biofilms.

Additional **evolutionarily driven morphotypes**, include variants having a higher specificity of phenotypes derived from divergent evolution. These morphotypes are weeded out based on mutational plasticity, optimized for particular niches. Often time, these variants are derived from isolates during chronic CF infections. These varied, yet specific, morphotypes have been shown to have a large number of varied SNP's with a specific group of common mutations. These mutations were reported to be located in regions of regulation involving stress response, QS, and alginate pathways that lock the cell variant into a solid mode of mucoidal growth geared for survival in the lung.

Together, cell morphotypes derived from regulation, mutations, and a combination of both mechanisms, achieve maximal diversity in a cell population against stressors. Changes are engineered on the bases of stimuli and progress to an optimized state in highly stressful environments.

1.4.D. The biofilm lifecycle

The biofilm lifecycle is a highly dynamic process, in which certain developmental pathways can occur under proper environmental parameters (Figure 1-7). Initially, cells start off as fast growing, freely motile, planktonic cells. These cells explore and establish attachment to a

surface while weakening the host immune system through toxin secretion. Initially, long range attachment occurs through positive Van der Waals forces with a surface. This force counters a net negative electrostatic charge possessed by many environmental surfaces. When closer in range, flagella and pili can contact the surface and aid in adhesion [78]. Attachment at this stage is reversible and cells can move closer together using pili using twitching motility. With time, the population increases on the surface forming aggregates of microcolonies.

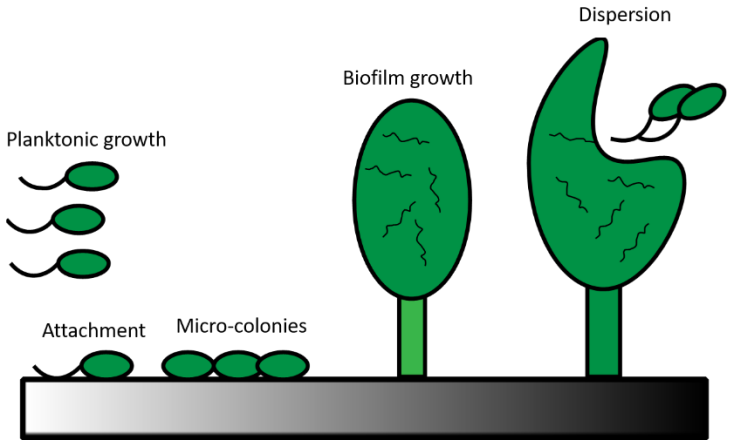

Figure 1- 7: The biofilm lifecycle. The biofilm lifecycle starts as planktonic growing cells. Cells attach to the surface and grow micro-colonies which develop into three-dimensional biofilm structures. Finally, dispersion occurs releasing clumps of planktonic cells.

After attachment, physiological changes can occur which help transition growing cells into the biofilm growth stage, where cells become irreversibly attached. It is believed that this switch is partially due to quorum sensing induction [79]. Many genes are activated including genes responsible for the production of compounds found in the matrix of developing biofilms, such as exopolysacharides [78]. This stage is characterized as sessile, slow growing cells, in

which biofilms grow from a single layer (from joined microcolonies), and progress to an advanced multilayer system. Biofilms eventually progress into well- developed three-dimensional communities [80]. After a certain amount of growth of biofilm is reached, a large group of cells are changed back into the planktonic growth stage in order to be released during dispersion to spread and colonize new areas for the next round of biofilm growth.

Additional morphotypes, in particular **persister cells**, play an important role in antibiotic resistance in biofilms. When biofilms are exposed to antibiotics that can penetrate the matrix, like fluoroquinolones, most of the population is eradicated. A small fraction of surviving persisters are able to remain however. When the drug is removed, biofilms can be reformed from these persister cells. This is one of the ways in which PA can survive through antibiotic treatment and continue the PA lifecycle [56]. These biofilms will then again disperse as planktonic to find new infection sites and the process continues. Overall, the biofilm cycle itself is an important component of the propagation of infection and disease persistence of PA in host systems and is an endless cycle if left untreated.

1.4.E. Lifestyle switching and regulation

In response to environmental changes, PA is able to switch from a planktonic (free swimming) to a sessile (biofilm forming) lifestyle. A planktonic lifestyle enables dispersion and travel to new environments, while a biofilm lifestyle offers protection as a community of cells in stressful environments [81, 82]). The transition between motile and sessile lifestyles is crucial for PA adaptation and requires the ability of PA to respond appropriately to changes in the environment [83]. Therefore, understanding the mechanisms that govern this lifestyle switch

may provide potential antibiotic targets for combatting infections. The biofilm lifecycle highlights the phenomenon of lifestyle switching between the planktonic and sessile growth states. This switching is essential for the propagation of the biofilm lifecycle and is the basis for the progression of infection. However, it is not exactly clear how this switching occurs.

One intriguing aspect of the lifestyle switching phenomenon, is that the changes in regulation affect not only the initial cell where change occurs, but for multiple dividing generations after it, often times, even if the signal is removed. This **epigenetic regulation** provides a powerful manner in which PA can alter the physiology of the entire community for multiple generations. This same phenomenon is also seen in scv generation and bi-stable virulence switching of the bexR regulon in which the effects are reversible yet present for multiple generations.

Much of what we know regarding lifestyle switching in *Pseudomonas aeruginosa* is in the form of **regulatory pathways** (Figure 1-8). PA possesses a large regulatory network of pathways which are highly dynamic and display a great deal of overlap for phenotypes attributable to each lifestyle. This overlap increases the complexity and response systems involved in the switching process, emphasizing the importance this process has on PA survival and adaptation. Condensins were found to be global regulators involving a number of virulence pathways related to biofilm formation and the different lifestyle states. It is speculated that they are involved in regulating a global switch involving several regulatory pathways. Here, we discuss some of the major known pathways involved in lifestyle switching with particular emphasis on pathways involved in biofilm formation in order to understand the scope in which condensins play in the overall lifestyle switching process.

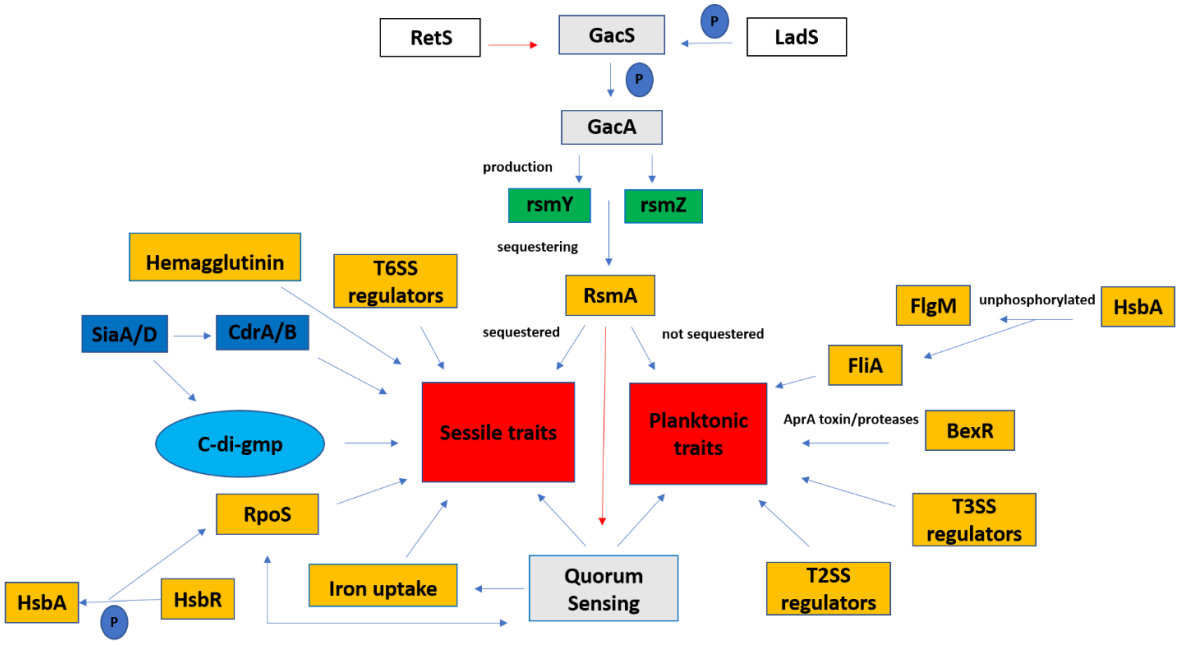

Figure 1- 8: Regulatory pathways in *P. aeruginosa* which contribute to sessile and planktonic traits.

There are three **quorum sensing systems** in PA. Two of these systems incorporate the AHL quorum sensing signal, *N*-Acyl homoserine lactone. These include the **Las and Rhl** systems. The **Las system** includes the transcriptional regulator, LasR, and the synthase, LasI, which synthesizes the AHL signal, N-(3-oxododecanoyl)-L-homoserine lactone (3-oxo-C12-HSL) [84, 85]. The Rhl system includes the transcriptional regulator, RhlR, and the synthase, Rhl, which synthesizes the AHL signal, N-butyryl-L-homoserine lactone (C4-HSL) [86]. The Las Quorum sensing system was found to be essential for the creation of mature biofilms, where LasI mutant formed very thin biofilms that lacked the three-dimensional architecture [87]. A link has also been reported between Las and the expression of the Pel polysaccharide, a component used in the biofilm matrix.

The **Rhl system**, however, has shown mixed results regarding its effect on biofilm formation. In some reports, Rhl is also a major factor by contributing through DNA release or directly via the synthesis of exopolysacharides. [88-90]. In other reports by contrast, no link could be found [87, 91]. These conflicting reports indicate that additional parameters play a role in the Rhl regulation of biofilm formation. Therefore, the two quorum sensing systems Las, and Rhl, have been found to play a role in the regulation of biofilm formation and toxin secretion and can contribute to the switch from a planktonic to sessile/biofilm lifestyle.

The **PQS system** (2-heptyl-3,4-dihydroxyquinoline) acts as a connector signal between the *las* and *rhl* quorum sensing systems [92]. Therefore, the QS systems have a great deal of overlap and internal regulation. The PQS system, like that of Las and Rhl systems have been connected to biofilm formation and virulence factors. Null mutations of the PQS system results in reduced biofilm formation and the decreased production of pyocyanin, elastase, PA-IL lectin and rhamnolipids and host immune responses [93]. In addition, the PQS system has also been found to be involved in iron uptake (pyocyanin and pyoverdine), the regulation of secreted toxins including ToxA and the protease PrpL, and the disruption of the host mitochondrial function [94, 95]. Overall, the PQS signal helps to maintain biofilms and regulates a number of virulence factors in both sessile and planktonic lifestyles.

The **IQS system** or Integrated Quorum Sensing system is the newest system discovered [96]. The IQS is able to enhance PQS production depending on the *P. aeruginosa* strain. The IQS system is tightly controlled by *las* under normal culture conditions but is also activated by phosphate limitation. Together, The QS systems are highly integrated and positively regulated by the las cascade [96].

RetS and LadS are sensor kinases involved in two-component signaling in PA [97]. Both RetS and LadS reciprocally regulate genes involved in the planktonic and sessile lifestyles. A RetS deficient strain showed a marked decrease in virulence from reduced toxin production (LipA and ToxA), an important aspect of planktonic growth, and an increased ability to form biofilms through the upregulation of psl and pel genes [98]. LadS in contrast, controls the expression of genes involved in producing exopolysacharides such as alginate and pel and psl. It also was found to negatively regulate swarming motility. Therefore, both RetS and LadS contribute to the control over the lifestyle switch.

RetS and LadS were found to converge on a master virulence regulator, **GacA.** Gac A is a response regulator that works with **GacS**, the sensor, in a conserved two-component system. RetS and LadS can influence levels of the small regulatory RNAs RsmZ and RsmY which regulate gene expression by binding to RsmA [97]. The GacS/GacA system regulates a broad range of virulence and stress response genes [99]. Overall, the GacS/GacA system has been proposed to control the reciprocal expression of the planktonic and sessile lifestyles, related to acute and chronic infection phenotypes [98].

The **c-di-GMP** second messenger is a signaling system that regulates many bacterial behaviors. Some of these include flagella rotation, type IV pili retraction, exo-polysacharide production (psl/pel), surface adhesion expression, antimicrobial resistance, stress responses, , secondary metabolite production, and biofilm dispersion. [100, 101]. Interestingly, the concentration of c-di-GMP was found to be associated with the lifestyle switch between planktonic and sessile lifestyles [102]. C-di-GMP has been found to be connected with the Gac/Rsm system, the **SagS** pathway and the Las quorum system which controls regulation of **biofilm formation**. The SagS

pathway**,** acts in concert with the two-component system, **BfiSR**, to enable *Pseudomonas aeruginosa* biofilm formation by altering **SadC** production levels of c-di-GMP [103]. High concentrations of c-di-GMP results in biofilm phenotypes while low concentrations are associated with motility and planktonic growth [104] . This association between lifestyle switching and c-di-GMP is present in several different species including (*Escherichia coli*, *Pseudomonas aeruginosa*, and *Salmonella enterica* serovar Typhimurium) [105]. **cAMP** is also involved with mediating PA biofilm formation. Almblad et al. showed that high levels of cAMP reduce c-di-GMP levels through the transcriptional regulator, **Vfr**, which reduces overall biofilm formation [106]. **Hemagglutinin** is a filamentous adhesion protein which also directly contributes to biofilm formation [107] [108]. Hemagglutinin mutants In *P. fluorescens* result in significant reductions in biofilm growth, extracellular matrix production, motility and overall attachment to host cells. In addition, mutants displayed marked reductions in infection ability implying a role as a virulence factor in pathogenicity [107].

RpoS (σ^S), is a major regulator of stress response and predominately expressed during stationary growth [109]. in PA, RpoS has also been shown to be upregulated in biofilms under stress conditions and is considered to be the master regulator of stress responses [110]. RpoS is post-translationally regulated by the HsbR-HsbA partner switching system [111]. HsbA, the anti-sigma factor, plays a role in lifestyle switching depending on its phosphorylation state. When phosphorylated, it binds to HsbR, the response regulator which binds to RpoS. When unphosphorylated, it binds to FlgM, the anti-sigma factor of HsbA. This plays a role in the release or sequestration of either of the two sigma factors which in turn, play a role in regulating growth states

The **SiaA/D** system also plays a role in biofilm formation by regulating the synthesis of c-di-GMP using the sensor kinase, SiaA, and diguanylate cyclase, siaD, [101, 112]. Increased c-di-GMP levels has been implicated in biofilm formation [102]. Other targets for SiaA/D mediated regulation include the psl polysaccharide, the CdrAB two-partner secretion system and the CupA fimbriae, all of which also activate biofilm formation in the sessile lifestyle [112]. **PpkA,** a serine/threonine kinase has also been reported to play a role in biofilm formation, as well as other virulence factors, in the type 6 secretion system [113]. PpkA, acts on the Fha1, a core scaffolding protein, through phosphorylation [114, 115] . This allows post-translational regulation of Hcp-PIS which is required for the assembly of PA T6SS HSI-1 [114, 115]**.** The type 6 secretion system (T6SS) is involved in a number of different functions. These include pathogenesis, biofilm formation and stress sensing [116]. **PppA**, a serine/threonine kinase, was found to act as a repressor for Hcp-1 export by acting as an antagonist for ppkA and acting on Fha1 [117] therefore, it can act as a repressor for biofilms. **PpyR** also affects biofilm formation by serving as an additional regulator in psl production through the psl operon. In addition, it has been found to contribute to the regulation of LasB, pyoverdine synthesis and PQS quorum sensing production, while reducing swimming motility [11].

A different type of factor for lifestyle control, was identified as the **BexR** virulence bi-stable switch [118]. This is a type of switching mechanism which allows large changes in regulation to be turned on and off, controlled by the BexR regulon (PA2432). When activated, a set of virulence genes, including the quorum sensing proteases, PA0572 and the *aprA* toxin gene from the type 1 secretion system, as well as lipase A, and the MexXY-OprM efflux pump, are upregulated, and when deactivated, they are turned off ensuring diversity in the overall

population. Overall, BexR acts as a switching point to control the expression of a diverse set of genes [118].

Iron also serves as a signal in *Pseudomonas aeruginosa* biofilm development and is a necessary component for PA survival [119]. Iron acquisition in PA occurs through the siderophores **pyoverdine and pyochelin** [120]. These siderophores are acquired though recognition at specific cell surface outer membrane receptors, TonB dependent receptors. Uptake of ferripyoverdine in *P. aeruginosa* PAO1 occurs through the FpvA receptor protein which utilizes the energy transducing protein TonB1. This binding sends a signal to the membrane-spanning anti-sigma factor FpvR which activates the sigma factors FpvI and PvdS [121]. PvdS regulates pyoverdine production and exo-toxin A [122]. FptA is an outer membrane receptor precursor of pyochelin which is regulated by the transcriptional regulator PchR (PA4227) [123].

Other heterologous siderophores, xeno-siderophores, ferrisiderophores and heme/hemophores can also be incorporated with TonB dependent receptor systems [120, 124]. Many of these systems are controlled by the central regulator, Fur, which can also regulate many sigma factors and other regulators [125]. **Pyocyanin**, a bluish green pigmented toxin has been able to contribute to iron uptake from transferrin [126] as well as its precursor, Phenazine-1-carboxylic acid (PCA) [124]. PCA and Pyocyanin can reduce ferric Fe^{3+} bound to host proteins to ferrous Fe^{2+} allowing uptake through the Feo system [127].

The precursor to pyocyanin, PCA, is regulated by a number of different factors including quorum sensing. The *phz1* operon is regulated by *P. aeruginosa* quinolones. Binding of the

Pseudomonas quinolone signal (PQS) to the transcriptional regulator, MvfR, is required for WT pyocyanine production [128]. The repressor QscR, encoded upstream of *phz2*, has a negative effect on the expression of both *phz* operons through an unknown mechanism [129]. Lastly, sequestering of RsmA by RsmZ and RsmY results in increased expression of pyocyanin along with the other previously described phenotypes [98].

The type I, 2 and 3 secretion systems play a role in the planktonic lifestyle state and are implicated during the acute infection state. These systems and the infection states are described in more detail in (section 1.1.F). This is a review of how these systems are regulated.

In the **Type 1 secretion system (T1SS)**, the HasAp haem uptake protein is regulated by the quorum sensing system in PA [130]. The virulence toxin, AprA is regulated by the BexR virulence regulator which controls bi-stability in PA [118].

The **type 2 secretion (T2SS)** is involved in toxin secretion. These include LasA, LasB, ToxA, and PlcH, PlcN (phospholipases). Inactivation of quorum sensing contributes to the downregulation T2SS expression including lipases [85]. The phoB/R genes (PA5360-PA5362) regulates PlcH and PlcN [131]. Regulation of Hxc T2SS genes is done by a cell surface signaling system, PUMA3 which includes genes in the vreAIR operon [132].

The **type 3 secretion system (T3SS)** is regulated by a number of ways. One major is by ExsA (PA1413) which binds upstream of the promoter to control genes in the regulon [133]. ExsD (PA1714) and PtrA(PA2808) act as anti-activators for ExsA. ExsC is an anti-anti activator of ExsD. When concentrations of Ca^{2+} are high, ExsE can bind to the anti-anti activator ExsC , freeing up ExsD to bind ExsA, preventing T3SS gene expression. Under Ca^{2+} limiting conditions,

ExsE is secreted, making ExsC free to bind to ExsD (the anti-activator). This frees ExsA to be able to activate T3SS expression [134]. ExsA is also activated by PsrA (3006) [135]. Although this is the primary mode of control, T3SS can also be suppressed by PtrB (rec-A mediated) under the stress of DNA damage [136].

Interestingly, **condensins** were discovered to be global regulators between these two physiological lifestyles. Regulation incorporated multiple pathways involved in biofilm formation and virulence factor expression. This discovery adds an additional component to our understanding of lifestyle switching. Overall, the causes of the physiological changes associated with PA adaptation involving lifestyle switching are undoubtedly multifactorial and still very much elusive. The discovery that condensins play a role in global regulation between lifestyles shows that chromosomal organization is somehow involved in the differentiation of lifestyle states. The duality of these phenotypes into a relative biphasic system also indicates the possibility that condensins play a role in epigenetic regulation. It is speculated that these proteins could act as a biphasic switch in response to environmental changes, enabling differentiation states in PA.

1.4.F. Chronic and acute infection states

PA is introduced into the human host as an environmental strain and transitions with time from an acute infection phase to a chronic infection phase [49]. During the **acute infection phase**, symptoms are exacerbated within the patient on account of the host immune system response. If diagnosed accurately and timely, acute infections are generally treatable with antibiotics. If not, PA can cause pneumonia, break down lung defenses, cause tissue necrosis,

enter the bloodstream, and even cause death. In contrast, during the **chronic infection phase**, patient symptoms are considered low-grade and sometimes even undetectable. One of the hallmarks of chronic infections is their extreme resistance to antibiotics and significant capacity for evading the host defenses.

In terms of the physiological attributes of bacteria during these infection phases, **the acute infection phase** is associated with a planktonic state. Phenotypes include increased motility (flagella and pili type IV also used for adherence) and enhanced toxin secretion from the type 1, 2 and type 3 secretion systems (Figure 1-9) [137, 138]. Both secretion types increase the severity of acute disease and are also less likely to be expressed during chronic infections [139]. Aspects of the type 1 secretion system has also been implicated in this infection type.

The type 1 secretion system (T1SS) utilizes an ABC (ATP-binding cassette) transporter with an outer membrane protein in order to export toxins [140]. T1SS encodes *has* (heme acquisition system) consisting of a heme receptor (*hasR*) and a protein that binds heme, HasAP, a haemophore [141]. This protein allows utilization of iron by binding haem from haemoglobin. This is an important step during the initial stages of infection. The other major protein involved in this system is AprA, an alkaline protease involved in various types of PA infections [142].

The type 2 secretion system (T2SS) is a membrane bound protein secretion machinery that is used to transport of a group of proteins, many being lipases, proteases, and other toxins, across the outer membrane into the extracellular space. Major toxins from the type 2 secretion system include elastases (LasA and LasB) (elastases), Protease IV (PrpL),a quorum sensing dependent endo-protease, ToxA (exotoxin A). In general, these proteins are associated with

the destruction of various tissues, which contributes to cell damage and disease. Exotoxin A is one of the most toxic virulence factors of PA. It is responsible for tissue necrosis by blocking protein synthesis [143]. Elastases A and B are also involved with tissue damage. LasB has been reported to degrade mucins and surfactant proteins which help to allow bacterial clearance [144]. Protease IV degrades surfactant proteins and inhibits surfactant host defense and biophysical functions [145].

The type 3 secretion system (T3SS) is a membrane-spanning structure and needle that can inject toxins directly into mammalian cells [146]. Major toxins of the T3SS system include ExoS/T/U/ and Y. ExoU, ExoS and ExoT cause death in animal models of pulmonary infection and possible humans [147]. Phospholipase C, a hemolysin, is another toxin which is secreted during the acute infection phase. These toxins are capable of interacting with the membranes of eukaryotic cells, causing hydrolysis of phosphatidylcholine and sphingomyelin, resulting in cell lysis [148]. Other virulence factors in the acute infection model include hydrogen cyanide and lipopolysaccharides [149, 150]. Cyanide can inhibit Cytochrome c oxidase, a terminal electron acceptor in the electron transport chain, effectively shutting down cellular respiration and causing cell death [151].

Lastly, in order to bypass direct interaction with the host, PA can use outer **membrane vesicles** as a mechanism for the long-distance delivery of multiple virulence factors to cause cytotoxicity. It has been shown that B-lactamase, alkaline phosphatase, hemolytic phospholipase C and Cif are delivered by PA into the host cytoplasm through outer membrane vesicles [152].

The chronic infection phase in PA is characterized by a distinct set of phenotypes which are associated with a biofilm lifestyle and specific virulence factors. Chronic infection phenotypes include enhanced biofilm formation and exopolysaccharide production, increased c-di-GMP levels, enhanced type 6 secretion effectors and frequently, increased antibiotic resistance and iron scavenging capabilities (Figure 1-9). Often, there are also reduced motilities and effector proteins of the type 3 secretion system and reduced virulence 19[153]. These common phenotypes are shared amongst *Pseudomonas aerugionsa*, *Staphylococus aureus*, and *Bhurholderia cepacia* strains during chronic infections, indicating that the chronic infection phase may possibly be an optimized cell lifestyle for sustained survival in the lung.

The type 6 secretion system (T6SS) involves a needle like complex resembling a phage like tail structure, [115] to inject toxins directly into both host cells as well as bacterial to fight off competition. There are three sub-types within this system incorporating different Hcp Secretion Island (HSI) genes, HSI-1, HSI-2, and HSI-3. Toxins produced from the HSI-system include Tse1, Tse2, and Tse3 [117]. HSI-1 is also involved in biofilm formation as described previously [154]. HSI-2 enhances bacterial internalization into host epithelial cells. Information for HSI-3 is limited.

In order to evade the host immune system, it has been reported that PA can synthesize structural homologs of the human α2-macroglobulin as a form of mimicry. Six gene elements are included in the overall complex formation and are found in the *magABCDEF* operon. The α2-macroglobulin complex is proposed to emulate the process by human α2-macroglobulin by trapping and inactivating external proteases aiding in bacterial defense and survival [155].

Bacteriophage is a virus capable of infecting and replicating in bacteria. It has been integrated into the chromosome of PA. Bacteriophage pf1 in particular, contribute to bacterial lysis functions which releases extracellular DNA that can contribute to the structure of biofilms [156]. It has been reported that bacteriophage pf1 genes are upregulated in biofilm cells [157].

As previously mentioned, studies have demonstrated that high iron concentrations favor the formation of biofilms [119, 158, 159]. However, in vivo conditions have low iron concentration since the host has iron sequestering mechanisms working to uptake iron such as lactoferrins in mucosal secretions and transferrins in serum [160]. In order to overcome this, PA has several pathways in place for iron uptake. Briefly, they including varying siderophores (pyoverdine, pyochelin and TonB dependent iron uptake), xeno-siderophores, and heme extractors (has and phu systems) [161] Pyocyanin and its precursor phenazine, can also contribute to iron acquisition through the FEO system [127] . Pyocyanin is a toxin secreted by PA which is capable of oxidizing and reducing other molecules [162]. This allows it to kill microbes which compete with it as well as mammalian host cells during infection. Pyocyanin is often detected in the sputum of cystic fibrosis patients during chronic lung infections [163].

In addition, iron-sulfur cluster biogenesis was shown to be upregulated in PA in response to iron starvation [164]. This trend was also seen in other strains including. *S. epidermidis* [165], and *Thermotoga maritima* [166] for cells growing in biofilms .

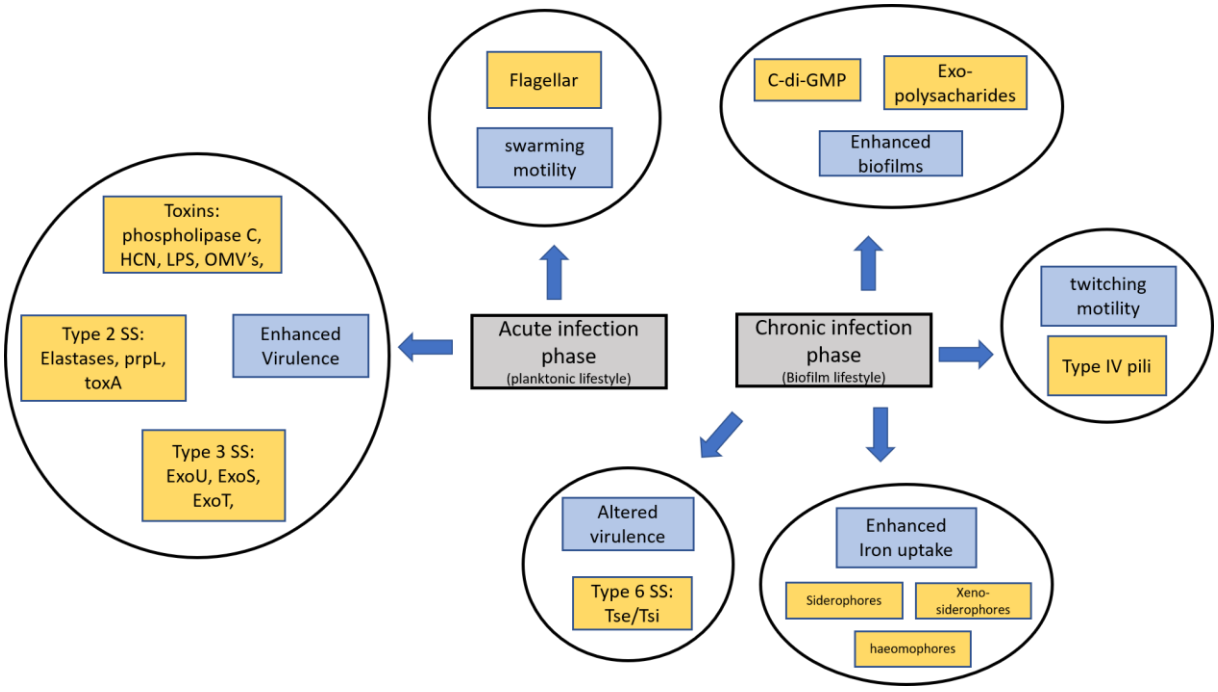

Figure 1- 9: General summary of acute and chronic infection phase phenotypes expressed in bacteria.

These characterizations of infection phases, however, are not black and white. During the chronic infection state, it has been reported that there is also a mix of cell types, albeit, with a higher prevalence for the sessile biofilm stage [167]. Additionally, virulence of the secretion systems also showed variation, with a higher prevalence for the chronic type 6 secretion, but there was always some degree of diversity in the population [168].

Populations with variation in lifestyle and virulence is necessary for diversity and is an essential component during infection stages. The ability to revert back and forth into these different physiologies ensures diversity and progression of infection. The evolution of PA during lung infections is of particular concern on account of its devastating impact on lung function for cystic fibrosis patients.

We report here that the two **condensins** in *Pseudomonas aeruginosa*, **SMC-ScpAB and MksBEF,** are involved in the differentiation of the bacterium and impose opposite physiological states. Understanding the switch in lifestyle could provide insight into the major transition between acute level and initial chronic infection stages of p.a. into advanced chronic infection levels. This finding could help illuminate ways to better target PA and treat infection, before changing into a state that is untreatable.

1.5 PAO1 and PA14 strains

PAO1 is a widely used laboratory strain while PA14 is considered a highly virulent clinical isolate. Both strains act as opportunistic human pathogens with intrinsic resistance to antibiotics and disinfectants. Included in their repertoire are a variety of extracellular virulence factors including proteases, hemolysins, pyocyanin, pili, lipopolysaccharide, alginate, and the type 3 secretion system effector proteins, ExoS, ExoT, ExoU, and ExoY. Additionally, lifestyle switching and the formation of biofilms with type 6 secretion system proteins inherent in both strain types.

Several studies involving different models of infection have reported that PA14 is more virulent than PAO1 [169-171] . The PAO1 and PA14 strains of *Pseudomonas aeruginosa* have a similar core genome where approximately 91.7% of PA14 genome exists in PAO1, and 95.8% PAO1 genome exists in PA14 [172]. The PAO1 chromosome (GenBank Assembly: GCF_000006765.1) is about 6.3 Mb with 5572 protein genes and 106 RNA genes while the UCBPP-PA14 (GenBank Assembly: GCA_000014625.1) is about 6.5 Mb having 5892 protein genes and 72 RNA genes (keg database: PAO1 PMID:17038190, PA14 PMID PMID:10984043

[173]. These differences in genome size account for 58, PA14 gene clusters that are absent in PAO1. Two pathogenicity islands (PAPI-1 and PAPI-2) have been identified in the PA14 genome [174]. The PAPI-1 island is about 108 kb while the PAPI-2 island is about 11 kb [174].

Different results have been reported for the impact of gene differences found on these islands. Harrison et al 2019 reported that the global contributions to virulence of both PAPI-1/2 together significantly attenuated virulence of PA14 in acute pneumonia and bacteremia models. In contrast, loss of one island did not show a measurable change [175].

Analysis of individual genes for several studies have shown link to virulence [174, 176]. Comparison of extra PA14 genes to other strains, however, did not show a correlation with virulence [172]. Lee et. al studied the 58, PA14 gene clusters that are absent in PAO1 to determine if any contributed to the enhanced virulence of PA14 in a *Caenorhabditis elegans* pathogenicity model. Of these extra genes, none were required or predictive of virulence in other strains. They concluded that the higher virulence in PA14 is multifactorial and combinatorial in terms of total pathogenicity related genes which interact differently in different genetic backgrounds [172].

Recent developments in RNA seq have illuminated roles for small RNAs in regulation. Comparison of PAO1 and PA14 show novel unique and conserved sRNA which were strain specific or had strain specific expression indicating a possible role in virulence regulation [177]. Supporting this, The PAPI-1 pathogenicity island encodes a small RNA PesA which was found to influence virulence and modulate pyocin S3 production, a virulence factor in PA14 [178].

Overall, enhanced virulence in could be combinatorial, residing on the overall global effects of how these genes are incorporated specifically into a particular strain with possible contributions for regulation by factors such as small RNAs. More progress needs to be made in order to better understand virulence and the differences between particular strains.

1.6 Nucleotide usage bias

There are four nucleotides which make up genetic code, Adenine (A), Guanine (G), Thymine (T) and Cytosine (C). When no selective pressure is present in a system, a random distribution of all four nucleotides among a single DNA strand is expected known as Chargaff or parity rule 2 [179] [180, 181]. However, in most prokaryotes, this distribution of nucleotides is not random.

Several types of nucleotide bias have been found encoded in bacterial genomes. One example in *E. coli* are the *Ter* sites, also known as DNA replication terminus binding-site. Ten closely related ter sites are present on the chromosome designated *TerA*, *TerB* up to *TerJ*. Each site has 23 base pairs. Depending on the strain, either the Tus or Tau proteins bind to *Ter* sites, preventing progress of the DNA replication fork from the opposite direction. Therefore, this system of blockage on *Ter* sites entraps the terminus of replication into a confined region of the chromosome [182].

Another example of nucleotide bias are KOPS (FtsK orienting polar sequences) sites which have the sequence GGGNAGGG, and are asymmetrically found in the two chromosome arms. FtsK, a DNA translocase protein, preferentially engages KOPS which guides it towards the terminus region at the chromosome dimer resolution, *dif*, site [183] a 28 bp sequence. Here, XerC

and XerD proteins bind at the two *dif* sites to form a complex followed by strand exchange, catalyzed by FtsK, and recombination which separates chromosome dimers [184] (Figure 1-10). KOPS sequences are present in most bacteria as well as FtsK and XerC and XerD homologs.

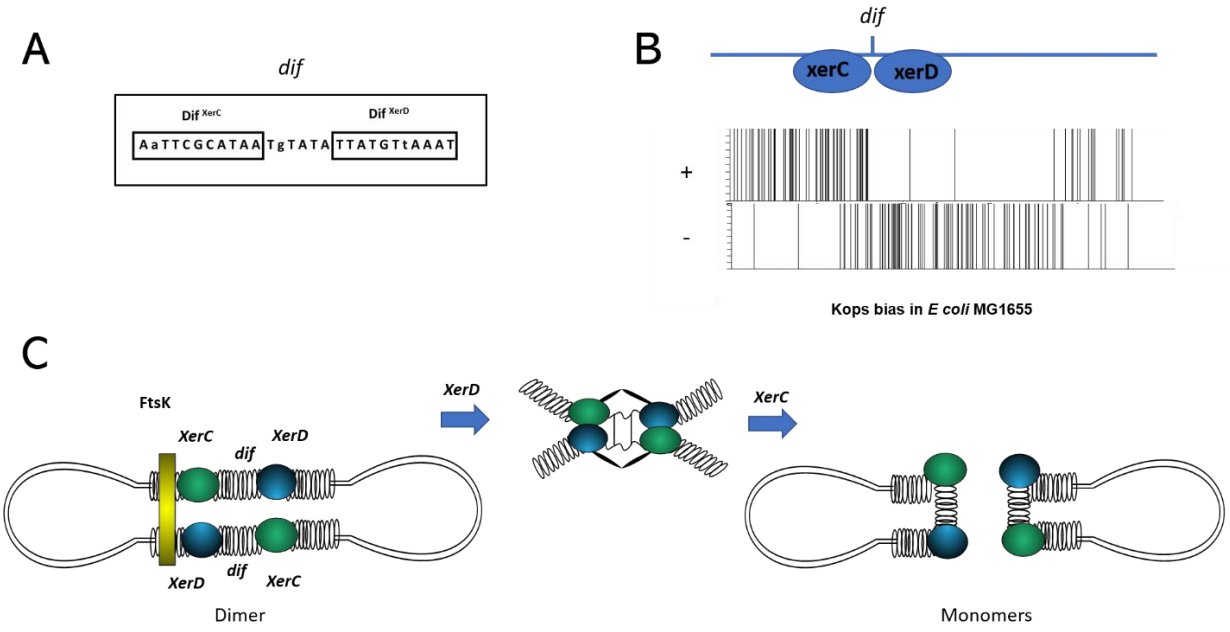

Figure 1- 10: *dif* and the XerC/D recombinase system. (A) The consensus *dif* sequence showing XerC and XerD binding sites. (B) Kops bias seen in leading and lagging strands for plus and minus strands in *E. coli* MG1655. These sequences align with the *dif* sequence. (C) Chromosome dimers are resolved by the XerC/XerD recombination system which occurs at the *dif* site. FtsK is a DNA translocase motor protein which brings together two *dif* sites guided by numerous KOPS (FtsK orienting polar sequences; 5'-GGGNAGGG-3'), which are distributed along both arms from *oriC* to dif. FtsK induces XerD catalytic activity required for the first DNA strand exchange. The second strand exchange event is modulated by XerC, completing the recombination reaction. Capital letters indicate >50% frequency in representative strains, lower-case <50% frequency.

In addition to these examples, global nucleotide compositions are typically found to be asymmetric with a clear nucleotide bias between the chromosome arms which overlap with the leading (G/T abundant) and lagging strands (A/C abundant) [181, 185]. This nucleotide bias phenomenon is known as GC skew and AT skew.

The cause for this phenomenon is still unclear. The current hypothesis is that it is primarily due to the higher incorporation of guanines versus cytosines in the leading strand during replication [186, 187]. Supporting this idea, GC-skew switches polarity at the origin of replication, *oriC*. Interestingly, the opposite GC-skew switch is found at the chromosomal dimer resolution site, *dif,* implying an alternative contribution to its origin [181, 188].

Nucleotide bias, therefore, serves as an inherent signaling code, switching polarity and thereby marking the location for *oriC and dif.* How this nucleotide bias is affected by chromosome asymmetry (placement of *dif* relative to *oriC*), and its coordination with segregation and replication has not been investigated. This thesis, therefore, looks at the coordination between nucleotide bias in conjunction with major processes of segregation and replication both in the PAO1 strain (model organism), and across all sequenced bacterial chromosomes in the NCBI database [6].

Chapter 2: Methods

2.1 Genome modification through allelic replacement

Modifications to the genome was done through bacterial conjugation using the method of Simon et. al (1986) [189]. Recipient *P. aeruginosa* cells and donor *E. coli* strain SM10 (*λpir*) cells carrying the suicide vectors were grown in LB medium at 37 °C to an OD_{600} of 0.2. Cells from each strain were then harvested and combined containing 5×10^7 of the SM10 (*λpir*) cells and 2×10^8 of *P. aeruginosa* cells in a total volume of 20 µl LB medium and spotted on an LB-agar plate. The conjugating cells were incubated 37 °C overnight, then collected, resuspended in 2 ml of 10 mM magnesium sulfate solution. Cells were then plated onto Vogel-Bonner minimal medium (VBMM: 0.083 M Magnesium sulfate, 0.48 M citric acid monohydrate, 2.87 M Dipotassium phosphate anhydrous, 1.28 M Sodium Ammonium Phosphate) agar plates supplemented with gentamicin (30 µg/ml). Colonies were re-streaked onto LB-agar plates containing 15% sucrose and incubated 37 °C. Strains generated using FRT cassettes (Flp recognition sequences) flanking drug resistance markers had their drug markers removed by electroporation with pFLP2 harboring the flippase (Flp) recombinase gene in order to recombine the FRT cassettes as done previously [190]. Colonies were then cross checked for sensitivity to carbenicillin which is present on the pEX18Ap and pFLP2 plasmids by streaking on LB plates supplemented with carbenicillin. Confirmation of genome modification was done by PCR and/or DNA sequencing.

2.2 Plasmid and strains

For experiments done with PAO1, PAO1-Lac (ATCC 47085) was used as the wild-type (WT). For experiments done with PA14, UCBPP-PA14 was used as the wild-type (WT). *E.coli* and *P. aeruginosa* cells were grown in Luria broth (LB medium or M9 medium plus 0.4% glycerol and 0.4% Casamino Acids (Difco) under aerobic conditions at 37^{o}C unless noted otherwise. Cell growth was measured by the optical density (OD) at 6_{00} nm (OD_{600}) using a UV-1601 UV-visible spectrophotometer. A complete list of plasmids is provided in Table 1, a list of strains in Table 2, and primers in Table 3 in the Appendix.

2.2.A Construction of plasmids

Constructs used to generate deletion and knock-in strains utilized the pEX18Ap suicide vector [190] as a backbone which incorporated the *ori*T region and the ColE1 origin of replication, the gentamicin resistance gene, GmR, flanked by FRT cassettes, the *sacB* gene and the ampicillin resistance gene, AmpR (Figure 2-1). The *sacB* gene encodes Levansucrase, an enzyme that converts sucrose to levan polysaccharides which accumulates in the periplasm and is toxic to cells [191]. Levansucrase activity confers sucrose sensitivity in *P. aeruginosa* in the presence of 10% sucrose, allowing it to be used as a counter selectable marker. The *ori*T region allows the plasmids to transfer from *E. coli* to *P. aeruginosa*. pEX-Δ*mksB* [1], used for condensin deletion constructs, was derived from pEX18Ap [190] and incorporates approximately 500 bp up and downstream of the *mksB* gene onto flanking regions of an FRT cassette containing a gentamicin resistance marker. pUCP-*mksB* [27], derived from the pUCPP22 vector [192], encodes MksB-His_8 and an *araC-*P_{araBAD} inducible promoter system. This construct was used for

the subcloning of an *sspB* gene to generate an arabinose inducible expression vector used in the degron system. The pYM101 vector [193] was used as a source for the *lacI*^{q} gene and the T7 early promoter $P_{T7(A1/04/03)}$ for generating conditional condensin mutants inducible by isopropyl-B-D-thiogalactopyranoside (IPTG).

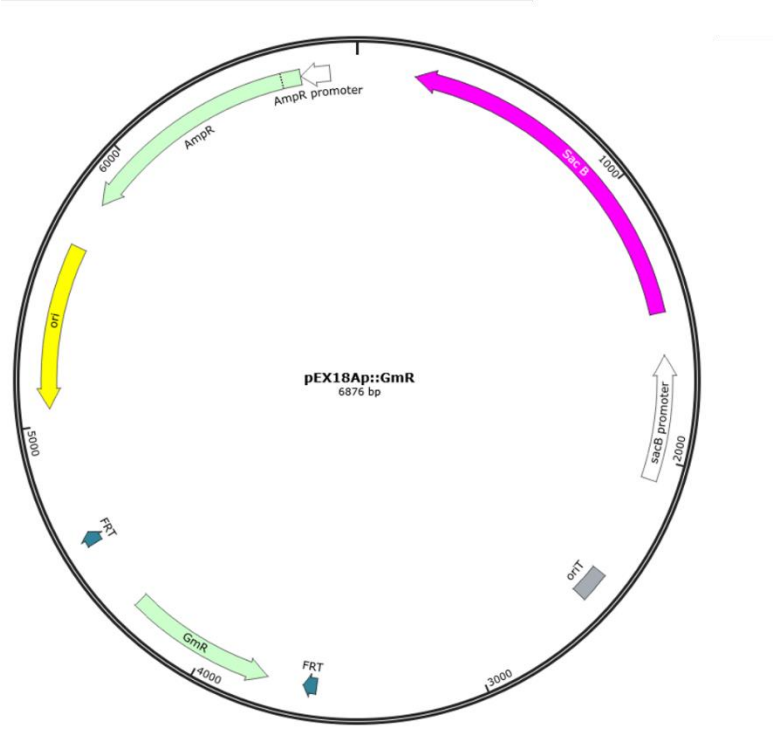

Figure 2- 1: Plasmid map of suicide vector pEX18Ap::GmR .

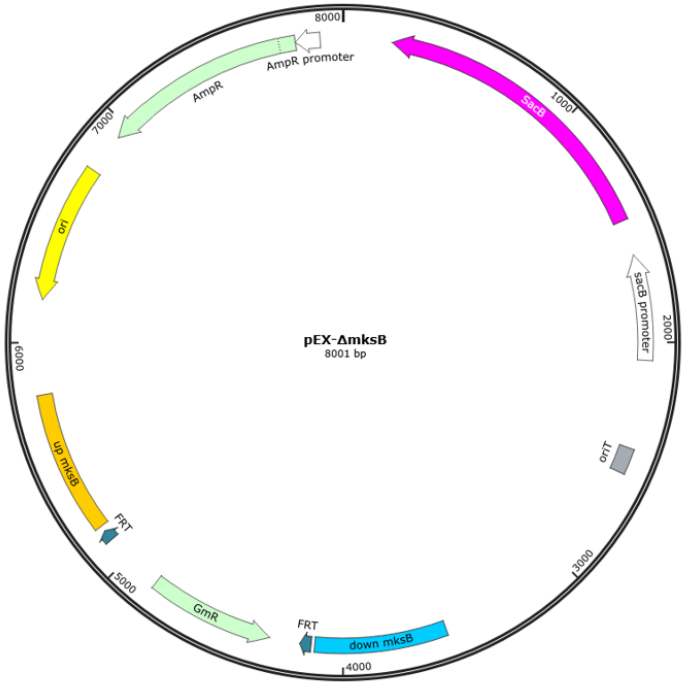

Figure 2- 2: Plasmid map of suicide vector pEX-Δ*mksB*

The **pEX-Δ*mksB*::*mksB*** plasmid was generated to incorporate a *mksB* gene into a Δ*mksB* strain (at the *mksB* locus) to test for complementation. To generate this construct, an FRT cassette (section 2.1) flanking a gentamicin resistance gene, FRT GmR, and an approximate 500 bp fragment of the downstream region of *mksB* was PCR amplified from the pEX-Δ*mksB* vector using primers Sbf1 forward and Opa30. This fragment was digested with the restriction enzymes SbfI and HindIII (New England Biolabs) and ligated with T4 DNA ligase (New England Biolabs) into the Sbf1/HindIII sites in the pEX18Ap suicide vector. Next, a fragment incorporating the entire *mksB* gene and approximately 500 bp upstream was PCR amplified from a PAO1 genomic template using primers Opa31 BamHI and Rev *mksB1* Blp1, then digested and ligated into the BamHI and SbfI sites.

To replace endogenous *mksB* by a DAS4-tagged version, the **pEX-*mksB*-Das4** plasmid was constructed. To this end, amplification of an approximate 600 bp fragment and the C-terminus of *mksB*, c-*mksB* , was obtained from genomic DNA just before the stop codon using primers degron 7 which incorporated a KpnI site and degron 8 which incorporated a DAS4 linker (For more details on primers used, see Table 3 of the Appendix). Amplification of the resulting fragment was done using primers degron 7 and degron 9 which added a Das4 tag, stop codon, and a BlpI restriction site. This was digested and ligated into the Kpn1 and Blp1 sites in the pEX-Δ*mksB* construct.

To incorate the sspB protein through inducible expression, the **pSspB** plasmid was generated. The sspB gene was amplified from a PAO1 genomic template using primers degron 10 and degron 11 and digested and ligated into the PacI and XbaI sites in a pUCP-*mksB* cloning vector, effectively replacing the *mksB* gene with *sspB*. The pUCP-*mksB* vector was obtained from our lab [27] .

To generate three different mksB ATPase mutants, the plasmids **pEX-*mksB*-D864A, pEX-*mksB*-E865Q,** and **pEX-*mksB*-S829R** were constructed. To this end, **pEX-*mksB*-D864A** was generated by PCR amplification of an approximate 600 bp fragment using primers opa180 and opa184 from PAO1 genomic DNA. This fragment is located about 240 bp upstream from the stop codon of *mksB*. Opa180 contains a restriction site for KpnI. The opa184 primer incorporates a single base pair change, cytosine, from an adenine, at the 2,591 bp position in the *mksB* gene. This changed the sequence from “GAC” to GCC”. A second fragment approximately 270 bp was generated using primers opa181 and opa183. Opa184 is the reverse complement of opa183. Both primers incorporate a single base pair change generating an

approximate 270 bp fragment. Opa181 contains the restriction site for BlpI. The two resulting fragments were joined using PCR mediated assembly, digested with KpnI and BlpI and inserted into pEX-Δ*mksB* obtained from our lab [1].

The **pEX-*mksB*-E865Q** plasmid was generated by PCR amplification of an approximate 600 bp fragment using primers opa180 and opa186 from PAO1 genomic DNA. This fragment is located about 240 bp upstream from the stop codon of *mksB*. Opa180 contains a restriction site for KpnI. The opa184 primer incorporates a single base pair change, cytosine from a guanine, at the 2,593 base pair position in the *mksB* gene. This changed the sequence from "GAG" to CAG. A second fragment approximately 270 bp was generated using primers opa181 and opa185. Opa186 is the reverse complement of opa185. Both primers incorporate a single base pair change generating an approximate 270 bp fragment. Opa181 contains the restriction site for BlpI. The two resulting fragments were joined using PCR mediated assembly, digested with KpnI and BlpI and inserted into pEX-Δ*mksB* obtained from our lab [1].

The **pEX-*mksB*-S829R** plasmid was generated by PCR amplification of an approximate 550 bp fragment using primers opa180 and opa188 from PAO1 genomic DNA. This fragment is located about 340 bp upstream from the stop codon of *mksB*. Opa180 contains a restriction site for KpnI. The opa188 primer incorporates two base pair changes, a cytosine and a guanine (in order), from a thymine and cytosine (in order), at the 2,485 and 2,486 base pair positions in the *mksB* gene. This changed the sequence from "TCC" to "CGC". A second fragment approximately 370 bp was generated using primers opa181 and opa187. Opa188 is the reverse complement of opa187. Both primers incorporate the two base pair changes generating an approximate 370 bp fragment. Opa181 contains the restriction site for BlpI. The two resulting

fragments were joined using PCR mediated assembly, digested with KpnI and BlpI and inserted into pEX-Δ*mksB* obtained from our lab [1].

To delete the *mksB2* gene in PA14, the **pEX-Δ*mksB*2** plasmid was generated. Construction of this plasmid included amplifying an approximate 500 bp fragment from the upstream region of *mksB*2 using primers Apa 1 and Apa 2 and cloned into the pEX-Δ*mksB* vector between KpnI and Blp1. Next, an approximate 500 bp fragment from the downstream region of *mksB*2 was amplified using primers Apa 3 and Apa 4 and cloned into the RsrII and HindIII sites.

To replace the original promoter upstream of the *mksB2* gene in PA14 with a *lacI*^{q}-P_{T7} inducible promoter, the **pEX-*lac*-*mksB*2 plasmid** was generated. To this end, a modified version of pEX18Ap with the EcoRI site removed, pEX18Ap*, was used for cloning. An approximate 300 bp fragment directly downstream of the *mksBEF*2 promoter was PCR amplified with primers containing SpeI (primer P3) and PstI (primer P4) sites. Next, an approximate 300 bp fragment, 200 bp upstream of the *mksBEF*2 promoter was amplified, with primers P1, containing the KpnI site and P2, containing the and EcoRI site. These amplified fragments were then combined using PCR mediated assembly, digested and ligated into the KpnI and PstI sites of of pEX18Ap*. The *lacI*^{q} gene and the T7 early promoter, P_{T7}, was then amplified from a pYM101 plasmid [193] and cloned in between the two fragments at the SpeI and EcoRI sites.

For deletion of both the *mksB2* and *mksG* genes in PA14, the **pEX-Δ*mksB2*-Δ*mksG*** plasmid was generated. For construction, amplification was done from PA14 genomic DNA of an approximate 500 bp fragment from the downstream region of the *mksG* gene using primers Apa 5 and Apa 6. This was followed by cloning into the pEX-Δ*mksB*2 vector at the RsrII and HindIII

sites.

2.2.B Construction of PAO1 strains

PAO1 *mksB*-E865Q was generated by mating SM10 (*λpir*) cells harboring the pEX-*mksB*-E865Q plasmid with the recipient PAO1 Δ*mksB* strain through allelic replacement. These steps include plating on VB 30 Gm followed by LB 10% sucrose which allowed counter-selection. The gentamicin resistance gene was removed by transforming cells which encodes Flp recombinase, followed by plating on LB 200 µg/ml carbenicillin [190]. Chromosomal insertion was verified using DNA sequencing and PCR.

PAO1 *mksB*-S829R, and **PAO1 *mksB*-D864A** were similarly generated as above, using their corresponding plasmids pEX *mksB*-S829R and pEX *mksB*-D864A respectively.

To test for *mskB* complementation, the ***PAO1 ΔmksB::mksB (ΔB::B)*** strain was generated which incorporated the *mksB* gene into a PAO1 Δ*mksB* strain. This strain was similarly generated as above using *the* plasmid pEX-Δ*mksB::mksB*. Chromosomal insertion was verified using PCR

2.2.B.1 Degron system strains

To construct **strains for DAS4 mediated degradation**, the *sspB* gene was first deleted from PAO1 Δ*mksB* [1] and wild-type PAO1-Lac using the allelic replacement method with pEXG2-Δ*sspB.* Next, the *mksB* gene was replaced by its DAS4-tagged version using the allelic exchange method with the pEX-*mksB*-Das4 plasmid. The gentamicin gene was removed as previously described generating **PAO1 Δ*sspB* Δ*mksB::mksB*-DAS4 *(*PAO1 Das4),** followed by transformation with either the pUCP22-SspB or pUCP22 plasmids generating **PAO1 Δ*sspB***

Δ*mksB::mksB-DAS4-PsSpB (*PAO1 Das4-PsSpB) and **PAO1 Δ*sspB* Δ*mksB::mksB*-DAS4-pUCP22 *(*PAO1 Das4-Pucp22)** respectively.

2.2.C Construction of PA14 strains

2.2.C.1 PA14 deletion strains

PA14 deletion strains were generated using the allelic exchange method as described in section 2.1 and are listed in Table 2 in the Appendix. Each condensin mutant listed below includes both a GmR strain (containing a gentamicin resistance marker flanked by an FRT cassette) and a ΔGm strain (gentamicin marker removed). For GmR strains, the GmR FRT cassette is located on the locus that was last to be replaced. Deletions were confirmed using PCR. The order in which each deletion was generated is indicated:

PA14 Δ*mksB1* was generated using pEX-Δ*mksB1*.

PA14 Δ*smc* was generated using pEX-Δ*smc*.

PA14 Δ*mksB2* was generated using pEX-Δ*smc*.

PA14 Δ*mksB1* Δ*mksB2* was generated using first, pEX-Δ*mksB1* then pEX-Δ*mksB*2.

PA14 Δ*mksB1* Δ*smc* was generated using first, pEX-Δ*smc* then, pEX-Δ*mksB1*.

PA14 Δ*mksB2* Δ*smc* was generated using first, pEX-Δ*smc* then, pEX-Δ*mksB2*.

PA14 Δ*mksB1* Δ*mksB2* Δ*smc* was generated using first, pEX-Δ*mksB1* then using pEX-Δ*mksB2*. then, pEX-Δ*smc*.

PA14 Δ*mksB2* Δ*mksG* was generated using pEX-Δ*mksB2*-Δ*mksG*

2.2.C.2 PA14 conditional mutant strains

Another set of PA14 deletions were generated in the same fashion as above, however, a *lacI*^{q}-P$_{T7}$ replaced the original promoter of the *mksB*2 gene. This promoter replacement was generated by conjugation of SM10 (*λpir*) cells harboring the pEX-*lacmksB*2 plasmid with PA14 WT cells followed by plating onto LB with 15% sucrose. Condensin deletions were then generated using this as a parent strain. Each mutant listed below (except for PA14 *lacB2*) includes both a GmR strain and a ΔGm strain. For GmR strains, the GmR is located on the locus that is last to be replaced. Deletions were confirmed using PCR. The order in which each deletion was generated is indicated:

PA14 *lacB2*

PA14 *lacB2* Δ*mksB1* generated using pEX-Δ*mksB1*

PA14 *lacB2* Δ*smc* generated using pEX-Δ*smc*

PA14 *lacB2* Δ*mksB1* Δ*smc* was generated using first, pEX-Δ*mksB1* then pEX-Δ*smc*.

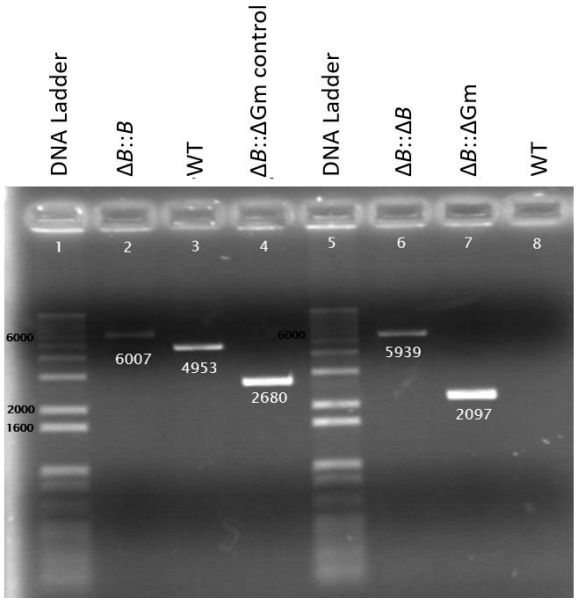

Figure 2- 3: PCR confirmation of PAO1 Δ*mksB:mksB (ΔB::B*). Rows 2 through 4 include samples PCR amplified using primers Opa11 and Opa42. Expected fragments include; Δ*B::B1* GmR: 6007 bp, WT: 4953 bp and Δ*B::*Δ*Gm*: 2680 bp. Rows 6 through 8 include samples PCR amplified using primers Opa11 and Opa22. Expected fragments include; Δ*B:B1* GmR: 5939 bp, Δ*B::*ΔGm: 2097 bp, and WT: no band.

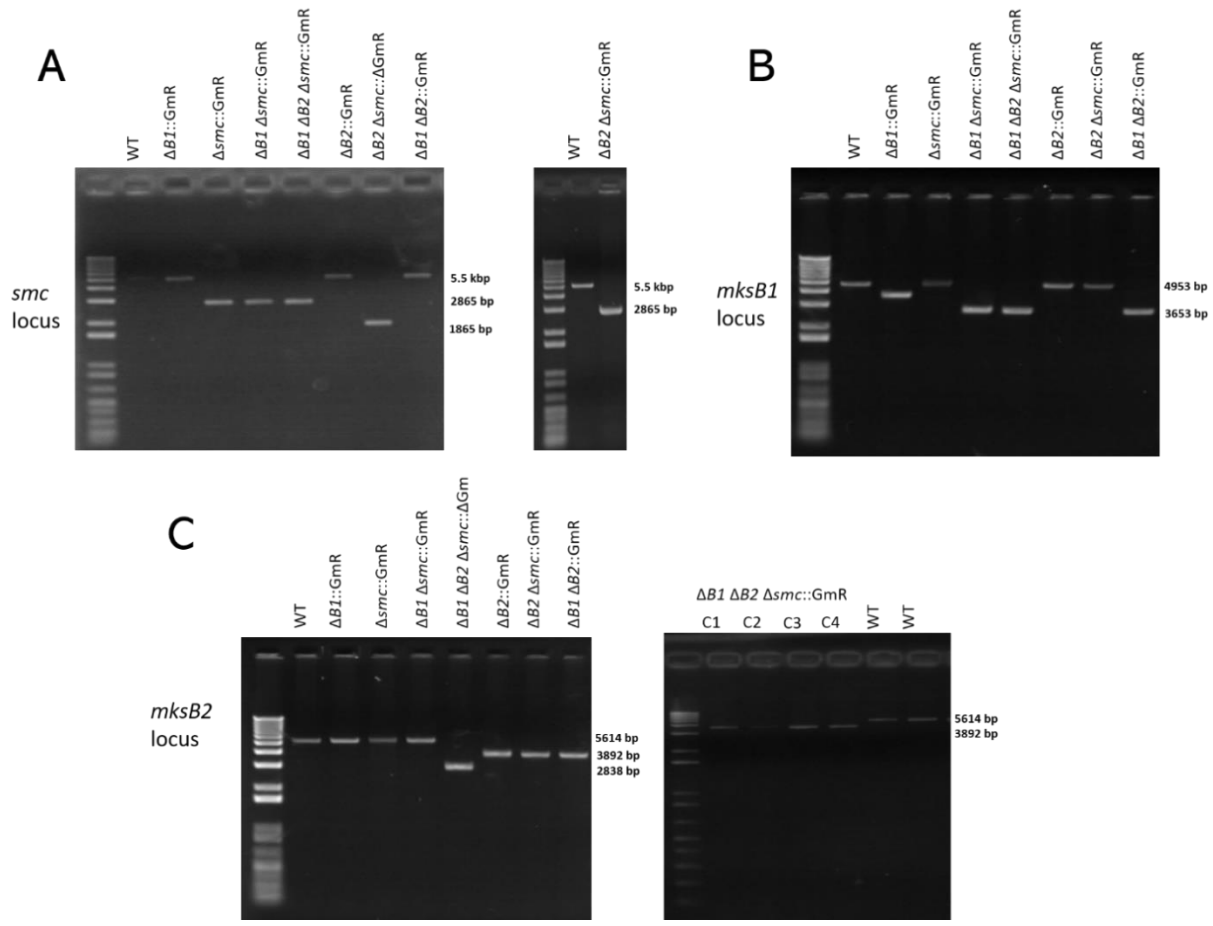

Figure 2- 4: PCR confirmation of PA14 condensin deletion strains containing a gentamicin resistance marker, Gm.

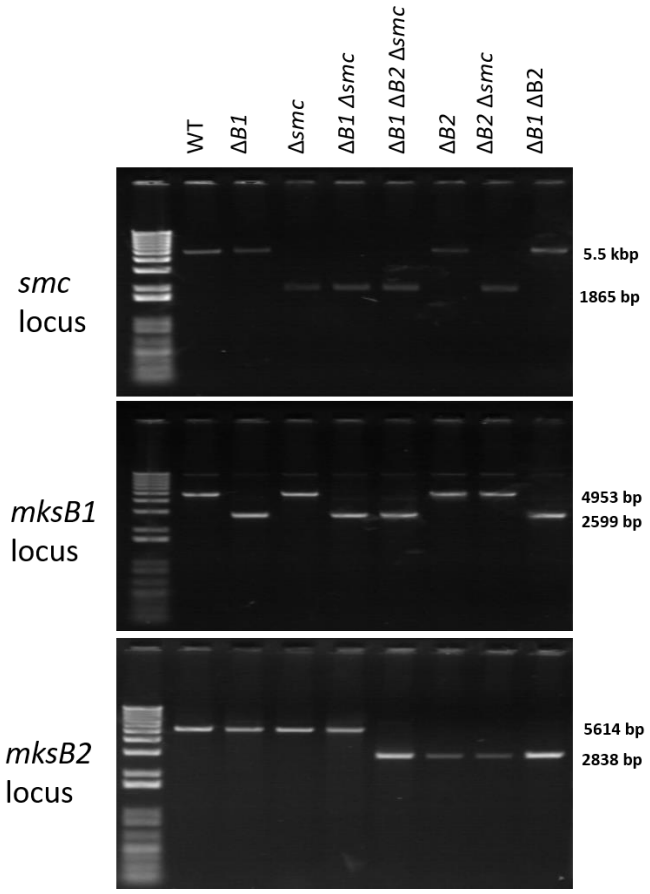

Figure 2- 5: PCR confirmation of PA14 condensin deletion strains with gentamicin removed.

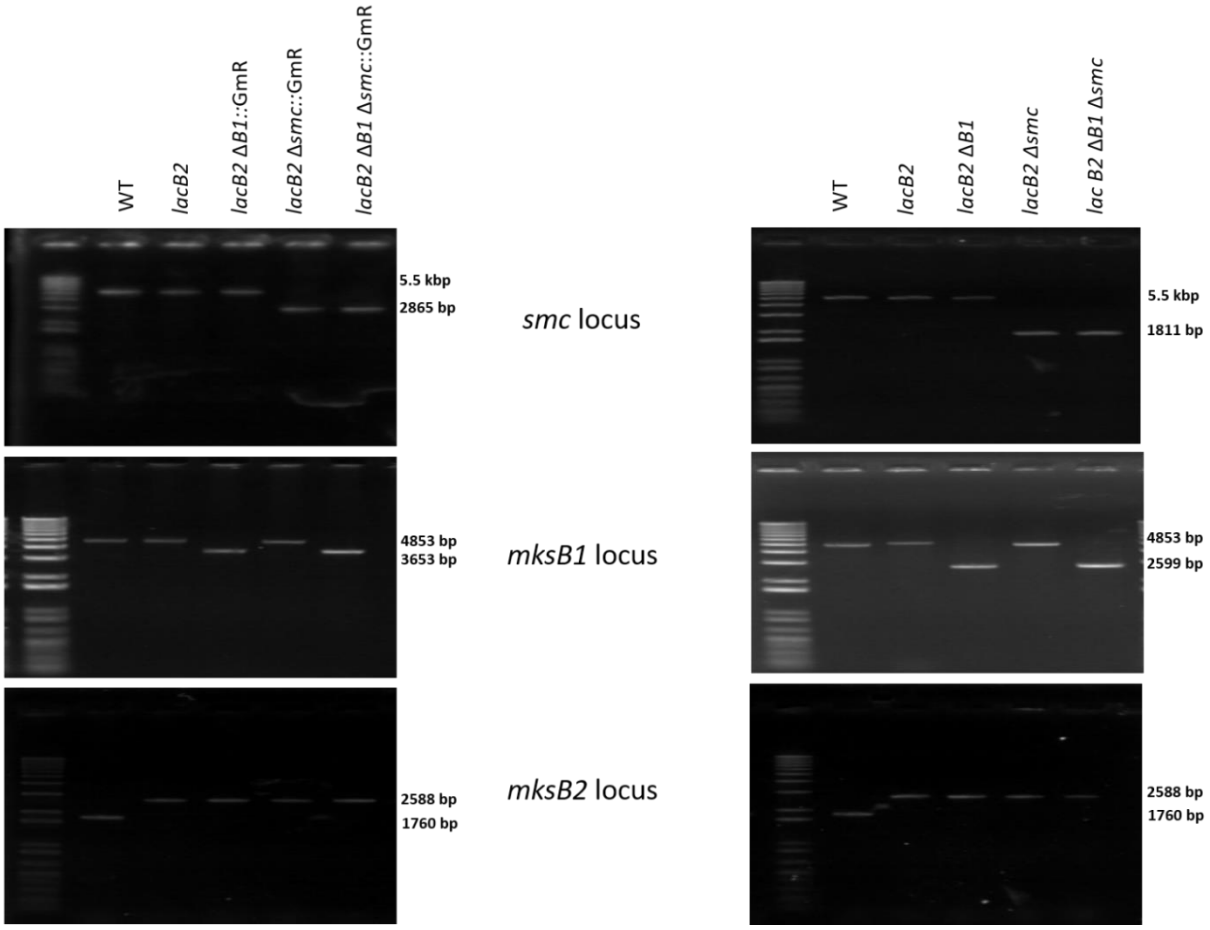

Figure 2- 6: PCR confirmation of PA14 condensin deletion strains with a *lacI*^{q}-P$_{T7}$ inducible promoter upstream of *mksB2*. Results include the *smc*, *mksB1* and *mksB2* loci.

2.3 The degron system

The degron system allows controlled degradation of proteins by the ClpXP protease. The system uses a Das4 tag (AANDENYSENYADAS), that binds to the C-terminus of the protein to be degraded. This tag is optimized for binding to both ClpXP as well as the adaptor protein, SspB, which makes degradation dependent on the presence of SspB.

For our study, a DAS4 tag was cloned at the 3`end of *mksB*. The *sspB* gene was removed from the chromosome through recombination using the deletion plasmid pEX-Δ*sspB* from

Castang et. al [194]. Next, the *mksB* gene was replaced by the DAS4 tagged version using the pEX-*mksB*-Das4 construct into the PAO1-ΔSspB strain. Finally, the SspB expression plasmid, p*SspB* was incorporated by electroporation into these strains. SspB was induced by adding 0.1 mM L-arabinose. Degradation was confirmed by western blot.

2.4 Biofilm formation

Biofilm formation was evaluated as previously described [195]. Cells were grown in LB or M9 medium supplemented with 0.4% Casamino acids and 0.4% glycerol to stationary phase then diluted 1:100 in M9 medium and 0.4% glycerol. 100 ul were placed into each well of a polyvinyl chloride (PVC) microplate and incubated at 37^{o}C for the indicted times. 0.1% crystal violet was used to stain 20 µl of cells for 10 minutes then the liquid was removed. Each well was then rinsed three times with phosphate buffered saline (PBS) and air dried for 15 min. The remaining cells were then resuspended in 100 ul of 95% ethanol. In order to measure the about of biofilm formation, absorbance readings were measured at 600 nm.

2.5 Fixed cell fluorescence microscopy

Anucleate cells were analyzed as previously described [196]. Cells were grown either LB or M9 medium supplemented with 0.4% Casamino acids and 0.4% glycerol to an OD_{600} of 0.6. 300 µl were then fixed in 70% ice cold ethanol and incubated on ice for 20 minutes. Cells were then rinsed with PBS (phosphate buffered saline). An aliquot of rinsed cells were then put onto poly-lysine coated microscope slides, stained with 100 nM DAPI and 1x Sypro-Orange. After staining, cells were observed by fluorescence microscopy. DAPI stains DNA and Sypro-Orange

stains proteins which makes it possible to view anucleate cells. Cells devoid of DNA do not fluoresce so they can be distinguished from normal cells which contain DNA.

2.6 Competition growth

To study competitive growth for condensin mutants, we used condensin strains which contained gentamicin resistance markers and the WT strain. Overnight cultures of mutant and WT were mixed at 1:1 ratios and approximately $2x10^4$ cells were put into fresh LB (5 ml). The cells were then further incubated at 37°C while shaking. Every 8 hours, the cell culture was reinoculated into fresh medium at an approximate OD_{600} of 0.2 to 0.5. Before each dilution, aliquots of the mixture were removed and spot plated onto LB agar plates as well as LB with 30 μg/ml gentamicin plates. This allowed us to calculate the total cells as well as mutant cells. The strain loss rate was determined by fitting the data to single exponential decay.

2.7 Minimal inhibitory concentration (MIC) analysis

To test susceptibility of mutants to antibiotics, overnight cultures of indicated strains were reinoculated and grown to an OD_{600} of approximately 1.0. Cells at a density of $5x10^4$ cells per ml were inoculated into each well place in the presence of antibiotic at 2 fold increasing concentrations. Cells were then grown approximately 20 hours at 37°C. The minimal inhibitory concentration was determined as the lowest concentration which inhibited growth.

2.8 RNA-Seq experimental methods

RNA-Seq analysis was performed for PAO1 condensin mutants during two separate experiments. The first experiment includes the first replica analyzing PAO1 WT, Δ*smc*, and ΔΔ. The second experiment included replicas 2 and 3 and analyzed PAO1 WT, Δ*smc*, Δ*mksB* and ΔΔ.

All together samples PAO1 WT, Δ*smc*, and ΔΔ had a total of three replicas, one replica from experiment 1 and two replicas from Experiment 2. Δ*mksB* included only two replicas derived from Experiment 2.

2.8.A Hot Phenol method

RNA in all replicas was extracted using the hot phenol method [197]. All samples were grown overnight in Luria-Bertani medium at 37 °C. The samples were reinoculated by diluting the sample 100x into fresh Luria-Bertani medium and grown to an OD_{600} of 0.6 for analysis of the exponenetial phase.

5 ml of culture was combined with 1:10 v/v of water saturated phenol ethanol (add 0.5 ml of water saturated phenol ethanol mixture) to the culture at room temperature. This was followed by centrifugation at 4,000 rpm at 4^{o}C for 10 mins to pellet the cells. The supernatant was removed and cells lysed with 800 µl of 0.5 mg/ml of lysozyme dissolved in TE pH 8.0. 80 ul of 10% SDS was added, mixed and the sample placed in a 65^{o}C water bath for 2 mins. 88 µl of 1 M NaOAc pH 5.2 and 1 ml of hot water saturated phenols prewarmed in 65^{o}C, was added and inverted 10 times. The mix was placed in a 65^{o}C water bath for 6 minutes, inverted every 60 seconds while in the bath. The tube was chilled on ice then centrifuged for 10 minutes at 4^{o}C 13,000 rpm. The top layer was pipetted off and put into a new centrifuge tube with equal volume of chloroform added and inverted 10 times then centrifuged again at a 4^{o}C at 13,000 rpm. Again, the top layer was pipetted off and put into another microfuge tube. Ethanol precipitation was then performed by adding 1/10 volume of 3 M NaOAc pH 4.2, 1 mM EDTA and 2-2.5 volumes of ice-cold ethanol to each sample. These samples were mixed and

incubated at -80^{o}C at least two hours. The RNA pellet was then pelleted by centrifugation at 13,000 rpm for 25 min s at a 4^{o}C, washed with ice cold 80% ethanol and centrifuged at 13,000 rpm for 5 mins at 4^{o}C. The ethanol was then removed and pellet air dried for 20 mins in a fume hood and resuspended in 100 µl DEPC water.

2.8.B DNase treatment

Genomic DNA was removed from the isolated RNA samples of PAO1 WT, Δ*smc*, Δ*mksB* and ΔΔ from using recombinant DNAse I treatment from Invitrogen, catalog number AM2235 [198]. The nucleic acid solution for all samples was diluted to 10 µg nucleic acid/50 µL. DNase I Buffer was added to 1X concentration in the RNA sample. 1 µL DNase I (2U) was added to 10 µg of RNA in a 50 µL reaction and incubated at 37°C for 30 minutes. The RNA sample was then extracted with phenol/chloroform to inactivate DNase I then Ethanol precipitated a final time.

2.8.C rRNA depletion

The total RNA that is obtained includes a pool of mRNA's, rRNA and small RNA's. rRNA generally comprises approximately 80 to 90% of total RNA. In order to ensure that a strong signal is obtained for mRNAs, the RNA population was enriched by the targeted removal of ribosomal RNAs using the **ribo-Zero rRNA depletion kit** (gram-negative bacteria) Magnetic kit by Illumina company catalog # MRZGN126, for replicas 2 and 3 and **MICROBExpress^{TM} Kit from Invitrogen catalog number : AM1905** from Thermal Fischer for replica 1.

2.8.D Sequencing

Alignment of counts to the PAO1-UW genome was performed by Oklahoma Medical Research Foundation, OMRF in Oklahoma City, Oklahoma resulting in a list of PAO1 genes with their corresponding number of reads.

2.9 RNA-Seq data normalization pipeline

Sequencing of trancript reads were done in the OMRF facility in Oklahoma City, Oklahoma using Illuminma. Counts were alligned to the PAO1 genome in order to obtain the number of reads for corresponding PAO1 genes processed at OMRF. These reads were then further processed for optimization of the signal to noise ratio.

2.9.A rRNA Exclusion

First, reads for rRNA were excluded in order to ensure that differences in rRNA reads across samples would not skew subsequent normalization of the data. rRNA genes that were excluded include the following: 16S rRNA (PA0668.1), PA0668.2, PA0668.3, 23S rRNA (PA0668.4), 23S rRNA (PA4280.2), PA4280.3, PA4280.4, 16S rRNA (PA4280.5), 23S rRNA (PA4690.2), PA4690.3, PA4690.4, 16S rRNA (PA4690.5), 23S rRNA (PA5369.2, PA5369.3, PA5369.4, 23S rRNA (PA5369.5).

2.9.B RPKMM calculation

Second, reads corresponding to PAO1 genes except rRNA genes, were converted to RPKMM values (Reads Per Kilobase per Million reads mapped). The extra M in this name denotes the removal of rRNA prior to RPKM calculation. The formula for the calculation of RPKMM is the following:

$$RPKMM = \frac{Read\ counts\ of\ transcript}{(gene\ length\ of\ transcript\ (Kb) * \sum all\ reads * 1x10\text{^}6)}$$ **Equation 2- 1 RPKMM calculation**

2.9.C Thresholding of noise

Third, thresholds were then applied to RNA reads as a means of filtering probable noise. This was needed due to the different sequencing depths between experiments (lower for replica 1). Genes having zero reads in either replicas 2 or 3 were removed from analysis and the resulting RPKMM list was indexed accordingly. In total, 117 genes having zero reads were removed.

2.9.D RPKMM averaging

Fourth, RPKMM values were averaged according to a conditional threshold on replica 1. Averaging was done on a conditional basis because replica 1 contained a significantly higher percentage of rRNA and therefore lower useable counts than replicas 2 or 3. A conditional cutoff was applied as <=1 for replica 1 in which the average RPKMM was calculated as either the sum of replicas 2 and 3 (when <=1), or the sum of all replicas (when >1).

2.9.E RPKMM ratios for each mutant

Lastly, ratios were determined as RPKMM of the sample/ RPKMM of WT in order to assess fold change values relative to each mutant.

2.10 RNA-Seq bioinformatic functions

All code, unless indicated, was written in house using the MATLAB R2017a platform [199].

2.10.A Hierarchical clustering

Clustering analysis was performed on the basis of hierarchical clustering. Hierarchical clustering generates clusters in a consecutive fashion from a set of datapoints based on proximity in space. At the beginning of clustering, each datapoint represents its own cluster. These clusters are then sequentially merged according to their similarity. Similarity is based on proximity of the objects in space [200].

The **city block method** was used in order to calculate the distance between the cluster or objects [201]. The *City block distance* between two points, *xs* and *xt*, with *n* dimensions is calculated as:

$$d_{st} = \sum_{j=1}^{n} |x_{sj} - x_{tj}|$$ **Equation 2- 2 City block distance**

Linkages establish how clusters are generated by defining the distance from a point or newly formed cluster to other clusters from the dataset. For our analysis, linkages of distances were established using the **average linkage method**. This is in contrast to other linkage methods such as single linkage (which links the closest distance of points in two adjacent clusters), or centroid linkage (which links by the distance of the centers of clusters). The average linkage method produces clusters with low within-cluster variance and similar sizes. Linkages are calculated as the average distances between all points within a cluster or object and another cluster or object.

When two objects, or clusters are considered the most similar based on linkages, they are merged to form a new cluster. Successive merging occurs until all points have been merged

into one large cluster. The results of the building of merges between objects is a hierarchical tree which can visualized in a dendrogram [202].

2.10.B Principle Component Analysis (PCA) with Cluster Analysis

Principle component analysis, or PCA, is a tool for dimension reduction of multivariate data while retaining trends and patterns. Thousands of dimensions can be reduced to a set of two or three, which contain most of the information from the original data set. This enables more intuitive visualization of large data sets.

PCA analysis linearly maps data using orthogonal transformation [203]. This mapping involves the projection of data onto principal components which are each, a single axis in space. Principle components are arranged orthogonally to one another eliminating redundancy of variables. Each principle component therefore, is a new variable generated by a linear combination of the original data. PCA ranks principle components based on having the greatest variance of projected data. This maximizes the information kept while reducing the number of dimensions. The first few principle components incorporates the majority of the original data, allowing a large number of variables to be interpreted in two to three dimensions.

PCA analysis (SVD method) was performed using MATLAB on data which overlaid data that was also clustered using the hierarchical clustering method with pdist set as city block and average in MATLAB properties as described in 2.3.A. Therefore, clusters could be visualized on the PCA plot relative to each other. This method of analysis allowed highlighting of statistically relevant outliers which correlated with differential gene expression.

Information regarding biological pathways was obtained from Kyoto Encyclopedia of Genes and Genomes (KEGG) [204], Virulence factor database (VFDB) [205], Pseudomonas Genome Database (Pseudomonas Genome Database (PseudoCAP)[206] [207] as well as other noted literature sources [104, 118, 121, 125, 155, 208-216]. A database was compiled of relevant pathways and used during the bioinformatic analysis.

2.10.C Violin and box plots

Violin plots with overlapping boxplots was generated using a modified script written by Bechtold, B. [217] which was run in MATLAB [199]. Violin plots overlaid with box plots indicate relative distributions of condensin mutant gene expression values as a log2 ratio (RPKMM sample/RPKMM WT). Red lines indicate 2 fold upregulation while green dashed lines indicate 2 fold downregulation. Box plots indicate the median value of each regulon as a central circle, the larger box portion indicates the 25^{th} and 75^{th} percentiles of gene distributions and the whiskers indicate QL + 1.5*QL and QL – 1.5*QL for the maximum and minimum respectively.

2.10.D Venn diagrams

Venn diagrams were generated using script written by Heil, J. [218] which was run in MATLAB.

2.10.E Elbow method (cluster optimization)

In order to separate the data into meaningful clusters, we estimated the optimal cluster number using the elbow method. The elbow method plots unexplained variance versus the postulated number of clusters. The elbow, or intersection point, indicates the point of lowest

unexplained variance (most compacted cluster) in which adding cluster numbers no longer has a significant effect on variance.

Script for the elbow method was written in MATLAB. The sum of square distances was calculated for each postulated cluster number up to 500 clusters. Each iteration calculated the square distances between individual datapoints and their designated centroids. These values were summed for each postulated cluster number and divided by the total sum of square distances for one cluster (representing the maximum unexplained variance). The unexplained variances for each cluster were then plotted against cluster number. Two lines were fitted against the data simultaneously, using linear regression analysis. The optimum cluster number was estimated as the determined elbow point of the two fitted lines.

Chapter 3: Physiological characterization of PA condensins

3.1 Introduction

Condensins are global regulators of gene expression (Chapter 4-1). Physiological studies on condensin deletion strains in PAO1 are in line with transcriptional analysis, showing opposite differentiation states where deletion of *smc* produced sessile biofilm growing cells and deletion of *mksB* produced planktonic growing cells with reduced biofilm formation [1]. Physiological studies in sections 3.2.B and 3.2.C in this chapter related to PAO1 have been previously published:

Zhao, H., Clevenger, A., Ritchey, J. W., Zgurskaya, H. I., & Rybenkov, V. V. (2016). *Pseudomonas aeruginosa* condensins support opposite differentiation states. *J Bacteriol*. doi:10.1128/JB.00448-16

Here, several parallel studies were performed in order to address the issue of complementation for *mksB* which revealed unexpected features regarding context dependence. In addition, we explored the roles that the PA condensins SMC-ScpAB and MksBEF have on PA14 cell physiology in order to determine the stability of phenotype across strains.

3.1.A Summary of PAO1 strains

Table 3- 1: Summary of PAO1 condensin mutant strains used in Section 3.2. *lacI^q-PT7* is an Isopropyl β-D-1-thiogalactopyranoside (IPTG) inducible promoter placed upstream of the *mksB* gene. Further details for strains are provided in Table 2 in the Appendix.

PAO1 Condensin Mutant Strains	Alternative names
lacI^q-P$_{T7}$-*mksB*	mks'
Δ*mksB*-P22-*mksB*	Δ*B*/p22-mksB
Δ*mksB*::*mksB*	Δ*B*::*B*
Δ*mksB*	Δ*B*
Δ*smc*	
Δ*mksB* Δ*smc*	Δ*B* Δ*smc* or ΔΔ
Δ*sspB*	
Δ*sspB* Δ*mksB*::*mksB*-DAS4	DAS4
ΔsspB ΔmksB::*mksB*-DAS4 -pUCP22-SspB	DAS4-pSspB
Δ*sspB* Δ*mksB*::*mksB*-DAS4 -pUCP22	DAS4-pUCP22
WT-pUCP22-SspB	WT-pSspB
mksB-E865Q	BEQ
mksB-S829R	BSR
mksB-D864A	BDA

3.2 Complementation of *mksB* reveals context dependence

3.2.A Conventional complementation tests reveal irrevocable alterations to the chromosome

Since the Δ*mkB* strain was found to be related to biofilm growth defects in both a physiological study as well as transcriptomic analysis [1] (Chapter 4), biofilm formation was used as a reporter for *mksB* phenotype. In order to test for complementation, the *mksB* gene was incorporated into a Δ*mkB* strain using several complementation strains and evaluated for its effect on biofilm formation. The complementation strains used included an IPTG inducible promoter upstream of *mksB* (*mks')* (Dr. Hang Zhao) , an IPTG inducible plasmid carrying *mksB* that was transformed into PAO1 Δ*B* (*PAO1* Δ*B*-P22-*mksB)* (Dr. Hang Zhao), and a knock-in *mksB* construct that was generated by inserting the *mksB* gene back onto the Δ*mksB* locus (PAO1 Δ*mksB::mksB*) (Figure 3-1). The *mks'* and PAO1 Δ*mksB*-P22-*mksB* strains expressed *mksB* in the presence of IPTG.

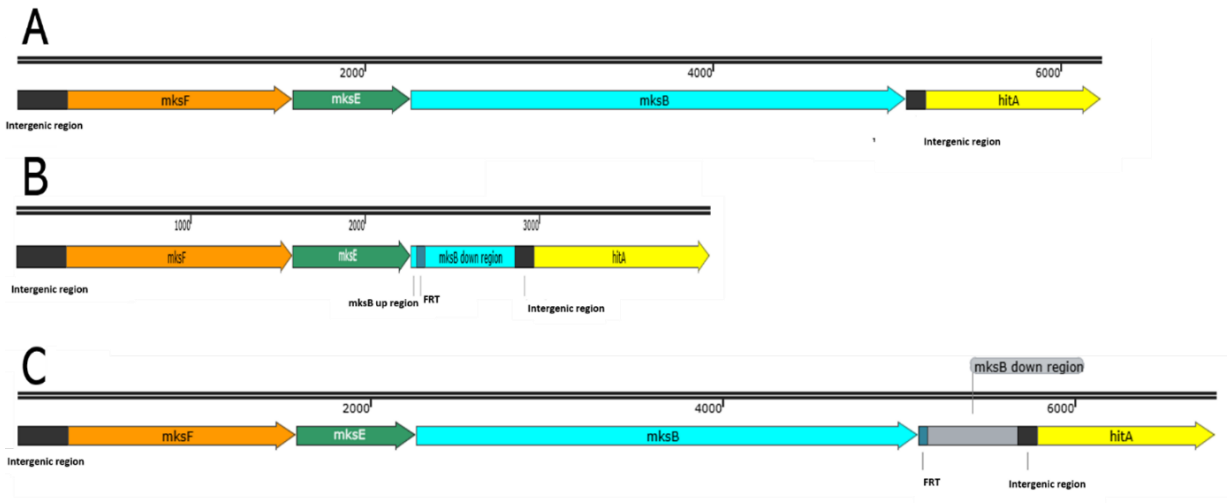

Figure 3- 1: *mksBEF* operon organization. The generation of PAO1 Δ*mksB*::*mksB* results in a FRT scar after removal of the FRT cassette as well as remnants of the *mksB* down region. (A) Full operon of *mksBEF* with no modifications to the chromosome (B) PAO1 Δ*mksB* showing an FRT scar flanked by the *mksB* up and down regions. (C) *mksB* knock-in construct PAO1 Δ*mksB*::*mksB* showing an FRT scar and residual *mksB* down region scar prior to the intergenic region.

Significant defects were observed for the Δ*B1 strain* as well as the PAO1 Δ*mksB*-P22-*mksB* (both with and without IPTG) and the knock-in strain (Figure 3-2), showing a lack of complementation of *mksB*.

This method can deduce if a link exists between MksB and biofilm formation with the condition that cis effects or secondary consequences of gene deletion do not impede complementation of *mksB*. In sections 3.2.B and 3.2.C, it is shown that *mskB* was complemented using both the degron system and ATPase point mutations. Therefore, the results here for conventional complementation tests show that a full *mksB* deletion and subsequent changes to cis or secondary effects resulted in irrevocable changes that could not be remediated with the incorporation of the *mksB* gene.

The *mks'* strain, both +/- IPTG, shows the same levels of biofilm formation as WT. This shows that there was not complete repression of *mksB* in *mks'* when the system was placed on the chromosome. This could be due to a possible leaky expression in the system which has been documented previously [219].

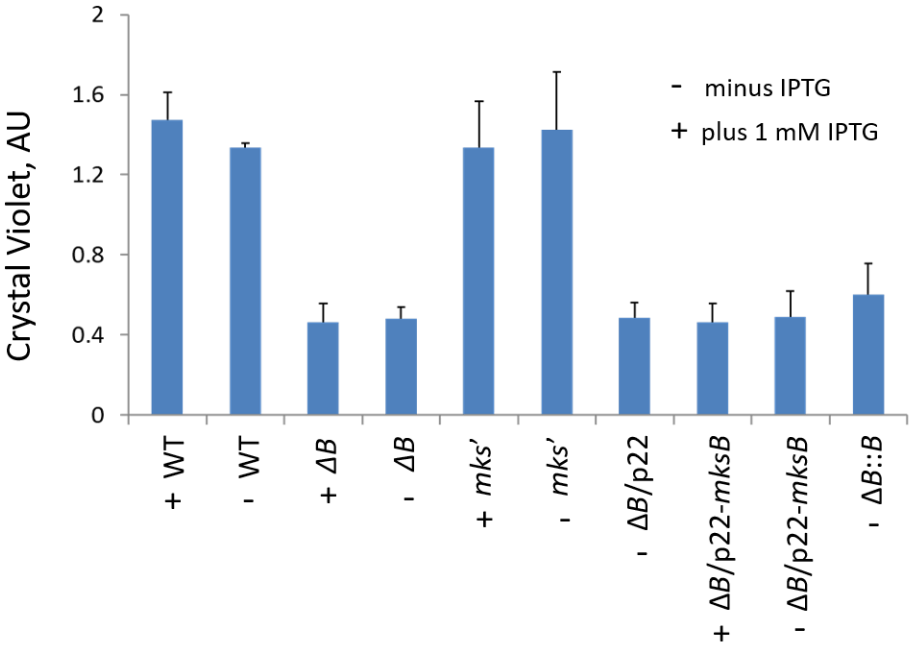

Figure 3- 2: Biofilm assay of PAO1 conventional complementation strains. Biofilm assay of WT, Δ*mksB* ΔGm (Δ*B*) (plus and minus IPTG), a lacI^{q}-P$_{T7}$ inducible promoter upstream of (*mks'*) (plus and minus IPTG), IPTG inducible plasmids (pUCP22) carrying *mksB* transformed into PAO1 Δ*B* (Δ*B*/p22, Δ*B*/p22-*mksB*, (Δ*B*/p22-*mksB*) and a knock-in *mksB* construct which inserted the *mksB* gene onto the Δ*mksB* locus (Δ*B::B*).

3.2.B A link between MksB and biofilm formation is confirmed using the degron system

On account of possible cis or secondary effects, complementation for *mksB* was tested using the degron system (Figure 3-3). The degron system incorporates a Das4 tag attached to the C-terminus of the protein which is recognized by the ClpXP mediated degradation system. The protein is degraded post-translationally, allowing an advantage in that it can bypass genetic

constraints. The control of degradation occurs because the Das-4 tag is optimized for binding to ClpXP in the presence of SspB. Therefore, generation of a system in which SspB presence is inducible, allows control of *mksB* degradation.

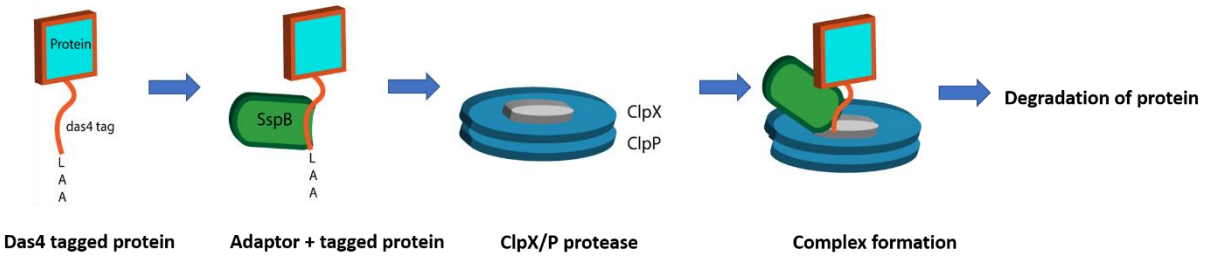

Figure 3- 3: Schematic for steps in the degron system of protein degradation. The protein of interest is tagged with a Das4 tag specific which is specific to the adaptor SspB protein. The adaptor and tagged protein combined with the ClpX/P protease to form a complex which leads to degradation of the tagged protein.

To set up the degron system for *mksB*, we first removed the gene for the protease adapter protein, *sspB* from PAO1 WT. The *mksB* gene was then replaced with a *mksB* gene containing a C-terminal Das4 tag. This tagged protein was affectively targeted for protease degradation in the presence of a plasmid that contains pUCP22-SspB (pSspB). pSspB was incorporated into the PAO1 Δ*sspB* Δ*mksB::mksB*-DAS4 strain using electroporation. A control strain was generated which incorporated an empty pUCP22 vector into PAO1 Δ*sspB* *mksB*::*mksB*-DAS4. Expression levels show a depletion of *mksB* in cells that express the plasmid pSspB, but not in the WT strain (Figure 3-4 A).

The biofilm assay shows that when *mksB* is absent, there are major defects in biofilm formation (Figure 3-4 B). All controls which include MksB including WT, WT-pSspB + Ara, and

PAO1 Δ*mksB*::*mksB*-Das4-pUCP22 + Ara show the same level of biofilm formation as WT. When the degron system is introduced and turned on, these levels drop significantly back down to that of Δ*mksB,* implicating *mksB* in biofilm growth.

Because the cell physiology changes in response to the production of the SspB protein, we conclude that the presence of MksB is linked with biofilm formation. Since MksB is associated with biofilm formation, yet the incorporation of *mksB* into PAO1 Δ*mksB* was not able to complement the phenotype, it can also be deduced that the deletion of *mksB* changed cis or secondary effects which resulted in irrevocable chromosomal changes.

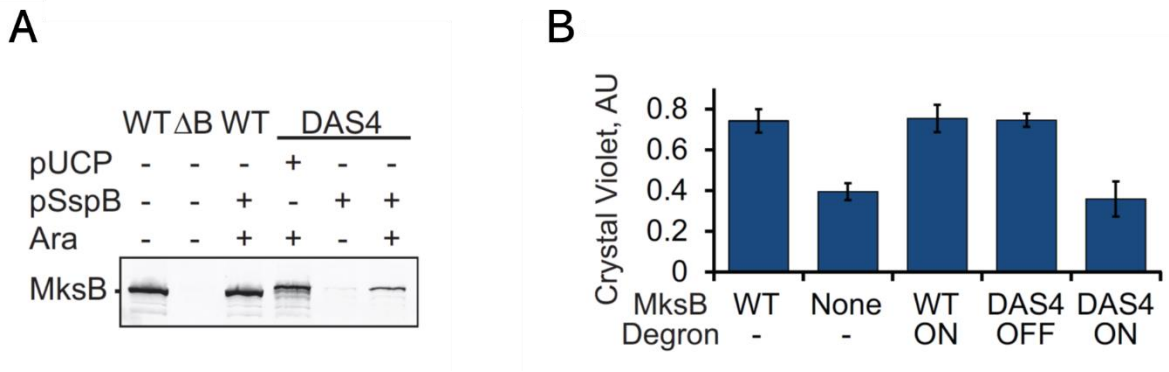

Figure 3- 4: Biofilm formation defects. (A) Depletion of MksB using the degron system. DAS4-tagged but not wild-type MksB is depleted in cells that express plasmid-encoded SspB (pSspB) as determined using immunoblotting. (B) Inducible depletion of MksB impairs biofilm formation. Biofilm formation (+/-SD; n=3) was measured for PAO1 WT, Δ*mksB* (none), or Δ*sspB mksB*::*mksB*-DAS4 (DAS4) cells that were transformed with the pUCP22 (OFF) or pSspB (ON) plasmid.

3.2.C The association of MksB with biofilm formation is dependent on conformation, not ATP turnover

ATP is essential for the function of condensins. The binding and hydrolysis of ATP is what modulates the opening and closing of the overall SMC protein. In order to gain insight into the role that ATPase activity plays on *mksB* function as well as providing an alternative method for complementation, we generated point mutations in the ATPase head domain of *mksB*. Point mutations result in the expression of MksB which are locked into specific intermediates in the ATPase cycle. This method gives insight into the role that ATPase activity plays on *mksB* function without introducing detrimental effects caused by a full *mksB* deletion.

Three types of *mksB* ATPase mutants were generated (Figure 3-5 A). The first is a D864A mutant in the Walker B region. This mutation prevents ATP binding and therefore, prevents dimerization of the SMC heads [2]. The second mutant included E864Q in the walker B region [3]. This mutant prevents ATP hydrolysis, but allows ATP binding which stabilizes the dimeric SMC heads. The third mutant included S829R in the C motif. This mutant interferes with head dimerization but allows ATP binding [185]. All of these mutations interfere with the dimerization of the SMC heads. These mutants were found to be expressed at normal levels (Figure 3-5 B).

Overall, two out of the three ATPase mutants including E864Q and S829R showed similar defects in biofilm as that of Δ*mksB* for biofilm formation (Figure 3-5 C). One of the mutants, D864A, however did not show any effect and had the same level of biofilm formation as that of WT. These results show that specific ATPase intermediates are essential for the function of *mksB* in the case of E864Q and S829R and that the D864A mutant results in an intermediate

that can still perform the regulatory function of MksB. Interestingly, this shows that MksB intermediate conformations rather than ATPase activity, are relevant for the regulatory function of MksB.

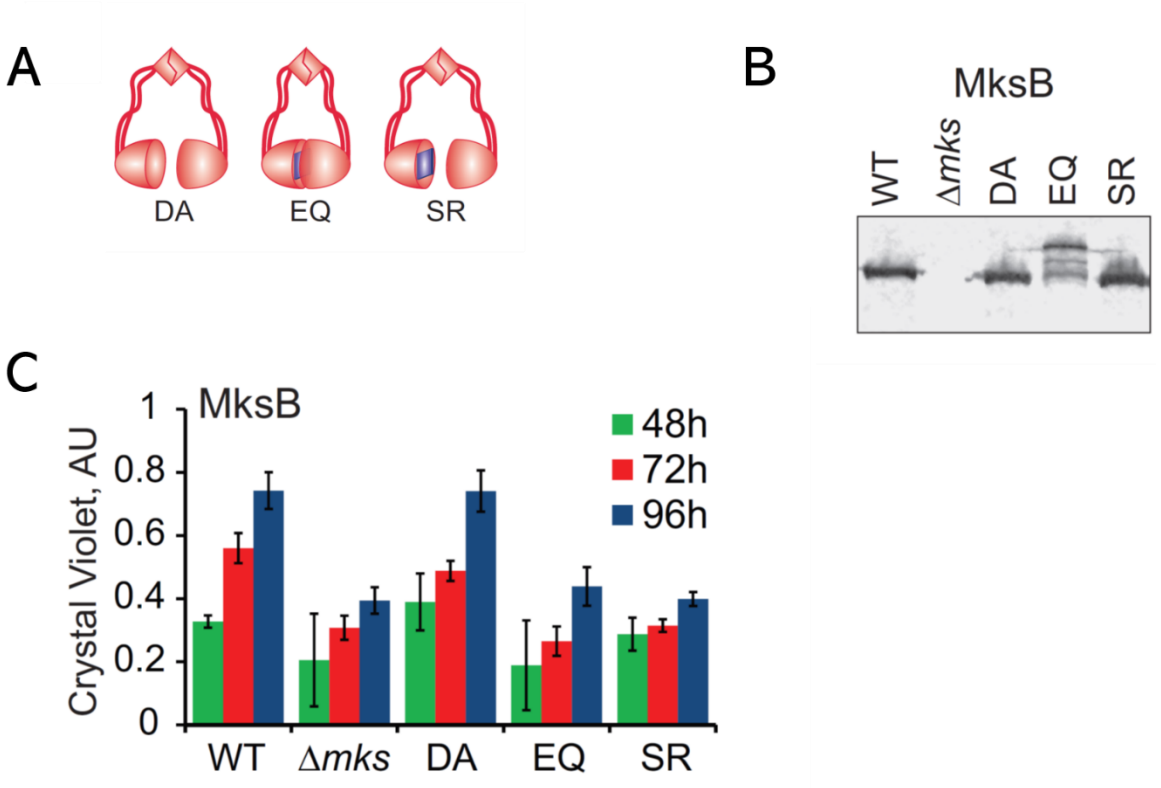

Figure 3- 5: Biofilm formation of MskB ATPase mutants. (A) Effects of ATPase mutations on the conformation of condensins. (B) Immunoblot analysis of expression levels for the tested mutants. (G) Biofilm formation by the indicated ATPase or deletion *mksB* mutants (+/- SD, n=6). Note formation of oligomers by MksBEQ, which is consistent with head disengagement defects expected for this mutant [1].

3.3 Condensin phenotypes are strain specific

PA14 has two copies of MksBEF, MksBEF1 and MksBEF2 in addition to SMC-ScpAB. Not much is known about this second copy of MksBEF. Because there are multiple versions of condensins, we hypothesized that the different versions play a specialized role in PA14 which possibly contribute to different lifestyle states as seen in PAO1. In order to analyze the role of condensins in PA14, several strains were generated which incorporated condensin deletions (Table 3-1). The *lacI*^{q}-P$_{T7}$ promoter was used in strains in order to replace the original promoter upstream of the *mksB2* gene for its controlled expression using IPTG. Deletions were generated using the allelic replacement method with the pEX-Δ*mksB1* [1] and pEX-Δ*smc* plasmids [27] and the pEX-Δ*mksB2* and pEX-Δ*G* plasmids. Strains were confirmed by PCR and/or sequencing (Figures 2-5 to 2-7).

Table 3- 2: Summary of PA14 condensin mutant strains used in section 3.3. Strains are named in the order that genes were deleted/modified. *lacI^q-P$_{T7}$,* is an Isopropyl β-D-1-thiogalactopyranoside (IPTG) inducible promoter system placed upstream of *mksB2*. Each condensin mutant listed below includes both a GmR strain (containing a gentamicin resistance marker flanked by an FRT cassette) and a ΔGm strain (gentamicin marker removed). Strains which include the GmR FRT cassette are always denoted as GmR. Further details for strains are provided in Table 2 in the Appendix.

PA14 Condensin Mutant Strains	Alternative names
lacI^q-P$_{T7}$-mksBEF2	*lacB2*
lacI^q-P$_{T7}$-mksBEF2 Δsmc	*lacB2 Δsmc*
lacI^q-P$_{T7}$-mksBEF2 ΔmksB1	*lacB2 ΔB1*
lacI^q-P$_{T7}$-*mksBEF2 ΔmksB1 Δsmc*	*lacB2 ΔmksB1 Δsmc*
ΔmksB2	*ΔB2*
ΔmksB1	*ΔB1*
Δsmc	
ΔmksB2 ΔmksB1	*ΔB2 ΔB1*
ΔmksB1 ΔmksB2	*ΔB1 ΔB2*
Δsmc ΔmksB2	*Δsmc ΔB2*
Δsmc ΔmksB1	*Δsmc ΔB1*
ΔmksB1 ΔmksB2 Δsmc	*ΔΔΔ*
ΔmksB2 ΔmksG	*ΔB2 ΔG*

3.3.A PA14 Condensin mutants show minor defects in biofilm formation

To test if condensins had any effect on biofilm growth, as was seen in PAO1, we grew cells in PVC well plates for 72 hours in M9 media supplemented with 0.4% glycerol. Cells that

grew biofilms adhered to the sides of the PVC well. Therefore, to quantify relative amounts of biofilm growth, the cells were stained with 0.1% crystal violet and measured for OD_{600}. Each sample was done in triplicate. Some slight reductions in biofilm were seen for the PA14 Δ*smc*, PA14 Δ*mksB2,* PA14 Δ*mksB1* Δ*smc* and the triple knock out PA14 Δ*mksB1* Δ*smc* Δ*mksB2*, with the largest reduction for PA14 Δ*mksB2* (Figure 3-6). All of these reductions, however, were within error bars of WT indicating they were not significantly changed. Therefore, the regulation of biofilm formation by MksB is unique to PAO1.

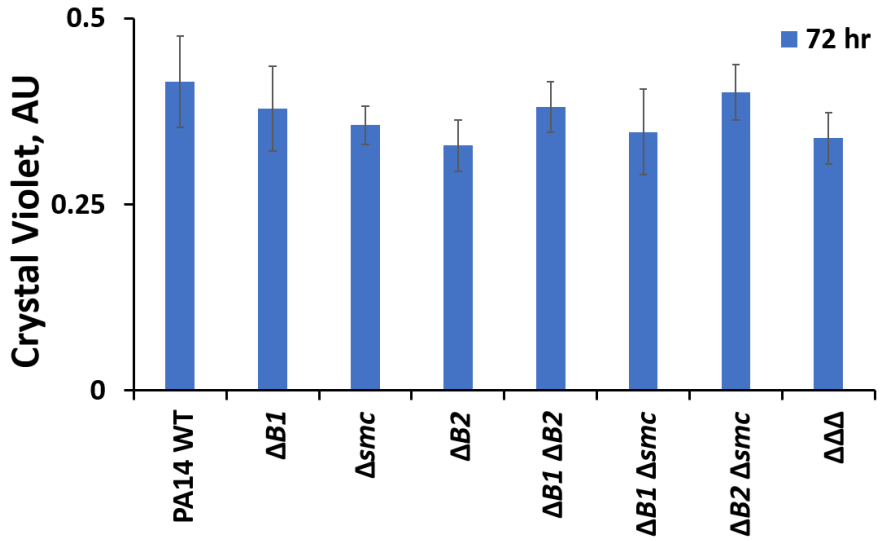

Figure 3- 6: Biofilm formation of PA14 deletion mutants. Cells were grown at 37°C for 72 hours. ΔΔΔ denotes Δ*mksB1* Δ*mksB2* Δ*smc*.

3.3.B PA14 condensin mutants exhibit growth and cellular fitness on par with WT

Condensins play a role in lifestyle states in PAO1 where each condensin contributes to

opposite physiological states. To test the role that condensins have in the PA14 strain, growth curves in planktonic media, growth on solid media, biofilm formation and competition growth were analyzed. For growth in planktonic medium, cells were grown in LB media at 37°C and checked for OD_{600} at the indicated time points. No changes from WT are seen for any of the mutants (Figure 3-7 A). For colony growth, CFU/OD was calculated for each mutant. These results were done in triplicate (Figure 3-7 B). Overall, no major deviations were seen between the mutants (CFU/OD). This shows that condensin mutants are nearly identical to WT with no significant defects.

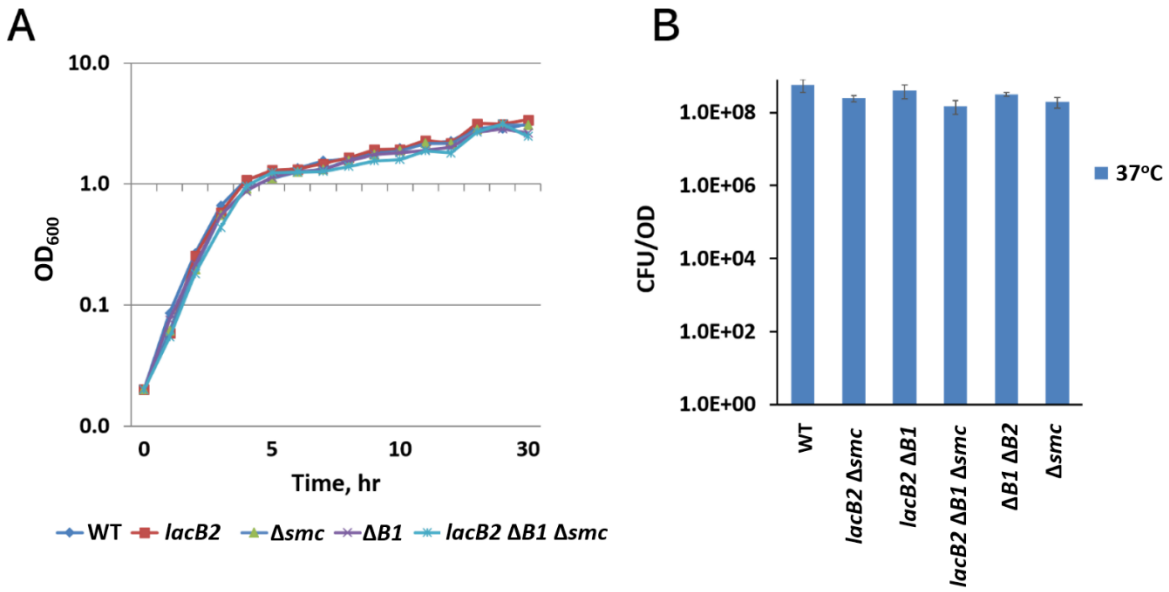

Figure 3- 7: Growth of PA14 condensin mutants. (A) Growth curve at 37°C in LB medium while shaking for the indicated condensin mutants. (B) Growth on solid LB agar plates for indicated mutants over night at 37°C. Colonies were counted and normalized to OD.

3.3.C Competitive growth of PA14 condensin mutants against WT result in slight strain losses

The competitive growth assay compares the cellular fitness of a particular strain against another. For our purpose, we compared condensin deletions against WT. Each mutant strain contained the gentamicin resistance marker. Cells were mixed at a 1:1 ratio, then inoculated into fresh LB medium and grown at 37°C with dilutions every 8 hours. Aliquots at each time interval were plated onto LB and LB plus gentamicin plates. Mutant cells were determined by the number of colonies on the gentamicin plate and the total number of cells were determined on the LB only plate and their CFU/OD calculated. The strain loss rate was calculated by fitting the data to its rate for single exponential decay.

All mutant strains showed some degree of strain loss rate. The results show a slightly higher strain loss rate for *lacB2* Δ*B1* with 0.5 mM IPTG (Figure 3-8). These values are significantly smaller than the effect seen in PAO1 which showed a strain loss rate for Δ*smc* at 0.4 [1], comparing to the highest result in PA14 at 0.025 for *lacB2* Δ*smc*. Overall, we see a small effect from condensin inactivation. Competition growth done less frequent dilutions including 12 and 24 hours resulted in no change. Also, when strains were grown individually, no change was seen. This result is apparent only when cells are growing during exponential phase and in the presence of WT. This indicates that cells are not sick by themselves but are slightly affected in growth in the presence of WT.

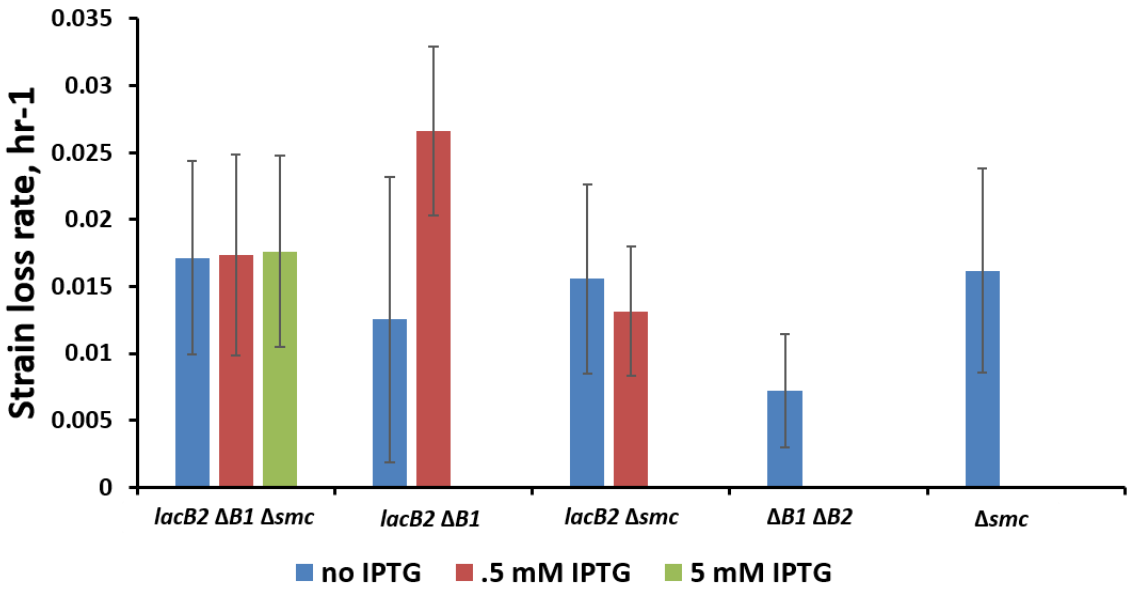

Figure 3- 8: Strain loss rate of competition growth for PA14 condensin mutants versus WT. Strain loss rate for competition growth of PA14 condensin mutants versus PA14 WT for the indicated strains. Cells were diluted into fresh LB media every 8 hours for 48 hours. Slopes for strain loss were calculated for each strain.

3.3.D A low frequency of anucleate cells is observed in condensin mutants

To test if condensin inactivation in PA14 affected chromosome compaction, we looked at the frequency of anucleate cells. Improper chromosome compaction yields one cell with unseparated DNA and the other cell lacking DNA entirely (anucleate). In order to analyze the frequency of anucleate cells, bacteria were grown in LB or M9 supplemented with 0.4 % glycerol as indicated.

Proteins were stained with Sypro-Orange and DNA with DAPI to allow visualization and distinction between DNA and the rest of the cell. Cells were counted as a total as well as the number of anucleate cells for each of the condensin deletion strains having a PA14 *lacI*^{q}-P_{T7}-

mksB2 background. The results show that very few cells were anucleate with a maximum of 3/909 or 0.3% for the *lacB2* Δ*B1* Δ*smc* strain and a single anucleate cell for the other strains (Figure 3-9). PA14 cells faired significantly well despite the inactivation of condensins.

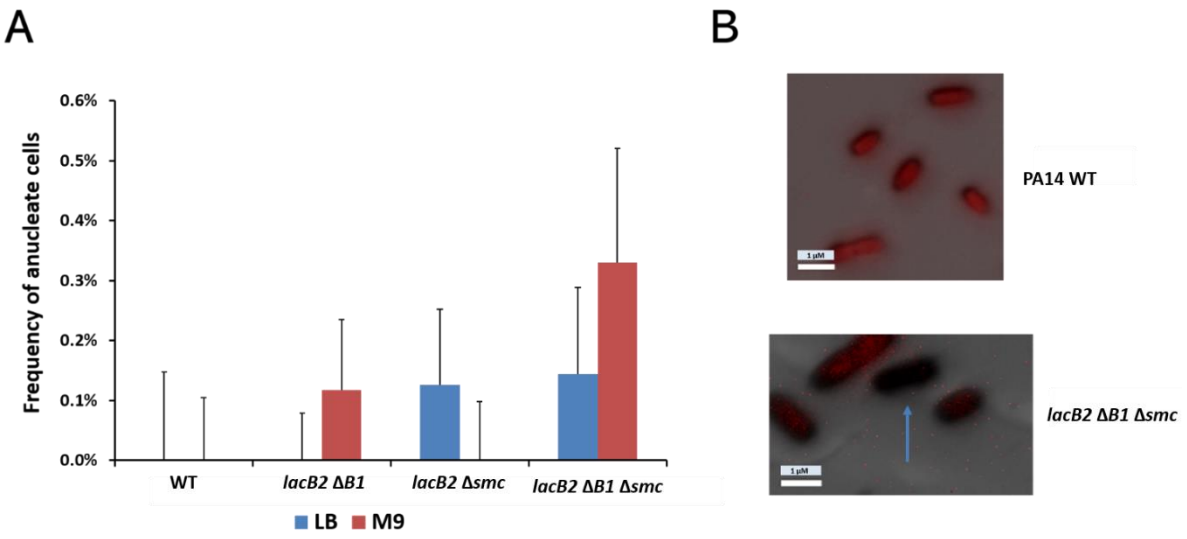

Figure 3- 9: Frequency of anucleate cells of PA14 condensin mutants. Cell were grown in LB and M9 at 37°C.

3.3.E Effect of antibiotics on growth

3.3.E.1 Antibiotic susceptibility is unchanged in PA14 mutants relative to WT

Minimal inhibitory concentration analysis of several antibiotics was tested on PA14 condensin deletions strains derived from a PA14 *lacB2* parent strain grown at 37°C in LB medium overnight (Table 3-3). These antibiotics have a range of targets including the ribosome, DNA gyrase, DNA, and the cell wall. The indicated minimum concentrations that inhibited growth in µg/ml are indicated for each strain. Results were done in duplicate. No changes

occurred that were greater than 2 fold relative to WT. Condensins, therefore, show no impact on drug susceptibility.

Table 3- 3: Minimal inhibitory concentration results. Table showing antibiotics and their effect on PA14 condensin mutants with a *lacB2* background

Target	Drug µg/ml	PA14 WT	*lacB2*	*lacB2 ΔB1*	*lacB2 Δsmc*	*lacB2 ΔB1 Δsmc*
Ribosome	Streptomycin	8 to 16	8 to 16	8 to 16	16	8
Ribosome	Kanamycin	62.5	62.5	62.5	62.5	62.5
Ribosome	Gentamicin	1 to 2	1	1	1	1
Ribosome	Chloramphenicol	4	4	4	4	4
Ribosome	Spectinomycin	500	500	500	500	500
DNA	Ethidium Bromide	2000	2000	2000	2000	2000
DNA	Mitomycin-C	2 to 4	2 to 4	2 to 4	4	2 to 4
DNA gyrase	Norfloxacin	0.5	0.5	0.5	0.5	0.5
cell wall formation	Carbenicillin	62.5 to 125	125	125	125	62.5
cell wall formation	Vancomycin	2000	2000	2000	2000	2000

3.3.E.2 Persister cell formation of condensin mutants is similar to WT

Persister cells are a morphotype in a small subpopulation in bacteria which allow survival in hostile environments. These persister cells can form prior to antibiotic or as a response to it. Typically, they are associated with slower growth which allows them to evade drug treatment

This mode of growth provides opportunities for multidrug tolerance and plays a major role during chronic infections.

In order to test the formation of persister cells and their variation among the generated condensin deletions, gentamicin, norfloxacin and streptomycin, were tested at 4x and 64 x concentrations greater than MIC concentration for a one hour and spot plated onto LB agar plates to determine colony growth at CFU/OD (Figure 3-10). The 64x concentration for gentamicin and streptomycin did not grow colonies. For gentamicin, additional testing was done on 12x and 20x concentrations. All mutant strains and WT showed decreased colony growth after the indicated treatments with antibiotics. Overall, no major variation was seen between WT or any of the condensin mutants indicating no major alterations occurred to persister cell formation on account of the inactivation of condensins.

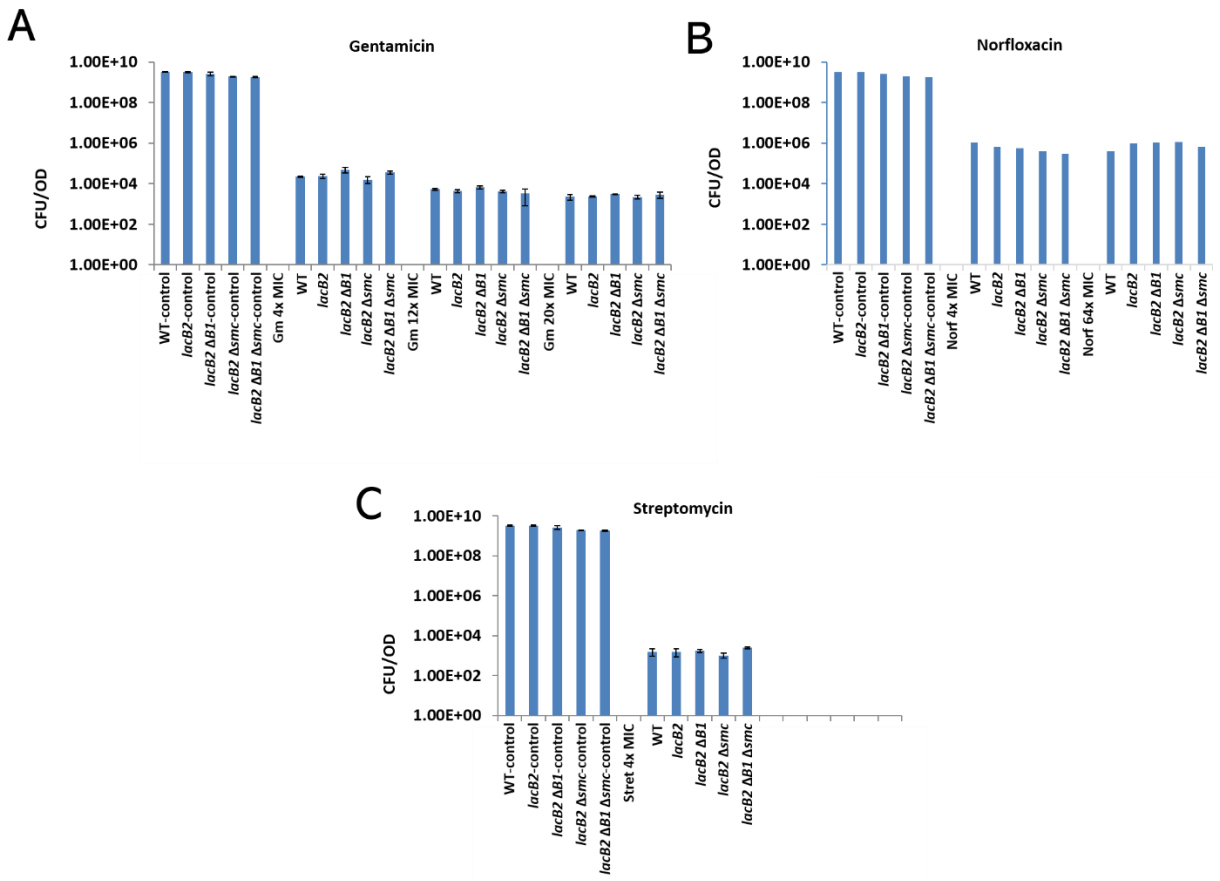

Figure 3- 10: CFU/OD of persister cell formation. Gentamicin, norfloxacin, and streptomycin at the indicated concentrations (either 4x, 12x, 20x, 64x relative to MIC) and were added to the indicated PA14 condensin mutants with a *lacB2* background for 1 hour at 37°C while shaking.

3.3.F Pigment production changes in PA14 condensin strains

During the generation of condensin deletion strains, pigment changes were observed for the PA14 Δ*B1* Δ*B2*::ΔGm *and PA14* Δ*B1* Δ*B2* Δ*smc*::ΔGm strains. Pigment production in *Pseudomonas aeruginosa* results from pyocyanin, seen as a bluish green color, and pyoverdine, seen as a greenish yellow (Figure 3-11). These pigments have been implicated in virulence and quorum sensing systems in PA. Here, we looked at the relative amount of pyocyanin and

pyoverdine production (Figures 3-12 and 3-13). Overall, the results show a significant decrease in pigment production, in particular for pyocyanin for cells that were grown at 37°C while shaking.

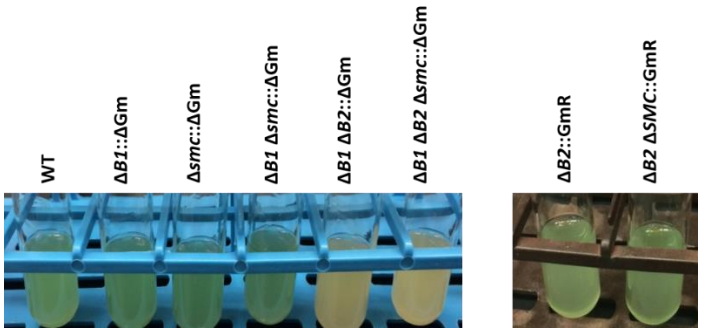

Figure 3- 11: Condensin mutant strains grown at 37°C while shaking for 16 hours.

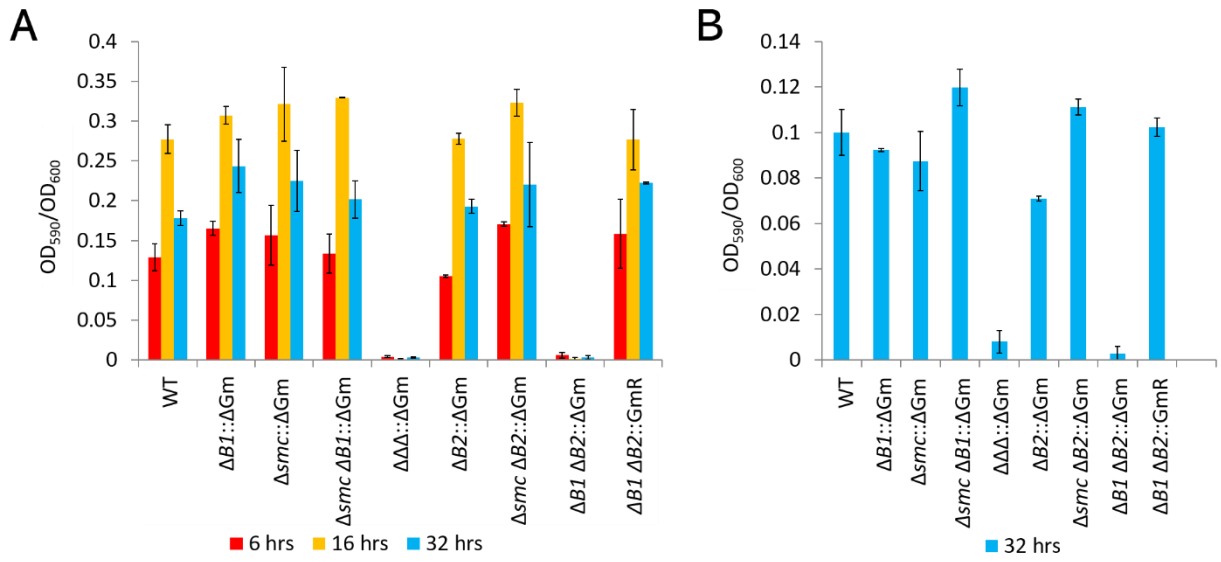

Figure 3- 12: Quantification of pyocyanin production in PA14. ΔΔΔ is the triple condensin mutant Δ*B2* Δ*B1* Δ*smc*. (A) Cells grown at 37°C while shaking for 6,16 and 32 hours. (B) Cells grown at 37°C no shaking for 32 hours.

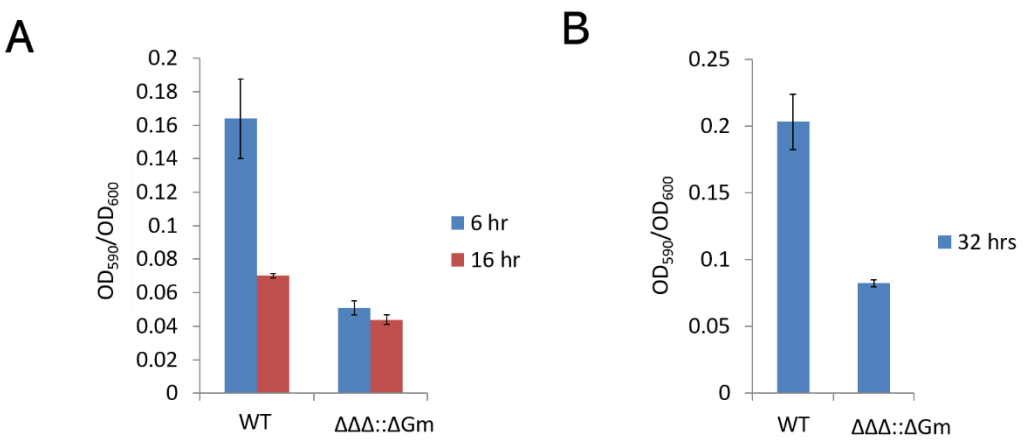

Figure 3- 13: Quantification of pyoverdine production in PA14. ΔΔΔ is the triple condensin mutant Δ*B2* Δ*B1* Δ*smc*. (A) Cells grown at 37°C while shaking for 6, and 16 hours. (B) Cells grown at 37°C no shaking for 32 hours.

In construction of the strains, Δ*B1* was deleted first, followed by Δ*B2* and then Δ*smc.* Δ*B1* Δ*B2*::GmR is green showing pyocyanin production while Δ*B1* Δ*B2*::ΔGm is yellow, indicating that the phenotypic change occurred during recombination while removing the gentamicin cassette. This indicates possible downstream polar effects after the removal of the GmR promoter. Since *mksG* is part of the *mksBEF2* operon and found directly downstream of *mksB2*, we hypothesized that removal of the gentamicin gene, may have blocked *mksG* expression after removal of the GmR promoter, possibly resulting in pigment change.

In order to assess if this phenotype is linked to *mksB2* and *mksG*, we generated a Δ*B2* Δ*G*::GmR strain to test its effect on pigment change. The results show that this strain maintained a green pigment (pyocyanin production) (Figure 3-14), indicating that *mksG* in the Δ*mksB2* background cannot alter pigment production. In line with this, a Δ*B2*::ΔGm strain also resulted in no pigment change.

However, other combinations of mutants were able to alter phenotype. In order to see if polar effects from a Δ*B1 and* Δ*B2*::ΔGm background were consistent, a second strain, Δ*B2* Δ*B1*::ΔGm was generated from a Δ*B2*::ΔGm parental strain. This is in contrast to the Δ*mksB1* Δ*B2::*ΔGmR showing green pigment which was generated from a Δ*B1*::ΔGm parental strain. The Δ*B2* Δ*B1*::GmR strain interestingly showed a change from green to yellow pigment (Figure 3-14).

Therefore, strains having a background of Δ*B1* combined with Δ*B2*::ΔGm resulted in pigment changes from green to yellow (reduced pyocyanin) indicating a possible association with this combination of mutations. These results show that Δ*B1* and Δ*B2* in combination with possible downstream polar effects resulted in pigment change. In order to fully elucidate if *mksG* is a contributor to this phenotype further studies will be necessary for deleting *mksG* in combination with both *mksB1* and *mksB2*.

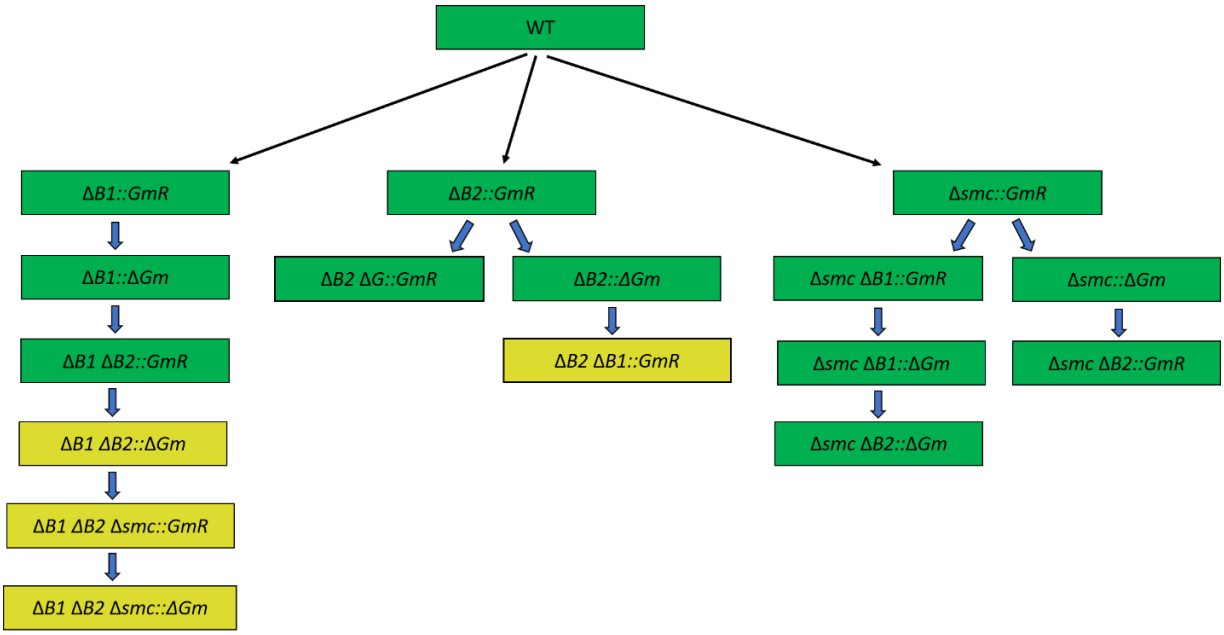

Figure 3- 14: PA14 generated strains and their resulting pigments. Cells were grown at 37°C with shaking and their resulting pigments.

Chapter 4: Transcriptomic analysis of PAO1 condensin mutants

4.1 Introduction

Physiological assays on PAO1 condensins revealed opposite differentiation states and a role in PA virulence [1]. Here, the regulatory role of PAO1 condensins was determined by transcriptomic analysis of condensin mutants using RNA-Seq which incorporates next-generation deep sequencing technology. To this end, we collected cells from our condensin mutant samples and PAO1 WT grown in exponential phase for RNA isolation and sequencing. RNA-Seq data was optimized to reduce noise using thresholds across samples. PCA analysis was performed based on hierarchical clustering of expression data. Integration of pathway information during clustering analysis highlighted major affected pathways for differentially expressed genes. Expression data for these pathways were further analyzed and compared across samples in order to derive transcriptomic profiles for each condensin mutant.

4.2 Removal of noise using thresholding

RNA was isolated from condensin mutant samples and PAO1 WT during the exponential phase of cell growth, sent for processing at the OMRF facility in Oklahoma City where it was sequenced using Illumina. The resulting transcript counts were further processed in the OMRF facility by allignment with the PAO1 genome resulting in the number of reads corresponding to each PAO1 gene. Experiment 1, which included the first replica (WT, Δ*smc* and ΔΔ) contained an average of 82% rRNA. Therefore, rRNA was first excluded from all replicas before further processing. RPKMM values (reads per thousand million excluding rRNA) were calculated using

the formula described in section 2.9.B. Reads were further processed in house for noise as described above.

The final plots after thresholding for noise for WT is shown in Figure 4-1. After thresholding, we see that the noise is reasonable (removal of straight lines at -1 (log2 of zero), and that most of the genes are equally expressed. Following noise thresholding, pair-wise comparisons were made as scatter plots of log2 average RPKMM values (Figure 4-2). These plots indicate that most genes have the same level of expression as evidenced by the fact that they lie mostly on the diagonal line over a long range. The diagonal line is where we expect no change between the two samples. There is a group of genes that are not equally expressed. These particular genes are more probable to be differentially expressed genes the further they are located away from the diagonal, a line indicating no change in expression. These are particularly likely to be differentially expressed for higher value RPKMM values in which noise becomes less likely a factor.

RPKMM values were then averaged according to the method described in section 2.9.D. and calculated for the corresponding ratios determined as RPKMM sample/RPKMM WT (fold changes) relative to each mutant.

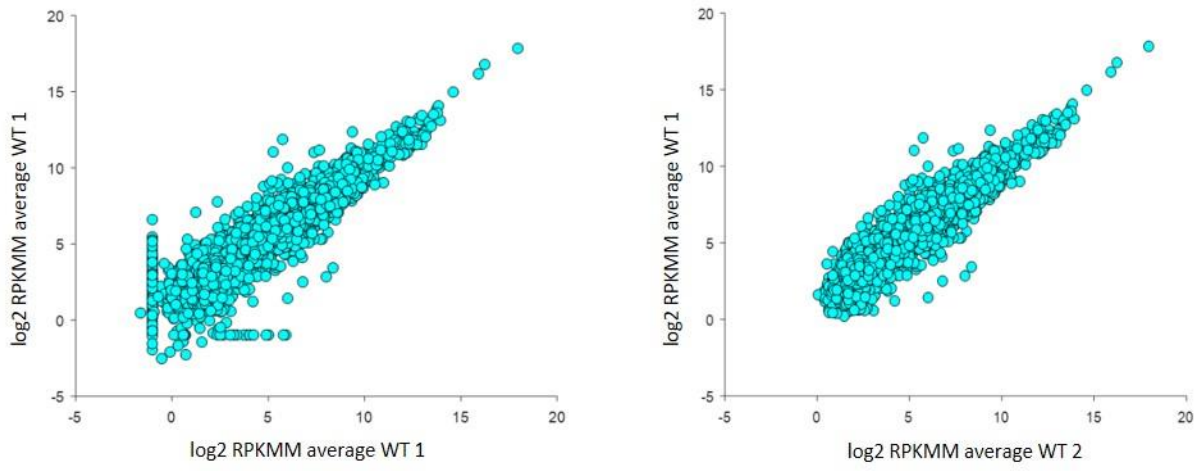

Figure 4- 1: Scatter plots of WT replica 1 vs WT replica 2. Plot with no threshold (left) and with threshold (right).

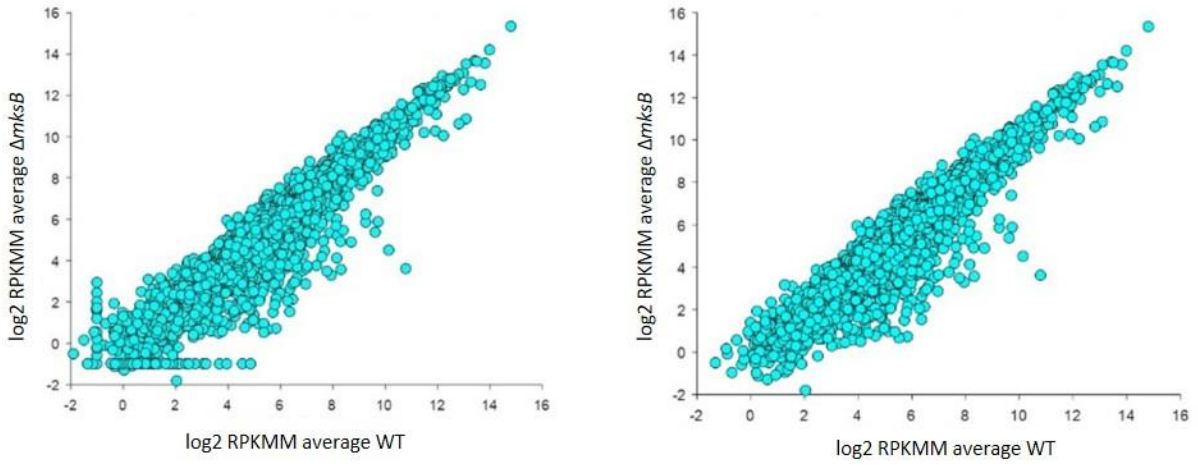

Figure 4- 2: Scatter plots of WT replica 1 vs *mksB* replica 1. Plot with no threshold (left) and with threshold (right)

4.3 Δ*smc*, Δ*mksB*, and Δ*smc* Δ*mksB* display distinct patterns of regulation

Differentially expressed genes for Δ*smc*, Δ*mksB* and Δ*smc* Δ*mksB* (ΔΔ*)* were determined as ratios of RPKMM values relative to PAO1 WT at a 2 fold threshold. Of the 5666 genes in PA, 612 genes were differentially upregulated and 645 were downregulated. However, a subset of differentially expressed genes was found to be unique for each condensin mutant.

Venn diagrams generated for differentially expressed genes showed that there is little overlap between condensin mutants for upregulated genes (Figure 4-3). 157 PAO1 Δ*smc* genes that were upregulated shared 6 genes with PAO1 Δ*mksB*, 25 with ΔΔ and only 7 with all three mutants. PAO1 Δ*mksB* showed 73 upregulated genes, sharing 12 of those with ΔΔ. 439 ΔΔ upregulated genes were found total. Overall, differentially expressed genes were found to be uniquely expressed for the individual mutants rather than overlapped. It is interesting that the ΔΔ mutant is actually different than either single mutant implying little synergystic effect for upregulated genes.

In contrast, downregulated genes showed much more overlap for differentially expressed genes between the PAO1 Δ*mksB* and PAO1 ΔΔ samples. Of the 512 PAO1 Δ*mksB* downregulated genes, 137 overlapped with PAO1 ΔΔ 15 with PAO1 Δ*smc* and 15 with all three mutants. For the PAO1 ΔΔ downregulated genes, only 1 was overlapped with PAO1 Δ*smc*. *PAO1* Δ*smc* showed 126 total downregulated genes. Overall, downregulated genes resulted in significant overlap between the PAO1 ΔΔ and PAO1 Δ*mksB* mutants, whereas PAO1 Δ*smc* remained differentiated for both up and downregulated genes. This indicates that ΔΔ is responsive to *mksB* for downregulated genes. In contrast, PAO1 Δ*smc* is completely

independent from PAO1 ΔΔ and PAO1 Δ*mksB* for both up and downregulated genes. This indicates that Δ*smc* has its own regulatory realms, while ΔΔ and Δ*mksB* share many regulatory pathways for downregulation.

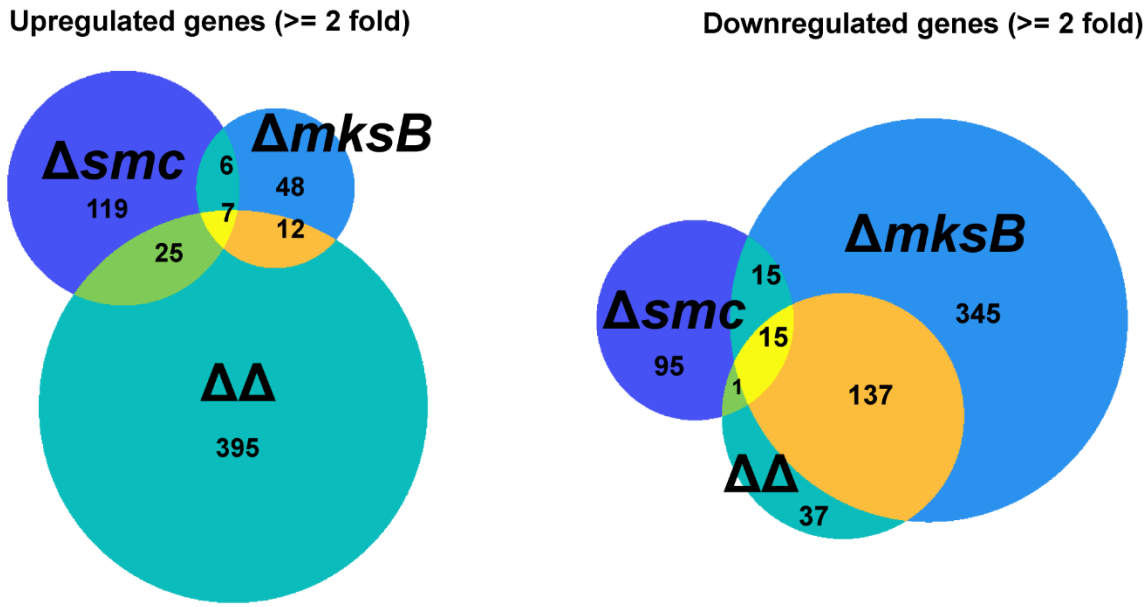

Figure 4- 3: Venn diagram of signficiant genes for condensin strains. Left: upregulated, right: downregulated.

Principle Component analysis, or PCA, was used to analyze fold change values (log2 RPKMM ratio) for 5484 genes for each PAO1 condensin mutant, a reflection of the total gene base. The results (Figure 4-4) show that PAO1 Δ*smc,* PAO1 Δ*mksB*, and PAO1 ΔΔ are opposite to one another along the first and second principle components (WT is located at 0,0). Therefore, alignment of any one particular sample to another sample was not seen, indicating overall distinct differences in their transcriptional profiles.

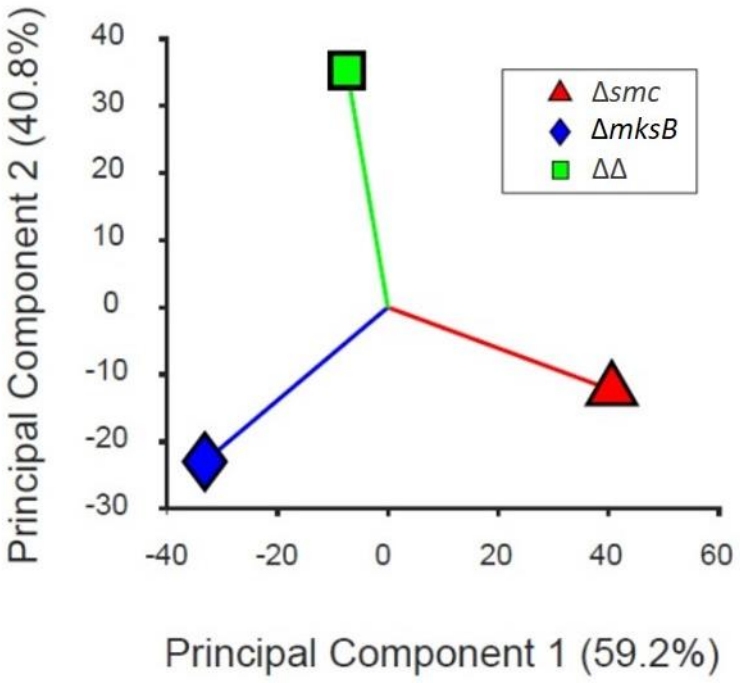

Figure 4- 4: PCA analysis of Δ*smc*, Δ*mksB* and ΔΔ. Reduced dimensions of genes into a single point.

4.4 Hierarchical clustering highlights statistically relevant gene groups

Hierarchical clustering was performed as described in section 2.3.A. This method highlights differentially expressed genes based on the statistical separation of datapoints based on log2 fold change values using the city block p-dist (Equation 2-2) and average linkage methods. The resulting dendrogram and accompanying heat map are found in Figure 4-5.

The heatmap presents differentially expressed genes that are upregulated above 1.5 fold change as red and downregulated as green, black for unchanged. The dendrogram based on each sample indicates a separation between Δ*smc* and the other two mutants Δ*mksB* and ΔΔ. A corresponding dendrogram based on individual genes shows that the majority of the

genes are within one larger group indicated by the fact that most nodes are found after an early split at the top. Outlier clusters can be found prior to this major node split.

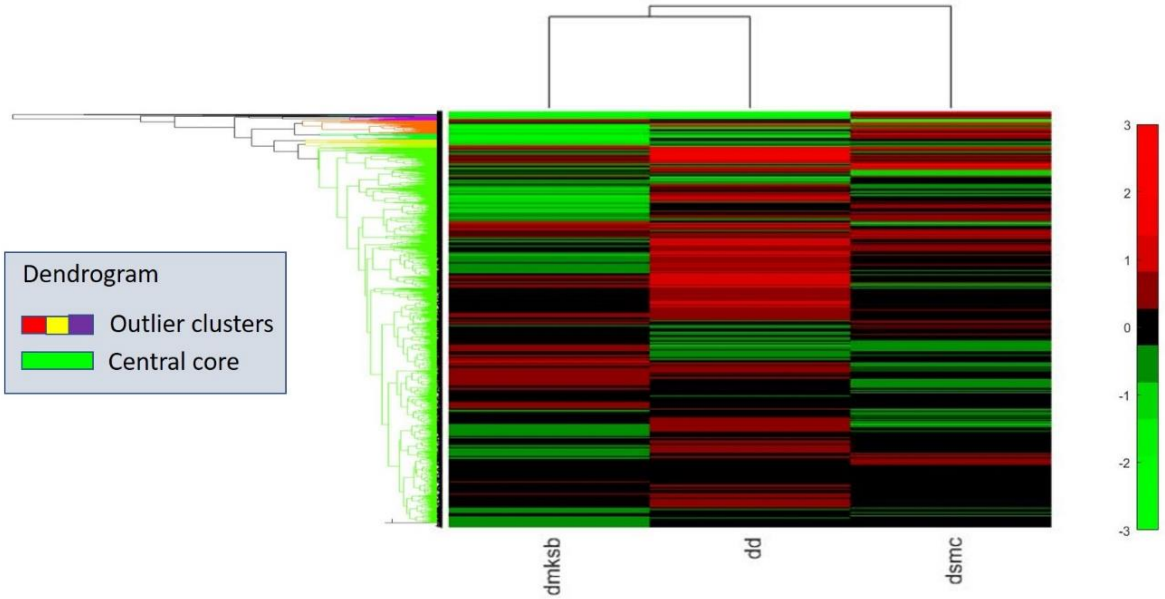

Figure 4- 5: Hierarchical clustering analysis of fold change values for PAO1 condensin strains. Expression values are represented in a heat map. Each gene is represented by a single row and each sample by a single column. Upregulated genes (>1.5 fold) are in red, downregulated genes (>1.5 fold) are in green. Dendrogram on the left shows genes separated into outlier clusters and the central core. Dendrogram on the top represents all three strains.

4.5 Clustering analysis reveals differentially regulated pathways in 9 major clusters

Hierarchical clustering allowed visual representation of the 5485 linkages determined in the dendrogram. In order to more efficiently process this large number of linkages for all three condensin mutants, we performed cluster analysis.

The first step for cluster analysis is determining how many differential clusters there are. The elbow method is one of many methods which provides a crude estimate of the optimal cluster number in a given dataset. This method estimates the optimum cluster number by approximating a relative elbow, or intersection point on a plot of unexplained variance vs postulated number of clusters. Using the elbow method as described in methods (section 2.10.E), it was determined that there were roughly 18 optimum clusters which is what we used as a starting point to begin analysis with as seen in Figure 4-6. This number allows splitting of the dendrogram into clusters of genes based on statistical relevance.

PCA analysis was performed based on this cluster determination as described in section 2.10.B. The PCA plot with 18 determined clustered is shown in Figure 4-7.

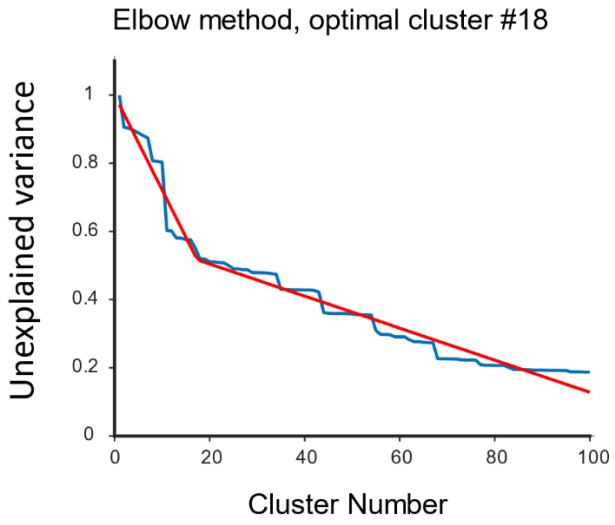

Figure 4- 6: Elbow method for determining optimum cluster number

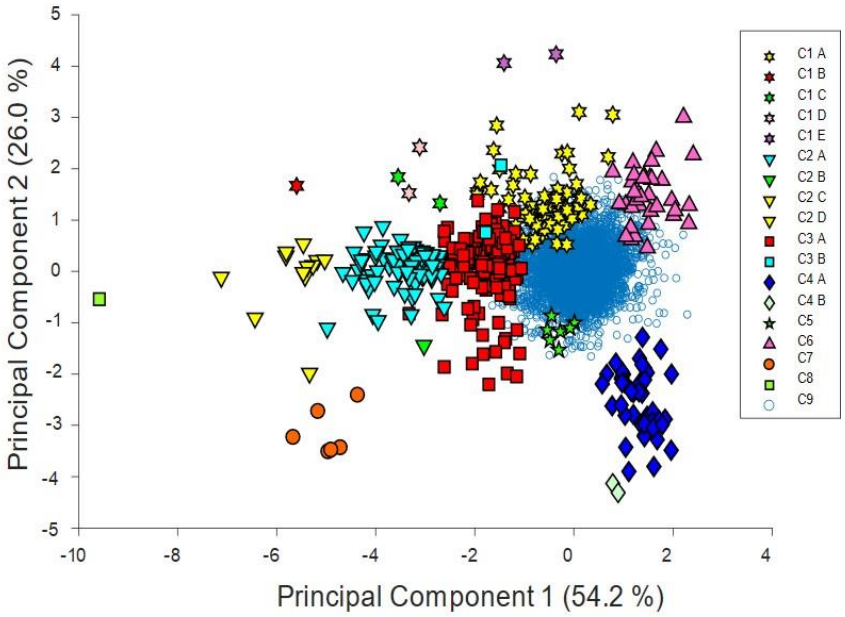

Figure 4- 7 PCA analysis of determined 18 clusters.

Utilizing a pathway database, we obtained information regarding the number of hits for each pathway. This pathways database was compiled as previously described (section 2.10.B).

Initial screening of our PCA plot indicated outlier genes which based on proximity and pathway, were merged with their associated larger cluster. This resulted in a total of 9 final clusters.

Summarization of the percent of biological pathways was performed for each cluster (using MATLAB) and is shown along with the merged PCA plot in Figure 4-8. This is summarized in a pie diagram in Figure 4-9 and in a Table 4-1.

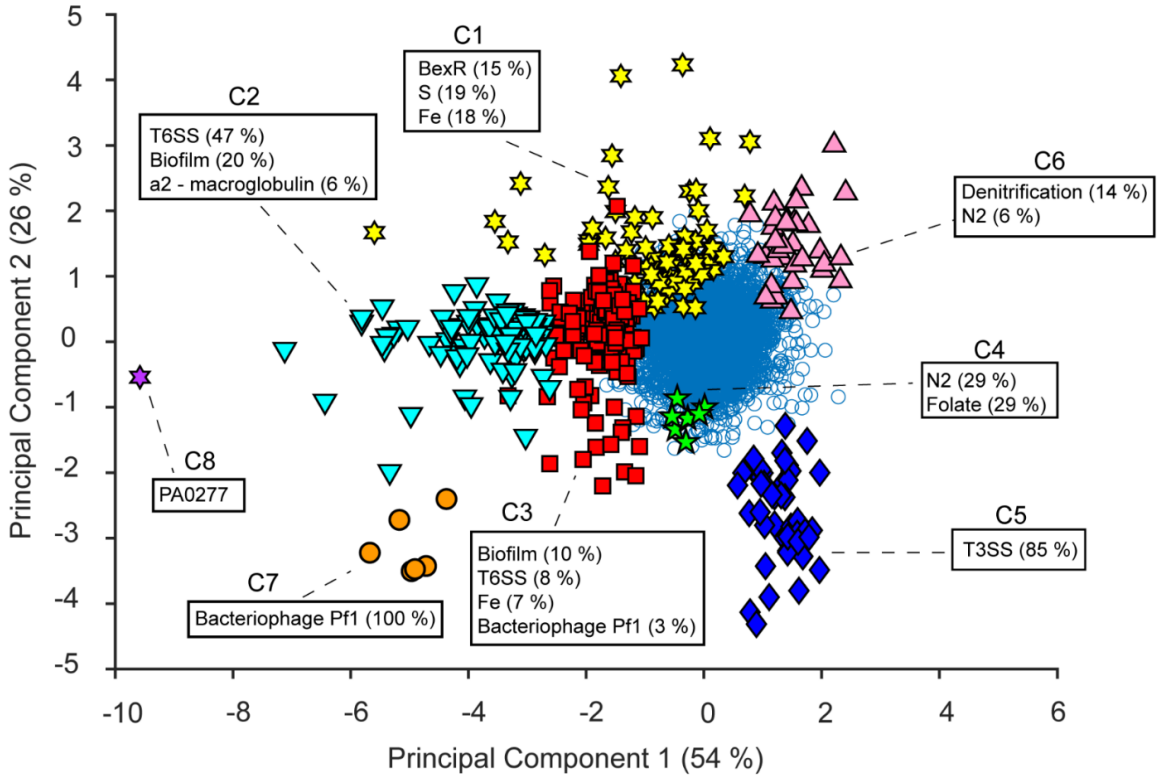

Figure 4- 8: PCA analysis of merged 9 clusters with pathways. Pathways show percent of contribution to each cluster.

4.6 Cluster Results show major pathways involved in virulence

Pathways which show distinct clusters indicate significant differentiation in gene expression based on hierarchical clustering. The following refers to Figure 4-8, Figure 4-9, and Table 4-1. Hypothetical genes with unknown function made up 33% (150/455) of genes in outlier clusters and 44% (2393/5485) of all genes.

The **type 3 secretion system (T3SS)** as previously discussed, is implicated in the acute infection phase. This pathway forms a single cluster which has no overlap or spread into other clusters. This indicates a concise regulation pattern throughout the regulon. **T3SS** genes made up 85% of cluster 5 and 95% of the entire regulon. This reveals differentiation of the entire T3SS regulon.

The type 6 secretion system (T6SS) as previously discussed, is implicated in the chronic infection phase. Genes in this path are spread widely across clusters 2 and 3 indicating a fairly widespread range for how the T6SS is regulated between mutants. T6SS made up 47% of cluster 2 and 8% of cluster 3. Further inquiry shows that T6SS HSI-1 was found in both clusters 2 and 3, however, only T6SS HSI-2 was found in cluster 2 (11 genes) while T6SS HSI-3 was found in cluster 3 (6 genes). This overlap indicates that there is a larger range of regulation for HSI-1, but HSI-2 and HSI-3 were clearly separated and regulated distinctly between the three condensin mutants.

Iron acquisition was found spread across two clusters, making up 18% of cluster 1 and 7% of cluster 3. (Figure)The iron uptake pathway is large, encompassing several different systems. These include the siderophores, pyochelin and pyoverdine as well and iron reducers

like pyocyanine. Iron (not including pyoverdine, pyocyanin or pyochelin or no p,p,p) also includes other TonB dependent siderophore, enterobactin, haemophore, and xenosiderophore uptake systems. The iron group was found to be differentiated for most iron groups. All affected pyochelin genes were distributed in cluster 3. In contrast, Iron (non p,p,p) which includes siderophore homologues and other groups just described was found primarily in cluster 1 (Table 4-1). Pyoverdine genes were distributed evenly between the two clusters at proximal regions of both clusters.

Biofilm (non pel/psl) genes were also distributed in two different clusters making up 20% in cluster 2 and 10% in cluster 3. This regulon coexists with the T6SS pathway and was therefore expected to be found in clusters 2 and 3. This pathway was partly separated on the basis of exopolysacharides, where all differentially regulated psl exo-polysaccharide genes were found in cluster 3 (9 genes). 18 non pel/psl genes were found in cluster 2 while 18 were found in cluster 3. The separation of biofilm genes coincides with type 6 secretion where biofilm genes related to T6SS HSI-3 are found in cluster 3 and those related to T6SS HSI-1 and T6SS HSI-2 are distributed in cluster 2.

The **BexR** regulon, involved in virulence switching, was found exclusively in cluster 1 making up 15% of the overall cluster. Many of the genes were found on the periphery and upper portions of the cluster indicating a high differentiation from the central insignificant cluster.

Five out of the 6 total **α2-macroglobulin homologue genes** (*magABCDEF* operon), were found in cluster 2. This distribution of nearly the entire gene set indicates clear differentiation

of these proteins. The proteins are proposed to be involved in host evasion through emulation of human α2-macroglobulin by trapping and inactivating external proteases aiding in bacterial defense and survival (1.4.F).

Bacteriophage pf1 genes showed some overlap between cluster 7 and cluster 3. Bacteriophage Pf1 genes made up the entire cluster 7 including 6 genes, while 5 genes were spread into cluster 3. As these clusters are spread fairly far apart, indicates either pockets within the regulon that were differentially regulated or stochastic behavior of the genes.

Sulfur genes were found exclusively in cluster 1 making 20% of the overall cluster.

Nitrogen was found in small numbers in significant clustering analysis. Two genes were found in cluster 4 and two genes were found in cluster 6. These clusters are spaced in different directions on the x and y coordinate indicating oppositely regulated genes.

Denitrification made up 14 percent of cluster 6 for a total of 5 genes. No overlap was seen with any other cluster indicating that these genes differentiated consistently.

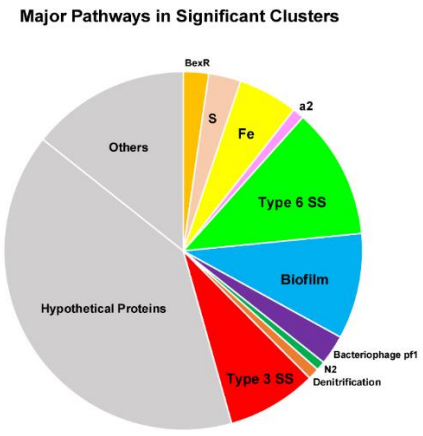

Figure 4- 9: Pie diagram of major pathways identified through clustering analysis.

Table 4- 1: Table for major identified pathways of transcriptomics study. Results shows pathways along with their associated groups (clusters) G1 through G8, number of gene hits, number of genes per regulon, and percent of genes within each group. N represents the total number of genes in the group along with the associated number of genes with known pathways. The pathway for Iron Acquisition (non p/p/p) stands for iron acquisition genes not including pyoverdine, pyocyanin, or pyochelin genes. Three pathways from the type 6 secretion system incorporating different groups from the Hcp Secretion Island (HSI) are represented as T6SS HS1-I, HS-2, and HS-3. Biofilm formation (non pel/psl) represents biofilm genes not including genes from the pel or psl pathways.

Groups	Pathways	# gene hits	# genes/regulon	% genes/group
G1 N = 74(59)	BexR Regulon	11	18	14.9
	Sulfur metabolism	14	51	18.9
	Iron Acquisition (non p/p/p)	10	58	13.5
	Iron Uptake: Pyoverdine	3	26	4.1
G2 N = 91(63)	α2-macroglobulin homolog synthesis	5	6	5.5
	Secretion System: Type 6 SS HSI-1	32	43	35.2
	Secretion System: Type 6 SS HSI-2	11	27	12.1
	Biofilm formation (non pel/psl)	18	91	20.1
G3 N = 184(96)	Iron Uptake: Pyochelin	5	11	2.7
	Iron Acquisition (non p/p/p)	2	58	1.1
	Iron Uptake: Pyoverdine	3	26	1.6
	Bacteriohage Pf1	5	15	3.8
	Secretion System: Type 6 SS HSI-1	8	43	4.3
	Secretion System: Type 6 SS HSI-3	6	26	3.3
	Biofilm: psl exopolysaccharide	9	15	4.9
	Biofilm formation (non pel/psl)	7	91	3.8
G4 N = 7(5)	Nitrogen metabolism	2	33	28.6
G5 N = 46(43)	Secretion System: Type III Secretion	39	41	84.8
G6 N = 36(22)	Nitrogen metabolism	2	33	5.6
	Denitrification	5	26	13.9
G7 N = 6(6)	Bacteriohage Pf1	6	15	100.0
G8 N = 1(0)	predicted Zn-dependent protease	1		100.0

Overall, major virulence pathways were found to make up the majority of the outlier clusters of differentially expressed genes. These groups included type 3 and type 6 secretion systems, iron uptake, sulfur metabolism, the bexR regulon, biofilm formation, Nitrogen metabolism, bacteriophage pf1 genes and toxins (included in the secretion systems).

4.7 Condensin mutants show unique transcriptomic profiles

Pathways which were identified using hierarchical statistical clustering and cluster analysis, were then analyzed for the individual condensin mutant profiles. The distributions for the most affected pathways are visualized as violin plots with overlaying box plots in **Figure 4-10** which are referenced to in the next three sections according to each condensin mutant. These include pathways for the T3SS, T6SS, BexR, psl, pel, biofilm, pyoverdine, pyochelin, and pyocyanin. Additional pathways include quorum sensing, two-component systems and cell motility pathways. A table incorporating fold change values for genes in affected pathways having at least one gene >1.5 fold from each mutant strain, are found in **Table 4** in the Appendix.

The percent of differentially expressed genes for affected pathways for either 2 fold, 1.5 to 2 fold, or no change was plotted in **Figure 4-11**. A corresponding table for the number of genes having fold changes of a minimum of 2 fold or between 1.5 and 2 fold is found in **Table 4-3**. Average fold changes for each path is found in **Table 4-2**. On account of their size and diversity, virulence factors effectors and virulence regulators were analyzed by looking at their sub-groups in Results 4-9, **Figures 4-12 and 4-13**. Metabolism is referred to in Table 4-3.

Together, this information is referenced in the next three sections relating to each condensin mutant. Gene descriptions are derived from KEGG, Virulence factor database (VFDB) and PseudoCAP. Additional information is derived from literature sources (see section 1.4.E and 2.10.B). Iron (non p,p,p) refers to the enterobactin, siderophore, and haemophore mediated iron uptake groups not including pyoverdine, pyocyanin or pyochelin. Biofilm (not pel/psl) includes the biofilm pathway not including the pel and psl groups. Significant fold changes are considered as >2 fold and moderate between 1.5 to 2 fold.

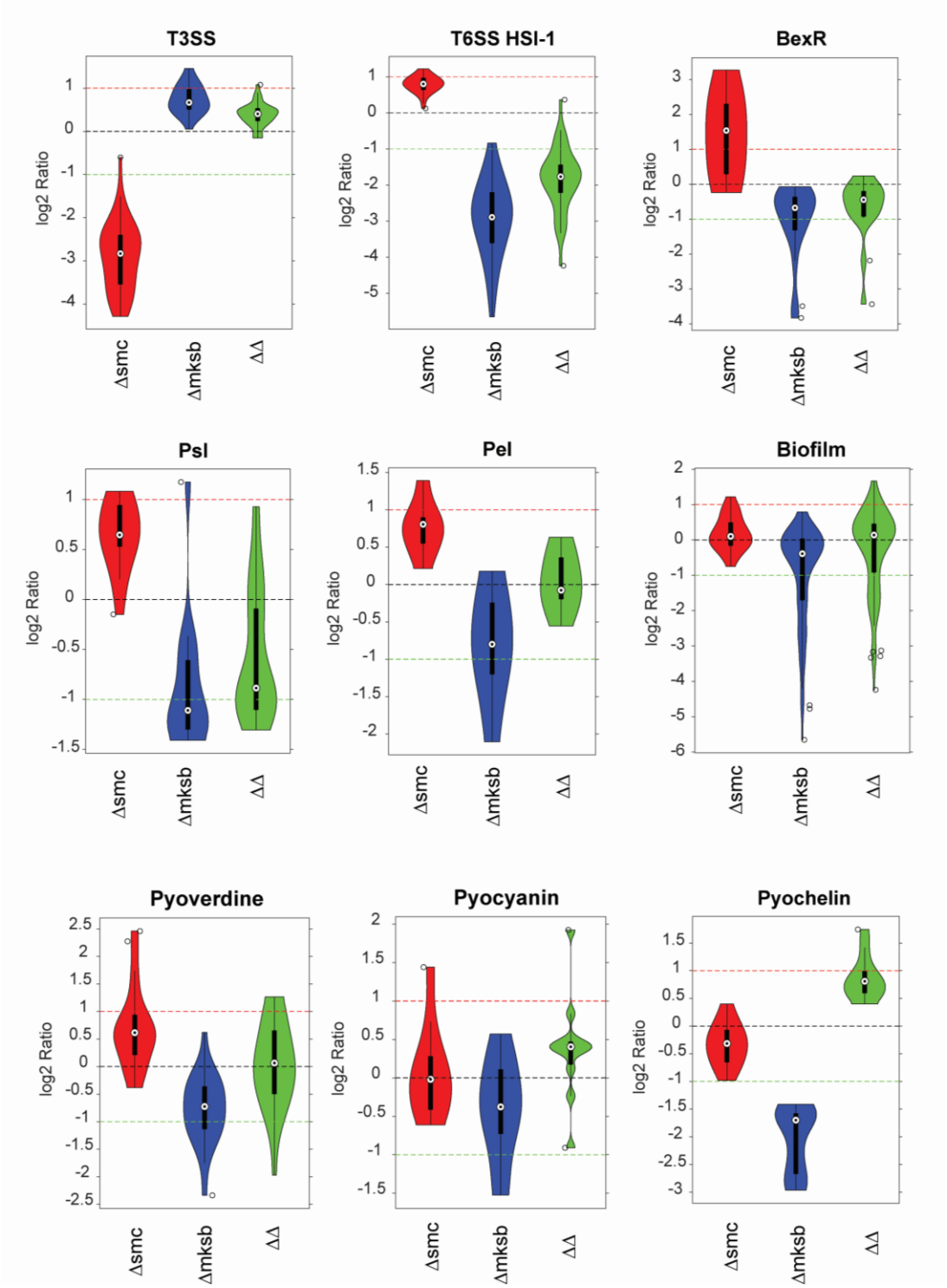

Figure 4- 10: Gene expression distributions for major identified pathways. Box plots and violin lots of log2 fold change values for each strain.

Table 4- 2: Table of average fold changes for major regulons. Dark green represents 2 fold and greater downregulation, light green represents 1.5 to 2 fold downregulation. Red represent 2 fold and greater upregulation, pink represent 1.5 to 2 fold upregulation. Types 2, 3 and 6 secretion systems are denoted as T2SS, T3SS, and T6SS respectively. The biofilm pathway not including pel or psl genes are show as biofilm (no pel/psl). Iron (non p,p,p) represents iron uptake genes not including pyoverdine, pyochelin or pyocyanin. TCS represents the two-component regulatory system.

Paths	Δsmc	ΔmksB	ΔΔ
T3SS	-8.62	1.72	1.13
T6SS HSI-1	1.75	-10.29	-4.29
T6SS HSI-2	0.93	-4.72	-1.63
T2SS	-0.35	-0.42	1.03
BexR	3.39	-3.02	-1.74
Psl	1.46	-1.78	-1.17
Pel	1.74	-1.70	-0.11
Biofilm (no pel/psl)	0.33	-3.23	-0.69
C-di-GMP	0.36	-0.62	0.11
Pyochelin	-0.93	-4.50	1.90
Pyoverdine	1.43	-1.79	0.04
Pyocyanin	0.01	-0.90	1.05
Iron (non p,p,p)	1.31	-0.94	0.88
Sulfur	3.08	-0.06	0.55
Bacteriophage	-3.46	-9.60	-5.80
Denitrification	1.07	-0.50	0.91
Nitrogen	-0.22	-0.33	0.60
Quorum sensing	0.09	-0.25	0.85
Viruence Regulators	0.22	-0.74	0.62
Simga factors	0.84	-0.37	0.95
Flagella	0.42	-0.58	1.16
Type IV Pili	-0.86	0.00	0.90
Chemotaxis	0.28	-0.18	1.13
Alginate	-0.39	-0.43	1.32
Fimbriae	0.75	-1.23	0.83
TCS	0.04	-0.13	0.68

4.7.A Δ*smc* transcriptomic profile

Several pathways were upregulated in the Δ*smc* strain. Significant upregulation was seen for the entire BexR regulon (Figure 4-10). The psl and pel exo-polysaccharide pathways, associated with biofilm formation, showed clear distributions of upregulation even at lower fold change values (Figure 4-10). The hemagglutinin gene, also associated with biofilm formation, was moderately upregulated by 1.8 fold. The type 6 secretion system HSI-1 (T6SS HSI-1), pyoverdine, sulfur, iron (non p,p,p), denitrification, and biofilm (non pel/psl) formation groups showed many significant upregulated genes while the majority showed generalized upregulated distributions at lower fold change values (Figure 4-10), Figure 4-11). In addition, all 6 genes for α2-macroglobulin homolog operon involved in protease inactivation and host evasion, were moderately upregulated (Table 4) (see section 1.4.F for more details on the α2-macroglobulin homolog).

Two pathways were found to be significantly downregulated in Δ*smc*, the type 3 secretion system (T3SS) and bacteriophage pf1 genes as seen by their fold change distributions (Figure 4-10).

Several sigma factors showed significantly increased expression for genes which regulate iron uptake including *pvdS* (PA2426) a regulator for pyoverdine, PA1300 for haem uptake, *fiuI* (PA0472) for ferrichrome uptake, *hasI* (PA3410) haem uptake, and a probable sigma factor for pyocin (PA4896) (Table 4). In addition, several virulence factors were significantly affected. Significantly increased expression of regulators include *bexR* (PA2432), which regulates *aprA* toxin in T1SS, *ppkA* (PA0074) and *pppA* (PA0075) which activate T6SS, and *ptrB*

(PA0612) which represses T3SS. *ppyR* (PA2663) was moderately increased which regulates psl production. Significantly decreased expression was seen in regulators *exsE* (PA1711), *exsD* (PA1714), *exsC* (PA1710), and *exsA* (PA1713) which are involved in the regulation of T3SS as well as *rsmY* (PA0527.1) a regulatory RNA gene (Table 4).

Significant upregulation was seen for the protease PA0277 and the *aprA* toxin gene found in the type 1 secretion system and the BexR regulon. Moderate upregulation was seen in the major hemolysin gene PA2462, as well as the hydrolase, PA0126 (Table 4). *hisJ* (PA2923), a histidine transport ATP-binding protein was down regulated significantly.

The c-di-GMP pathway, also associated with biofilm formation, was only slightly upregulated in some genes but did not include the *wsp* genes (Figure 4-11, Table 4). Slight reductions, with mostly no changes were seen in pyochelin and alginate and the two-component system (TCS) (Figure 4-10, Figure 4-11)). No major effect was seen in quorum sensing, HCN toxins, pyocyanin, or the type 2 secretion system (T2SS) (Table 4).

Overview of downregulated Δ*smc* genes:

Type 3 secretion system (T3SS): The entire distribution of T3SS genes in Δ*smc* was significantly downregulated with an average of -8.6 fold across the regulon (Figure 4-10) (Table 4-2). 98% of T3SS (40/41) were significantly downregulated >2 fold (Table 4-3, Figure 4-11). Included in this are the toxins *exoT* (-11 fold), *exoY* (-14 fold), and *exoS* (-16 fold). 17 *psc* genes ranged from -2.8 to -9.6 fold change. *exsC/E/D*, and *exoS* genes were also downregulated (-5 to -8 fold change. The *ptrB* gene, coding for a negative regulator of T3SS, was found to be

significantly upregulated (2.1 fold) and *exsA*, a gene coding for a transcriptional activator of T3SS, was downregulated -6 fold (Table 4).

Bacteriophage pf1: Most bacteriophage pf1 genes were downregulated significantly with two genes showing moderate upregulation (between 1.5 and 2 fold), giving an average of -3.6 fold for the regulon. 73% (11/15) of genes were downregulated >2 fold (Table 4-3) (Figure 4-11).

Pyochelin genes showed a slight distribution of downregulation where all genes are distributed below 2 fold. The average for the regulon is -0.9 fold (Figure 4-10). No genes were changed greater than 2 fold. 36% (4/11) genes were downregulated between 1.5 and 2 fold (Table 4-3) (Figure 4-11).

Alginate was only slightly reduced with 14% (4/28) of genes downregulated between 1.5 and 2 fold. The *algF* gene was slightly reduced by 1.7 fold (Table 4-3, Figure 4-11).

***hisJ*,** a gene coding for a histidine transport ATP-binding protein was downregulated significantly at -3.5 fold.

Overview of upregulated Δ*smc* genes:

Type 6 secretion system HSI-1 (T6SS-HSI-1): T6SS HSI-1 genes showed a clear but moderate upregulation in its distribution with a pocket of genes > 2 fold and an overall regulon average of 1.8 fold (Figure 4-10). 16% (7/43) of genes were upregulated greater than 2 fold. The majority of the regulon, 65% (28/43) genes, was expressed between 1.5 and 2 fold (Figure 4-11) where 5 of these showed 1.9 fold change (Table 4-3). *ppka*, a gene coding for a post-

translational regulator of Hcp-HSI which acts on Fha1, a core scaffolding protein, was moderately upregulated (1.8 fold) as well as *fha1* (moderate 1.8 fold) (Table 4).

BexR: The majority of the BexR regulon shows a significant distribution for upregulated genes in Δ*smc* with an average of 3.4 fold change for the entire regulon (Figure 4-10, Table 4-2). 61% (11/18) of genes in the BexR regulon were upregulated greater than 2 fold (Figure 4-11, Table 4-3) For Δ*smc*, the *bexR* regulator gene itself was significantly upregulated by 9.2 fold. The *aprA* gene, encoding metalloproteinase, was upregulated by 2.3 fold. Other distinctly highly regulated genes included PA1202, a probably hydrolase (9.6 fold), and a number of hypothetical genes affected by the BexR regulator, PA1203 (4.6 fold), PA2430 (7.3 fold), PA2431(5.4 fold), and PA2598 (4.3 fold) (Table 4).

Sulfur: The sulfur uptake regulon showed significant upregulation with several genes above 10 fold, giving an overall average of 3.1 for the regulon (Table 4-2, Table 4-3). 37% (19/51) of genes were upregulated > 2 fold. 3 of these genes are in the *cys* operon with *cysA* being upregulated 6.0 fold and *cysW* being upregulated 4.4 fold. The greatest affected genes included PA3442 though PA3446 which are involved in the transport of sulfonate under sulfur starvation. The fold change values include the following: PA3442 (6.2 fold), PA3443 (46.6 fold), PA3444 (26.7 fold), PA3445 (11.5 fold), and PA3446 (3.6 fold). 9.8% (5/53) additional genes were upregulated between 1.5 and 2 fold (1.4.F).

Pyoverdine: Pyoverdine genes were mostly moderately upregulated with a pocket of genes showing significant upregulation >2 fold with an overall regulon average of 1.4 fold (Figure 4-10). Overall, 23% (6/26) genes were upregulated > 2 fold. Two genes were

particularly high, *pvdS*, encoding a pyoverdine sigma factor, upregulated at 5.5 fold and pvdA upregulated at 4.8 fold. Most genes were upregulated moderately under 2 fold (Figure 4-11). 27% (7/26) genes were upregulated between 1.5 and 2 fold. Uptake of ferripyoverdine in *P. aeruginosa* occurs via the FpvA receptor protein and requires the energy-transducing protein TonB1. PvdS is a sigma factor which activates expression of FpvA (see section 1.4.E for details). Δ*smc* showed significant upregulation for *pvdS* (5.5 fold), *tonB1* (2.1 fold), and *fpvA* (moderate 1.8).

Psl: The psl path showed a clear but moderate distribution of upregulation even at lower fold change values (Figure 4-10) with an average regulation change of 1.5 fold. 13% (2/15) of genes were upregulated greater than 2 fold while 47% (7/15) were upregulated between 1.5 and 2 fold. A single gene was downregulated between 1.5 and 2 fold. Therefore, most psl genes were slightly upregulated for Δ*smc*.

Pel: Pel, was mostly moderately upregulated in Δ*smc* with one gene above 2 fold and a total average of 1.7 (Figure 4-10). 14% **(**1/7) of genes was upregulated greater than 2 fold and 43% (3/7) genes between 1.5 and 2 fold.

Hemagglutinin (PA0041): Hemagglutinin, a filamentous adhesion protein associated with biofilm formation and pathogenicity was also up regulated moderately by 1.8 fold (see section 1.4.E for details).

Biofilm (non pel/psl): Although most of the distribution of biofilm (non pel/psl) genes showed no change at zero, pockets of genes were found both moderately up and downregulated with a group of genes upregulated greater than 2 fold (Figure 4-10). On

account of fluctuation throughout this larger regulon, the average was at 0.3 fold (Figure 4-1). 6.6% (6/91) genes were upregulated greater than 2 fold. These genes are the same genes also involved in the type 6 HSI-1 secretion system which is related to biofilm formation (Table 4). 13% (12/91) of genes of Δ*smc* were upregulated between 1.5 and 2 fold (6 of these from Type 6 SS HSI-1). Four genes were moderately down regulated between 1.5 and 2 fold). Δ*smc* moderately upregulated both *siaA* (PA0172) 1.8 fold , encoding a threonine kinase regulator, and *siaD*, 1.9 fold, encoding a diguanylate cyclase that synthesizes c-di-GMP. An affect was also seen on the *cdrA/B* genes encoding proteins that promote biofilm, with *cdrA* (PA4625) upregulated at 2.3 fold and *cdrB* (PA4624) upregulated at 2.3 fold.

Pyocyanin: Most of the distribution for pyocyanin showed minimal change with an overall average of 0.01 (Figure 4-1). A single gene, *phzF2* (PA1904) was found out of 17 which upregulated at 2.7 fold, and a single gene, *phzB2* (PA1900), was upregulated between 1.5 and 2 fold.

Iron not including pyoverdine, pyochelin or pyocyanin (iron non p/p/p): The iron pathway was distributed widely with the largest density of distribution showing genes at 1.5 fold and higher indicated most are moderately upregulated. The overall average of the regulon is 1.3 (Table 4-2). 26% (15/58) genes were significantly upregulated above 2 fold. Most genes were moderately upregulated with 20% (12/58) of the genes being upregulated between 1.5 and 2 fold. Together, this shows that almost 50% of the genes are upregulated greater than 1.5 fold change (Figure 4-11). Of the 13 significant genes, three of are xenosiderophore genes, 3 heme uptake and degradation genes and one probable iron/ascorbate oxidoreductase. The xeno-siderophore genes included *optJ* (PA0434) 2.5 fold, *fvbA* (PA4156) 2.0 fold, and *optR*

(PA3268) 3.5 fold. The heme uptake and degradation genes included *hemO* (heme oxygenase) (5.1 fold), PA4709 *phuS* (hemin uptake) (2.9 fold), and *phuR* (3.1 fold). The iron oxido-reducatase (PA4191) was upregulated at 4.6 fold. Only 1 gene was significantly downregulated, *fepD* (PA4160) at -2.6 fold and 2 genes were down regulated between 1.5 and 2 fold. Iron sigma factors were upregulated including PA0472 (2.2 fold), and PA1300 (2.4 fold), *pvdS* (PA2426) at 5.5 fold, and a factor for pyocin (PA4896) by 2.6 fold (Table 4).

Denitrification: The overall distribution shows upregulation of more than half of the genes in the regulon (Figure 4-11) although the average for the regulon was around 1 fold. Upregulated genes corresponded to all operons except the *nar* genes which showed genes with moderate and slight downregulation. 27% (7/26) genes were significantly upregulated greater than 2 fold and 31% (8/26) were moderately upregulated between 1.5 and 2 fold. Only 4% (1/26) was downregulated between 1.5 and 2 fold (Table 4-3).

a2-macro globulin homolog operon: All 6 genes for α2-macroglobulin homolog operon were moderately upregulated (Table 4).

C-di-GMP: C-di-GMP genes mostly showed no change with a small number being upregulated. 10.5% (2/19) of genes were significantly upregulated greater than 2 fold. These included PA4624 and PA4625. 10.5% (2/19) were moderately upregulated between 1.5 to 2 fold (Figure 4-11). These included genes PA0169 and PA0170. Genes in the *wsp* operon were not affected here (Table 4).

Additional affected genes included upregulation of the **protease PA0277** at 2.4 fold and a moderate upregulation of **PA0126** (1.8 fold)**,** a key responder gene to oxidative stress. A **DNA**

repair protein PA4172 was found to be upregulated by 2.2 fold. The hemolysin gene **(PA2462)** was found to increase by 1.7 fold.

Sigma factors and Virulence regulators:

Sigma factors: Several sigma factors were upregulated. 13% (4/31) sigma factor genes were significantly upregulated while 19% (6/31) were upregulated moderately between 1.5 and 2 fold (Figure 4-11). Significantly upregulated genes included ***pvdS*** (**PA2426),** a pyoverdine sigma factor regulator at 5.5 fold and three RNA polymerase sigma factors associated with iron uptake; **PA1300** (2.4 fold), **PA0472** (2.3 fold). **PA3410** was upregulated at 2.0 fold. A probable sigma-70 factor (ECF) for pyocin, **PA4896,** was upregulated 2.6 fold in Δ*smc* (Table 4).

Virulence Regulators: Several virulence regulators were both up and downregulated. 3/95 genes were significantly upregulated while 7/95 genes were moderately upregulated**.** ***ppkA*** (PA0074) was upregulated 1.8 fold. The significantly upregulated genes include ***bexR*** (PA2432) at 9.2 fold, and ***ptrB*** encoding a protein which represses T3SS, at 2.1 fold. The ***ppyR*** **gene, encoding a regulator of the psl operon,** was moderately upregulated at 1.6 fold as well as ***pppA*** (PA0075) encoding a protein which phosphorylates FhaI and acts on pyocyanin and T6SS, at 1.6 fold. 4/100 genes were significantly downregulated while 1/100 genes were down regulated moderately. Significantly downregulated genes include ***exsC*** (PA1710) at -4.7 fold, ***exsE*** (PA1711) at -5.5 fold, ***exsA*** (PA1713) at -5.9 fold, and ***exsD*** (PA1714) at -5.3 fold. ***rsmZ*** was downregulated by -4.6 fold ***rsmY*** was unchanged. *rsmA* however, was not affected (Table 4-3, Table 4).

Notable pathways with no major effect:

As a note, **quorum sensing genes** and genes in the GacA/RsmA system, and HCN genes (Figure 4-10) were not affected in Δ*smc* (see table sigma factors and regulators). **T2SS:** The entire regulon for T2SS was unaffected (Table 4). In addition, cellular motility including Type IV pili, flagella and chemotaxis genes were not affected.

4.7.B Δ*mksB* transcriptomic profile

Δ*mksB* showed marked decreases in regulation for a number of different pathways. Significant downregulation was seen for the entire T6SS HSI-1 and pyochelin pathways. The majority of gene distribution was down regulated for the BexR, bacteriophage pf1, psl and the T6SS HSI-2 pathways (Figure 4-10, Figure 4-11).

The pyoverdine (iron uptake), pel (exo-polysacharide contributing to biofilms), and biofilm (non pel/psl) groups showed significantly downregulated genes while the majority showed a generalized down regulated distribution at nearly 2 fold (Figure 4-10, Figure 4-11). The hemagglutinin gene, also associated with biofilm formation, was downregulated -5.7 fold. Iron (non p/p/p) significantly downregulated many genes while the main distribution showed slight downregulation less than 1.5 fold. T2SS and c-di-GMP showed moderate downregulation (Figure 4-11). In addition, all 6 genes for α2-macroglobulin homolog operon involved in host evasion, were significantly down regulated (Table 4).

T3SS was the only group upregulated in Δ*mksB*. Many genes were upregulated significantly in T3SS with the main distribution showing upregulation just below 2 fold (Figure 4-10).

Several toxins were reduced. Significant downregulation was seen for the hydrogen cyanide genes, *hcnA/B/C*, the hemolysin gene, PA2462, a phospholipase gene, *pldA*, and a stress responding hydrolase, PA0126. A protease, PA0277, was downregulated greater than 100 fold.

In addition, genes for a heat shock protein, *dnaJ* and *dnaK* were significantly down regulated. *ligD*, (PA2138), encoding DNA ligase, was significantly down regulated. *hisJ*, a histidine transport ATP-binding protein was down regulated moderately.

Denitrification showed significant up and downregulation. Upregulated genes were expressed in the *nos* the operon. Significantly downregulated genes were seen in the *nor* and *nap* operons.

Several sigma factors and virulence regulators showed significantly decreased expression. Affected genes include regulators for iron uptake, quorum sensing, T6SS, T3SS and virulence. Significantly downregulated iron uptake regulators include *pchR* (PA4227), a regulator for pyochelin, and PA2384, a probable Fur, Fe^{2+}/Zn^{2+} uptake regulation protein. Moderate downregulation was seen for *pvdS* (PA2426), a regulator for pyoverdine and *femI* (PA1912) involved in mycobactin/ carboxymycobactin uptake. Decreased expression was seen for *ppka*, which regulates T6SS as well as *pppa*, a PpkA antagonist. A repressor for T3SS (*prtB*), the virulence bi-stable switch regulator (*bexR*), and a virulence regulator (*vreI*) were significantly decreased. The quorum sensing regulators PA1196 were significantly decreased as well as two quorum sensing repressor genes *qteE* (PA2593) and *qscR* (PA1898). Upregulated

regulators affected include *exsC* (PA1710), a regulator for T3SS, and *ppyR* (PA2663), a regulator of psl (Table 4).

More significant downregulated genes were seen than upregulated that affected metabolism. About 35 different metabolic groups were affected. Most of these were slight with 1-3 genes affected. Groups with 4 or more genes down regulated include the biosynthesis of amino acids (7/143 genes), aminoacyl-tRNA biosynthesis (5/101 genes), carbon metabolism (6/127 genes), glycerophospholipid metabolism (4/28 genes), and arginine biosynthesis (4/29 genes) (Table 4-3).

Pyocyanin was significantly downregulated in some genes with most of the pathway showing no change. Quorum sensing didn't show many affected genes. Those affected included significant downregulation of two phenazine genes, *phzF1* (PA4215) and *phzD2* (PA1902) as well as *lasI* (PA1432) encoding an autoinducer synthesis protein, and the previous mentioned QS regulators.

The two-component regulatory system (TCS) was moderately affected overlapping with pathways for chemotaxis and C4-dicarboxylate transport. Cellular motility in general was largely unaffected. Chemotaxis was largely unaffected but showed inconsistency with some significant genes that were both up and downregulated. Fimbriae (related to biofilm) showed mostly no change in the regulon with significant downregulation of the *cupB2* gene.

Overview of downregulated Δ*mksB* genes:

Type 6 secretion system (T6SS HSI-1): Δ*mksB* shows significant downregulation in the entire distribution of genes with an average fold change of -10.2 (Figure 4-10). 95% (41/43)

genes were significantly downregulated > 2 fold where 30 of these genes were downregulated greater than 5 fold. (Table 4-3). No genes were downregulated in this regulon. *ppka* (PA0074), encoding a T6SS regulator, was downregulated (-5.9 fold), as well as *fha1* (PA0081) encoding the scaffolding protein required for T6SS at -2 fold.

BexR: The BexR regulon was significantly downregulated with the greatest distribution being found below the 2 fold mark (Figure 4-10). The overall average of the regulon is -3 fold. 39% (7/18) were downregulated greater than 2 fold and 17% (3/17) were downregulated between 1.5 and 2 fold. The *bexR* regulator gene (PA2432) itself was found to be downregulated by -4.6 fold. *aprA*, encoding the metalloprotease regulated by BexR, was reduced moderately at -1.5 fold. PA1202, a probable hydrolase was reduced -14.3 fold, PA2483 by -11 fold and the hydrolase (PA1203) by -2.5 fold). Other genes in this regulon included hypothetical genes (Table 4).

Pyochelin: Δ*mksB* revealed significant and consistent downregulation of all pyochelin genes giving an average of -4.5 for the regulon (Figure 4-10). 100% (11/11) genes were downregulated below -2 fold with 5 genes being downregulated below -4 fold in the *phc* operon (average -4.5). The *fptA* receptor gene for pyochelin was down regulated by -3.2 fold. Δ*mksB* is clearly downregulated for pyochelin (Table 4-3, Table 4).

Psl: The majority of the psl regulon was downregulated with more than half distributed below the 2 fold mark. The overall average of the regulon is -1.8 fold (Figure 4-10). 60% (9/15) of genes were downregulated greater than 2 fold while 13% (2/15) genes were

downregulated between 1.5 and 2 fold. Interestingly, a single outlier was upregulated, the psl regulator gene *ppyR* (PA2663) at 2.3.

Pel: Pel genes shows downregulation of genes with the greatest density just below the 2 fold region giving an average fold change of the regulon of -1.7 (Figure 4-1). 29% (2/7) genes were downregulated significantly while 43% (3/7) of genes were down regulated between 1.5 and 2 fold.

Biofilm (non pel/psl): Although the main distributions of genes are nominal, a large group of genes are significantly downregulated in Δ*mksB* with an average of -3.2 fold for the entire regulon (Figure 4-1). 33% (30/91) genes were downregulated > 2 fold and 6.6% (6/91) of genes between 1.5 and 2 fold. A single gene was up regulated moderately between 1.5 and 2 fold. (Table 4-1, Figure 4-2). The significantly affected genes mostly belong to the T6SS HSI-1 and T6SS HSI-2 secretion systems with fold change ranging from -2 to -50. 3 genes that were downregulated between 1.5 and 2 fold are attributed to quorum sensing. Δ*mksB* downregulated both *siaA* and *siaD* genes with *siaA* (PA0172) at -3.3 fold and *siaD* (PA0169) at -3.2 fold. Downregulation was also seen on the *cdrA/B* genes with *cdrA* (PA4625) downregulated at -2.3 fold and *cdrB* (PA4624) downregulated at 2.1 fold (Table 4).

Pyoverdine: Pyoverdine was downregulated in Δ*mksB* with the greatest distribution of genes just below 2 fold. The average of the regulon is -1.8 (Figure 4.10). 31% (8/26) genes were significantly downregulated while 27% (7/26) were downregulated moderately (1.5 to 2 fold) 4% (1/26) were upregulated moderately (Table 4-3, Figure 4-11). The *fpvA* gene was significantly downregulated at -5 fold. FpvA is a receptor protein for the uptake of pyoverdine.

7 genes were downregulated between 1.5 and 2 fold and 1 was upregulated 1.5 and 2 fold. Δ*mksB* also showed downregulation for *pvdS*, a gene for the pyoverdine sigma factor regulator, (-1.9 fold), and *tonB1* (-1.1 fold).

Pyocyanin: Most of the distribution for pyocyanin showed minimal change with a couple of genes which were significantly downregulated giving an average of -.9 out of 17 genes total (Figure 4-1 (Figure 4-1). The two significantly downregulated genes included *phzD2* (PA1902) at -2.9 fold and *phzF1* (PA4215) at --2.7 fold.

Iron (non p/p/p). The majority of the distribution of iron (non p/p/p) genes were moderately downregulated with a smaller group of genes that were significantly down regulated around -4 fold. The overall average for the regulon is -0.9 (Figure 4-3). About 14% (8/58) genes were significantly downregulated greater than 2 fold and about 7% (4/58) down regulated between 1.5 and 2 fold. The significantly affected genes include those from enterobactin and siderophore mediated iron uptake. These genes include *fepG* (PA4161) -2.1 fold, *tonB2*(PA0197) -4.6 fold), and *exbB1* (PA0198) -3.4 fold, *fiuR* (PA0471 fold) -2.4, and *viuB* (PA2033) -2.6 fold, and *femR* (PA1911) -3.4 fold. The single upregulated gene included *fecA* (PA3901) 2.0 fold. Three additional genes were downregulated between 1.5 and 2 fold, including *femA* and two sigma factors, *femI* (PA1912) and PA3899 (Table 4-3, Table 4).

Bacteriophage pf1: Bacteriophage pf1 genes were significantly downregulated with the greatest part of its distribution downregulated greater than 8 fold. The average of the regulon is -9.6 (Figure 4-2). 73% (11/15) genes were significantly downregulated while a single gene was moderately downregulated (1.5 to 2 fold). The most significantly affected genes are

hypothetical and include PA0717 through PA0720 and PA0722 which downregulated in a range from -8 to -15 fold.

Quorum sensing: A small number of genes were significantly affected in quorum sensing (Figure 4-2). 3/99 were significantly downregulated. Those include*, lasI* which was downregulated at -2.6 fold, *phzD2* (PA1902) at -2.9 fold, and *phzF1* (PA4215) at -2.7 fold. In addition to these, a regulator of RhlrI, PA1196, was downregulated by -2.4 fold. Additional quorum sensing sigma factor genes that were affected included *qscR* (-2.9 fold) and *qteE* (-2.4 fold), anti-sigma factors. 11/99 genes were moderately downregulated. 1/99 genes were significantly upregulated while 7/99 genes were moderately upregulated. The moderately affected genes were both up and downregulated. The upregulated gene is a hypothetical protein, PA3320 (Table 4-3, Table 4).

α2-macroglobulin homolog operon: All 6 genes for α2-macroglobulin homolog operon were significantly downregulated (Table 4).

Type 6 secretion system HSI-2 (T6SS HSI-2): Δ*mksB* showed significant differentially expressed genes for the majority of the T6SS-HS2 system. Δ*mksB* showed significant downregulation in this pathway with an average fold change of -4.7 (Figure 4-11). 52% (14/27) of genes were downregulated greater than 2 fold. Three genes were moderately downregulated (1.5 to 2 fold) and zero were upregulated. All genes in the order from PA1656 to PA1670 were significantly affected ranging from -3.8 to -15 fold decrease in expression.

Hydrogen cyanide genes ***hcnA/B/C*** were all significantly downregulated at -2.4, -2.6, and -3.5 fold respectively.

The **hemolysin gene PA2462** was also significantly downregulated at -5.8 fold.

The **hemagglutinin gene PA0041** was significantly downregulated at -5.7 fold.

Additional affected genes included significant downregulation of the **protease PA0277** at -146 fold and a key responder gene to oxidative stress **PA0126** at -19 fold.

dnaJ*,** a gene encoding a heat shock protein involved in bacterial translocation across host cells, was found to be downregulated by -2.3 fold. ***dnaK, encoding another heat shock protein, was downregulated by -2.5 fold.

***hisJ*,** encoding a histidine transport ATP-binding protein was downregulated moderately at -1.9 fold.

pldA (PA3487), encoding a phospholipase gene, was downregulated -2.5 fold. Other phospholipases were not affected (Table 4).

ligD (PA2138), a gene for for DNA ligase, was significantly downregulated at -3.5 fold.

Metabolism: A large number of metabolic genes were affected> 2 fold in *mksB* (Table 4-3). Of these, about three times as many genes were downregulated as compared to upregulated. These ranged across 35 different metabolic groups. The number of genes affected in each metabolic group mostly ranged from 1 to 2 genes for upregulated and 1 to 3 for downregulated genes. Groups that showed a slight affect with 4 or more downregulated genes include: Biosynthesis of amino acids (7 /143 genes), aminoacyl-tRNA biosynthesis (5/101 genes), carbon metabolism (6/127 genes), glycerophospholipid metabolism (4/28 genes), and arginine biosynthesis (4/29 genes).

Type 2 secretion system (T2SS): shows moderate downregulation (with a couple of significantly downregulated genes) of about 25% of the gene distribution (Figure 4-2).

C-di-GMP: c-di-GMP shows only moderate downregulation (no significantly affected genes) of about 20% of the regulon. 21% (4/19) of genes were signficantly downregulated between >2 fold. (Figure 4-2). (Table 4).

Two-component regulatory system (TCS): TCS was moderately affected showing several significant up and downregulated genes. Of the 202 genes in this regulon, 2 were significantly upregulated and 6 were significantly downregulation. TCS genes overlapped with several other pathways. For upregulated genes, 2 TCS genes are involved in chemotaxis. In down regulated genes, two overlapped with C4-dicarboxylate transport, two with chemotaxis, one with biofilm and one with antibiotic resistance (PA0749).

Overview of upregulated Δ*mksB* genes:

Type 3 secretion system (T3SS): T3SS shows a clear upregulation in its distribution of genes with a large pocket of genes greater than 2 fold and an overall regulon average of 1.7 fold (Figure 4-10). 24% (10/41) genes were upregulated greater than 2 fold and 42% (17/41) between 1.5 and 2 fold (Table 4-3). The *ptrB* gene was found to be significantly downregulated at -2.7 fold which acts in repressing type 3 secretion.

Notable pathways with no major effect:

The following pathways showed mostly no change however, many had at least one significantly affected gene so they are discussed.

Sulfur: Sulfur genes were mostly unaffected. Most of the distribution of sulfur genes in Δ*mksB* is insignificantly up and downregulated with a few significantly downregulated genes giving an average fold change of -0.06 (Figure 4-1). 8% (4/51) genes were downregulated >2 fold while 10% (5/51) were downregulated moderately. 13.7% (7/51) were upregulated moderately (Table 4-3).

Chemotaxis: Δ*mksB* did not show a consistent distribution in the chemotaxis regulon. Both up and downregulation of genes were seen with an overall average of -0.2 fold (Figure 4-11). 6.7% (3/45) of genes were significantly upregulated, 11% (5/45) genes were moderately upregulated. Significantly upregulated genes included the *pctA*, PA2561, and PA4502 genes. Moderately upregulated genes include *pctC* and *pctB*. 4% (2/45) were significantly downregulated and 11% (5/45) were moderately downregulated. Downregulated genes included those in the chemotaxis methyl-esterase operon.

Type IV pili was largely unaffected in Δ*mksB* (Figure 4-11). Type IV pili showed one significantly downregulated gene *fimT* (PA4549) at -2.5 fold with an overall average of 0.004. Two genes were moderately up and 2 genes were moderately downregulated in this regulon.

Flagella: flagella genes were largely unaffected (Figure 4-11)

Fimbriae: The overall distribution of cup genes involved in Fimbriae was largely unaffected, however *cupB2* (PA4085) showed a significant downregulation at -5.5 fold. Two other genes were moderately affected, *cupA5* (PA2132) and *cupB4* (PA4083) was moderately upregulated.

Pathways with distinct up and downregulation:

Denitrification: Denitrification showed significant up and downregulation. Upregulated genes were expressed in the *nos* operon. Significantly downregulated genes were seen in the *nor* and *nap* operons. 19% (5/26) of genes were significantly upregulated while 27% (7/26) of genes were significantly downregulated.

Sigma factors and Virulence regulators:

Sigma factors: One sigma factor gene was significantly downregulated and 6 moderately out of 31 genes. The significantly downregulated gene included **PA0472** (-2.2 fold), which is involved in iron uptake. Moderately downregulated genes include ***algU***, ***mucA*** **and the iron uptake sigma factor, and *pvdS***. No sigma factor genes were significantly upregulated. Two genes were moderately upregulated.

Virulence Regulators: most virulence regulators were down significantly downregulated. 13/95 genes were significantly downregulated while 11/95 genes were moderately downregulated. A full list of genes affected and their fold change values are in Table 4-4. Significantly downregulated genes that regulate iron uptake include, ***pchR*** and **PA2384**. Some of the significant genes include ***ppka*** (5.9 fold) associated with T6SS, and **pppA** (-10 fold) a T6SS post translational antagonist. Also affected included ***prtB*** (-2.4 fold) a repressor for T3SS, ***bexR*** (-4.6 fold), and ***vreI*** , a gene encoding a virulence regulator, at -2.5 fold. Quorum sensing sigma factor regulator genes affected include the quorum sensing repressor gene, ***qscR*** (-2.9 fold), the quorum sensing post translational repressor *gene,* ***qteE*** (-2.4 fold). Iron uptake sigma factors affected include ***pchR*** (PA4227) pyochelin regulator at -3.1 fold, and **PA2384** (-5.8 fold) regulator for iron uptake a haemolysin regulator **PA2463** (-3.1). In

addition, ***rsmZ*** was downregulated by -16.6 fold. ***rsmY*** was downregulated by -4.1 fold. The ***rsmA* gene involved in signaling** was downregulated -2.1 fold. 2/95 genes were significantly upregulated while 3/95 genes was upregulated moderately. The significantly upregulated genes include ***exsC***, an anti-activator of *exsA* which regulates T3SS at 2.0 fold and ***ppyR*** (a regulator of psl) at 2.3 fold. The ***gacA*** gene did not show any significant effects on Δ*mksB* (Table 4).

4.7.C Δ*smc* Δ*mksB* transcriptomic profile

Two pathways were found to be significantly downregulated in the delta double strain across the entire regulon, T6SS HSI-1 and bacteriophage pf1 genes (Figure 4-10). The T6SS HSI-2 and psl pathways show a large portion of the regulon downregulated with a small pocket of moderately upregulated genes (Figure 4-11). In contrast to T6SS, T3SS showed moderate upregulation with the majority of genes being upregulated just below 1.5 fold. Pyochelin showed significant upregulation for the majority of its gene distribution. The hemagglutinin gene, associated with biofilm formation, was downregulated -3 fold.

Biofilm (non pel/psl), TCS and the denitrification pathways show distinct patterns of up and downregulation. For biofilm, downregulated genes overlapped with the T6SS and *rsmA* (PA0905) while upregulated genes overlapped with quorum sensing genes and *gacA* (PA2586). For TCS, downregulated genes overlapped with chemotaxis (5 genes), C4-dicarboxylate transport (5 genes), and biofilm (3 genes) while downregulated genes overlapped with cytochrome b/c genes (6 genes). Denitrification showed general upregulation which included

the *nos*, *nar* and *nor* operons. Marginal downregulation of denitrification was seen in the *nap* operon.

BexR showed moderate downregulation of roughly 30% of its genes > 1.5 fold including a small pocket of significantly down regulated genes (Figure 4-10). T2SS, denitrification and iron (non p,p,p) showed moderate upregulation with roughly 30% of its gene distribution including small pockets of significant gene expression. Quorum sensing, T2SS, and iron (non p,p,p), significantly upregulated several genes showing an overall moderate upregulation in its distribution for 20-30% of the regulons. Many quorum sensing genes were affected for the *rhl*, phenazine and *pqs* genes, with the majority showing moderate upregulation. Some of the significantly affected genes include *rhlB* (PA3473) and *pqsA* (PA0096) and *phzF2* (PA1904) (Table 4-3) . In addition, 5/6 genes for α2-macroglobulin homolog operon involved in host evasion were significantly downregulated (Table 4).

C-di-GMP was stochastic with affected genes, showing some significantly downregulated genes as well as a general moderate (1.5 to 2 fold) upregulation of the regulon (60%). Sulfur, pel, pyocyanin, and Type IV pili showed largely no affect with only minor distributions above no fold change.

Marginal affects were seen in other groups including alginate, chemotaxis, nitrogen metabolism and pyoverdine. These groups showed slight upregulation of roughly 20 percent of the regulon including small pockets of significant upregulation and a few down regulated genes.

Significant downregulation was seen for the protease PA0277 (-76 fold), a responder to oxidative stress PA0126 (-29 fold), HCN genes, a hemolysin gene (PA2462), and a histidine

transport ATP-binding protein gene, *hisJ* (PA2923). Two DNA repair genes including *sbcD* (PA4281) was significantly upregulated while *ung* (PA0750) was significantly downregulated. A probable DNA invertase gene for DNA recombination (PA3867) was also significantly upregulated. Genes for Lipase A (PA2862 *lipA*) and Lipase B (PA3997 *lipB*) were both upregulated at just under 2 fold (Table 4).

Several sigma factors and virulence regulators were significantly affected which are involved in alginate, iron uptake, quorum sensing, T6SS, T3SS, virulence as well as cell division. Affected sigma factors include significant upregulation of *algU* (PA0762) for alginate regulation, as well as *fpvI* (PA2387) a sigma factor in pyoverdine uptake, PA4896 for siderophore uptake and two quorum sensing regulators, *mvfR* (PA1003) and *amiC* (PA3364).

Upregulated virulence regulators include *mexR* (PA0424), which negatively regulates multidrug efflux systems, *psrA* a positive transcriptional regulator gene of T3SS, *mvfR* (PA1003), a regulator gene in the quorum sensing path, *tpbA* (PA3885) which negatively regulates biofilm, *mraZ* (PA4421) encoding a transcriptional regulator and cell division protein, *gacA* (PA2586), a response regulator gene, and *wzz* (PA3160), an o-antigen chain length regulator (Table 4-4). As a note*, rsmA* (PA0905) and the central iron regulator gene, *fur* (PA4764), were not changed. Downregulated virulence regulator genes include PA2384, an iron uptake regulator, *ppkA* which regulates T6SS, *pppA* an antagonist of PpkA, *ptrB* a negative regulator for T3SS, *bexR* a virulence bi-stable switch regulator involving the *aprA* toxin gene, and both *rsmZ* and *rsmY*, small RNA regulators (Table 4).

More significant upregulated genes were seen than downregulated that affected metabolism. About 35 different metabolic groups were affected. Most of these were slight with 1-3 genes affected (Table 4-3). Groups with 4 or more genes upregulated include: Valine, leucine, isoleucine degradation (7/47 /genes), arginine and proline metabolism (6/47 genes), butanoate metabolism (4/41 genes), pentose phosphate pathway (6/26 genes), phenylalanine metabolism (6/26 genes), Glycolysis/glucogenesis 4/35, propanoate metabolism 6/47, biosynthesis of amino acids 9/143, pyruvate metabolism 4/59, and carbon metabolism 11/127.

Overview of downregulated ΔΔ genes:

Type 6 secretion system HSI-1 (T6SS HSI-1): ΔΔ showed significant downregulation for nearly the entire regulon with an average of -4.3 fold (Figure 4-10). Almost all of the genes were significantly downregulated. 81% (35/43) of genes were significantly upregulated greater than 2 fold. 9 of these genes were affected over 5 fold. *ppka* was downregulated (-3.5 fold), however, fha1 showed no change in expression compared to WT (1.3 fold) (Table 4).

BexR. The bexR regulon was significantly downregulated with the majority of the distribution below 2 fold. The average of the regulon was -1.7. (Figure 4-10). 11% (2/18) of genes were significantly downregulated greater than 2 fold while 1 gene was downregulated significantly. 28% (5/18) of genes were downregulated moderately. The *bexR* (PA2432) regulator gene was downregulated at -4.6 fold which activates both *aprA* (-1.0 fold) and hydrolase PA1202 (-10.9 fold) and other downstream genes (PA1203 at -1.9 fold).

Psl: ΔΔ distinctly showed significant downregulation of the majority of the regulon giving an average of -1.2 fold). 33% (5/15) of genes in the Psl regulon were significantly down

regulated, greater than 2 fold (Figure 4-1). 27% (5/15) of genes upregulated between 1.5 and 2 fold. The outliers were determined to be PA5452 (*wbpW*) at 1.9 fold, involved in phosphomannose isomerase/GDP-mannose, *algA* at 1.29 fold, and *pslA* at 1.2 fc (Table 4-3).

Type 6 secretion system HSI-2 (T6SS HSI-2): ΔΔ showed significant differentially expressed genes in the T6SS-HIS-2 system with downregulation seen in the majority of the regulon. ΔΔ showed downregulation in this pathway with an average fold change of -1.6 (Table 4-2). 44% (12/27) of genes were downregulated greater than 2 fold. Two genes were moderately downregulated and four moderately upregulated (1.5 to 2 fold). All genes in the order from PA1657 to PA1669 (except PA1667 qt -1.9 fold) were significantly affected ranging from -2 to -5.9 fold decrease in expression (Table 4-3). These genes are all hypothetical.

Bacteriophage pf1: ΔΔ was significantly downregulated for bacteriophage pf1 genes with average of -5.8 (Figure 4-1). 60% (9/15) of genes for ΔΔ were downregulated greater than 2 fold.

Additional affected genes included significant downregulation of the **protease PA0277** at -76 fold and **PA0126**, a key responder gene to oxidative stress at -29 fold.

Toxins for hydrogen cyanide genes ***hcnA/B/C*** were all significantly downregulated at -14 fold, -3 fold, and -2 fold respectively. The hemolysin gene PA2462 was also significantly downregulated at -5.8 fold.

sbcD (PA0750), encoding a base excision repair protein was downregulated -2 fold.

hisJ**,** encoding a histidine transport ATP-binding protein was downregulated -2.3 fold.

The **hemolysin gene PA2462** was also significantly downregulated at -3 fold.

In addition, 5/6 genes for **α2-macroglobulin homolog** operon were significantly down regulated (Table 4).

Overview of upregulated ΔΔ genes:

Type 3 secretion system (T3SS): ΔΔ revealed moderate to low upregulation of T3SS with most of the distribution below around 1.5 fold for an average of 1.1 for the entire regulon (Figure 4-10). Only one gene was upregulated significantly, *exoS* (PA3841) at 2.5 fold. 10% (4/41) of genes were upregulated moderately between 1.5 and 2 fold. These genes included (*pscT, pcrG, pcrH,* and *exsB*). No genes were downregulated (Table 4-1). *ptrB* was found to be significantly downregulated (-2.7 fold) which encodes a protein that acts in deactivating type 3 secretion. The *psrA gene*, encoding an activator of T3SS was significantly upregulated at 3.2 fold.

Pyochelin: ΔΔ was clearly upregulated for pyochelin genes showing most of the distribution of genes upregulated slight under 2 fold with an average of the regulon at 1.9 (Figure 4-10). 27% (3/11) of genes were significantly upregulated while 55% (6/11) were moderately upregulated (1.5 to 2 fold). Significantly upregulated genes include *pchA* (PA4231) at 2.0 fold and *pchB* (PA4230) at 3.4 genes and *fptA* (PA4221) at 2.7 fold (Table 4).

Iron (non p/p/p). The overall distribution shows a slightly greater density of upregulated genes just below 1.5 fold. The average of the regulon is 0.9. 9% (5/58) of genes were significantly upregulated while 29% (17/58) genes were moderately upregulated. The upregulated genes include siderophore mediated iron uptake genes; PA2307 at 2.0 fold, *fpvI* at

2.4 fold, *bfrB* at 2.3 fold, and PA4156 at 2.1 fold. Only a single gene was significantly downregulated and no genes were moderately down regulated. The downregulated gene includes *oprC* at -3.2 fold (Table 4-3, Table 4).

Lipases were upregulated in ΔΔ. Lipase A and Lipase B were both upregulated at just under 2 fold (1.99 FC).

Quorum sensing: Many quorum sensing genes were significantly upregulated including some for *rhl*, *las* and *pqs* genes. The overall distribution shows moderate upregulation for almost 30 percent of genes and slight upregulation for more than 75% of genes. %10 (10/99) genes were significantly upregulated while 17% (17/99) were moderately upregulated. Some of the significantly upregulated genes include *plcH* (PA0844) at 2.9 fold, *braD* (PA1073) at -2.2 fold, *phzD2* (PA1902) at 3.8 fold, *pqsA* (PA0996) at 2.9 fold, *amiC* (PA3364) at 2.6 fold, and *rhlB* (PA3473) at 2.5 fold . *rhlI* was upregulated at 1.7 fold. *mvfR*, a quorum sensing transcriptional regulator gene, was upregulated 2.0 fold. lasI and PA1196 were moderately upregulated showing a 1.4 fold for both genes. *mexG* and *mexH* were moderately down regulated at -1.6 fold and -1.9 fold respectively (Table 4).

Fimbriae: ΔΔ cup genes encoding fimbriae shows upregulation *cupB* and *cupC* genes and downregulation or no change for *cupA* genes. The overall average of all cup genes was 0.96. 21% (2/14) genes. Significantly upregulated genes included *cupC2* at 3 fold, *cupB3* at 3.1 fold. Moderately upregulated genes included *cupB1*,cupB4, and cupB6. No significant downregulation was seen. The two moderately down regulated genes included *cupA1* and *cupA2* (Table 4-3).

Chemotaxis: ΔΔ shows upregulation for some chemotaxis genes with an average of 1.1 fold. 13% 6/45) of genes were significantly upregulated while 22% (10/45) genes were moderately upregulated. No genes were significantly downregulated, and 4% (2/45 genes) were moderately downregulated.

Alginate: Alginate was upregulated for some genes showing a slight upregulation for the pathway at an average of 1.3 fold. 2/28 genes were upregulated significantly, 6/28 were upregulated moderately. Most of the regulon was unchanged. The two significantly upregulated genes include *algU* and PA4033. No genes were significantly downregulated, and 1 gene was moderately downregulated.

Type 2 secretion system (T2SS): T2SS shows moderate upregulation with 9% (4/45) of genes were significantly upregulated and 24% (11/45) of genes were moderately upregulated. No genes were downregulated. The remaining 65% are found just below 15 fold.

Base excision repair proteins/DNA repair: *sbcD* (PA4281) encoding a base excision repair protein/DNA repair was upregulated 2 fold. The DNA invertase/DNA recombination gene **PA3867** was upregulated 3 fold.

Metabolism: A large number of metabolic genes were affected> 2 fold in ΔΔ (Table 4-3). Of these, about five times as many genes were upregulated as compared to downregulated. These ranged across 35 different metabolic groups. Groups that showed an affect of 4 or more upregulated genes include: Valine, leucine, isoleucine degradation (7/47 /genes), arginine and proline metabolism (6/47 genes), butanoate metabolism (4/41 genes), pentose phosphate pathway (6/26 genes), phenylalanine metabolism (6/26 genes), glycolysis/glucogenesis 4/35 ,

propanoate metabolism 6/47, biosynthesis of amino acids 9/143, pyruvate metabolism 4/59, and carbon metabolism 11/127.

Pathways with distinct up and downregulation:

Biofilm (non pel/psl): Significant genes for biofilm are both upregulated and downregulated in ΔΔ. Overall, a pattern could be found that ΔΔ was downregulated in the biofilm pathway related to T6SS and *rsmA* genes, but upregulated in terms of quorum sensing and *gacA* genes.

The main distribution of biofilm genes in ΔΔ is seen slightly above zero. Pockets of significantly up and downregulated genes are expressed with a greater distribution of significant genes that are downregulated (Figure 4-10). The average of the regulon is-0.7 fold. 23% (21/91) of genes were significantly downregulated while 4% (4/91) were moderately downregulated. Of the downregulated genes greater than 2 fold in ΔΔ, 13 genes belong to T6SS HSI-1, 4 genes to T6SS HSI-2, and two genes to T6SS HSI-3.

8% (7/91) of genes were significantly upregulated while 12% (11/91) of genes were moderately upregulated. The six upregulated genes greater than 2 fold include the following, *gacA* involved in the regulation of biofilm, *rhlB* involved in quorum sensing, *mvfR*, encoding a transcriptional regulator, and two genes that are part of the HptB dependent secretion system. Additionally, 10 genes were upregulated for ΔΔ between 1.5 and 2 fold including 3 genes from the *wsp* operon and *alg44*. Two genes included *pqsB* and *phnB* associated with quorum sensing. In addition, ΔΔ downregulated both *siaA* and *siaD* genes with *siaA* (PA0172) at -2.2 fold and

siaD (PA0169) at -2.8 fold. Downregulation was also moderately seen on the *cdrA/B* genes with *cdrA* (PA4625) downregulated at -1.4 fold and *cdrB* (PA4624) at -1.4 fold (Table 4-3, Table 4).

Two-component regulatory system (TCS): of the 202 genes in this regulon, 18 were significantly upregulated (32 moderately). 6 genes were significantly downreguled (14 moderately). The upregulated TCS genes overlapped with several other pathways. For upregulated genes, five TCS genes are involved in C4-dicarboxylate transport, five in chemotaxis, three in biofilm, three as regulators and one in iron uptake. The six significantly down regulated genes were found to be exclusively apart of Cytochrome c/b genes (Table 4).

Denitrification: Denitrification showed general upregulation which included the *nos*, *nar* and *nor* operons. Marginal downregulation of denitrification was seen in the *nap* operon. Denitrification shows most of the distribution is upregulated with almost half being greater than 1.5 fold.4% One gene was significantly upregulated while 42% (11/26) of genes were moderately upregulated. The *nos* genes were significantly downregulated while three from the *nap* operon were downregulated moderately (Table 4).

C-di-GMP: C-di-GMP genes were stochastic with affected genes, showing several significantly downregulated genes along with a general moderate upregulation of the regulon. 10.5% (2/19) of genes were significantly downregulated greater than 2 fold. 26% (5/19) were moderately upregulated between 1.5 to 2 fold (Figure 4-1) (Table 4).

Notable pathways with no major effect:

Pel: ΔΔ did not present any significant regulation (average -0.1 fold) (Figure 4-10).

Pyoverdine: Most genes were unchanged with a small pocket of significant genes that are upregulated and a single gene that was significantly downregulated. The average of the regulon is 0.04 fold. 12% (3/26) of genes were upregulated significantly while 15% (4/26) were upregulated moderately. Significantly upregulated genes include *pvcA*, *pvcD* and *tonB1*, the energy transducer for pyoverdine was upregulated 2.3 fold and *fpvI*, encoding a sigma factor for pyoverdine was upregulated 2.4 fold. *fpvR*, encoding the anti-sigma factor was not changed. 4% (1/26) of genes were downregulated significantly with 12% (3/26) of genes downregulated moderately. The significantly down regulated gene included *fpvA* , the pyoverdine receptor by -3.9 fold. *pvdS* was downregulated by -1.9 fold (Table 4-3)

Pyocyanin: ΔΔ did not show significant regulation changes in the pyocyanin pathway (average of 1.0 fold). Out of 17 total genes in the regulon, one gene, *phzF2*, was significantly upregulated greater than 2 fold. One gene was moderately upregulated and one downregulated between 1.5 and fold.

Sulfur: Overall, the majority of this distribution was insignificant with the majority of its gene distribution above and below a fold change of 1 with an overall average of 0.6. The one significant gene that was upregulated was PA2595 at 3.3 fold. ΔΔ showed downregulation of a specific pocket of *cys* operon genes including *cysA* at -2.1 fold, and *cysI* at -3.1 fold. An additional gene in the same operon which was closely regulated was *cysW* at -1.95 fold (Table 4-3, Table 4).

Type IV Pili had little affect with slight upregulation for some genes. 6/34 genes were upregulated between 1.5 and 2 fold.

Flagella: Only 2/47 genes were affected in the flagella pathway indicating not much change. 2/47 genes were significantly upregulated, *motA* (PA4854) and PA3526. Most genes had no change, and no genes were downregulated.

Sigma factors and Virulence regulators:

Sigma factors were slightly upregulated for some genes in ΔΔ. 3/31 genes were significantly upregulated, eight were upregulated moderately. Only one gene was moderately down regulated. Significantly affected upregulated genes included ***algU*** (PA0762) at 2.3 fold, ***fpvI*** (PA2387) at 2.4 fold, and **PA4896** involved in iron uptake for pyocin at 6 fold.

Virulence Regulators: Significant genes were both up and downregulated in ΔΔ with more genes being upregulated. 8/95 genes were significantly upregulated while 17/95 genes were moderately upregulated. Several genes were significantly upregulated including ***mexR*** **(2.9 fold),** ***psrA*** **(3 fold),** a quorum sensing transcriptional regulator gene**,** ***mvfR*** (2 fold), a quorum sensing repressor gene**,** ***qscR*** (1.9 fold), and ***amiC*** (PA3364 2.6 fold). ***tpbA*** **(2 fold)** encoding a repressor of biofilms with significantly upregulated. ***mraZ*** (PA4421) encoding a transcriptional regulator and cell division protein was upregulated 2 fold and ***gacA*** at 2 fold, and an o-antigen chain length regulator, ***wzz*** (PA3160) at 2 fold.

9/100 were significantly down regulated while 2/100 were moderately. Some of significantly down regulated genes include ***ppkA*** (-3.5 fold), ***ptrB*** (-2.7 fold), and ***bexR*** (-4.5 fold), ***pppA*** (-3.7 fold), **PA2384** (-2.2 fold) a response regulator for iron uptake, a haemolysin regulator **PA2463** (-2.9 fold). ***rsmZ*** was downregulated by -4 fold. ***rsmY*** was downregulated by -

2 fold. ***rsmA*** was not changed. A full list of genes affected and their fold change values are in Table 4.

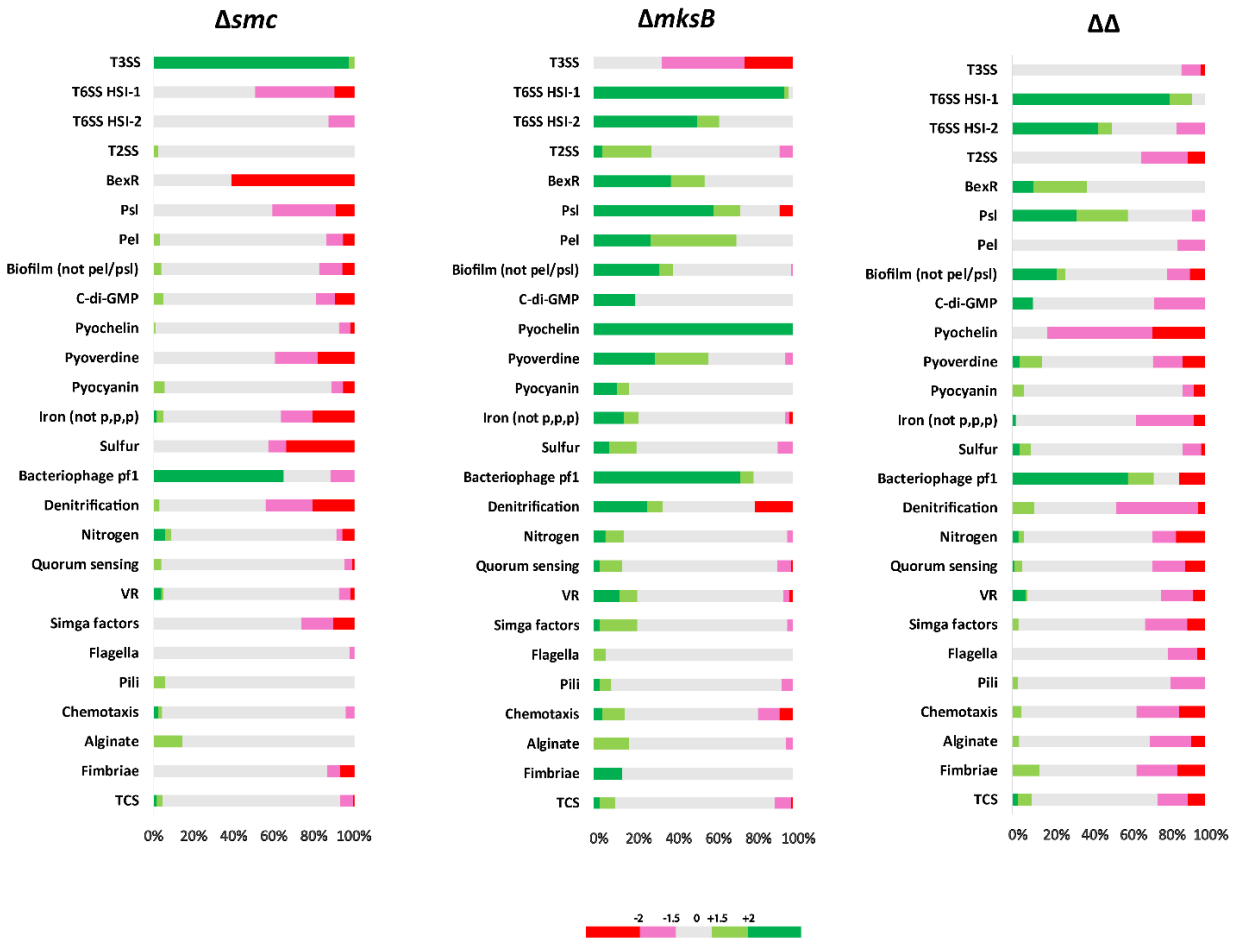

Figure 4- 11: Summary of affected pathways for each PAO1 condensin deletion strain.

Affected pathways summarized in a plot as the percent of total genes in each path that are changed by either 2 fold, 1.5 to 2 fold, or no change (Figure 4-2).

4.8 Comparison of relative expression levels in pathways for condensin mutant strains shows both an overlap and marked differences

Δ*mksB* and Δ*smc* are oppositely regulated for biofilm (non pel/psl), psl, T3SS, T6SS HSI-I, the BexR regulon and α2-macroglobulin homologs. ΔΔ expression overlaps with Δ*mksB* in these pathways while showing unique upregulation of some biofilm genes. Δ*mksB* and ΔΔ expression levels in T3SS are overlapped and directly opposite to the expression levels of Δ*smc*. Both *ΔmksB* and ΔΔ moderately increase expression levels in T3SS while Δ*smc* shows a marked reduction (Figure 4-1). The opposite trend is seen for T6SS HSI-1, where both *ΔmksB* and ΔΔ are overlapped showing significant downregulation, while Δ*smc* is moderately upregulated (Figure 4-10). This same pattern of overlap is observed for several pathways including T6SS HSI-2, BexR and psl (Figure 4-10, Figure 4-11). It should be noted that the ΔΔ strain shows less pronounced expression level changes in these pathways when overlapped as seen in their averages for each regulon (Table 4-2) and general expression levels (Table 4). This observation also holds when observing effector expression levels (Figure 4-12).

Overlap between Δ*mksB* and ΔΔ is also seen in the biofilm pathways. In this path, Δ*smc* shows pockets of upregulation while Δ*mksB* has a larger distribution of genes that are downregulated. ΔΔ shows both up and downregulated genes (Figure 4-11). The downregulated genes overlap with those in Δ*mksB* but the upregulated genes occur in a different set other than those affected in Δ*smc*. Therefore, ΔΔ shows overlap with Δ*mksB* for down regulated biofilm genes, while having unique divergence for some upregulated biofilm genes. Several toxins and genes for host evasion genes were downregulated in both Δ*mksB* and ΔΔ, including HCN toxins, hemolysin (PA2462) protease (PA0277), a stress hydrolase (PA1202)

and the α2-macroglobulin homolog genes. Δ*smc* showed significant upregulation for the PA0277 protease and PA1202 hydrolase and a moderate upregulation of hemolysin as well as all α2-macroglobulin homolog genes.

Δ*mksB* and Δ*smc* are oppositely regulated for several iron uptake genes and specific operons in denitrification. ΔΔ shows overlap for both strains in the pyoverdine path, while primarily showing overlap with Δ*smc* in the iron (non p,p,p) and denitrification groups. In addition, ΔΔ uniquely shows moderate upregulation of an additional denitrification operon. In the pyoverdine pathway, ΔΔ shows a combination of overlap for both Δ*mksB* and Δ*smc*. Δ*smc* shows a clear general upregulation while Δ*mksB* shows significant downregulation. In the ΔΔ strain, the overall result is a stochastic effect in regulation for pyoverdine pathway with no major shift in overall distribution (Figure 4-10). Δ*smc* is significantly upregulated for many genes in the iron (non p,p,p) path while Δ*mksB* shows many significantly down regulated genes. ΔΔ shows overlap with Δ*smc* for many of the affected upregulated genes (Table 4). Denitrification shows a large set of upregulated genes in Δ*smc* that is associated with the *nor* and *nos* gene operons. Δ*mskB* shows downregulation of genes in the *nap* operon and upregulation for genes in the *nos* operon. ΔΔ expression levels shows overlap between both Δ*mksB* and Δ*smc* with upregulation in the *nor* and *nos* operons and downregulation of the *nap* operon. In addition to this overlap, ΔΔ also uniquely shows moderate upregulation of genes in the *nar* operon. As a note, ΔΔ expression levels are more moderate compared to either strain (Table 4).

Similar regulation for all strains: Bacteriophage pf1 genes showed similar expression patterns for all three strains. Genes are overlapped between all three strains showing

significant downregulation. HCN toxins were reduced in all strains, although substantially more for Δ*mksB* and ΔΔ compared to Δ*smc*.

All three strains show unique regulation in certain pathways. For the sulfur pathway, Δ*smc* shows upregulation and Δ*mksB* shows downregulation. ΔΔ is stochastically regulated with no overlap for either Δ*mksB* or Δ*smc* and is overall, marginally affected. The ΔΔ strain shows a marked divergence from either single deletion for the majority of the pyochelin pathway which is expressed at an average of almost 2 fold while Δ*mksB* is markedly reduced and Δ*smc* shows no change. Quorum sensing genes were for the most part unaffected in both Δ*smc* and Δ*mksB* with exceptions in some outlier genes. ΔΔ shows a clear but moderate upregulation indicating ΔΔ uniquely regulates aspects of quorum sensing. Flagella, Type IV pili, chemotaxis and alginate show no change in Δ*smc*, and nominal downregulation of some genes in Δ*mksB*. ΔΔ shows unique upregulation of pockets of genes in these regulons. Proteases on average are moderately increased in Δ*smc* while decreased in Δ*mksB* and not affected in ΔΔ (Figure 4-5). Lipases show increased expression for ΔΔ but no change for the other strains (Figure 4-5). Nitrogen metabolism showed clear downregulation in Δ*mksB* however, Δ*smc* and ΔΔ are both stochastically regulated. For the nitrogen pathway, there is little overlap between the three strains (Table 4).

Overall, Δ*smc* and Δ*mksB* revealed opposite expression trends for growth and virulence genes as well as the major secretion systems, T3SS and T6SS. ΔΔ revealed overlap for Δ*mksB* for growth and secretion systems while showing overlap with Δ*smc* for iron uptake genes. In addition, Large groups of genes were uniquely expressed across all samples indicating independent regulatory pathways.

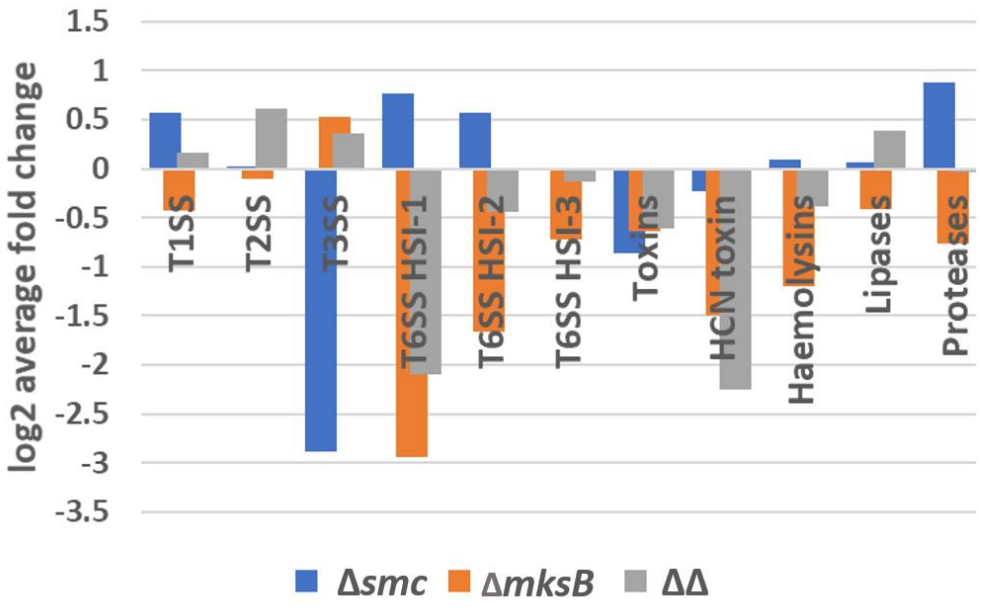

Figure 4- 12: Average fold change of virulence effectors.

4.9 Many affected virulence regulators show both overlap and marked differences between strains

The fold change values for affected virulence regulators and sigma factors are plotted in Figure 4-13. For iron uptake regulators, Δ*smc* showed significant upregulation while ΔΔ showed generally moderate increases (except for PA2384). Δ*mksB* was for the most part, downregulated for regulators in iron uptake (Figure 4-5). PA4896, a sigma factor for pyocin, was significantly upregulated in both Δ*smc* and ΔΔ and moderately upregulated in Δ*mksB*. Δ*smc* significantly upregulated the sigma factor for pyoverdine regulation, *pvdS*. In contrast Δ*mksB* was significantly decreased and ΔΔ decreased slightly. The haem uptake regulator *hasI* (PA3410), was significantly upregulated in Δ*smc* and nearly 2 fold in ΔΔ while *ΔmksB* was

negligible. PA1300, encoding a haem uptake regulator gene (similar to *fecI)* as well as *fiuI* (PA0472), encoding a regulator for ferrichrome uptake, was significantly upregulated in Δ*smc* and marginally upregulated in ΔΔ. In contrast, Δ*mksB* showed no effect for PA1300 and was significantly decreased in *fiuI* (PA0472). *fpvI*, encoding a sigma factor for pyoverdine, was significantly down regulated in ΔΔ and moderately in Δsmc. PA2050, involved in metal uptake, showed a moderate increase in expression for Δ*smc* and a slight decrease in expression for ΔΔ. *pchR* was significantly downregulated in Δ*mksB* with no effect seen in Δ*smc* or ΔΔ (Figure 4-5). PA2384, a Probable Fur, Fe^{2+}/Zn^{2+} uptake regulation protein gene, was significantly downregulated in both Δ*mksB* and ΔΔ.

Overlap between Δ*mksB* and ΔΔ is seen for several regulators related to biofilm and the T6SS HSI-1 pathways which is opposite to Δ*smc* expression, with the exception of the ppyR regulator. The *siaA* and *siaD* and *cdrA* and *cdrB* genes as well as *ppkA* and *pppA* regulators were downregulated in both Δ*mksB* and ΔΔ and upregulated in Δ*smc* coinciding with the regulatory pattern in the biofilm pathways. Interestingly, *ppyR*, a regulator for psl production and pyoverdine, was moderately upregulated in Δ*smc* and significantly up regulated in Δ*mksB* which is in conflict with the expression levels seen from both psl and biofilm (non pel/psl). The alginate regulators, *algU*, and the alginate/twitching motility regulator, *amrZ* ,were upregulated in ΔΔ. However, *tbpA*, which encodes a protein that acts as a negative repressor of biofilms, was significantly upregulated in ΔΔ with no affect in the other strains (Figure 4-5).

The *bexR* regulator gene (PA2432) was downregulated in both Δ*smc* and ΔΔ while upregulated almost 9 fold in Δ*smc*. This regulon is a bi-stable switch for virulence factors

including genes *apr*A, protease PA1202. *vreI*, another virulence regulator gene, was also down regulated in Δ*mksB* however, no affect was seen in other strains.

Regulators for T3SS showed overlapped expression levels for Δ*mksB* and ΔΔ which were opposite to Δ*smc* regulation. Both Δ*mksB* and ΔΔ showed reduced expression of several T3SS regulators while Δ*smc* showed increased expression. Both Δ*mksB* and ΔΔ showed significant decreased expression of *ptrB*, a repressor of the T3SS, while Δ*smc* was upregulated coinciding with the T3SS pathway being decreased in Δ*smc* and increased in Δ*mksB* and ΔΔ. In addition, Δ*smc* showed significantly decreased expression of the *exs* genes involved in regulating ExsA, an activator for T3SS. These genes include *exsE/C/D/A*. In contrast, these genes were moderately upregulated for both Δ*mksB* and ΔΔ. *exsC* was significantly upregulated in Δ*mksB.* In addition, the gene for the *psrA* activator of ExsA was upregulated in ΔΔ, highlighting another manner in with T3SS could be switched on.

rsmZ and *rsmY* were significantly down regulated for all three strains (zero for *rsmY* Δ*smc*). The *gacA* gene was significantly upregulated for ΔΔ but no affect was seen for the other strains. *rsmA* was significantly down regulated in Δ*mksB* and significantly upregulated in ΔΔ with no change in Δ*smc*. Downregulation of *rsmZ* and *rsmY* does not look attributable to GacA. RsmA regulation, however, could be affected from a lack of sequestering by rxmZ and rsmY.

Several quorum sensing regulators and genes were upregulated in ΔΔ. Δ*mksB* showed marginal change and ΔΔ was largely unaffected. In Δ*mksB*, the *qscR* and *qteE* repressor genes were significantly downregulated, including a gene for the LasI autoinducer. ΔΔ showed significant upregulation in the quorum sensing regulator genes, *mvfR*, *amiC* and the *qscR*

quorum sensing repressor. Several genes were affected including the *rhlI* and *lasI* autoinducer genes (Table 4-4).

Interestingly, ΔΔ uniquely showed upregulation of the alginate regulator (*algU* (PA0762) and the alginate and twitching motility regulator, *amrZ* (PA3385)), a multidrug resistance operon repressor gene, *mexR* (PA0424), a gene encoding a regulator and cell division protein, *mraZ* and an O-antigen chain length regulator gene, *wzz* (PA3160).

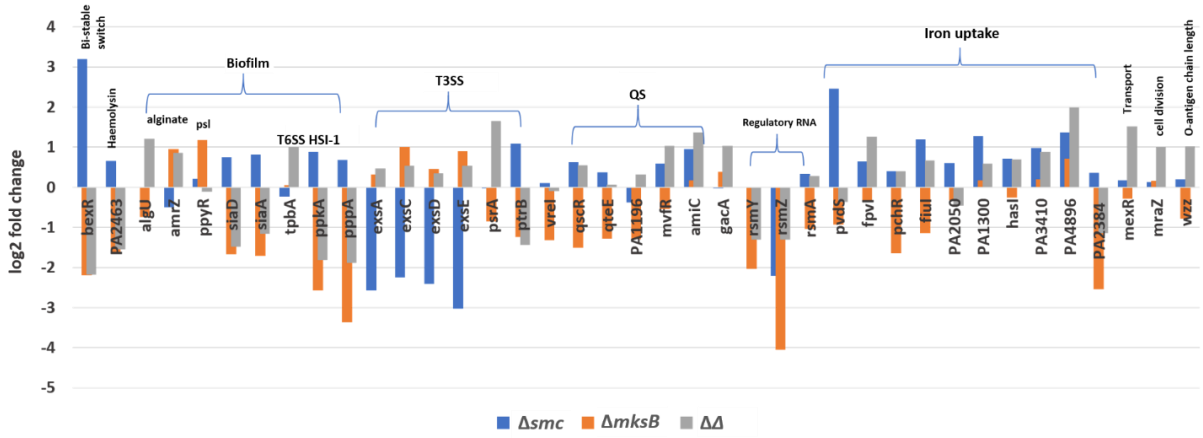

Figure 4- 13: log2 fold change of virulence regulators and sigma factors.

4.10 Condensin Mutant Profiles Summary

Each condensin mutant exhibits a unique transcriptomic profile

Analysis of the differentially expressed genes in these pathways revealed unique regulation for each condensin mutant (Figure 4-14). For many of these pathways, opposite regulation was seen between Δ*smc* and Δ*mksB* condensin mutants . Intriguingly, Δ*smc* followed patterns of chronic infection (sessile/biofilm growth state with enhanced T6SS) and

Δ*mksB* followed patterns for acute infection (planktonic growth state with enhanced T3SS) (Figure 4-6). Major pathways that were oppositely regulated included T3SS, T6SS HSI-1, BexR, iron uptake, biofilm formation (psl, hemagglutinin) and sulfur metabolism.

ΔΔ showed overlap with Δ*mksB* that was opposite to Δ*smc* for many pathways related to growth and secretion systems including the T6SS, T3SS, bexR, biofilm formation (psl and hemagglutinin). In contrast, ΔΔ overlapped with Δ*smc* for several iron regulation genes (iron sigma factors/regulators, TonB1 and siderophore mediated iron uptake). Interestingly, ΔΔ also showed unique expression for several pathways and genes.

Overall, all three strains maintained unique profiles including the ΔΔ strain which reflected more than just the sum of the single deletions. The unique regulatory patterns for each strain was partially indicated previously with a Venn diagram depicting 2 fold overlap of significant genes (Figure 4-3). This reveals that condensin regulation is more than additive and includes independent regulatory pathways.

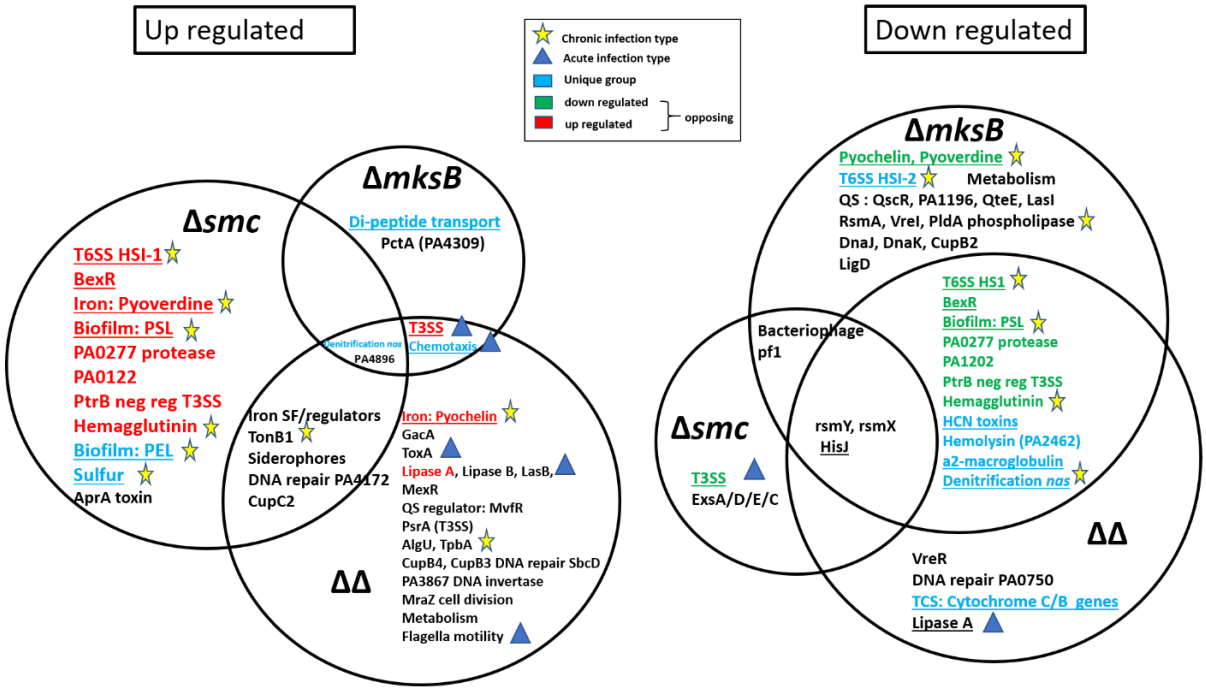

Figure 4- 14: Venn diagram showing overlapping pathways and genes for PAO1 condensin strains.

4.11 Regulators correlate with many pathways affected in condensin deletions

Many regulators show relative expression levels that correlate with down stream pathways. Figure 4-6 maps regulators with expected down stream phenotypes as reported in literature along with the fold change for each mutant.

Both the *ptrB* repressor and *exsA* activator show correlation of expression levels with T3SS in all three strains as indicated (Figure 4-6). The *pchR* regulator for pyochelin correlated with expression levels of the pyochelin regulon for Δ*mksB*. *pchR* upregulated slighly at 1.3 fold for both the Δ*smc* and ΔΔ strains however, the expression levels for pyochelin were differed. Δ*smc* was slightly downregulated for pyochelin while ΔΔ was moderately upregulated, including

several signficantly affected genes. Therefore no correlation was seen in Δ*smc* and only a slight correlation is seen for ΔΔ.

Pyoverdin matched well with the expression levels of *pvdS* and the pyoverdin regulon for both Δ*smc* as well as Δ*mksB*. On account of the stochastic up and downregulation of pyoverdin genes in ΔΔ, *pvdS* only partially correlated with phenotype in ΔΔ.

Expression of the *bexR* regulator (PA2432) correlated very well with nearly all genes in the BexR regulon with the highest correlation with PA1202 for all mutants. An exception is seen for the *aprA* toxin gene which is strain dependent. In Δ*smc*, expression levels of the *aprA* toxin gene strongly correlated with the *bexR*, however, at a lower magnitude (9 fold vs 2 fold). In Δ*mksB, bexR only* moderately correlated with expression of *aprA* whereas, no correlation was seen in ΔΔ.

RsmA pathway: *rsmZ* and *rsmY* sequester RsmA, resulting in sessile characteristics including T6SS production, biofilm, and pel/psl production. In addition, sequestering results in increased pyocyanin and HCN production. In contrast, free RsmA produces planktonic phenotypes including T2SS, T3SS, cell motility and lipases. *rsmY* and *rsmZ* were signficantly downregulated for all strains (*rsmY* = 0 in Δ*smc*). In addition rsmA was signficiantly downregulated in Δ*mksB* while unchanged in Δ*smc* and ΔΔ. *rsmY/Z* and *rsmA* expression levels do are not correlate with phenotypes in Δ*smc* which shows expression patterns related to a sessile lifstyle, slight reductions in HCN genes and no change in pyocyanin. *rsmY and rsmZ* are correlated with phenotypes *in* Δ*mksB* which shows reduced biofilm regulation, reduced HCN and upregulated T3SS.

For the ΔΔ strain, the RsmA pathway is correlated with phenotypes related to the planktonic state however, it is only partially correlated with the pycyanine phenotype which is stochastic in ΔΔ.

The T6SS and biofilm formation pathways are highly connected in which they share many genes for both pathways. The *siaA*/*siaD* genes directly affect c-di-GMP levels which in turn promotes biofilm formation. Expression levels of *siaA* and *siaD* shows a strong correlation to biofilm phenotype for all three strains. This is also true for the *cdrA/B* genes which also promotes biofilm formation by activating psl production.

ppyR, a regulator for pyoverdine and an activator of psl production (and biofilm) shows increased expression in Δ*mksB* and no change for the other strains. This regulator shows a negative correlation with expression levels of psl in Δ*mksB* strain, and no correlation with the other strains.

T6SS HSI-1 is regulated by the phophorlation of the FHA domain of the Fha1 protein by the PpkA regulator. Its antagonist is the PppA regulator. For all strains, *ppkA* shows a strong correlation for T6SS expression. *pppA* shows no correlation despite its high expression changes in all strains.

For quorum sensing regulators in condensin deletion strains, correlation is only partial for phenotypes and is strain dependent. No correlation was seen for *vreI* which acts on the LasR regulator. In addition, no correlation was seen for *qteE*, encoding a repressor of LasR, as well as *qscR,* which encodes a repressor of LasR and RhlR. Downregulation of PA1196 in Δ*mksB* was correlated with reduced *hcn* genes and the *aprA* toxin gene. However, there was no

correlation for the expression of *xcpP/R, lasB*, *toxA* or pyocyanin expression levels. PA1196 shows no correlation for the other strains.

MvfR positively regulates a number of downstream genes including T6SS HSI-2 , aprA, xcpP, lasB, toxA, hcn genes (through PQS), pyocyanin (through PQS), rhlA/rhlB (through PQS and LasRI/RhlRI regulation), lasA, xcpR, rpoS. In addition, it negatively regulates the T6SS HSI-1 system. For all strains, *mvfR* was only partially correlated with phenotype. *mvfR* was upregulated by 2 fold in ΔΔ which correlated with upregulation of *lasB*, *toxA*, and *xcpP* and significant downregulation of T6SS HSI-1. *mvfR* however, did not correlate with other downstream phenotypes.

In Δ*smc, mvfR* was only moderately correlated with the expression of the *aprA* toxin gene but no other phenotypes. Similarly, in Δ*mksB*, *mvfR* was only correlated with reduced HCN gene expression, but no other phenotypes.

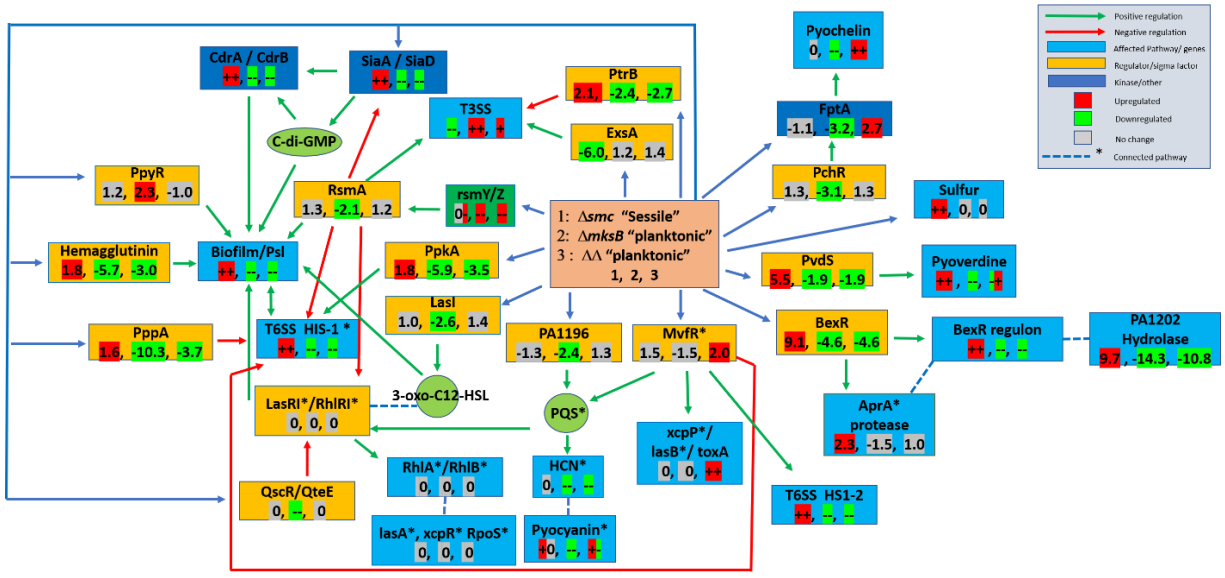

Figure 4- 15: Map of pathways and regulators related to their expression levels. A diagram depicting the expression levels of regulators in orange and pathways in blue. Post translational regulators are marked in dark blue. Green arrows indicate positive regulation, red negative regulation. The three numbers in each box correlate to each condensin mutant. On the left, 1, represents the fold change value for Δ*smc*, 2 represents the fold change value for Δ*mksB* and 3 represents the fold change value for ΔΔ. * indicates connected pathways. The effect of RsmA is conditionally based on if it is sequestered by *rsmY* and *rsmX* and is represented with dashed lines.

Table 4- 3 Number of significant and moderately affected genes in each pathway. Table for the number of genes having fold changes of a minimum of 2 fold or between 1.5 and 2 fold for each strain for the indicated pathways. Pathways shown include those with at least one significantly affected gene (>=2 fold) across samples.

Pathways	*Δsmc* up 2 fold change	*Δsmc* up 1.5-2 fold change	*Δsmc* down 1.5-2 fold change	*Δsmc* down 2 fold change	*ΔmksB* up 2 fold change	*ΔmksB* up 1.5-2 fold change	*ΔmksB* down 1.5-2 fold change	*ΔmksB* down 2 fold change	*ΔΔ* up 2 fold change	*ΔΔ* up 1.5-2 fold change	*ΔΔ* down 1.5-2 fold change	*ΔΔ* down 2 fold change	# genes
Type I Secretion System	1	1	0	0	0	0	2	0	0	1	0	0	5
Type 3 Secretion System	0	0	1	40	10	17	0	0	1	4	0	0	41
Type 6 secretion system HSI-1	7	28	0	0	0	0	1	41	0	0	5	35	43
Type 6 Secretion System HSI-2	0	4	0	0	0	0	3	14	0	4	2	12	27
Type 6 Secretion System HSI-3	2	6	1	0	0	0	2	11	1	3	4	2	26
Type 2 Secretion System	0	0	1	0	0	3	11	2	4	11	0	0	45
BexR Regulon	11	0	0	0	0	0	3	7	0	0	5	2	18
Psl exopolysaccharide	2	7	0	0	1	0	2	9	0	1	4	5	15
Pel exopolysaccharide	1	3	0	0	0	0	3	2	0	1	0	0	7
Biofilm formation (non pel/psl)	6	12	4	0	0	1	6	30	7	11	4	21	91
C-di-GMP signalling pathway	2	2	1	0	0	0	0	4	0	5	0	2	19
Pyochelin	0	0	4	0	0	0	0	11	3	6	0	0	11
Pyoverdine	6	7	0	0	0	1	7	8	3	4	3	1	26
Pyocyanin	1	1	1	0	0	0	1	2	1	1	1	0	17
Iron Acquisition (non p/p/p)	15	12	2	1	1	2	4	8	5	17	0	1	58
Sulfur relay system	1	1	2	1	0	3	1	0	5	7	1	0	19
Sulfur metabolism	19	5	0	0	0	4	7	4	1	5	3	2	51
Bacteriohage pf1	0	2	0	11	0	0	1	11	2	0	2	9	15
Denitrification	7	8	1	0	5	0	2	7	1	11	3	0	26
Nitrogen metabolism (no denitrification)	2	1	1	2	0	1	3	2	5	4	1	1	33
Quorum sensing	1	4	4	0	1	7	11	3	10	17	4	1	99
Virulence Factors	13	20	8	3	0	5	20	47	13	37	10	16	223
Virulence Regulators	3	7	1	4	2	3	9	14	8	17	1	8	95
Sigma Factors	4	6	0	0	0	1	6	1	3	7	1	0	31
Flagellar assembly	0	1	0	0	0	0	3	0	2	7	0	0	47
Type IV pili	0	0	2	0	0	2	2	1	0	6	1	0	34
Bacterial chemotaxis	0	2	1	1	3	5	5	2	6	10	2	0	45
Alginate	0	0	4	0	0	1	5	0	2	6	1	0	28
Fimbriae	1	1	0	0	0	0	0	2	2	3	2	0	14
Two-component system	1	14	7	3	2	17	16	6	18	32	14	6	202
α2-macroglobulin homolog synthesis	0	6	0	0	0	0	0	6	0	0	1	5	6
Lipases	0	1	0	0	0	0	3	1	0	2	0	0	7
HCN toxin	0	0	0	0	0	0	0	3	0	0	0	3	3
Haemolysins	0	1	0	0	0	0	0	1	0	0	0	1	2
Proteases	2	0	0	0	0	0	2	2	2	1	0	1	11
Toxins	1	1	0	3	0	2	2	5	1	1	0	5	13
Phospholipases	0	1	0	0	0	0	2	1	0	1	0	0	5
Phenazine biosynthesis	1	2	2	0	0	0	3	3	2	5	2	0	29
Ribosome	0	0	1	1	0	2	0	1	1	1	5	1	68
RNA degradation	0	0	0	0	0	1	1	2	1	2	1	0	15
Protein export	0	0	0	0	0	1	0	1	0	1	1	1	18
Base excision repair	1	0	0	0	0	0	0	0	1	0	0	1	13
Non-homologous end-joining	0	0	1	0	0	0	0	1	0	0	0	0	2
Adherence: LPS O-antigen	0	0	0	0	0	0	2	1	2	4	0	0	20
Rhamnolipid biosynthesis	0	0	1	0	0	0	1	0	1	0	0	0	3
Peptidases	1	0	0	0	0	0	2	0	0	2	0	0	6
Lipopolysaccharide biosynthesis proteins	0	0	0	0	0	0	1	0	1	0	0	0	1
Polyketide biosynthesis proteins	0	0	1	0	0	0	0	1	0	1	0	0	1
Transcription factors	0	0	0	0	1	2	11	3	5	20	1	0	81
Transcription machinery	4	5	0	0	0	2	6	1	4	6	1	0	26
Transfer RNA biogenesis	0	1	0	0	0	1	0	0	1	0	0	0	7
Chaperones and folding catalysts	0	0	0	0	0	0	0	3	1	5	0	0	15
Chromosome and associated proteins	0	0	0	0	0	1	1	0	1	7	0	0	28
DNA repair and recombination proteins	0	0	0	0	0	1	0	0	1	1	0	0	7
Exosome	0	0	1	0	0	1	0	1	0	2	0	0	5
Antimicrobial resistance genes	0	4	1	1	0	0	4	5	7	8	2	1	49
Glycolysis / Gluconeogenesis	1	2	0	0	1	3	2	2	4	9	2	1	35
Citric acid cycle (TCA cycle)	0	3	0	0	1	3	2	1	2	5	4	0	31
Pentose phosphate pathway	1	1	1	0	1	1	2	1	6	1	1	0	26
Biosynthesis of unsaturated fatty acids	0	0	0	0	0	1	1	1	0	2	0	0	13
Biosynthesis of siderophore group nonribosomal peptides	0	0	1	0	0	0	0	6	2	4	0	0	7
Biosynthesis of secondary metabolites	5	9	10	0	5	36	18	18	24	55	19	9	336
Microbial metabolism in diverse environments	5	15	7	3	5	21	30	13	29	49	14	4	280
Biosynthesis of antibiotics	5	10	8	1	3	28	16	13	23	38	20	5	267
Carbon metabolism	0	6	3	0	2	17	7	6	11	17	8	5	127
2-Oxocarboxylic acid metabolism	1	0	1	0	1	2	0	2	3	4	0	0	30

Pentose and glucuronate interconversions	0	0	0	0	0	1	2	0	1	1	1	0	7
Galactose metabolism	0	1	0	0	0	0	1	0	1	0	1	0	5
Fatty acid biosynthesis	0	2	0	1	1	9	2	2	0	4	0	1	26
Fatty acid degradation	0	2	2	0	0	5	4	2	3	8	0	0	32
Synthesis and degradation of ketone bodies	2	1	1	0	0	2	2	1	0	2	0	0	10
Ubiquinone and other terpenoid-quinone biosynthesis	1	0	0	0	0	1	0	2	1	3	0	0	18
Oxidative phosphorylation	2	2	1	1	2	10	3	1	3	3	7	6	57
Arginine biosynthesis	0	1	1	0	0	1	0	4	2	4	1	0	29
Purine metabolism	0	0	4	0	1	7	3	2	4	9	3	0	84
Pyrimidine metabolism	0	0	4	0	0	8	2	2	1	1	1	0	45
Alanine, aspartate and glutamate metabolism	1	1	3	0	0	7	2	0	2	4	3	0	37
Glycine, serine and threonine metabolism	3	2	1	1	1	6	1	2	2	9	5	4	49
Monobactam biosynthesis	1	0	0	0	0	0	0	1	1	0	1	0	9
Cysteine and methionine metabolism	1	1	0	0	0	2	2	2	0	3	5	1	41
Valine, leucine and isoleucine degradation	3	5	1	0	1	5	9	2	7	8	1	0	47
Geraniol degradation	0	1	1	0	0	1	1	0	3	6	0	0	16
Valine, leucine and isoleucine biosynthesis	0	0	1	0	1	0	0	1	2	4	0	0	20
Lysine biosynthesis	0	0	0	0	0	0	0	2	2	0	0	0	15
Lysine degradation	0	2	1	0	0	4	3	0	0	4	1	0	19
Arginine and proline metabolism	2	1	1	2	2	1	5	3	6	5	9	0	47
Histidine metabolism	0	2	1	0	0	2	2	1	2	7	2	0	24
Tyrosine metabolism	2	1	0	0	0	1	2	3	2	9	1	0	27
Phenylalanine metabolism	1	1	0	0	1	3	1	1	6	8	1	0	26
Tryptophan metabolism	0	2	2	0	1	3	6	0	1	7	2	0	27
Phenylalanine, tyrosine and tryptophan biosynthesis	0	0	0	0	0	2	1	0	1	9	1	0	30
beta-Alanine metabolism	1	1	2	1	1	5	4	2	3	3	3	0	26
Taurine and hypotaurine metabolism	2	2	1	0	0	0	3	1	0	1	0	0	9
Phosphonate and phosphinate metabolism	0	1	1	0	1	0	2	0	1	1	0	0	10
Cyanoamino acid metabolism	0	1	3	0	0	2	1	3	0	1	0	5	11
Glutathione metabolism	0	2	1	0	1	1	2	1	2	5	2	0	26
Starch and sucrose metabolism	1	0	1	0	0	0	2	2	1	5	1	0	16
Amino sugar and nucleotide sugar metabolism	0	2	0	0	0	1	6	0	2	4	3	0	36
Streptomycin biosynthesis	0	0	0	0	0	0	0	0	1	1	0	0	8
Peptidoglycan biosynthesis	0	0	0	1	0	0	0	0	0	2	0	0	20
Glycerolipid metabolism	0	0	0	1	0	0	0	1	0	6	0	0	14
Glycerophospholipid metabolism	0	1	0	0	0	0	1	4	1	4	1	2	28
alpha-Linolenic acid metabolism	0	0	0	0	0	0	0	0	1	0	0	0	3
Sphingolipid metabolism	0	0	0	0	0	0	0	1	0	0	0	0	2
Pyruvate metabolism	1	5	1	0	2	8	7	2	4	13	2	0	59
Xylene degradation	0	0	0	2	0	0	3	0	0	0	1	0	5
Chloroalkane and chloroalkene degradation	0	0	0	0	0	0	0	1	0	1	0	0	8
Naphthalene degradation	0	0	0	0	0	0	0	1	0	0	0	0	2
Aminobenzoate degradation	0	0	1	0	1	1	4	1	1	6	0	0	15
Glyoxylate and dicarboxylate metabolism	0	3	4	1	0	7	4	0	3	11	3	3	56
Nitrotoluene degradation	0	0	0	0	0	1	1	0	1	0	0	0	2
Propanoate metabolism	1	5	1	0	1	9	7	2	6	8	1	0	47
Styrene degradation	1	1	0	0	1	0	2	1	2	5	0	0	12
Butanoate metabolism	2	1	3	0	1	5	4	2	4	8	2	0	41
C5-Branched dibasic acid metabolism	0	0	1	0	1	0	0	2	1	3	0	2	14
One carbon pool by folate	0	0	1	0	0	2	0	0	2	3	0	3	18
Methane metabolism	0	1	1	0	0	5	1	1	1	5	4	2	26
Thiamine metabolism	1	1	0	0	0	2	1	0	1	2	1	0	13
Riboflavin metabolism	2	0	0	0	0	0	0	0	1	2	0	0	11
Vitamin B6 metabolism	0	0	0	0	0	1	0	1	0	0	1	0	9
Pantothenate and CoA biosynthesis	0	0	3	0	1	3	3	1	2	3	1	0	23
Biotin metabolism	0	2	0	0	0	2	1	2	0	2	0	1	21
Folate biosynthesis	0	0	1	3	0	3	4	2	9	6	0	0	29
Porphyrin and chlorophyll metabolism	0	1	2	0	1	4	3	1	2	4	5	0	43
Aminoacyl-tRNA biosynthesis	0	2	1	3	0	0	0	5	1	3	2	4	101
Fatty acid metabolism	0	3	1	1	1	13	5	3	3	8	0	1	48
Degradation of aromatic compounds	0	0	0	2	0	0	6	2	3	3	1	0	26
Biosynthesis of amino acids	3	2	4	0	1	13	3	7	9	21	7	4	143
beta-Lactam resistance	0	1	0	3	0	0	1	3	2	2	1	0	27
Vancomycin resistance	0	1	0	0	0	1	0	1	0	0	1	0	8
Cationic antimicrobial peptide (CAMP) resistance	1	1	1	1	0	1	2	2	1	2	2	0	28
ABC transporters	17	12	6	4	10	8	23	16	20	41	6	5	193

Chapter 5: Nucleotide bias, replication and segregation in asymmetric chromosomes

5.1 Introduction

Sections 5.2, 5.4 and 5.5 of this chapter has been published in the following: Segregation but Not Replication of the *Pseudomonas aeruginosa* Chromosome Terminates at *Dif.* Bijit K. Bhowmik, April L. Clevenger, Hang Zhao, Valentin V. Rybenkov mBio Oct 2018, 9 (5) e01088-18; DOI: 10.1128/mBio.01088-18.

Deletion of the *mksB* condensin gene causes a large chromosomal inversion in the PAO1 genome, significantly altering alignment of *oriC*, the origin of replication, and *dif*, the chromosomal dimer resolution site [4]. These markers are prominent sites related to a nucleotide usage bias known as GC skew. GC skew is an underlying signaling code in bacterial DNA where there is an abundance of guanines on the leading strand and cytosines on the lagging strand. GC skew is utilized as a prediction tool for locating *oriC* and *dif* based on GC skew switch points (switch in abundance between guanines and cytosines).

Typically, bacteria have symmetrical layouts where their terminus of replication and *dif* site align (Figure 5-1 A). Segregation and replication are highly coordinated at their start sites indicated by the close proximity between *oriC* and *parS*, the initiation site in segregation. This coordination allows greater efficiency during growth and decreases the probability of developing problems on account of stalled processes. How dependent these processes are on each other is not exactly clear as symmetrical alignment makes it difficult to distinguish replication and segregation models

PAO1-UW has an asymmetric chromosome where one arm is 56% longer than the other. In this strain, the chromosome is longitudinally aligned between *oriC* and *dif*, where *dif* is asymmetrically aligned from the opposite of *oriC* [5] (Figure 5-1 B).

Here, we used the asymmetrical PAO1-UW as a model strain for studying the coordination between segregation, replication and nucleotide bias. The terminus of replication was determined to be directly opposite from *oriC* [16] (Figure 5-2). In contrast, the terminus of segregation ends asymmetrically at the *dif* site [5]. This confirmation of markers for segregation and replication in an asymmetric strain allowed us to study their coordination with nucleotide bias. In this chapter, we performed GC skew analysis on the asymmetric PAO1-UW strain, as well as on a larger scale for all sequenced bacterial chromosomes in the NCBI database [6], using bioinformatic analysis.

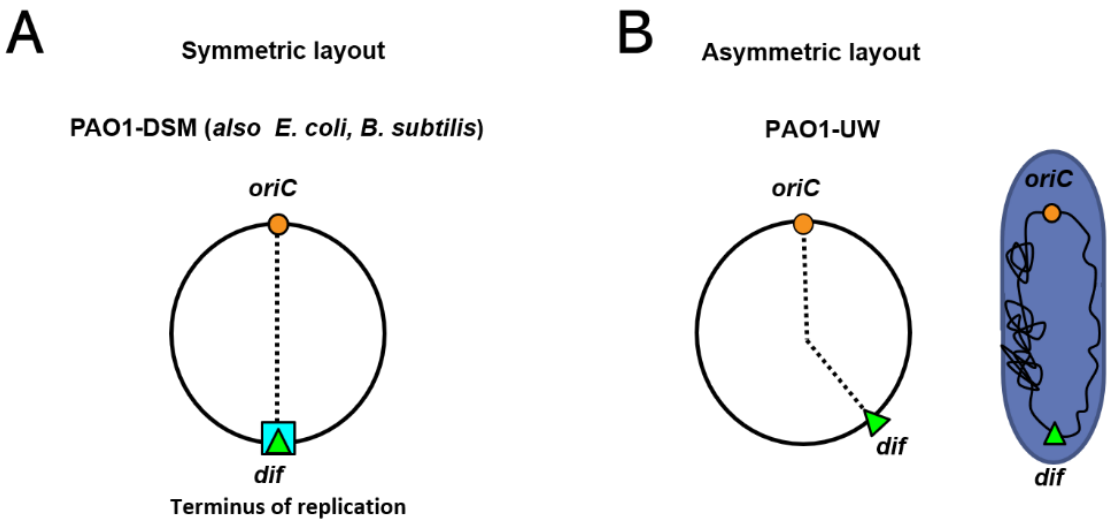

Figure 5- 1: Symmetric and asymmetric chromosomal layouts. (A) symmetric chromosomal layout where *dif* and the terminus of replication align and are opposite from *oriC*. (B)

Asymmetric layout in PAO1 where *dif*, the chromosomal dimer resolution site, is misaligned relative to the opposite of *oriC*.

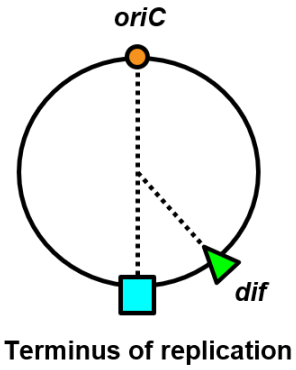

Figure 5- 2: Chromosome map of the asymmetrical PAO1-UW strain. The map shows the terminus of replication directly opposite from *oriC* and the terminus of segregation at the asymmetrical *dif* [5].

5.2 GC-skew switches polarity at *dif*, not opposite from *oriC* for PAO1-UW

GC skew analysis was first performed on the PAO1-UW strain with code generated in MATLAB (Figure 5-3). GC skew was calculated as (G-C)/(G+C) where G represents the number of guanines and C, the number of cytosines from the positive DNA strand. Analysis was done using a 1 kb sliding window. *oriC* was determined as the first switch in GC skew polarity which initiated a positive GC skew. The terminus of replication was determined directly opposite of *oriC* as verified experimentally using marker frequency analysis [5]. The *dif* site for Xer C/D recombination includes the sequence (GATTCGCATAATGTATATTATGTTAAAT) [220] which is located at 2.4 Mbp. The results show that there is an abundance of guanines between *oriC* and the *dif* site and an abundance of cytosines on the rest of the chromosome (on the positive

strand). GC skew switches polarity approximately 15 kb from the *dif* site, 682 kb away from the terminus of replication. Therefore, in the asymmetrical PAO1-UW chromosome, GC switches at *dif* but not the terminus of replication.

FtsK is a DNA translocase motor protein which brings together two *dif* sites guided by numerous KOPS (FtsK orienting polar sequences; 5'-GGGNAGGG-3'), which are distributed asymmetrically along both arms from *oriC* to *dif*) [221]. KOPS sequences were therefore plotted for both the plus and minus strand as a comparison to GC skew. The KOPS skew shows correlation and switching at the same point that GC skew switches raising the question as to whether GC skew and KOPS skew are related phenomena.

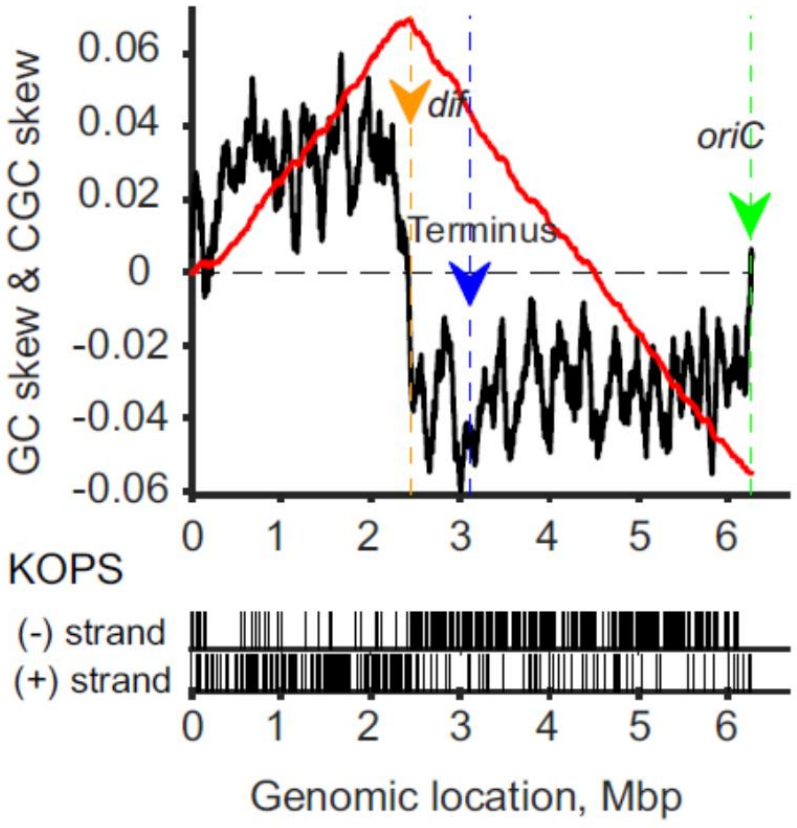

Figure 5- 3: GC, CGC, and KOPS skew of PAO1-UW. (A) Distribution of *dif* locations in the bacterial genomes GC-skew (black) and CGC-skew (red), with *oriC*, *dif*, and the replication terminus (top) and locations of KOPS sites (bottom) in the chromosome of PAO1-UW indicated.

5.3 KOPS sequences are independent from GC skew

Analysis of the number of KOPS sequences on each strand showed that 153 and 34 KOPS were on the positive and negative strands of the short chromosome arm. On the long arm, 75 and 57 KOPS were found on the negative and positive strands. Calculation of the contribution of excessive guanines shows that 595 guanines were contributed to the short arm and 1,070 to the long arms. Total guanine excess for the short arm is 45,815 and 81,859 for the long arm. KOPS sequences therefore do not significantly contribute to GC skew.

To test if these processes are independent, we analyzed how other sequences similar to KOPS with varying % G and % C would contribute to the excessive GC skew. The excess KOPS hits and excessive GC-skew for both the short and long chromosomal arms were calculated as the following (Equations 5-1, 5-2):

Equation 5- 1 Excess KOPS hits

Excess KOPS hits = KOPS hits (plus strand) – KOPS hits (minus strand)

Equation 5- 2 Excess GC-skew

Excess GC-skew = $\frac{Excess\ KOPS\ hits * (KOPS\ G's - KOPS\ C's)}{total\ G's + total\ C's}$

The KOPS sequence modified with two permutations was tested for a total of 16 queries along with one extra query. The actual KOPS sequence is query 10 - GGGCAGGG. Five controls were used that show the effect of excess guanines in different ways. The results for KOPS analysis is found in Figure 5.4. Interestingly, a modified version of KOPS, query 2 - GAGCAGGG, contributed the highest frequency of excess KOPS hits and overall highest percentage of excessive guanines. This sequence, however, did not contain the greatest number of guanines. KOPS still showed a high frequency of hits and contribution to excessive guanines relative to the other sequences including those with a higher number of guanines in their sequence. Overall, the results show that the prevalence of KOPS hits and ultimately contribution to excessive guanines is not based on sheer number of guanines within the KOPS sequence. This indicates that KOPS specificity to the chromosome is independent of GC skew.

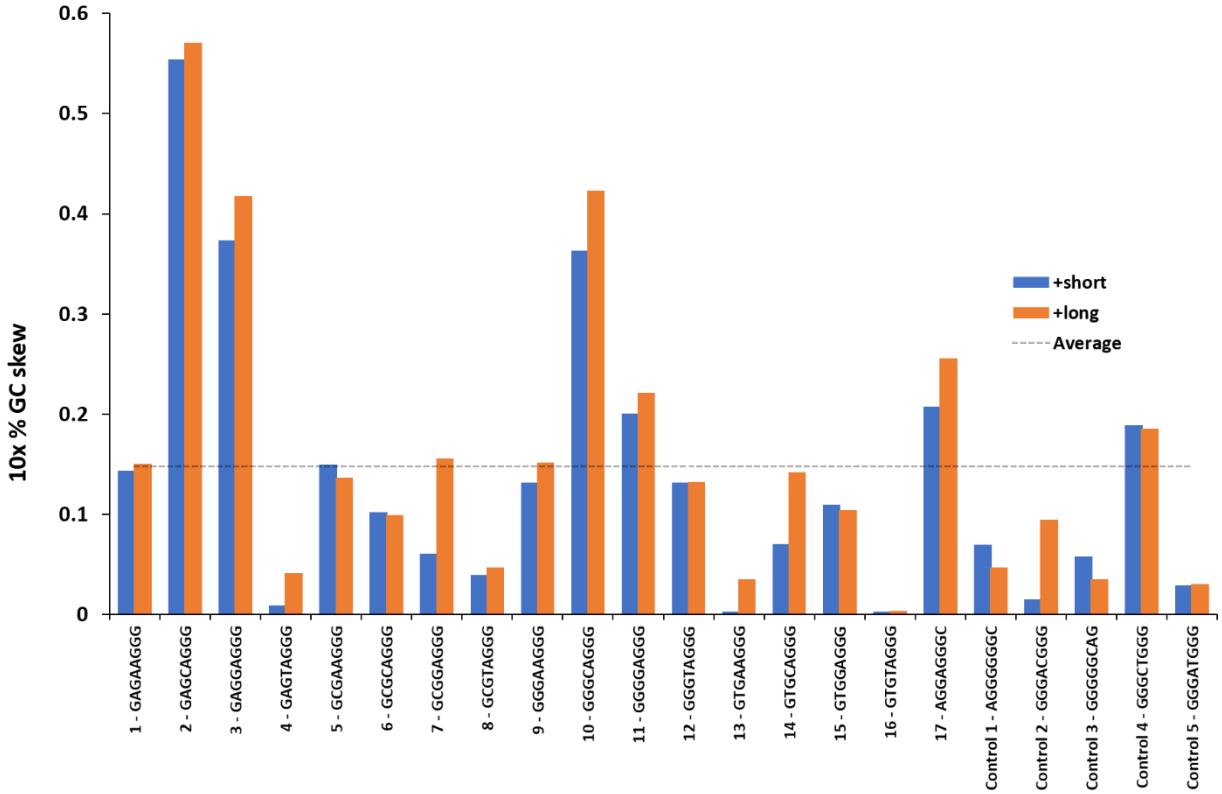

Figure 5- 4: 10x % excess G-C skew contribution for varying KOPS query sequences. Plot shows values for both the short and long arms of the chromosome.

5.4 6% of analyzed chromosomes are asymmetric

After determining that the PAO1-UW chromosome is asymmetric for *dif* relative to *oriC*, we next determined the prevalence of asymmetry across all bacterial strains. In order to do this, we first performed a blast analysis of 8,530 complete sequenced chromosomes obtained from the NCBI database [6] with a consensus *dif* sequence (AATTCGCATAATGTATATTATGTTAAAT). Approximately half (4,055) of the chromosomes were found to have a full *dif* sequence. Next, chromosomes were filtered for having two consistent GC skew domains, one with abundant guanines and the other with abundant cytosines. The

location for *oriC* was determined from the first GC skew switch point. The terminus of replication was calculated directly opposite from *oriC* as experimentally determined in the PAO1 model organism [5].

Overall, about 6% of all chromosomes are asymmetric for *dif* relative to the terminus of replication (for more details and figures [5]). Asymmetrical chromosomes were defined as having a significant (5% or greater) distance between *dif* and the terminus of replication. This range was outside of 3.3 standard deviations of a Guassian fit (99% confidence interval) (Figure 5-5).

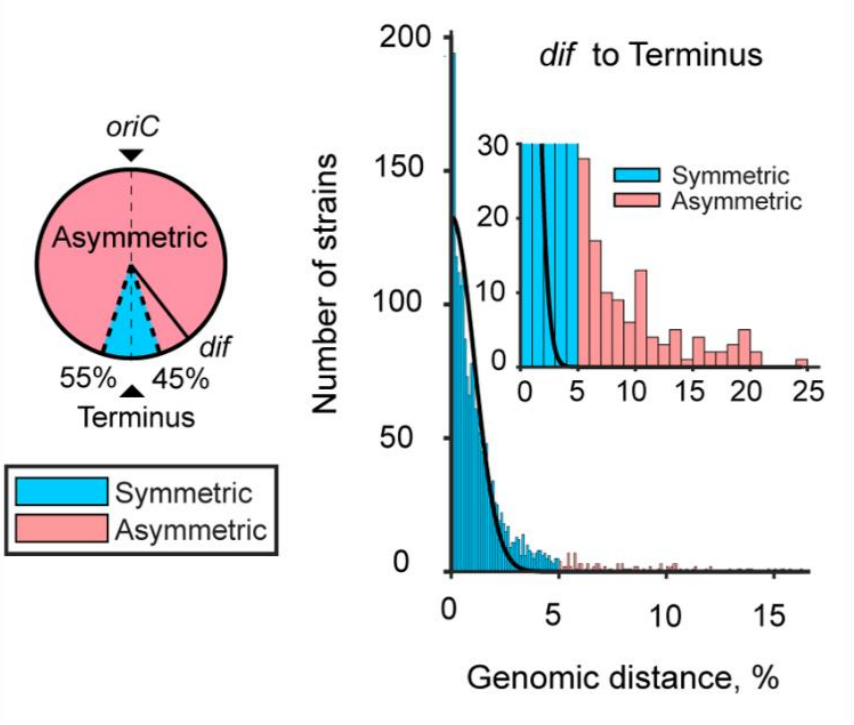

Figure 5- 5: Prevalence of asymmetric chromosomes. Numbers of chromosomes with the indicated genomic separation between *dif* and the replication terminus. The data were fit to a Gaussian distribution. Chromosomes where dif was located more than 5% away from the

predicted terminus of replication were considered asymmetric resulting in 6% asymmetric chromosomes.

5.5 GC skew aligns with *dif*, not the terminus of replication for both symmetrical and asymmetrical chromosomes

Next we analyzed the overall distributions of distances between the GC skew switch points and *dif* as well as the GC skew switch points and the terminus for both symmetrical and asymmetrical chromosomes. On average, *dif* was 13 kb away from the switch as opposed to 71 kb for the terminus of replication[5]). The overall results show that GC switch aligns with *dif* but not the terminus of replication (Figure 5-6). This was found to be true in in both symmetric and asymmetric chromosomes. In addition, the overall distribution of distances between the GC-switch and *dif* was indistinguishable between the two types of chromosomes (Figure 5-7) (for more details and figures on this topic, see the referenced paper [5]).

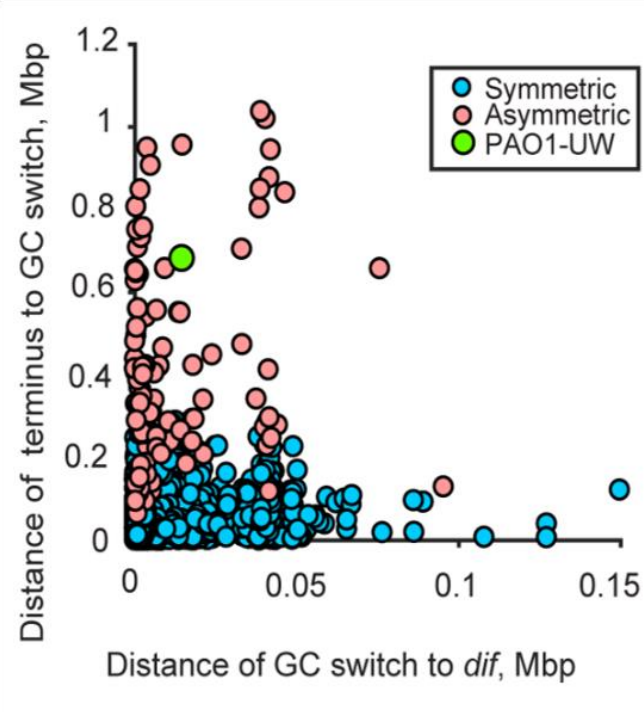

Figure 5- 6: Comparison of the distribution of distances of the GC-switch to *dif* and the expected terminus of replication for symmetric and asymmetric chromosomes.

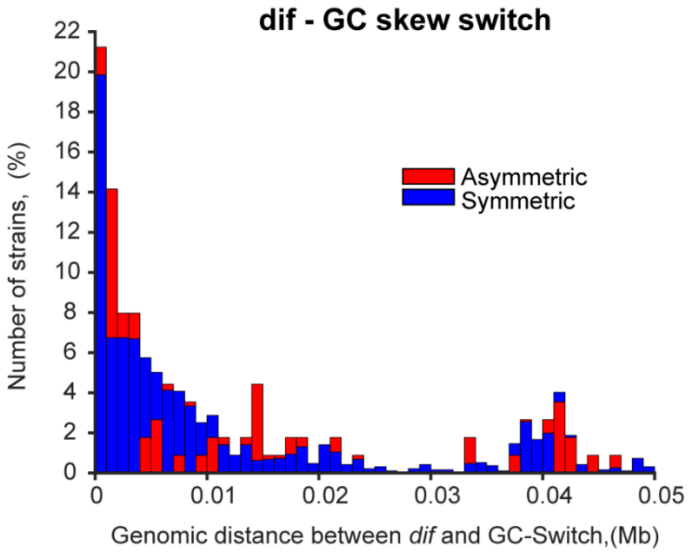

Figure 5- 7: Distribution of distances between GC-switch and *dif* for the percent of symmetric and asymmetric chromosomes.

Discussion

Pseudomonas aeruginosa is a major opportunistic pathogen capable of causing a variety of acute and chronic infections. The progression into different infection states is due in part to lifestyle switching. PA is equipped with a large regulatory network geared for adapting and circumventing environmental stressors. The ability to form biofilms is an intrinsic aspect for its survival.

Two different families of condensins are in *P. aeruginosa*, MksBEF and SMC-ScpAB. Physiological assays revealed opposite lifestyle states for the Δ*mksB* and Δ*smc* strains where deletion of *smc* produced sessile biofilm growing cells and deletion of *mksB* produced planktonic growing cells with reduced biofilm formation [1]. Transcriptomic analysis coincided with physiological assays while revealing that PAO1 condensins are global regulators of gene expression. These changes affected a number of different virulence and growth pathways. Remarkably, Δ*mksB* reflected expression profiles in the acute infection phase while Δ*smc* reflected those in the chronic infection phase implying a significant role of condensins in infection progression.

Phenotype for the double deletion strain in physiological assays was dominated by Δ*mksB [1].* This control over the growth state implicates MksB as a dominant factor for growth regulation. Expression patterns for the double deletion strain revealed overlap for growth genes with Δ*mksB* and iron uptake genes with Δ*smc*. Together, each condensin profile revealed hundreds of uniquely regulated genes including the double deletion strain indicating that many regulatory pathways are non-additive and independently regulated.

Regulation by MksB was found to be dependent on conformation through an ATPase mutation study. Additional physiological assays revealed that condensin phenotype is both context and strain dependent. Complementation analysis of *mksB* revealed an underlying genetic context resulting in regulatory plasticity. Investigation of PA14 revealed strain dependence of condensin phenotypes implying that regulatory plasticity may contribute to diversity in different strains.

Condensins are global regulators involved in infection progression:

Transcription analysis revealed broad global regulation patterns between condensin deletion strains in PAO1. For single deletion strains, Δ*smc* and Δ*mksB*, regulatory patterns for growth and virulence were strikingly opposite and reminiscent of acute and chronic infection phases. Δ*smc* upregulated genes involved in biofilm formation including a number of adhesion genes, the BexR regulon, T6SS, and iron uptake. Downregulated genes included the T3SS pathways. This profile reflects the sessile lifestyle state and chronic infection phase. Δ*mksB* downregulated T6SS, the BexR regulon, biofilm formation, iron uptake and adhesion genes and upregulated T3SS reflecting planktonic growth and the acute infection phase.

These trends correlate with the expression levels of several virulence regulators; PtrB and ExsA/B/C/D/E which regulate T3SS, the SiaA/D and CdrA/B genes which regulate c-di-GMP and biofilm, PvdS which regulates pyoverdine, BexR which regulates AprA toxin and other virulence factors, and PpkA which regulates T6SS. These findings implicate condensins as global regulatory factors for infection progression.

Interestingly, the double deletion strain showed overlap with Δ*mksB* for genes related to growth including biofilm and adhesion genes as well as the Types 3 and 6 secretion systems and the BexR regulon including associated virulence regulators. In this regard, the double deletion strain reflected planktonic growth and the acute infection phase. Overlap with Δ*smc* was also seen for several iron uptake genes. However, a major affected iron uptake pathway in ΔΔ, pyochelin, did not resemble either single deletion strain.

Overall, all three condensin mutant strains revealed hundreds of uniquely regulated genes. These results show that the manner of regulation by condensins is not merely additive. While growth regulation was dominated by *mksB*, each deletion strain contributed a unique transcriptional profile where the delta double strain reflected more than just the sum of the single deletion strains. This implies that condensins are independently integrated into the regulatory network with special programs.

For all condensin mutant strains, both virulence and growth programs were significantly affected implying an inherent link in regulation between these regulatory pathways. A connection between growth and virulence pathways can allow easier conversion between major infection phases where alterations in growth subsequently results in major changes to virulence programs. This link implicates PAO1 condensins as global regulators of infection progression.

The study on ATPase point mutations illuminated aspects of how condensins control gene expression. Interestingly, MksB phenotype is conformational dependent and does not require ATPase activity as much as it does specific MksB intermediate states. This was also seen

for the Δ*smc* strain [1]. How these specific conformations contribute to regulation remains to be determined. Regulatory effects by condensins could very well be related to their roles as chromosome maintainers. One possibility is that specific conformations are necessary in chromosome scaffolding, which may contribute to overall chromosome structure and subsequent regulatory effects.

Context dependence of condensin phenotypes reveals regulatory plasticity; a possible mechanism for adaptation and evolution:

Physiological assays showed that condensin phenotype is both context and strain dependent. Using the degron system and ATPase point mutations, we showed that MksB is linked with biofilm formation; however, significant *cis* effects or even secondary consequences of the *mksB* deletion prevented complementation through the reincorporation of *mksB*. Cis effects include a number of factors including cis regulatory elements (CRE's) (i.e. silencers and enhancers) and epigenetic factors (such as methyl groups, miRNA, or sRNA) which can regulate gene expression. Less direct factors related to chromosome structuring could also play a role in gene expression. This study highlights irrevocable changes to the chromosome resulting from a *mksB* deletion, however, further studies are necessary to confirm the exact nature of how the chromosome has been altered.

One possibility for secondary effects includes a recent discovery by Dr. Bijit Bhowmik, which showed that a *mksB* deletion results in a large chromosomal inversion between two rRNA sites 2.2 Mbp away [4]. This finding raises the possibility that chromosomal rearrangement occurring in the Δ*mksB* strain may permanently alter *mksb* phenotype. MksB

may play a role in holding the chromosome in a particular stable topology which prevents inversion. Its removal or decrease could result in instability in maintaining this particular topology, resulting in inversion and irreversible alterations to the chromosome. Subsequently, *mksB* regulation of gene expression may reside in how it maintains chromosome integrity.

Overall, context dependence of condensin phenotypes reveals regulatory plasticity. *mksB* phenotype is dependent on more than just the association of genes to functions, it also resides on a genetic context. This genetic context to condensin regulation allows additional diversity within the regulatory network.

Physiological studies on PA14 revealed that condensin phenotypes are strain dependent. PA14 condensin displayed markedly smaller effects on phenotype than PAO1. These results implicate differences in how condensins are integrated into their regulatory network. This study, however, is limited in that phenotypes are determined by physiological assays alone and does not include gene expression profiles. Further transcriptomic analysis on PA14 condensin mutations is needed to better illuminate their regulatory effects which may be diminished by additional factors.

Regulatory plasticity could allow greater diversity across strains and species, serving as a possible mode for adaptation and species formation. The PAO1 system may have incorporated condensins in a manner that allowed substantial regulatory benefits that contribute to disease progression and virulence in addition to their roles in chromosome maintenance. Regulatory plasticity may contribute to overall organism variability, helping drive adaptation and evolution

GC skew alignment with *dif* but not the terminus of replication is possibly due to integration during early bacterial evolution:

An inversion in the chromosome caused by *mksB* illuminated a major shift of the chromosome dimer resolution site, *dif* relative to the origin of replication, *oriC* [4]. This asymmetry provided a unique opportunity to study aspects of segregation and replication which are otherwise indiscernible in symmetric chromosomes. The chromosome is highly integrated into an inherent code known as GC skew. This code has been used as prediction markers for *oriC* and *dif.* One of the prominent proposals regarding the origin of GC skew is that it is due to a higher incorporation of guanines in the leading strand during replication. This proposal is consistent for its alignment with *oriC*, however, it does not explain the consistent alignment with *dif* and whether this skew is also aligned with the terminus of replication. This study differentiated segregation and replication processes in an asymmetrical chromosome model to study their coordination along with GC skew.

Using marker frequency analysis, replication was found to terminate opposite from *oriC*, despite asymmetry of the PAO1-UW chromosome [5]. In contrast, segregation terminated at the asymmetric *dif* [5] . This allowed confirmation of the relative locations for both the terminus of replication and the terminus of segregation in asymmetric chromosome types and showed that they are not coordinated.

GC skew analysis of the PAO1 model organism revealed alignment with dif but not the terminus of replication. This finding showed that in the asymmetric chromosome in which segregation and replication termini are clearly differentiated, GC skew is aligned with dif, found

at the terminus of segregation, rather than the expected terminus of replication. Extending this study to all sequenced bacterial chromosomes also showed that *dif*, not the terminus of replication, exclusively aligns with GC skew in both symmetric and asymmetric chromosomes (6% of the chromosomes analyzed).

In order to reconcile these observations for GC skew alignment on the premise that GC skew is generated during replication, we propose that the *dif* sequence likely integrated itself near the GC skew switch early in evolution. The XerC/D recombinase system recombines DNA at *dif* sites, helping to separate chromosome dimers. It is possible that *dif* sites, found in ancient DNA, may have recombined with each other and were integrated at the GC switch point proximal to the terminus of replication early in bacterial evolution. This could explain why most bacterial chromosomes having a full *dif* sequence are symmetrically aligned for *dif* and the terminus of replication along with GC skew. Subsequent alterations to chromosomes across bacterial strains during evolution would affect the orientation between *oriC* and *dif* while maintaining their locations at GC skew switch points. This could account for the lack of alignment of GC skew observed for the terminus of replication. Further analysis will be required to better understand the ancient origins of *dif* integration onto the GC skew switch sites.

References

1. Zhao, H., et al., *Pseudomonas aeruginosa Condensins Support Opposite Differentiation States.* J Bacteriol, 2016. **198**(21): p. 2936-2944.

2. Petrushenko, Z.M., et al., *Mechanics of DNA bridging by bacterial condensin MukBEF in vitro and in singulo.* EMBO J, 2010. **29**(6): p. 1126-35.

3. Hirano, T., *Condensin-Based Chromosome Organization from Bacteria to Vertebrates.* Cell, 2016. **164**(5): p. 847-57.

4. Bhowmik, B.K., *Chromosome Organization and Segregation in Pseudomonas Aeruginosa*, in *Chemistry and Biochemistry*. 2007, University of Oklahoma: Norman, Ok.

5. Bhowmik, B.K., et al., *Segregation but Not Replication of the Pseudomonas aeruginosa Chromosome Terminates at Dif.* MBio, 2018. **9**(5).

6. National Center for Biotechnology Information. *Genome*. 2019; Available from: https://www.ncbi.nlm.nih.gov/.

7. Centers for Disease Control and Prevention. *ANTIBIOTIC RESISTANCE THREATS in the United States, 2013*. 2013; Available from: https://www.cdc.gov/drugresistance/threat-report-2013/pdf/ar-threats-2013-508.pdf.

8. Yamazaki, K.-i., et al., *Isolation and characterization of nucleoid proteins from Escherichia coli.* Molecular and General Genetics MGG, 1984. **196**(2): p. 217-224.

9. Azam, T.A. and A. Ishihama, *Twelve Species of the Nucleoid-associated Protein from Escherichia coli : SEQUENCE RECOGNITION SPECIFICITY AND DNA BINDING AFFINITY.* Journal of Biological Chemistry, 1999. **274**(46): p. 33105-33113.

10. Ohniwa, R.L., et al., *Proteomic analyses of nucleoid-associated proteins in Escherichia coli, Pseudomonas aeruginosa, Bacillus subtilis, and Staphylococcus aureus.* PLoS One, 2011. **6**(4): p. e19172.

11. Attila, C., A. Ueda, and T.K. Wood, *PA2663 (PpyR) increases biofilm formation in Pseudomonas aeruginosa PAO1 through the psl operon and stimulates virulence and quorum-sensing phenotypes.* Appl Microbiol Biotechnol, 2008. **78**(2): p. 293-307.

12. Dillon, S.C. and C.J. Dorman, *Bacterial nucleoid-associated proteins, nucleoid structure and gene expression.* Nat Rev Microbiol, 2010. **8**(3): p. 185-95.

13. Ali Azam, T., et al., *Growth phase-dependent variation in protein composition of the Escherichia coli nucleoid.* J Bacteriol, 1999. **181**(20): p. 6361-70.

14. Claret, L. and J. Rouviere-Yaniv, *Variation in HU composition during growth of Escherichia coli: the heterodimer is required for long term survival.* J Mol Biol, 1997. **273**(1): p. 93-104.

15. Calvo, J.M. and R.G. Matthews, *The leucine-responsive regulatory protein, a global regulator of metabolism in Escherichia coli.* Microbiol Rev, 1994. **58**(3): p. 466-90.

16. Dame, R.T., M.C. Noom, and G.J. Wuite, *Bacterial chromatin organization by H-NS protein unravelled using dual DNA manipulation.* Nature, 2006. **444**(7117): p. 387-90.

17. Grant, R.A., et al., *The crystal structure of Dps, a ferritin homolog that binds and protects DNA.* Nat Struct Biol, 1998. **5**(4): p. 294-303.

18. Ohniwa, R.L., et al., *Dynamic state of DNA topology is essential for genome condensation in bacteria.* EMBO J, 2006. **25**(23): p. 5591-602.

19. Rouviere-Yaniv, J., M. Yaniv, and J.E. Germond, *E. coli DNA binding protein HU forms nucleosomelike structure with circular double-stranded DNA.* Cell, 1979. **17**(2): p. 265-74.

20. Swinger, K.K., et al., *Flexible DNA bending in HU-DNA cocrystal structures.* EMBO J, 2003. **22**(14): p. 3749-60.

21. Valens, M., et al., *Macrodomain organization of the Escherichia coli chromosome.* EMBO J, 2004. **23**(21): p. 4330-41.

22. Delius, H. and A. Worcel, *Letter: Electron microscopic visualization of the folded chromosome of Escherichia coli.* J Mol Biol, 1974. **82**(1): p. 107-9.

23. Petrushenko, Z.M., et al., *Mechanics of DNA bridging by bacterial condensin MukBEF in vitro and in singulo.* The EMBO Journal, 2010. **29**(6): p. 1126-1135.

24. Albert, A.-C., et al., *Hyper-Negative Template DNA Supercoiling During Transcription of the Tetracycline-Resistance Gene in topA Mutants is Largely Constrained In Vivo.* Nucleic Acids Research, 1996. **24**(15): p. 3093-3099.

25. Petrushenko, Z.M., et al., *DNA reshaping by MukB. Right-handed knotting, left-handed supercoiling.* J Biol Chem, 2006. **281**(8): p. 4606-15.

26. Lammens, A., A. Schele, and K.P. Hopfner, *Structural biochemistry of ATP-driven dimerization and DNA-stimulated activation of SMC ATPases.* Curr Biol, 2004. **14**(19): p. 1778-82.

27. Petrushenko, Z.M., W. She, and V.V. Rybenkov, *A new family of bacterial condensins.* Molecular microbiology, 2011. **81**(4): p. 881-896.

28. Jones, P.M. and A.M. George, *Subunit interactions in ABC transporters: towards a functional architecture.* FEMS Microbiology Letters, 1999. **179**(2): p. 187-202.

29. Niki, H., et al., *E.coli MukB protein involved in chromosome partition forms a homodimer with a rod-and-hinge structure having DNA binding and ATP/GTP binding activities.* The EMBO journal, 1992. **11**(13): p. 5101-5109.

30. Haering, K.N.a.C.H., *THE STRUCTURE AND FUNCTION OF SMC AND KLEISIN COMPLEXES.* Annual Review of Biochemistry, 2005. **74**: p. 595-648.

31. Woo, J.S., et al., *Structural studies of a bacterial condensin complex reveal ATP-dependent disruption of intersubunit interactions.* Cell, 2009. **136**(1): p. 85-96.

32. Petrushenko, Z.M., C.H. Lai, and V.V. Rybenkov, *Antagonistic interactions of kleisins and DNA with bacterial Condensin MukB.* J Biol Chem, 2006. **281**(45): p. 34208-17.

33. Kim, H. and J.J. Loparo, *Multistep assembly of DNA condensation clusters by SMC.* Nat Commun, 2016. **7**: p. 10200.

34. Hirano, M. and T. Hirano, *Positive and negative regulation of SMC-DNA interactions by ATP and accessory proteins.* EMBO J, 2004. **23**(13): p. 2664-73.

35. Palecek, Jan J. and S. Gruber, *Kite Proteins: a Superfamily of SMC/Kleisin Partners Conserved Across Bacteria, Archaea, and Eukaryotes.* Structure, 2015. **23**(12): p. 2183-2190.

36. Tran, N.T., et al., *Permissive zones for the centromere-binding protein ParB on the Caulobacter crescentus chromosome.* Nucleic Acids Research, 2017. **46**(3): p. 1196-1209.

37. Surtees, J.A. and B.E. Funnell, *Plasmid and chromosome traffic control: how ParA and ParB drive partition.* Curr Top Dev Biol, 2003. **56**: p. 145-80.

38. Walter, J.C., et al., *Surfing on Protein Waves: Proteophoresis as a Mechanism for Bacterial Genome Partitioning.* Phys Rev Lett, 2017. **119**(2): p. 028101.

39. Gruber, S. and J. Errington, *Recruitment of condensin to replication origin regions by ParB/SpoOJ promotes chromosome segregation in B. subtilis.* Cell, 2009. **137**(4): p. 685-96.

40. Adachi, S., et al., *Localization of replication forks in wild-type and mukB mutant cells of Escherichia coli.* Mol Genet Genomics, 2005. **274**(3): p. 264-71.

41. Badrinarayanan, A., et al., *The Escherichia coli SMC complex, MukBEF, shapes nucleoid organization independently of DNA replication.* J Bacteriol, 2012. **194**(17): p. 4669-76.

42. Li, Y., et al., *Escherichia coli condensin MukB stimulates topoisomerase IV activity by a direct physical interaction.* Proc Natl Acad Sci U S A, 2010. **107**(44): p. 18832-7.

43. Nicolas, E., et al., *The SMC complex MukBEF recruits topoisomerase IV to the origin of replication region in live Escherichia coli.* MBio, 2014. **5**(1): p. e01001-13.

44. Adachi, S. and S. Hiraga, *Mutants suppressing novobiocin hypersensitivity of a mukB null mutation.* J Bacteriol, 2003. **185**(13): p. 3690-5.

45. Sawitzke, J.A. and S. Austin, *Suppression of chromosome segregation defects of Escherichia coli muk mutants by mutations in topoisomerase I.* Proc Natl Acad Sci U S A, 2000. **97**(4): p. 1671-6.

46. Vallet-Gely, I. and F. Boccard, *Chromosomal organization and segregation in Pseudomonas aeruginosa.* PLoS genetics, 2013. **9**(5): p. e1003492-e1003492.

47. World Health Organization. *WHO PRIORITY PATHOGENS LIST FOR R&D OF NEW ANTIBIOTICS* 2017; Available from: https://www.who.int/medicines/publications/WHO-PPL-Short_Summary_25Feb-ET_NM_WHO.pdf.

48. Korgaonkar, A.K. and M. Whiteley, *Pseudomonas aeruginosa enhances production of an antimicrobial in response to N-acetylglucosamine and peptidoglycan.* J Bacteriol, 2011. **193**(4): p. 909-17.

49. Folkesson, A., et al., *Adaptation of Pseudomonas aeruginosa to the cystic fibrosis airway: an evolutionary perspective.* Nat Rev Microbiol, 2012. **10**(12): p. 841-51.

50. Filiatrault, M.J., et al., *Identification of Pseudomonas aeruginosa genes involved in virulence and anaerobic growth.* Infect Immun, 2006. **74**(7): p. 4237-45.

51. Haussler, S. and M.R. Parsek, *Biofilms 2009: new perspectives at the heart of surface-associated microbial communities.* J Bacteriol, 2010. **192**(12): p. 2941-9.

52. Lu, T.K. and J.J. Collins, *Dispersing biofilms with engineered enzymatic bacteriophage.* Proc Natl Acad Sci U S A, 2007. **104**(27): p. 11197-202.

53. Whitchurch, C.B., et al., *Extracellular DNA required for bacterial biofilm formation.* Science, 2002. **295**(5559): p. 1487.

54. Colvin, K.M., et al., *The Pel and Psl polysaccharides provide Pseudomonas aeruginosa structural redundancy within the biofilm matrix.* Environ Microbiol, 2012. **14**(8): p. 1913-28.

55. Ernst, J., et al., *Polyester-based particles to overcome the obstacles of mucus and biofilms in the lung for tobramycin application under static and dynamic fluidic conditions.* Eur J Pharm Biopharm, 2018. **131**: p. 120-129.

56. Lewis, K., *Riddle of biofilm resistance.* Antimicrob Agents Chemother, 2001. **45**(4): p. 999-1007.

57. Stoodley, P., et al., *Structural deformation of bacterial biofilms caused by short-term fluctuations in fluid shear: an in situ investigation of biofilm rheology.* Biotechnol Bioeng, 1999. **65**(1): p. 83-92.

58. Ma, L., et al., *Assembly and development of the Pseudomonas aeruginosa biofilm matrix.* PLoS Pathog, 2009. **5**(3): p. e1000354.

59. Stoodley, P., D. Debeer, and Z. Lewandowski, *Liquid flow in biofilm systems.* Appl Environ Microbiol, 1994. **60**(8): p. 2711-6.

60. Ma, L., et al., *Pseudomonas aeruginosa Psl is a galactose- and mannose-rich exopolysaccharide.* J Bacteriol, 2007. **189**(22): p. 8353-6.

61. Franklin, M.J., et al., *Biosynthesis of the Pseudomonas aeruginosa Extracellular Polysaccharides, Alginate, Pel, and Psl.* Front Microbiol, 2011. **2**: p. 167.

62. Byrd, M.S., et al., *The Pseudomonas aeruginosa exopolysaccharide Psl facilitates surface adherence and NF-kappaB activation in A549 cells.* MBio, 2010. **1**(3).

63. Zegans, M.E., et al., *Pseudomonas aeruginosa exopolysaccharide Psl promotes resistance to the biofilm inhibitor polysorbate 80.* Antimicrobial agents and chemotherapy, 2012. **56**(8): p. 4112-4122.

64. Irie, Y., et al., *Self-produced exopolysaccharide is a signal that stimulates biofilm formation in Pseudomonas aeruginosa.* Proc Natl Acad Sci U S A, 2012. **109**(50): p. 20632-6.

65. Jennings, L.K., et al., *Pel is a cationic exopolysaccharide that cross-links extracellular DNA in the Pseudomonas aeruginosa biofilm matrix.* Proceedings of the National Academy of Sciences of the United States of America, 2015. **112**(36): p. 11353-11358.

66. Liang, Z.X., *The expanding roles of c-di-GMP in the biosynthesis of exopolysaccharides and secondary metabolites.* Nat Prod Rep, 2015. **32**(5): p. 663-83.

67. Colvin, K.M., et al., *The pel polysaccharide can serve a structural and protective role in the biofilm matrix of Pseudomonas aeruginosa.* PLoS pathogens, 2011. **7**(1): p. e1001264-e1001264.

68. Colvin, K.M., et al., *The Pel and Psl polysaccharides provide Pseudomonas aeruginosa structural redundancy within the biofilm matrix.* Environmental Microbiology, 2012. **14**(8): p. 1913-1928.

69. Ma, L., et al., *Assembly and development of the Pseudomonas aeruginosa biofilm matrix.* PLoS pathogens, 2009. **5**(3): p. e1000354-e1000354.

70. Wei, Q. and L.Z. Ma, *Biofilm matrix and its regulation in Pseudomonas aeruginosa.* Int J Mol Sci, 2013. **14**(10): p. 20983-1005.

71. Rehm, B.H. and S. Valla, *Bacterial alginates: biosynthesis and applications.* Appl Microbiol Biotechnol, 1997. **48**(3): p. 281-8.

72. Sutherland, I., *Biofilm exopolysaccharides: a strong and sticky framework.* Microbiology, 2001. **147**(Pt 1): p. 3-9.

73. Kadurugamuwa, J.L. and T.J. Beveridge, *Virulence factors are released from Pseudomonas aeruginosa in association with membrane vesicles during normal growth and exposure to gentamicin: a novel mechanism of enzyme secretion.* J Bacteriol, 1995. **177**(14): p. 3998-4008.

74. Kuhn, M.J., et al., *Bacteria exploit a polymorphic instability of the flagellar filament to escape from traps.* Proc Natl Acad Sci U S A, 2017. **114**(24): p. 6340-6345.

75. Balaban, N.Q., et al., *Bacterial Persistence as a Phenotypic Switch.* Science, 2004. **305**(5690): p. 1622.

76. Dörr, T., K. Lewis, and M. Vulić, *SOS response induces persistence to fluoroquinolones in Escherichia coli.* PLoS genetics, 2009. **5**(12): p. e1000760-e1000760.

77. Brauner, A., et al., *Distinguishing between resistance, tolerance and persistence to antibiotic treatment.* Nature Reviews Microbiology, 2016. **14**: p. 320.

78. Garrett, T.R., M. Bhakoo, and Z. Zhang, *Bacterial adhesion and biofilms on surfaces.* Progress in Natural Science, 2008. **18**(9): p. 1049-1056.

79. Miller, M.B. and B.L. Bassler, *Quorum sensing in bacteria.* Annu Rev Microbiol, 2001. **55**: p. 165-99.

80. Davey, M.E. and A. O'Toole G, *Microbial biofilms: from ecology to molecular genetics.* Microbiol Mol Biol Rev, 2000. **64**(4): p. 847-67.

81. O'Toole, G.A., *Jekyll or hide?* Nature, 2004. **432**(7018): p. 680-681.

82. Flemming, H.-C., et al., *Biofilms: an emergent form of bacterial life.* Nature Reviews Microbiology, 2016. **14**: p. 563.

83. Kolter, R. and E.P. Greenberg, *The superficial life of microbes.* Nature, 2006. **441**(7091): p. 300-302.

84. Gambello, M.J. and B.H. Iglewski, *Cloning and characterization of the Pseudomonas aeruginosa lasR gene, a transcriptional activator of elastase expression.* Journal of bacteriology, 1991. **173**(9): p. 3000-3009.

85. Passador, L., et al., *Expression of Pseudomonas aeruginosa virulence genes requires cell-to-cell communication.* Science, 1993. **260**(5111): p. 1127-30.

86. Ochsner, U.A., et al., *Isolation and characterization of a regulatory gene affecting rhamnolipid biosurfactant synthesis in Pseudomonas aeruginosa.* Journal of bacteriology, 1994. **176**(7): p. 2044-2054.

87. Davies, D.G., et al., *The involvement of cell-to-cell signals in the development of a bacterial biofilm.* Science, 1998. **280**(5361): p. 295-8.

88. Sakuragi, Y. and R. Kolter, *Quorum-sensing regulation of the biofilm matrix genes (pel) of Pseudomonas aeruginosa.* Journal of bacteriology, 2007. **189**(14): p. 5383-5386.

89. Allesen-Holm, M., et al., *A characterization of DNA release in Pseudomonas aeruginosa cultures and biofilms.* Mol Microbiol, 2006. **59**(4): p. 1114-28.

90. Barken, K.B., et al., *Roles of type IV pili, flagellum-mediated motility and extracellular DNA in the formation of mature multicellular structures in Pseudomonas aeruginosa biofilms.* Environ Microbiol, 2008. **10**(9): p. 2331-43.

91. Heydorn, A., et al., *Statistical analysis of Pseudomonas aeruginosa biofilm development: impact of mutations in genes involved in twitching motility, cell-to-cell signaling, and*

stationary-phase sigma factor expression. Applied and environmental microbiology, 2002. **68**(4): p. 2008-2017.

92. McGrath, S., D.S. Wade, and E.C. Pesci, *Dueling quorum sensing systems in Pseudomonas aeruginosa control the production of the Pseudomonas quinolone signal (PQS).* FEMS Microbiol Lett, 2004. **230**(1): p. 27-34.

93. Cao, H., et al., *A quorum sensing-associated virulence gene of Pseudomonas aeruginosa encodes a LysR-like transcription regulator with a unique self-regulatory mechanism.* Proc Natl Acad Sci U S A, 2001. **98**(25): p. 14613-8.

94. Kim, K., et al., *HHQ and PQS, two Pseudomonas aeruginosa quorum-sensing molecules, down-regulate the innate immune responses through the nuclear factor-kappaB pathway.* Immunology, 2010. **129**(4): p. 578-88.

95. Kang, D., K.E. Turner, and N.V. Kirienko, *PqsA Promotes Pyoverdine Production via Biofilm Formation.* Pathogens, 2017. **7**(1).

96. Lee, J., et al., *A cell-cell communication signal integrates quorum sensing and stress response.* Nat Chem Biol, 2013. **9**(5): p. 339-43.

97. Records, A.R. and D.C. Gross, *Sensor kinases RetS and LadS regulate Pseudomonas syringae type VI secretion and virulence factors.* J Bacteriol, 2010. **192**(14): p. 3584-96.

98. Goodman, A.L., et al., *A signaling network reciprocally regulates genes associated with acute infection and chronic persistence in Pseudomonas aeruginosa.* Dev Cell, 2004. **7**(5): p. 745-54.

99. Lapouge, K., et al., *Gac/Rsm signal transduction pathway of gamma-proteobacteria: from RNA recognition to regulation of social behaviour.* Mol Microbiol, 2008. **67**(2): p. 241-53.

100. Römling, U., M.Y. Galperin, and M. Gomelsky, *Cyclic di-GMP: the first 25 years of a universal bacterial second messenger.* Microbiology and molecular biology reviews : MMBR, 2013. **77**(1): p. 1-52.

101. Ha, D.-G. and G.A. O'Toole, *c-di-GMP and its Effects on Biofilm Formation and Dispersion: a Pseudomonas Aeruginosa Review.* Microbiology spectrum, 2015. **3**(2): p. 10.1128/microbiolspec.MB-0003-2014-2014.

102. Valentini, M. and A. Filloux, *Biofilms and Cyclic di-GMP (c-di-GMP) Signaling: Lessons from Pseudomonas aeruginosa and Other Bacteria.* The Journal of biological chemistry, 2016. **291**(24): p. 12547-12555.

103. Petrova, O.E. and K. Sauer, *SagS contributes to the motile-sessile switch and acts in concert with BfiSR to enable Pseudomonas aeruginosa biofilm formation.* J Bacteriol, 2011. **193**(23): p. 6614-28.

104. Cornelis, P., S. Matthijs, and L. Van Oeffelen, *Iron uptake regulation in Pseudomonas aeruginosa.* Biometals, 2009. **22**(1): p. 15-22.

105. Simm, R., et al., *GGDEF and EAL domains inversely regulate cyclic di-GMP levels and transition from sessility to motility.* Mol Microbiol, 2004. **53**(4): p. 1123-34.

106. Almblad, H., et al., *High levels of cAMP inhibit Pseudomonas aeruginosa biofilm formation through reduction of the c-di-GMP content.* Microbiology, 2019. **165**(3): p. 324-333.

107. Sun, Y.Y., H. Chi, and L. Sun, *Pseudomonas fluorescens Filamentous Hemagglutinin, an Iron-Regulated Protein, Is an Important Virulence Factor that Modulates Bacterial Pathogenicity.* Front Microbiol, 2016. **7**: p. 1320.

108. Relman, D.A., et al., *Filamentous hemagglutinin of Bordetella pertussis: nucleotide sequence and crucial role in adherence.* Proc Natl Acad Sci U S A, 1989. **86**(8): p. 2637-41.

109. Fujita, M., et al., *Transcription of the principal sigma-factor genes, rpoD and rpoS, in Pseudomonas aeruginosa is controlled according to the growth phase.* Mol Microbiol, 1994. **13**(6): p. 1071-7.

110. Xu, K.D., et al., *Spatial physiological heterogeneity in Pseudomonas aeruginosa biofilm is determined by oxygen availability.* Appl Environ Microbiol, 1998. **64**(10): p. 4035-9.

111. Bouillet, S., et al., *Connected partner-switches control the life style of Pseudomonas aeruginosa through RpoS regulation.* Sci Rep, 2019. **9**(1): p. 6496.

112. Colley, B., et al., *SiaA/D Interconnects c-di-GMP and RsmA Signaling to Coordinate Cellular Aggregation of Pseudomonas aeruginosa in Response to Environmental Conditions.* Frontiers in Microbiology, 2016. **7**(179).

113. Pan, J., et al., *Serine/threonine protein kinase PpkA contributes to the adaptation and virulence in Pseudomonas aeruginosa.* Microb Pathog, 2017. **113**: p. 5-10.

114. Hsu, F., S. Schwarz, and J.D. Mougous, *TagR promotes PpkA-catalysed type VI secretion activation in Pseudomonas aeruginosa.* Mol Microbiol, 2009. **72**(5): p. 1111-25.

115. Chen, L., et al., *Composition, function, and regulation of T6SS in Pseudomonas aeruginosa.* Microbiol Res, 2015. **172**: p. 19-25.

116. Bernard, C.S., et al., *Nooks and crannies in type VI secretion regulation.* J Bacteriol, 2010. **192**(15): p. 3850-60.

117. Hood, R.D., et al., *A type VI secretion system of Pseudomonas aeruginosa targets a toxin to bacteria.* Cell Host Microbe, 2010. **7**(1): p. 25-37.

118. Turner, K.H., I. Vallet-Gely, and S.L. Dove, *Epigenetic control of virulence gene expression in Pseudomonas aeruginosa by a LysR-type transcription regulator.* PLoS Genet, 2009. **5**(12): p. e1000779.

119. Patriquin, G.M., et al., *Influence of quorum sensing and iron on twitching motility and biofilm formation in Pseudomonas aeruginosa.* J Bacteriol, 2008. **190**(2): p. 662-71.

120. Llamas, M.A., et al., *The heterologous siderophores ferrioxamine B and ferrichrome activate signaling pathways in Pseudomonas aeruginosa.* J Bacteriol, 2006. **188**(5): p. 1882-91.

121. Shirley, M. and I.L. Lamont, *Role of TonB1 in pyoverdine-mediated signaling in Pseudomonas aeruginosa.* J Bacteriol, 2009. **191**(18): p. 5634-40.

122. Hunt, T.A., et al., *The Pseudomonas aeruginosa alternative sigma factor PvdS controls exotoxin A expression and is expressed in lung infections associated with cystic fibrosis.* Microbiology, 2002. **148**(Pt 10): p. 3183-93.

123. Heinrichs, D.E. and K. Poole, *PchR, a regulator of ferripyochelin receptor gene (fptA) expression in Pseudomonas aeruginosa, functions both as an activator and as a repressor.* J Bacteriol, 1996. **178**(9): p. 2586-92.

124. Cornelis, P. and J. Dingemans, *Pseudomonas aeruginosa adapts its iron uptake strategies in function of the type of infections.* Front Cell Infect Microbiol, 2013. **3**: p. 75.

125. Luscher, A., et al., *TonB-Dependent Receptor Repertoire of Pseudomonas aeruginosa for Uptake of Siderophore-Drug Conjugates.* Antimicrob Agents Chemother, 2018. **62**(6).

126. Cox, C.D., *Role of pyocyanin in the acquisition of iron from transferrin.* Infect Immun, 1986. **52**(1): p. 263-70.

127. Wang, Y. and D.K. Newman, *Redox reactions of phenazine antibiotics with ferric (hydr)oxides and molecular oxygen.* Environ Sci Technol, 2008. **42**(7): p. 2380-6.

128. Deziel, E., et al., *The contribution of MvfR to Pseudomonas aeruginosa pathogenesis and quorum sensing circuitry regulation: multiple quorum sensing-regulated genes are*

modulated without affecting lasRI, rhlRI or the production of N-acyl-L-homoserine lactones. Mol Microbiol, 2005. **55**(4): p. 998-1014.

129. Chugani, S.A., et al., *QscR, a modulator of quorum-sensing signal synthesis and virulence in Pseudomonas aeruginosa.* Proc Natl Acad Sci U S A, 2001. **98**(5): p. 2752-7.

130. Schuster, M., et al., *Identification, timing, and signal specificity of Pseudomonas aeruginosa quorum-controlled genes: a transcriptome analysis.* J Bacteriol, 2003. **185**(7): p. 2066-79.

131. Filloux, A., et al., *Phosphate regulation in Pseudomonas aeruginosa: cloning of the alkaline phosphatase gene and identification of phoB- and phoR-like genes.* Mol Gen Genet, 1988. **212**(3): p. 510-3.

132. Bleves, S., et al., *Protein secretion systems in Pseudomonas aeruginosa: A wealth of pathogenic weapons.* Int J Med Microbiol, 2010. **300**(8): p. 534-43.

133. Frank, D.W., *The exoenzyme S regulon of Pseudomonas aeruginosa.* Mol Microbiol, 1997. **26**(4): p. 621-9.

134. Dasgupta, N., et al., *A novel anti-anti-activator mechanism regulates expression of the Pseudomonas aeruginosa type III secretion system.* Mol Microbiol, 2004. **53**(1): p. 297-308.

135. Shen, D.K., et al., *PsrA is a positive transcriptional regulator of the type III secretion system in Pseudomonas aeruginosa.* Infect Immun, 2006. **74**(2): p. 1121-9.

136. Wu, W. and S. Jin, *PtrB of Pseudomonas aeruginosa suppresses the type III secretion system under the stress of DNA damage.* J Bacteriol, 2005. **187**(17): p. 6058-68.

137. Sandkvist, M., *Type II secretion and pathogenesis.* Infect Immun, 2001. **69**(6): p. 3523-35.

138. Furukawa, S., S.L. Kuchma, and G.A. O'Toole, *Keeping their options open: acute versus persistent infections.* Journal of bacteriology, 2006. **188**(4): p. 1211-1217.

139. Roy-Burman, A., et al., *Type III protein secretion is associated with death in lower respiratory and systemic Pseudomonas aeruginosa infections.* J Infect Dis, 2001. **183**(12): p. 1767-74.

140. Morgan, J.L.W., J.F. Acheson, and J. Zimmer, *Structure of a Type-1 Secretion System ABC Transporter.* Structure, 2017. **25**(3): p. 522-529.

141. Wandersman, C. and P. Delepelaire, *Bacterial iron sources: from siderophores to hemophores.* Annu Rev Microbiol, 2004. **58**: p. 611-47.

142. Guzzo, J., et al., *Pseudomonas aeruginosa alkaline protease: evidence for secretion genes and study of secretion mechanism.* J Bacteriol, 1991. **173**(17): p. 5290-7.

143. Wolf, P. and U. Elsasser-Beile, *Pseudomonas exotoxin A: from virulence factor to anti-cancer agent.* Int J Med Microbiol, 2009. **299**(3): p. 161-76.

144. Kuang, Z., et al., *Pseudomonas aeruginosa elastase provides an escape from phagocytosis by degrading the pulmonary surfactant protein-A.* PLoS One, 2011. **6**(11): p. e27091.

145. Bradshaw, J.L., et al., *Pseudomonas aeruginosa Protease IV Exacerbates Pneumococcal Pneumonia and Systemic Disease.* mSphere, 2018. **3**(3): p. e00212-18.

146. Quinaud, M., et al., *The PscE-PscF-PscG complex controls type III secretion needle biogenesis in Pseudomonas aeruginosa.* J Biol Chem, 2005. **280**(43): p. 36293-300.

147. Shaver, C.M. and A.R. Hauser, *Relative contributions of Pseudomonas aeruginosa ExoU, ExoS, and ExoT to virulence in the lung.* Infect Immun, 2004. **72**(12): p. 6969-77.

148. Titball, R.W., *Bacterial phospholipases C.* Microbiological reviews, 1993. **57**(2): p. 347-366.

149. Gallagher, L.A. and C. Manoil, *Pseudomonas aeruginosa PAO1 kills Caenorhabditis elegans by cyanide poisoning.* J Bacteriol, 2001. **183**(21): p. 6207-14.

150. Zaidi, T.S., et al., *Lipopolysaccharide outer core is a ligand for corneal cell binding and ingestion of Pseudomonas aeruginosa.* Invest Ophthalmol Vis Sci, 1996. **37**(6): p. 976-86.

151. Spiro, S., *The FNR family of transcriptional regulators.* Antonie Van Leeuwenhoek, 1994. **66**(1-3): p. 23-36.

152. Bomberger, J.M., et al., *Long-distance delivery of bacterial virulence factors by Pseudomonas aeruginosa outer membrane vesicles.* PLoS Pathog, 2009. **5**(4): p. e1000382.

153. Hogardt, M. and J. Heesemann, *Adaptation of Pseudomonas aeruginosa during persistence in the cystic fibrosis lung.* Int J Med Microbiol, 2010. **300**(8): p. 557-62.

154. Southey-Pillig, C.J., D.G. Davies, and K. Sauer, *Characterization of temporal protein production in Pseudomonas aeruginosa biofilms.* J Bacteriol, 2005. **187**(23): p. 8114-26.

155. Robert-Genthon, M., et al., *Unique features of a Pseudomonas aeruginosa alpha2-macroglobulin homolog.* MBio, 2013. **4**(4).

156. Webb, J.S., et al., *Cell death in Pseudomonas aeruginosa biofilm development.* J Bacteriol, 2003. **185**(15): p. 4585-92.

157. Danese, P.N., L.A. Pratt, and R. Kolter, *Exopolysaccharide production is required for development of Escherichia coli K-12 biofilm architecture.* J Bacteriol, 2000. **182**(12): p. 3593-6.

158. Singh, P.K., *Iron sequestration by human lactoferrin stimulates P. aeruginosa surface motility and blocks biofilm formation.* Biometals, 2004. **17**(3): p. 267-70.

159. Banin, E., M.L. Vasil, and E.P. Greenberg, *Iron and Pseudomonas aeruginosa biofilm formation.* Proc Natl Acad Sci U S A, 2005. **102**(31): p. 11076-81.

160. Nairz, M., et al., *The struggle for iron – a metal at the host–pathogen interface.* Cellular Microbiology, 2010. **12**(12): p. 1691-1702.

161. Minandri, F., et al., *Role of Iron Uptake Systems in Pseudomonas aeruginosa Virulence and Airway Infection.* Infection and Immunity, 2016. **84**(8): p. 2324.

162. Hassan, H.M. and I. Fridovich, *Mechanism of the antibiotic action pyocyanine.* Journal of bacteriology, 1980. **141**(1): p. 156-163.

163. Usher, L.R., et al., *Induction of neutrophil apoptosis by the Pseudomonas aeruginosa exotoxin pyocyanin: a potential mechanism of persistent infection.* J Immunol, 2002. **168**(4): p. 1861-8.

164. Nelson, C.E., et al., *Proteomic analysis of the Pseudomonas aeruginosa iron starvation response reveals PrrF sRNA-dependent iron regulation of twitching motility, amino acid metabolism, and zinc homeostasis proteins.* J Bacteriol, 2019.

165. Guan, C.P., et al., *Global Transcriptome Changes of Biofilm-Forming Staphylococcus epidermidis Responding to Total Alkaloids of Sophorea alopecuroides.* Pol J Microbiol, 2018. **67**(2): p. 223-226.

166. Pysz, M.A., et al., *Transcriptional analysis of biofilm formation processes in the anaerobic, hyperthermophilic bacterium Thermotoga maritima.* Appl Environ Microbiol, 2004. **70**(10): p. 6098-112.

167. Clark, S.T., et al., *Phenotypic diversity within a Pseudomonas aeruginosa population infecting an adult with cystic fibrosis.* Sci Rep, 2015. **5**: p. 10932.

168. Czechowska, K., et al., *Cheating by type 3 secretion system-negative Pseudomonas aeruginosa during pulmonary infection.* Proc Natl Acad Sci U S A, 2014. **111**(21): p. 7801-6.

169. Kukavica-Ibrulj, I., et al., *In vivo growth of Pseudomonas aeruginosa strains PAO1 and PA14 and the hypervirulent strain LESB58 in a rat model of chronic lung infection.* J Bacteriol, 2008. **190**(8): p. 2804-13.

170. Mikkelsen, H., R. McMullan, and A. Filloux, *The Pseudomonas aeruginosa reference strain PA14 displays increased virulence due to a mutation in ladS.* PLoS One, 2011. **6**(12): p. e29113.

171. Carilla-Latorre, S., et al., *Dictyostelium transcriptional responses to Pseudomonas aeruginosa: common and specific effects from PAO1 and PA14 strains.* BMC Microbiol, 2008. **8**: p. 109.

172. Lee, D.G., et al., *Genomic analysis reveals that Pseudomonas aeruginosa virulence is combinatorial.* Genome Biol, 2006. **7**(10): p. R90.

173. Stover, C.K., et al., *Complete genome sequence of Pseudomonas aeruginosa PAO1, an opportunistic pathogen.* Nature, 2000. **406**(6799): p. 959-64.

174. He, J., et al., *The broad host range pathogen Pseudomonas aeruginosa strain PA14 carries two pathogenicity islands harboring plant and animal virulence genes.* Proc Natl Acad Sci U S A, 2004. **101**(8): p. 2530-5.

175. Harrison, E.M., et al., *Pathogenicity islands PAPI-1 and PAPI-2 contribute individually and synergistically to the virulence of Pseudomonas aeruginosa strain PA14.* Infect Immun, 2010. **78**(4): p. 1437-46.

176. Choi, J.Y., et al., *Identification of virulence genes in a pathogenic strain of Pseudomonas aeruginosa by representational difference analysis.* J Bacteriol, 2002. **184**(4): p. 952-61.

177. Ferrara, S., et al., *Comparative profiling of Pseudomonas aeruginosa strains reveals differential expression of novel unique and conserved small RNAs.* PLoS One, 2012. **7**(5): p. e36553.

178. Ferrara, S., et al., *The PAPI-1 pathogenicity island-encoded small RNA PesA influences Pseudomonas aeruginosa virulence and modulates pyocin S3 production.* PLoS One, 2017. **12**(6): p. e0180386.

179. Chargaff, E., *Chemical specificity of nucleic acids and mechanism of their enzymatic degradation.* Experientia, 1950. **6**(6): p. 201-9.

180. Sueoka, N., *Intrastrand parity rules of DNA base composition and usage biases of synonymous codons.* J Mol Evol, 1995. **40**(3): p. 318-25.

181. Lobry, J.R., *Asymmetric substitution patterns in the two DNA strands of bacteria.* Mol Biol Evol, 1996. **13**(5): p. 660-5.

182. Mulcair, M.D., et al., *A molecular mousetrap determines polarity of termination of DNA replication in E. coli.* Cell, 2006. **125**(7): p. 1309-19.

183. Lee, J.Y., et al., *Single-molecule imaging of DNA curtains reveals mechanisms of KOPS sequence targeting by the DNA translocase FtsK.* Proc Natl Acad Sci U S A, 2012. **109**(17): p. 6531-6.

184. Shimokawa, K., et al., *FtsK-dependent XerCD-dif recombination unlinks replication catenanes in a stepwise manner.* Proc Natl Acad Sci U S A, 2013. **110**(52): p. 20906-11.

185. Xia, X., *DNA replication and strand asymmetry in prokaryotic and mitochondrial genomes.* Current genomics, 2012. **13**(1): p. 16-27.

186. Necsulea, A. and J.R. Lobry, *A new method for assessing the effect of replication on DNA base composition asymmetry.* Mol Biol Evol, 2007. **24**(10): p. 2169-79.

187. Chen, C.-L., et al., *Replication-Associated Mutational Asymmetry in the Human Genome.* Molecular Biology and Evolution, 2011. **28**(8): p. 2327-2337.

188. McLean, M.J., K.H. Wolfe, and K.M. Devine, *Base composition skews, replication orientation, and gene orientation in 12 prokaryote genomes.* J Mol Evol, 1998. **47**(6): p. 691-6.

189. Simon, R., et al., *Plasmid vectors for the genetic analysis and manipulation of rhizobia and other gram-negative bacteria.* Methods Enzymol, 1986. **118**: p. 640-59.

190. Hoang, T.T., et al., *A broad-host-range Flp-FRT recombination system for site-specific excision of chromosomally-located DNA sequences: application for isolation of unmarked Pseudomonas aeruginosa mutants.* Gene, 1998. **212**(1): p. 77-86.

191. Li, X.T., et al., *Positive and negative selection using the tetA-sacB cassette: recombineering and P1 transduction in Escherichia coli.* Nucleic Acids Res, 2013. **41**(22): p. e204.

192. West, S.E., et al., *Construction of improved Escherichia-Pseudomonas shuttle vectors derived from pUC18/19 and sequence of the region required for their replication in Pseudomonas aeruginosa.* Gene, 1994. **148**(1): p. 81-6.

193. Morita, Y., et al., *Application of an inducible system to engineer unmarked conditional mutants of essential genes of Pseudomonas aeruginosa.* J Microbiol Methods, 2010. **82**(3): p. 205-13.

194. Castang, S., et al., *H-NS family members function coordinately in an opportunistic pathogen.* Proc Natl Acad Sci U S A, 2008. **105**(48): p. 18947-52.

195. O'Toole, G.A. and R. Kolter, *Initiation of biofilm formation in Pseudomonas fluorescens WCS365 proceeds via multiple, convergent signalling pathways: a genetic analysis.* Mol Microbiol, 1998. **28**(3): p. 449-61.

196. Wang, Q., et al., *Chromosome condensation in the absence of the non-SMC subunits of MukBEF.* J Bacteriol, 2006. **188**(12): p. 4431-41.

197. Thermofisher, *Application and Tehniques.* 2012.

198. Thermofisher. *DNase I (RNase free) manual*. 2012; Available from: https://assets.thermofisher.com/TFS-Assets/LSG/manuals/4393898B.pdf.

199. MATLAB, *version R2017a*. 2019, The MathWorks Inc.: Natick, Massachusetts.

200. MATLAB. *Hierarchical Clustering*. 2019; Available from: https://www.mathworks.com/help/stats/hierarchical-clustering.html.

201. MATLAB. *pdist*. 2019; Available from: https://www.mathworks.com/help/stats/pdist.html.

202. MATLAB. *dendrogram*. 2019; Available from: https://www.mathworks.com/help/stats/dendrogram.html.

203. Jolliffe, I.T. and J. Cadima, *Principal component analysis: a review and recent developments.* Philos Trans A Math Phys Eng Sci, 2016. **374**(2065): p. 20150202.

204. Laboratories, K., *KEGG: Kyoto Encyclopedia of Genes and Genomes*. 2019.

205. NHC Key Laboratory of Systems Biology of Pathogens, I.o.P.B., CAMS&PUMC, *Virulence Factors of Pathogenic Bacteria.* 2019.

206. University, T.B.L.a.S.F., *Pseudomonas Genome Database.* 2019.

207. Winsor, G.L., et al., *Enhanced annotations and features for comparing thousands of Pseudomonas genomes in the Pseudomonas genome database.* Nucleic Acids Res, 2016. **44**(D1): p. D646-53.

208. Pissaridou, P., et al., *The Pseudomonas aeruginosa T6SS-VgrG1b spike is topped by a PAAR protein eliciting DNA damage to bacterial competitors.* Proc Natl Acad Sci U S A, 2018. **115**(49): p. 12519-12524.

209. Whitney, J.C., et al., *An interbacterial NAD(P)(+) glycohydrolase toxin requires elongation factor Tu for delivery to target cells.* Cell, 2015. **163**(3): p. 607-19.

210. Hachani, A., et al., *The VgrG proteins are "a la carte" delivery systems for bacterial type VI effectors.* J Biol Chem, 2014. **289**(25): p. 17872-84.

211. Boyer, F., et al., *Dissecting the bacterial type VI secretion system by a genome wide in silico analysis: what can be learned from available microbial genomic resources?* BMC Genomics, 2009. **10**: p. 104.

212. Llamas, M.A., et al., *A Novel extracytoplasmic function (ECF) sigma factor regulates virulence in Pseudomonas aeruginosa.* PLoS Pathog, 2009. **5**(9): p. e1000572.

213. Webb, J.S., M. Lau, and S. Kjelleberg, *Bacteriophage and phenotypic variation in Pseudomonas aeruginosa biofilm development.* J Bacteriol, 2004. **186**(23): p. 8066-73.

214. Borrero-de Acuna, J.M., et al., *Protein Network of the Pseudomonas aeruginosa Denitrification Apparatus.* J Bacteriol, 2016. **198**(9): p. 1401-13.

215. Hayashi, N.R., et al., *The nirQ gene, which is required for denitrification of Pseudomonas aeruginosa, can activate the RubisCO from Pseudomonas hydrogenothermophila.* Biochim Biophys Acta, 1998. **1381**(3): p. 347-50.

216. Alvarez-Ortega, C. and C.S. Harwood, *Responses of Pseudomonas aeruginosa to low oxygen indicate that growth in the cystic fibrosis lung is by aerobic respiration.* Mol Microbiol, 2007. **65**(1): p. 153-65.

217. Bechtold, B. *Violin Plot*. 2016; Available from: https://github.com/bastibe/Violinplot-Matlab/blob/master/Violin.m.

218. Heil, J. *Venn Diagram (vennx)*. 2004; Available from: https://www.mathworks.com/matlabcentral/fileexchange/6116-proportional-venn-diagrams.

219. Rosano, G.L. and E.A. Ceccarelli, *Recombinant protein expression in Escherichia coli: advances and challenges.* Front Microbiol, 2014. **5**: p. 172.

220. Carnoy, C. and C.-A. Roten, *The dif/Xer recombination systems in proteobacteria.* PloS one, 2009. **4**(9): p. e6531-e6531.

221. Hendrickson, H. and J.G. Lawrence, *Selection for chromosome architecture in bacteria.* J Mol Evol, 2006. **62**(5): p. 615-29.

Appendix

Table 1: List of plasmids used in studying *P. aeruginosa* physiology

Plasmids	Description	Source or reference
General vectors		
pFLP2	ApR; Site-specific excision vector	[190]
pUCP22	ApR; shuttle plasmid	[192]
pEXG2	GmR; Scarless deletion plasmid	[194]
pEX18Ap	ApR; Deletion plasmid	[190]
pYM101	ApR; Source of *lacI*^{q} gene and the T7 early promoter $P_{T7(A1/04/03)}$	[193]
PAO1 study		
pEX-Δ*mksB*::*mksB*	ApR; GmR; *mksB* knock-in plasmid for mksB1 used for complementation	This study
pEX-*mksB*-D864A	ApR; GmR; *mksB*-D864A ATPase point mutation plasmid	This study
pEX-*mksB*-E865Q	ApR; GmR; *mksB*-E865Q ATPase point mutation plasmid	This study
pEX-*mksB*-S829R	ApR; GmR; *mksB*-S829R ATPase point mutation plasmid	This study
pEX-*mksB*-Das4	ApR; GmR; ClpXP mediated degradation of MksB protein	This study
pEXG2-*sspB*	GmR; *sspB* deletion plasmid	[194]
pUCP22-*SspB* (pSspB)	ApR; SspB expression vector under *araC*-P_{araBAD} control	This study
pUCP-*mksB*	ApR; MksB-His_8 expression vector under *araC*-P_{araBAD} control	[27]
PA14 study		
pEX-Δ*smc*	ApR; GmR*; smc* deletion plasmid	[27]
pEX-Δ*mksB*	ApR; GmR*; mksB* deletion plasmid	[1]

pEX-Δ*mksB*2	ApR; GmR; *mksB2* deletion plasmid for *mksB2* in PA14	This study
pEX-*lac*-*mksB*2	ApR; GmR; *lacI*^{q}-P$_{T7}$ insertion plasmid for *mksB2*	This study
pEX-Δ*mksB*2 Δ*mksG*	ApR; GmR; *mksB2-mksG* deletion plasmid in PA14	This study

Table 2: List of strains used in studying *P. aeruginosa* physiology. GmR-FRT designates a gentamicin resistance marker flanked by two FRT sequences. ΔGm-scar designates removal of GmR-FRT by flippase (Flp) recombination at the FRT sequences, leaving an FRT sequence at the noted locus.

Strain	Relevant genotype or description	Source or reference
***E. coli* strains**		
SM10 (*λ pir*)	*thi thr leu tonA lacY supE recA::RP4-2-Tc::Mu KmR λpir*	[190]
DH5α	*supE44 DlacU169 hsdR17 recA1 endA1 gyrA96 thi-1 relA1*	Novagen
PAO1 strains		
PAO1 WT	*lacI^{q+} delta(lacZ)M15^{+} tetA^{+} tetR^{+}*	ATCC 47085
PAO1 Δ*smc*	PAO1-Lac Δ*smc*::ΔGm	[1]
PAO1 Δ*mksB*	PAO1-Lac Δ*mksB*::ΔGm	[1]
PAO1 Δ*smc* Δ*mksB*	PAO1-Lac Δ*smc* Δ*mksB*::ΔGm	[1]
PAO1 Mks’	PAO1-Lac *lacI^{q}*-P$_{T7}$-*mksB;* used for *mksB* complementation	[1]
PAO1 Δ*mksB*-P22-*mksB*	PAO1-Lac Δ*mksB +* pUCP22-*mksB;* used for *mksB* complementation	[1]
PAO1 Δ*mksB*::*mksB*	PAO1-Lac Δ*mksB*::*mksB*-scar; knock-in strain used for *mksB* complementation	This study
PAO1 *mksB*-E865Q	PA01-Lac *mksB*-E865Q	This study
PAO1 *mksB*-S829R	PA01-Lac *mksB*-S829R	This study
PAO1 *mksB*-D864A	PA01-Lac *mksB*-D864A	This study

PAO1 Δ*sspB*	PA01-Lac Δ*sspB;* used in the degron system	This study
PAO1 Das4	PAO1-Lac Δ*sspB mksB::mksB*-Das4; used in the degron system	This study
PAO1 Das4-pUCP22	PAO1-Lac-Δ*sspB mksB::mksB*-Das4 + pUCP22 empty vector; used in the degron system	This study
PAO1 Das4-PsspB	PAO1-Lac Δ*sspB mksB::mksB*-Das4 +pUCP22-SspB expression vector; used in the degron system	This study
PA14 strains		
PA14 WT	Clinical isolate UCBPP-PA14	[172]
PA14 *lacB2*	PA14-*lacI*^{q}-P$_{T7}$-*mksBEF2*	This study
PA14 *lacB2* Δ*smc*::GmR	PA14-*lacI*^{q}-P$_{T7}$-*mksBEF2* Δ*smc*::GmR-FRT	This study
PA14 *lacB2* Δ*smc*	PA14-*lacI*^{q}-P$_{T7}$-*mksBEF* Δ*smc::*ΔGm-scar	This study
PA14 *lacB2* Δ*B1*::GmR	PA14-*lacI*^{q}-P$_{T7}$-*mksBEF2* Δ*mksB1*::GmR-FRT	This study
PA14 *lacB2* Δ*B1*	PA14-*lacI*^{q}-P$_{T7}$-*mksBEF2* Δ*mksB1*::ΔGm-scar	This study
PA14 *lacB2* Δ*smc* Δ*mksB1*::GmR	PA14-*lacI*^{q}-P$_{T7}$-*mksBEF2* Δ*smc* Δ*mksB1*::GmR-FRT	This study
PA14 *lacB2 mksB1* Δ*smc*	PA14-*lacI*^{q}-P$_{T7}$-*mksBEF2* Δ*mksB1* Δ*smc*::ΔGm-scar	This study
PA14 Δ*B2*::GmR	PA14 Δ*mksB2*::GmR-FRT	This study
PA14 Δ*B2*	PA14 Δ*mksB2*::ΔGm-scar	This study
PA14 Δ*B1*::GmR	PA14 Δ*mksB1*::GmR-FRT	This study
PA14 Δ*B1*	PA14 Δ*mksB1*::ΔGm-scar	This study
PA14 Δ*smc*::GmR	PA14 Δ*smc*::GmR-FRT	This study
PA14 Δ*smc*	PA14 Δ*smc*::ΔGm-scar	This study

PA14 Δ*B2* Δ*B1*::GmR	PA14 Δ*mksB2* Δ*mksB1*::GmR-FRT	This study
PA14 Δ*B2* Δ*B1*	PA14 Δ*mksB2* Δ*mksB1*::ΔGm-scar	This study
PA14 Δ*B1* Δ*B2*::GmR	PA14 Δ*mksB1* Δ*mksB2*::GmR-FRT	This study
PA14 Δ*B1* Δ*B2*	PA14 Δ*mksB1* Δ*mksB2*::ΔGm-scar	This study
PA14 Δ*smc* Δ*B2*::GmR	PA14 Δ*smc* Δ*mksB2*::GmR-FRT	This study
PA14 Δ*smc* Δ*B2*	PA14 Δ*smc* Δ*mksB2*::ΔGm-scar	This study
PA14 Δ*smc* Δ*B1*::GmR	PA14 Δ*smc* Δ*mksB1*::GmR-FRT	This study
PA14 Δ*smc* Δ*B1*	PA14 Δ*smc* Δ*mksB1*::ΔGm-scar	This study
PA14 ΔΔΔ::GmR	PA14 Δ*mksB1* Δ*mksB2* Δ*smc*::GmR-FRT	This study
PA14 ΔΔΔ	PA14 Δ*mksB1* Δ*mksB2* Δ*smc*::ΔGm-scar	This study
PA14 Δ*B2* Δ*G*::GmR	PA14 Δ*mksB2* Δ*mksG*::GmR-FRT	This study

Table 3: List of Primers

Primer name	Nucleotide sequence	Description
Apa1	CCGCCGGTACCCTGACGGCGGAGCCCATG	For generating pex-Δ*mksB2* left flank, forward primer + KpnI site, 384 bp upstream from the *mksB2* start codon (GTA).
Apa2	CCGCCGCTAAGCCACGCCAGAGTAGTGCCT	For generating pEX-Δ*mksB2* left flank, reverse primer + BlpI site, 5bp downstream of *mksB2* start codon.
Apa3	CCGCCGGTCCGCCTGCTCAAGGATGCCTGC	For generating pEX-Δ*mksB2* right flank, forward primer + RsrII site, 476 bp upstream from *mksB2* stop codon.
Apa4	CCGCCAAGCTTCGACGCGGCACCTTCGAAG	For generating pEX-Δ*mksB2* right flank, reverse primer + HindIII site, 546 bp downstream from *mksB2* stop codon.
Apa5	CCGCCAAGGAATACAGTCGTCGAGC	For generating pEX-Δ*mksB2*-Δ*mksG* right flank, forward primer + RsrII site, 149 bp upstream from *mksG* stop codon.
Apa6	CCGCCAACGTTGTTGATCCGGGCTTCCAG	For generating pEX-Δ*mksB2*-Δ*mksG* right flank, reverse primer + HindIII site, 412 bp downstream from *mksG* stop codon.
Apa7	CGATCGAGTTCGTCCGAC	PCR check primer for *mksB2* deletion located 480 bp downstream from *mksG* stop codon
P1	CCGCCGGTACCCCGAGATTCGTGGGCAGG	For replacement of *mksBEF2* promoter with *LacI*^{q}-P_{T7} promoter, forward primer + KpnI site, 783 bp upstream of *mksR* start codon.

P2	TTCTTGGGAATTCGACTAGTTTCAACCGT CTCCTGGAG	For replacement of *mksBEF2* promoter with *LacI^q-P$_{T7}$*, reverse primer + SpeI and EcoRI sites, located 500 upstream of *mksF* start codon.
P3	GGTTGAAACTAGTGGAATTCCCAAGAAG GGTCTCGGCT	For replacement of *mksBEF2* promoter with *LacI^q-P$_{T7}$*, forward primer + SpeI and EcoRI sites, 22 bp upstream from *mksF* start codon.
P4	CCGCC CTGCAG ATTCGCGCCTTTGGAAC	For replacement of *mksBEF2* promoter with *LacI^q-P$_{T7}$*, reverse primer + PstI site, 939 bp downstream of *mksF* start codon.
Rev *mksB1* Blp1	CTTCTTGCTGAGCTCACGCCGGTTCGCCG GCTT	For generating pEX-Δ*mksB::mksB* complementation plasmid left flank, reverse primer + BlpI site, located at the *mksB* stop codon, used to amplify upstream portion of *mksB* and entire *mksB* gene.
Opa31 BamHI	CCTGGTGGATCCCGAGCTGGTCTGCGAT ACCC	For generating pEX-Δ*mksB::mksB* complementation plasmid left flank, forward primer + BamHI site, 520 bp upstream of the *mksB* start codon (used to amplify upstream portion of *mksB* and entire *mksB* gene).
Sbf1 forward	CTTCTTCCTGCAGGCGAATTAGCTTCAAA AGCGCTC	For generating pEX-Δ*mksB::mksB* right flank, forward primer + SbfI site, used to amplify *FRT-down mksB* fragment from pEX-Δ*mksB.*
Opa30	CCCAAGCTTAGTCCACGGCCCT GTCAGGC	For generating pEX-Δ*mksB::mksB* complementation plasmid right flank, reverse primer + HindIII site, used to amplify *FRT-down mksB* fragment from pEX-Δ*mksB.*

degron 7	GCTGGTACCTCTCGGTGTTCGACCTGAC C	For generating pEX-*mksB*-Das4, forward primer + KpnI site, 528 bp upstream of *mksB* stop codon.
degron 8	GTCGTTGGCGGCTGCGGCCGCATATATG AGCTCACTAGTGAATTCAAGCTTCGCCG GTTCGCCGGCTTCC	For generating pEX-*mksB*-Das4, reverse primer + Das4 linker, located at the *mksB* stop codon.
degron 9	CTTCTTGCTTAGCtcaTCGCTGGCGTCGG CGTAGTTCTCGCTGTAGTTCTCGTCGTTG GCGGCTGCGGC	For generating pEX-*mksB*-Das4, reverse primer complementary to degron 8 + Das4 tag + stop codon + BlpI.
degron 10	TCACCCTTAATTAATGAATTCCAGCCGTC CCTATC	For generating pUCP22-*sspB*, forward primer + PacI site, located at the start codon of *sspB* gene, used to amplify *sspB* gene and clone into pUCP22.
degron 11	AACAAGAGATCTTTACTTGACCACCTTCA GGGATG	For generating pUCP22-*sspB*, reverse primer + XbaI site, located at the stop codon of *sspB* gene, used to amplify *sspB* gene and clone into pUCP22
Opa180	CCTGGTACCTGCGCCTGAAGGGCGTCG	For generating *mksB* ATPase point mutation constructs, forward primer + KpnI site, 866 bp upstream from *mksB* start codon, cloned into pEX18AP.
Opa181	CTTCTTGCTTAGCTCACGCCGGTTCGCCG G	For generating *mksB* ATPase point mutation constructs, reverse primer + BlpI site, located at the *mksB* stop codon, cloned into pEX18AP.
Opa183	CCCTACTACCTGGCCGAGGCGGCGGAC	For generating pEX-*mksB*-D864A, forward primer, 237 bp upstream of the *mksB* stop codon, contains point mutations for D864A (GAC to GCC).

Opa184	GTCCGCCGCCTCGGCCAGGTAGTAGGG	For generating pEX-*mksB*-D864A, reverse primer, 237 bp upstream of the *mksB* stop codon, contains point mutations for D864A (GAC to GCC).
Opa185	CCTACTACCTGGACCAGGCGGCGGACATC	For generating pEX-*mksB*-E865Q, forward primer, 237 upstream of the *mksB* stop codon, contains point mutations for E865Q (GAG to CAG).
Opa186	GATGTCCGCCGCCTGGTCCAGGTAGTAGG	For generating pEX-*mksB*-E865Q, reverse primer, 237 upstream of the *mksB* stop codon, contains point mutations for E865Q (GAG to CAG).
Opa187	GACGGCGCCGCCCGCAATGGCACCACC	For generating pEX-*mksB*-S829R, forward primer, 345 bp from the *mksB* stop codon, contains point mutations for S829R (TCC to CGC)
Opa188	GGTGGTGCCATTGCGGGCGGCGCCGTC	For generating pEX-*mksB*-S829R, reverse primer 345 bp from the *mksB* stop codon, contains point mutations for S829R (TCC to CGC).

Table 4 Table of fold change values for PAO1 condensin mutants in affected pathways.

(minimum 1.5 fold for any sample)

T3SS

Locus Tag	General Description and Gene Name	*Δsmc*	*ΔmksB*	*ΔΔ*
PA0044	exoenzyme T (exoT)	-10.9	1.3	1.5
PA2191	adenylate cyclase ExoY (exoY)	-13.7	1.5	-1.0
PA3841	exoenzyme S (exoS)	-15.7	1.5	2.1
PA1692	translocation protein in type III secretion (PA1692)	-6.1	1.7	1.3
PA1693	type III secretion system protein (pscR)	-3.8	1.9	1.4
PA1694	type III secretion system protein (pscQ)	-9.6	1.9	1.1
PA1695	translocation protein in type III secretion (pscP)	-8.6	2.7	1.3
PA1696	translocation protein in type III secretion (pscO)	-8.1	2.2	1.1
PA1697	type III secretion system ATPase (PA1697)	-11.6	1.9	1.1
PA1698	Type III secretion outer membrane protein PopN precursor (popN)	-19.5	1.6	-1.1
PA1699	hypothetical protein (PA1699)	-8.0	2.2	1.3
PA1700	hypothetical protein (PA1700)	-8.0	2.6	1.0
PA1701	hypothetical protein (PA1701)	-18.5	2.1	1.1
PA1702	hypothetical protein (PA1702)	-5.0	2.0	1.2
PA1703	type III secretory apparatus protein PcrD (pcrD)	-9.1	1.4	1.1
PA1704	transcriptional regulator protein PcrR (pcrR)	-4.1	2.1	1.3
PA1705	regulator in type III secretion (pcrG)	-11.8	1.8	1.7
PA1706	type III secretion protein PcrV (pcrV)	-13.7	1.6	1.4
PA1707	regulatory protein PcrH (pcrH)	-17.5	1.6	1.7
PA1708	translocator protein PopB (popB)	-15.4	1.5	1.5
PA1709	translocator outer membrane protein PopD precursor (popD)	-12.2	1.6	1.5
PA1710	ExsC (exsC)	-4.7	2.0	1.5
PA1711	ExsE (exsE)	-5.5	1.9	1.4
PA1712	exoenzyme S synthesis protein B (exsB)	-5.0	1.6	1.7
PA1713	transcriptional regulator ExsA (exsA)	-5.9	1.2	1.4
PA1714	ExsD (exsD)	-5.3	1.4	1.3
PA1715	type III export apparatus protein (pscB)	-8.5	1.3	1.2
PA1716	Type III secretion outer membrane protein PscC precursor (pscC)	-5.5	1.3	1.4
PA1717	type III export protein PscD (pscD)	-5.1	1.3	1.4
PA1718	type III export protein PscE (pscE)	-5.9	2.1	1.2
PA1719	type III export protein PscF (pscF)	-6.5	1.6	1.3
PA1720	type III export protein PscG (pscG)	-11.6	2.0	1.4
PA1721	type III export protein PscH (pscH)	-5.6	1.5	1.2
PA1722	type III export protein PscI (pscI)	-7.0	1.6	1.5
PA1723	type III export protein PscJ (pscJ)	-7.1	1.4	1.4
PA1724	type III export protein PscK (pscK)	-5.6	1.4	1.2
PA1725	type III secretion system protein (pscL)	-4.8	1.3	-1.1
PA2191	adenylate cyclase ExoY (exoY)	-13.7	1.5	-1.0
PA3217	hypothetical protein (cyaB)	-1.5	1.0	-1.1
PA3841	exoenzyme S (exoS)	-15.7	1.5	2.1
PA3842	chaperone (PA3842)	-15.5	2.5	1.4

T6SS HSI-1

PA0070	hypothetical protein (PA0070)	2.0	-10.7	-5.4
PA0071	hypothetical protein (PA0071)	1.6	-2.8	-1.8
PA0072	hypothetical protein (PA0072)	2.0	-6.0	-3.3
PA0073	ABC transporter ATP-binding protein (PA0073)	1.7	-12.6	-4.5
PA0074	serine/threonine protein kinase PpkA (ppkA)	1.8	-5.9	-3.5
PA0075	PppA (pppA)	1.6	-10.3	-3.7
PA0076	hypothetical protein (PA0076)	1.7	-7.5	-2.7
PA0077	IcmF1 (icmF1)	2.2	-7.9	-3.2
PA0078	hypothetical protein (PA0078)	2.0	-7.6	-3.7
PA0079	hypothetical protein (PA0079)	1.7	-6.1	-2.7
PA0080	hypothetical protein (PA0080)	1.5	-13.6	-2.8
PA0081	Fha1 (fha1)	1.8	-2.0	1.3
PA0082	hypothetical protein (PA0082)	2.2	-12.0	-2.9
PA0083	hypothetical protein (PA0083)	2.3	-25.6	-9.8
PA0084	hypothetical protein (PA0084)	2.3	-27.4	-9.0
PA0085	Hcp1 (hcp1)	2.0	-50.3	-18.9
PA0086	hypothetical protein (PA0086)	2.0	-6.9	-4.6
PA0087	hypothetical protein (PA0087)	1.7	-35.1	-4.9
PA0088	hypothetical protein (PA0088)	2.0	-19.1	-7.3
PA0089	hypothetical protein (PA0089)	1.9	-18.4	-10.1
PA0090	ClpV1 (clpV1)	2.1	-17.4	-8.8
PA0091	VgrG1 (vgrG1)	1.8	-12.2	-7.2
PA0092	hypothetical protein (PA0092)	1.4	-3.5	-3.4
PA0093	hypothetical protein (PA0093)	1.7	-5.5	-3.6
PA0094	hypothetical protein (PA0094)	1.8	-6.2	-4.5
PA0095	hypothetical protein (PA0095)	1.7	-4.0	-2.4
PA0096	hypothetical protein (PA0096)	1.9	-4.2	-3.0
PA0097	hypothetical protein (PA0097)	1.5	-14.1	-4.3
PA0098	3-oxoacyl-(acyl carrier protein) synthase (PA0098)	1.7	-8.0	-2.8
PA0099	hypothetical protein (PA0099)	1.8	-6.2	-1.6
PA0100	hypothetical protein (PA0100)	1.5	-2.9	-1.8
PA0101	hypothetical protein (PA0101)	1.5	-3.2	-2.2
PA1844	hypothetical protein (PA1844)	1.5	-9.7	-6.0
PA1845	hypothetical protein (PA1845)	1.2	-8.0	-4.3
PA2684	hypothetical protein (PA2684)	1.7	-5.3	-2.7
PA2685	hypothetical protein (PA2685)	1.8	-3.6	-1.5
PA2702	hypothetical protein (PA2702)	1.5	-4.1	-3.2
PA2774	hypothetical protein (PA2774)	1.6	-4.6	-3.9
PA2775	hypothetical protein (PA2775)	1.6	-4.8	-2.0
PA3484	hypothetical protein (PA3484)	1.8	-7.3	-3.4
PA3485	hypothetical protein (PA3485)	1.3	-7.7	-2.9
PA5267	secreted protein Hcp (hcpB)	1.1	-1.8	-1.4

T2SS

Locus Tag	General Description and Gene Name	*Δsmc*	*ΔmksB*	*ΔΔ*
PA0677	putative type II secretion system protein (PA0677)	1.5	-1.4	1.7
PA0679	hypothetical protein (PA0679)	-1.1	-1.6	-1.3
PA0681	HxcT pseudopilin (PA0681)	-1.5	-1.7	1.1
PA0682	putative type II secretion system protein (PA0682)	-1.1	-1.7	-1.0
PA0685	putative type II secretion system protein (PA0685)	1.1	-1.7	-1.2
PA0686	putative type II secretion system protein (PA0686)	-1.0	-1.8	1.2
PA0844	hemolytic phospholipase C precursor (plcH)	1.4	-1.6	1.3
PA1382	type II secretion system protein (PA1382)	1.2	-1.3	2.0
PA1871	LasA protease precursor (lasA)	-1.1	-1.6	1.2
PA1948	membrane protein component of ABC ribose transporter (rbsC)	1.3	-2.4	2.4
PA2671	hypothetical protein (PA2671)	-1.1	1.2	2.0
PA2672	type II secretion system protein (PA2672)	-1.3	-2.3	-1.1
PA2673	type II secretion system protein (PA2673)	-1.2	-1.8	1.6
PA2674	type II secretion system protein (PA2674)	-1.3	1.5	1.2
PA2675	type II secretion system protein (PA2675)	1.1	1.0	1.8
PA2676	type II secretion system protein (PA2676)	1.2	-2.0	1.6
PA2862	lactonizing lipase precursor (lipA)	-1.3	1.1	1.9
PA3096	general secretion pathway protein L (xcpY)	-1.2	1.1	1.6
PA3098	general secretion pathway protein J (xcpW)	-1.8	1.1	1.6
PA3100	general secretion pathway outer membrane protein H precursor (xcpU)	-1.0	1.7	1.7
PA3102	general secretion pathway protein F (xcpS)	-1.1	-1.0	1.6
PA3104	secretion protein XcpP (xcpP)	-1.1	1.6	2.0
PA3296	alkaline phosphatase (phoA)	-1.2	-1.7	1.4
PA3319	non-hemolytic phospholipase C precursor (plcN)	1.0	1.1	1.6
PA3724	elastase LasB (lasB)	1.0	1.4	3.2
PA4813	lipase LipC (lipC)	-1.3	-2.0	1.3

T6SS HSI-2

PA1653	transcriptional regulator (PA1653)	1.1	1.2	1.6
PA1655	putative glutathione S-transferase (PA1655)	1.2	-1.1	1.6
PA1656	hypothetical protein (PA1656)	1.1	-6.6	-1.5
PA1657	hypothetical protein (PA1657)	1.4	-10.5	-5.4
PA1658	hypothetical protein (PA1658)	1.4	-10.3	-4.3
PA1659	hypothetical protein (PA1659)	1.1	-9.0	-2.6
PA1660	hypothetical protein (PA1660)	1.1	-5.2	-2.0
PA1661	hypothetical protein (PA1661)	1.1	-6.0	-4.1
PA1662	ClpA/B-type protease (PA1662)	1.4	-5.3	-3.0
PA1663	putative transcriptional regulator (PA1663)	1.3	-9.6	-5.9
PA1665	hypothetical protein (PA1665)	1.2	-15.0	-5.0
PA1666	hypothetical protein (PA1666)	1.4	-8.8	-3.3
PA1667	hypothetical protein (PA1667)	1.4	-3.9	-1.9
PA1668	hypothetical protein (PA1668)	1.5	-9.3	-3.4
PA1669	hypothetical protein (PA1669)	1.3	-5.6	-4.0
PA1670	serine/threonine phosphoprotein phosphatase Stp1 (stp1)	1.7	-6.4	-2.7
PA1671	serine-threonine kinase Stk1 (stk1)	1.6	-2.0	-1.0
PA1672	hypothetical protein (PA1672)	1.7	1.1	1.6
PA1673	hypothetical protein (PA1673)	-1.1	-1.4	-1.6
PA1675	hypothetical protein (PA1675)	1.2	-1.5	1.3
PA1676	hypothetical protein (PA1676)	-1.4	-1.8	1.2
PA1677	hypothetical protein (PA1677)	1.1	-1.0	1.7

BexR

PA0572	hypothetical protein (PA0572)	2.4	-1.3	1.2
PA1202	putative hydrolase (PA1202)	9.7	-14.3	-10.8
PA1203	hypothetical protein (PA1203)	4.9	-2.5	-1.9
PA1204	hypothetical protein (PA1204)	3.7	-1.7	-1.2
PA1205	hypothetical protein (PA1205)	3.5	-2.1	-1.3
PA1249	alkaline metalloproteinase precursor (aprA)	2.3	-1.5	1.1
PA2430	hypothetical protein (PA2430)	7.3	-2.5	-1.2
PA2431	hypothetical protein (PA2431)	5.5	-2.5	-1.7
PA2432	bistable expression regulator BexR	9.2	-4.6	-4.6
PA2433	hypothetical protein (PA2433)	4.6	-11.3	-1.1
PA2698	putative hydrolase (PA2698)	4.3	-1.7	-1.9
PA4205	hypothetical protein (mexG)	1.2	-1.3	-1.6
PA4206	RND efflux membrane fusion protein precursor (mexH)	1.1	-1.4	-1.9

a2-Macroglobulin Homologue

PA4487	hypothetical protein (PA4487)	1.6	-4.3	-3.7
PA4488	hypothetical protein (PA4488)	1.5	-5.1	-2.9
PA4489	hypothetical protein (PA4489)	1.7	-6.6	-4.5
PA4490	hypothetical protein (PA4490)	1.6	-5.0	-4.0
PA4491	hypothetical protein (PA4491)	1.6	-5.5	-4.4
PA4492	hypothetical protein (PA4492)	1.7	-2.4	-1.7

Pyocyanin

PA1900	phenazine biosynthesis protein (phzB2)	1.7	-1.7	1.4
PA1902	phenazine biosynthesis protein PhzD (phzD2)	-1.4	-2.9	-1.9
PA1904	phenazine biosynthesis protein (phzF2)	2.7	1.5	3.8
PA4212	phenazine biosynthesis protein PhzC (phzC1)	1.0	1.2	1.8
PA4215	phenazine biosynthesis protein (phzF1)	-1.4	-2.7	1.3
PA4217	hypothetical protein (phzS)	-1.5	-1.0	1.3

Psl

Locus Tag	General Description and Gene Name	*Δsmc*	*ΔmksB*	*ΔΔ*
PA2232	phosphomannose isomerase/GDP-mannose pyrophosphorylase (psl	1.56	-1.86	-1.38
PA2233	glycosyl transferase (pslC)	1.56	-1.60	-1.06
PA2234	PslD (pslD)	2.09	-2.24	-1.73
PA2235	hypothetical protein (pslE)	2.12	-2.16	-2.22
PA2236	hypothetical protein (pslF)	1.98	-2.57	-1.89
PA2237	putative glycosyl hydrolase (pslG)	1.94	-2.46	-1.85
PA2238	hypothetical protein (pslH)	1.88	-2.05	-2.27
PA2239	putative transferase (pslI)	1.44	-2.65	-2.00
PA2240	hypothetical protein (pslJ)	1.57	-2.46	-1.85
PA2241	hypothetical protein (pslK)	1.46	-2.23	-2.47
PA2242	hypothetical protein (pslL)	1.68	-2.62	-2.20
PA2663	psl and pyoverdine operon regulator, PpyR	1.15	2.26	-1.07
PA5452	phosphomannose isomerase/GDP-mannose WbpW (wbpW)	1.15	-1.29	1.90

Pel

PA3058	PelG (pelG)	1.16	-1.06	1.55
PA3059	PelF (pelF)	1.45	-1.74	1.17
PA3060	PelE (pelE)	1.75	1.13	1.33
PA3061	PelD (pelD)	1.89	-2.51	-1.47
PA3062	PelC (pelC)	1.79	-4.30	-1.05
PA3063	PelB (pelB)	2.62	-1.64	-1.16
PA3064	PelA (pelA)	1.50	-1.78	-1.10

Biofilm (no Pel/Psl)

PA0074	serine/threonine protein kinase PpkA (ppkA)	1.84	-5.92	-3.52
PA0075	PppA (pppA)	1.61	-10.27	-3.69
PA0076	hypothetical protein (PA0076)	1.74	-7.54	-2.71
PA0077	IcmF1 (icmF1)	2.17	-7.94	-3.20
PA0079	hypothetical protein (PA0079)	1.68	-6.07	-2.66
PA0081	Fha1 (fha1)	1.81	-2.03	1.29
PA0082	hypothetical protein (PA0082)	2.19	-11.99	-2.86
PA0083	hypothetical protein (PA0083)	2.33	-25.57	-9.76
PA0084	hypothetical protein (PA0084)	2.30	-27.39	-8.96
PA0085	Hcp1 (hcp1)	2.02	-50.33	-18.88
PA0089	hypothetical protein (PA0089)	1.87	-18.40	-10.05
PA0090	ClpV1 (clpV1)	2.10	-17.43	-8.76
PA0169	hypothetical protein (PA0169)	1.68	-3.19	-2.79
PA0172	hypothetical protein (PA0172)	1.76	-3.28	-2.24
PA0263	secreted protein Hcp (hcpC)	1.89	1.45	-1.03
PA0649	anthranilate synthase component II (trpG)	1.10	-1.21	1.59
PA0905	carbon storage regulator (rsmA)	1.26	-2.06	1.22
PA0996	coenzyme A ligase (pqsA)	-1.07	1.30	2.87
PA0997	beta-keto-acyl-acyl-carrier protein synthase-like protein (pqsB)	-1.48	1.06	1.59
PA1000	quinolone signal response protein (pqsE)	-1.56	-1.58	-1.02
PA1001	anthranilate synthase component I (phnA)	1.11	-1.58	-1.62
PA1002	anthranilate synthase component II (phnB)	1.33	-1.16	1.72
PA1003	Transcriptional regulator MvfR (mvfR)	1.50	-1.45	2.04
PA1432	autoinducer synthesis protein LasI (lasI)	1.07	-2.64	1.43
PA1657	hypothetical protein (PA1657)	1.41	-10.51	-5.38
PA1658	hypothetical protein (PA1658)	1.43	-10.33	-4.31
PA1661	hypothetical protein (PA1661)	1.06	-6.04	-4.11
PA1662	ClpA/B-type protease (PA1662)	1.40	-5.30	-3.03
PA1667	hypothetical protein (PA1667)	1.40	-3.89	-1.88
PA1669	hypothetical protein (PA1669)	1.34	-5.63	-3.96
PA1670	serine/threonine phosphoprotein phosphatase Stp1 (stp1)	1.71	-6.44	-2.70
PA1976	sensor histidine kinase	1.07	-1.58	-1.03
PA2360	hypothetical protein (PA2360)	1.25	-3.84	-1.14
PA2361	hypothetical protein (PA2361)	1.41	-1.81	1.12
PA2363	hypothetical protein (PA2363)	1.11	-2.26	-1.18
PA2365	hypothetical protein (PA2365)	1.71	-2.75	-1.89
PA2366	uricase PuuD (PA2366)	1.65	-2.13	-1.64
PA2367	hypothetical protein (PA2367)	1.20	-3.69	-4.05
PA2370	hypothetical protein (PA2370)	1.13	-3.43	-2.10
PA2371	putative ClpA/B-type protease (PA2371)	1.07	-3.07	1.81
PA2569	hypothetical protein (PA2569)	-1.10	-1.23	2.03
PA2586	response regulator GacA (gacA)	-1.02	1.30	2.04
PA2824	sensor/response regulator hybrid (PA2824)	-1.12	1.09	1.64
PA3217	hypothetical protein (cyaB)	-1.52	1.04	-1.10
PA3345	hypothetical protein (PA3345)	-1.36	1.12	1.95
PA3346	putative two-component response regulator (PA3346)	-1.20	1.06	2.00
PA3347	hypothetical protein (PA3347)	-1.01	1.73	3.17
PA3476	autoinducer synthesis protein RhlI (rhlI)	1.25	-1.30	1.71
PA3478	rhamnosyltransferase chain B (rhlB)	-1.13	-1.10	2.48
PA3479	rhamnosyltransferase chain A (rhlA)	-1.68	-1.59	-1.36
PA3542	alginate biosynthesis protein Alg44 (alg44)	1.13	1.04	1.51
PA3703	chemotaxis-specific methylesterase (wspF)	-1.03	1.42	1.88
PA3704	putative chemotaxis sensor/effector fusion protein (wspE)	-1.57	1.28	1.32
PA3707	hypothetical protein (wspB)	-1.17	1.23	1.79
PA3708	putative chemotaxis transducer (wspA)	-1.17	1.06	1.82
PA5267	secreted protein Hcp (hcpB)	1.09	-1.78	-1.40

Bacteriophage pf1

Locus Tag	General Description and Gene Name			
PA0715	hypothetical protein (PA0715)	1.8	1.4	3.3
PA0716	hypothetical protein (PA0716)	1.9	-1.1	2.7
PA0717	hypothetical protein (PA0717)	-7.1	-29.4	-14.4
PA0718	hypothetical protein (PA0718)	-6.6	-28.8	-8.3
PA0719	hypothetical protein (PA0719)	-4.0	-13.0	-8.0
PA0720	helix destabilizing protein of bacteriophage Pf1 (PA0720)	-7.8	-16.6	-13.6
PA0722	hypothetical protein (PA0722)	-5.7	-10.7	-16.2
PA0723	coat protein B of bacteriophage Pf1) (coaB)	-7.1	-14.7	-14.4
PA0724	putative coat protein A of bacteriophage Pf1 (PA0724)	-3.4	-5.4	-3.2
PA0725	bacteriophage protein (PA0725)	-2.1	-3.1	-2.3
PA0726	hypothetical protein (PA0726)	-2.1	-4.6	-1.8
PA0727	hypothetical protein (PA0727)	-2.9	-3.4	-2.3
PA0728	bacteriophage integrase (PA0728)	-2.2	-3.2	-1.6
PA0729	hypothetical protein (PA0729)	-1.2	-1.6	-1.2

Pyoverdine

PA2254	pyoverdine biosynthesis protein PvcA (pvcA)	-1.2	1.5	1.8
PA2256	pyoverdine biosynthesis protein PvcC (pvcC)	-1.0	-1.6	1.0
PA2257	pyoverdine biosynthesis protein PvcD (pvcD)	1.5	-1.3	2.2
PA2385	3-oxo-C12-homoserine lactone acylase PvdQ (pvdQ)	2.1	-3.4	-1.5
PA2386	L-ornithine N5-oxygenase (pvdA)	4.8	-2.4	-2.0
PA2387	FpvI (fpvI)	1.6	-1.3	2.4
PA2392	PvdP (pvdP)	1.6	-1.9	-1.5
PA2393	putative dipeptidase precursor (PA2393)	1.8	-1.4	1.2
PA2394	PvdN (pvdN)	1.4	-2.0	-1.3
PA2395	PvdO (pvdO)	2.9	-1.6	1.6
PA2396	pyoverdine synthetase F (pvdF)	1.6	-1.7	-1.0
PA2397	pyoverdine biosynthesis protein PvdE (pvdE)	-1.0	-1.8	1.6
PA2398	ferripyoverdine receptor (fpvA)	1.8	-5.1	-3.9
PA2399	pyoverdine synthetase D (pvdD)	1.4	-2.2	-1.1
PA2400	probable non-ribosomal peptide synthetase (pvdJ)	1.2	-2.6	-1.4
PA2402	peptide synthase (PA2402)	1.6	-2.2	-1.1
PA2413	diaminobutyrate--2-oxoglutarate aminotransferase (pvdH)	3.3	-2.6	1.1
PA2424	peptide synthase (pvdL)	1.5	-2.2	-1.5
PA2426	extracytoplasmic-function sigma-70 factor (pvdS)	5.5	-1.9	-1.9
PA4168	second ferric pyoverdine receptor FpvB (fpvB)	-1.1	-1.3	1.8
PA5531	transporter TonB	2.1	-1.1	2.3

Pyochelin

PA4221	Fe(III)-pyochelin outer membrane receptor precursor (fptA)	-1.12	-3.25	2.67
PA4222	ABC transporter ATP-binding protein (PA4222)	-1.63	-2.97	1.52
PA4223	ABC transporter ATP-binding protein (PA4223)	-1.51	-3.04	1.45
PA4224	pyochelin biosynthetic protein PchG (pchG)	-1.98	-7.80	1.51
PA4225	pyochelin synthetase (pchF)	-1.27	-5.39	1.75
PA4226	dihydroaeruginoic acid synthetase (pchE)	-1.24	-4.35	1.66
PA4227	transcriptional regulator PchR (pchR)	1.32	-3.13	1.32
PA4228	pyochelin biosynthesis protein PchD (pchD)	-1.24	-6.73	1.78
PA4229	pyochelin biosynthetic protein PchC (pchC)	-1.60	-7.33	1.77
PA4230	isochorismate-pyruvate lyase (pchB)	-1.03	-2.66	3.35
PA4231	salicylate biosynthesis isochorismate synthase (pchA)	1.04	-2.85	2.06

Denitrification

PA0516	heme d1 biosynthesis protein NirF (nirF)	1.5	1.1	1.3
PA0518	cytochrome c-551 precursor (nirM)	1.6	1.4	1.0
PA0520	regulatory protein NirQ (nirQ)	1.8	-1.5	1.5
PA0521	putative cytochrome c oxidase subunit (PA0521)	1.5	-2.1	1.1
PA0522	hypothetical protein (PA0522)	1.7	-2.7	1.5
PA0523	nitric-oxide reductase subunit C (norC)	1.6	-1.4	1.8
PA0524	nitric-oxide reductase subunit B (norB)	1.9	-1.5	1.7
PA0525	putative dinitrification protein NorD (PA0525)	2.2	-1.1	1.6
PA1172	cytochrome c-type protein NapC (napC)	2.2	-2.5	1.0
PA1173	cytochrome c-type protein NapB precursor (napB)	1.6	-2.3	-1.9
PA1174	nitrate reductase catalytic subunit (napA)	1.1	-1.8	-1.0
PA1175	NapD protein of periplasmic nitrate reductase (napD)	1.3	-2.3	-1.1
PA1176	ferredoxin protein NapF (napF)	-1.2	-2.2	-1.9
PA1177	periplasmic nitrate reductase protein NapE (napE)	1.1	-2.6	-1.6
PA3392	nitrous-oxide reductase (nosZ)	2.5	3.0	1.8
PA3393	NosD protein (nosD)	2.5	2.5	2.2
PA3394	NosF protein (nosF)	2.0	2.4	1.6
PA3395	NosY protein (nosY)	2.2	2.2	1.7
PA3396	NosL protein (nosL)	2.4	2.6	1.3
PA3872	respiratory nitrate reductase gamma chain (narI)	-1.1	-1.3	1.6
PA3873	respiratory nitrate reductase delta chain (narJ)	-1.2	-1.2	1.8
PA3874	respiratory nitrate reductase beta chain (narH)	-1.4	-1.3	1.8
PA3875	respiratory nitrate reductase alpha chain (narG)	-1.7	-1.5	2.0

Sigma Factors

Locus Tag	General Description and Gene Name	*Δsmc*	*ΔmksB*	*ΔΔ*
PA0472	RNA polymerase sigma factor (PA0472)	2.3	-2.2	1.6
PA0762	RNA polymerase sigma factor AlgU (algU)	1.0	-1.7	2.3
PA0763	anti-sigma factor MucA (mucA)	-1.0	-1.7	1.3
PA1300	ECF subfamily RNA polymerase sigma-70 factor (PA1300)	2.4	1.1	1.5
PA1351	ECF subfamily RNA polymerase sigma-70 factor (PA1351)	1.6	-1.2	1.6
PA1363	ECF subfamily RNA polymerase sigma-70 factor (PA1363)	1.6	-1.5	1.3
PA1912	ECF sigma factor, FemI	1.5	-1.8	-1.0
PA2050	RNA polymerase sigma factor (PA2050)	1.5	-1.3	-1.4
PA2093	RNA polymerase sigma factor (PA2093)	1.5	-1.7	1.4
PA2387	FpvI (fpvI)	1.6	-1.3	2.4
PA2426	extracytoplasmic-function sigma-70 factor (pvdS)	5.5	-1.9	-1.9
PA2467	Anti-sigma factor FoxR (foxR)	1.4	-1.1	1.6
PA2896	RNA polymerase sigma factor (PA2896)	1.4	-1.0	1.6
PA3410	ECF subfamily RNA polymerase sigma-70 factor (PA3410)	2.0	1.1	1.8
PA3899	RNA polymerase sigma factor (PA3899)	1.3	-1.8	1.6
PA4896	RNA polymerase sigma factor (PA4896)	2.6	1.6	4.0

Virulence Regulators

PA0074	serine/threonine protein kinase PpkA (ppkA)	1.8	-5.9	-3.5
PA0075	PppA (pppA)	1.6	-10.3	-3.7
PA0169	hypothetical protein (PA0169)	1.7	-3.2	-2.8
PA0172	hypothetical protein (PA0172)	1.8	-3.3	-2.2
PA0424	multidrug resistance operon repressor MexR (mexR)	1.1	-1.2	2.9
PA0527.1	regulatory RNA RsmY	0.0	-4.1	-2.5
PA0610	transcriptional regulator PrtN (prtN)	1.4	-1.6	-1.2
PA0611	transcriptional regulator PrtR (prtR)	1.5	-1.2	-1.0
PA0612	repressor, PtrB ' (ptrB)	2.1	-2.4	-2.7
PA0707	transcriptional regulator ToxR (toxR)	-1.0	-1.9	1.8
PA0763	anti-sigma factor MucA (mucA)	-1.0	-1.7	1.3
PA0764	negative regulator for alginate biosynthesis MucB (mucB)	1.1	-1.9	1.2
PA0905	carbon storage regulator (rsmA)	1.3	-2.1	1.2
PA0929	two-component response regulator (PA0929)	7.1	-1.5	3.0
PA1003	Transcriptional regulator MvfR (mvfR)	1.5	-1.5	2.0
PA1196	putative transcriptional regulator (PA1196)	-1.3	-2.4	1.3
PA1431	regulatory protein RsaL (rsaL)	1.4	-1.5	1.3
PA1432	autoinducer synthesis protein LasI (lasI)	1.1	-2.6	1.4
PA1710	ExsC (exsC)	-4.7	2.0	1.5
PA1711	ExsE (exsE)	-5.5	1.9	1.4
PA1713	transcriptional regulator ExsA (exsA)	-5.9	1.2	1.4
PA1714	ExsD (exsD)	-5.3	1.4	1.3
PA1799	two-component response regulator, ParR	1.1	-1.2	-1.5
PA1898	putative transcriptional regulator (qscR)	1.5	-2.9	1.9
PA2259	transcriptional regulator PtxS (ptxS)	1.4	-1.5	1.9
PA2384	hypothetical protein (PA2384)	1.3	-5.8	-2.2
PA2432	bistable expression regulator BexR	9.2	-4.6	-4.6
PA2463	hypothetical protein (PA2463)	1.6	-3.1	-2.9
PA2467	Anti-sigma factor FoxR (foxR)	1.4	-1.1	1.6
PA2492	transcriptional regulator MexT (mexT)	-1.1	1.2	1.8
PA2523	putative two-component response regulator (PA2523)	-1.0	-1.1	1.8
PA2586	response regulator GacA (gacA)	-1.0	1.3	2.0
PA2591	transcriptional regulator (PA2591)	1.4	-1.4	1.5
PA2593	quorum threshold expression protein QteE	1.3	-2.4	1.0
PA2663	psl and pyoverdine operon regulator, PpyR	1.2	2.3	-1.1
PA2686	two-component response regulator PfeR (pfeR)	1.4	1.6	1.4
PA3006	transcriptional regulator PsrA (psrA)	-1.0	-1.8	3.2
PA3269	putative transcriptional regulator (PA3269)	-1.0	1.2	1.9
PA3364	aliphatic amidase expression-regulating protein (amiC)	-1.1	1.1	2.6
PA3385	alginate and motility regulator Z (amrZ)	-1.4	1.9	1.8
PA3476	autoinducer synthesis protein RhlI (rhlI)	1.2	-1.3	1.7
PA3542	alginate biosynthesis protein Alg44 (alg44)	1.1	1.0	1.5
PA3621.1	regulatory RNA RsmZ	-4.6	-16.6	-2.5
PA3649	hypothetical protein (PA3649)	1.0	1.2	1.6
PA3708	putative chemotaxis transducer (wspA)	-1.2	1.1	1.8
PA3879	transcriptional regulator NarL (narL)	-1.5	-1.0	1.7
PA3885	protein tyrosine phosphatase TpbA	-1.2	1.0	2.0
PA3947	RocR (rocR)	1.0	1.1	1.7
PA4080	putative response regulator (PA4080)	-1.0	-1.0	1.9
PA4196	protein BfiR	-1.2	-1.5	1.3
PA4227	transcriptional regulator PchR (pchR)	1.3	-3.1	1.3
PA4421	cell division protein MraZ (PA4421)	1.1	1.1	2.0
PA5346	hypothetical protein (PA5346)	1.0	1.1	1.8
PA5483	two-component response regulator AlgB (algB)	-1.1	-1.7	1.2

C-di-GMP

PA0169	hypothetical protein (PA0169)	1.7	-3.2	-2.8
PA0172	hypothetical protein (PA0172)	1.8	-3.3	-2.2
PA2870	hypothetical protein (PA2870)	-1.3	-1.1	1.5
PA3343	hypothetical protein (PA3343)	-1.3	-1.0	1.5
PA3703	chemotaxis-specific methylesterase (wspF)	-1.0	1.4	1.9
PA3704	putative chemotaxis sensor/effector fusion protein (wspE)	-1.6	1.3	1.3
PA3707	hypothetical protein (wspB)	-1.2	1.2	1.8
PA3708	putative chemotaxis transducer (wspA)	-1.2	1.1	1.8
PA4624	hypothetical protein (PA4624)	2.3	-2.1	-1.4
PA4625	hypothetical protein (PA4625)	2.3	-2.3	-1.4

Iron (no p,p,p)

Locus Tag	General Description and Gene Name	*Δsmc*	*ΔmksB*	*ΔΔ*
PA0197	transporter TonB	1.7	-4.6	1.3
PA0198	transport protein ExbB (exbB1)	1.4	-3.4	1.8
PA0434	hypothetical protein (PA0434)	2.5	1.2	1.3
PA0470	Ferrichrome receptor FiuA (fiuA)	1.0	-1.2	1.6
PA0471	putative transmembrane sensor (PA0471)	1.9	-2.4	-1.1
PA0472	RNA polymerase sigma factor (PA0472)	2.3	-2.2	1.6
PA0672	heme oxygenase (hemO)	5.2	-2.5	-1.1
PA0929	two-component response regulator (PA0929)	7.1	-1.5	3.0
PA0931	outer membrane receptor FepA (pirA)	1.7	-1.3	-1.1
PA1300	ECF subfamily RNA polymerase sigma-70 factor (PA1300)	2.4	1.1	1.5
PA1302	putative heme utilization protein precursor (PA1302)	1.7	-1.0	1.3
PA1322	putative TonB-dependent receptor (PA1322)	1.1	-1.6	1.1
PA1363	ECF subfamily RNA polymerase sigma-70 factor (PA1363)	1.6	-1.5	1.3
PA1910	ferric-mycobactin receptor, FemA	-1.0	-1.7	1.2
PA1912	ECF sigma factor, FemI	1.5	-1.8	-1.0
PA1922	putative TonB-dependent receptor (PA1922)	-1.3	-1.3	1.7
PA2033	hypothetical protein (PA2033)	-1.3	-2.6	1.1
PA2034	hypothetical protein (PA2034)	-1.1	-1.2	1.6
PA2050	RNA polymerase sigma factor (PA2050)	1.5	-1.3	-1.4
PA2335	TonB-dependent receptor (PA2335)	1.8	1.2	1.5
PA2384	hypothetical protein (PA2384)	1.3	-5.8	-2.2
PA2466	Ferrioxamine receptor FoxA (foxA)	1.7	-1.4	1.8
PA2467	Anti-sigma factor FoxR (foxR)	1.4	-1.1	1.6
PA2686	two-component response regulator PfeR (pfeR)	1.4	1.6	1.4
PA3268	TonB-dependent receptor (PA3268)	3.5	-1.1	1.6
PA3269	putative transcriptional regulator (PA3269)	-1.0	1.2	1.9
PA3407	heme acquisition protein HasAp (hasAp)	-1.6	-1.3	-1.2
PA3408	heme uptake outer membrane receptor HasR precursor (hasR)	-1.1	1.2	1.7
PA3410	ECF subfamily RNA polymerase sigma-70 factor (PA3410)	2.0	1.1	1.8
PA3530	hypothetical protein (PA3530)	1.5	-1.0	1.7
PA3531	bacterioferritin (bfrB)	-1.3	1.3	2.3
PA3899	RNA polymerase sigma factor (PA3899)	1.3	-1.8	1.6
PA3901	Fe(III) dicitrate transport protein FecA (fecA)	1.4	2.0	1.2
PA4156	TonB-dependent receptor (PA4156)	2.0	-1.1	2.1
PA4160	ferric enterobactin transport protein FepD (fepD)	-2.6	-1.3	1.1
PA4161	ferric enterobactin transport protein FepG (fepG)	-1.1	-2.1	1.0
PA4191	iron/ascorbate oxidoreductase (PA4191)	4.4	-1.1	-1.2
PA4514	outer membrane receptor for iron transport (PA4514)	5.5	-1.2	1.7
PA4675	putative TonB-dependent receptor (PA4675)	2.3	-1.3	-1.4
PA4708	Heme-transport protein, PhuT ' (phuT)	1.7	-1.4	-1.0
PA4709	putative hemin degrading factor (PA4709)	2.9	-1.4	1.3
PA4710	heme/hemeoglobin uptake outer membrane receptor PhuR precursor (p	3.2	-1.3	1.2
PA4837	outer membrane protein precursor (PA4837)	-1.5	-1.3	1.7
PA4896	RNA polymerase sigma factor (PA4896)	2.6	1.6	4.0
PA5217	putative binding protein component of ABC iron transporter (PA5217)	2.4	-1.2	1.4
PA5531	transporter TonB	2.1	-1.1	2.3

Sulfur

PA0184	ABC transporter ATP-binding protein (PA0184)	-1.2	-1.8	1.1
PA0186	binding protein component of ABC transporter (PA0186)	-1.0	-1.2	1.6
PA0193	hypothetical protein (PA0193)	2.0	1.1	1.3
PA0280	sulfate transport protein CysA (cysA)	6.0	1.2	-2.1
PA0281	sulfate transport protein CysW (cysW)	4.5	1.1	-2.0
PA0282	sulfate transport protein CysT (cysT)	2.9	-1.1	-1.9
PA0283	sulfate-binding protein precursor (sbp)	2.5	1.2	-1.5
PA0518	cytochrome c-551 precursor (nirM)	1.6	1.4	1.0
PA0589	thiosulfate sulfurtransferase (glpE)	1.1	1.0	1.8
PA1393	adenosine 5'-phosphosulfate (APS) kinase (cysC)	1.1	-1.9	1.3
PA1838	sulfite reductase (cysI)	1.4	1.3	-3.0
PA2104	cysteine synthase (PA2104)	1.3	-2.1	1.1
PA2105	acetyltransferase (PA2105)	1.2	-1.7	1.3
PA2310	hypothetical protein (PA2310)	2.2	-1.6	1.3
PA2357	NADH-dependent FMN reductase MsuE (msuE)	2.3	1.3	-1.3
PA2595	hypothetical protein (PA2595)	1.6	-1.1	3.3
PA2596	hypothetical protein (PA2596)	2.4	-1.1	1.3
PA2598	hypothetical protein (PA2598)	3.0	-1.3	1.1
PA2600	hypothetical protein (PA2600)	2.1	1.6	1.4
PA3107	O-succinylhomoserine sulfhydrylase (metZ)	-1.3	1.7	1.1
PA3442	aliphatic sulfonates transport ATP-binding subunit (ssuB)	6.2	-1.2	1.4
PA3443	ABC transporter permease (PA3443)	46.6	1.5	1.1
PA3444	alkanesulfonate monooxygenase (PA3444)	26.7	-2.1	1.2
PA3445	hypothetical protein (PA3445)	11.5	-2.2	-1.2
PA3446	NAD(P)H-dependent FMN reductase (PA3446)	3.6	1.2	1.3
PA3447	ABC transporter ATP-binding protein (PA3447)	-1.1	-1.6	1.6
PA3448	ABC transporter permease (PA3448)	3.1	1.9	1.8
PA3449	hypothetical protein (PA3449)	2.1	1.1	-1.1
PA3935	taurine dioxygenase (tauD)	3.4	-1.1	1.0
PA3936	taurine ABC transporter permease (PA3936)	2.4	-1.8	1.4
PA3937	taurine ABC transporter ATP-binding protein (PA3937)	3.9	-2.1	1.3
PA3938	periplasmic taurine-binding protein precursor (PA3938)	2.0	-1.5	1.2
PA3954	hypothetical protein (PA3954)	1.0	1.4	1.8
PA4442	cysN	1.3	1.5	-1.7
PA4513	oxidoreductase (PA4513)	1.9	-1.3	1.1

Nitrogen (no detnitrification)

Locus Tag	General Description and Gene Name	*Δsmc*	*ΔmksB*	*ΔΔ*
PA1566	hypothetical protein (PA1566)	1.8	1.4	1.9
PA1779	assimilatory nitrate reductase (PA1779)	-1.4	-1.5	1.2
PA1780	assimilatory nitrite reductase small subunit (nirD)	2.2	1.4	1.4
PA1783	nitrate transporter (nasA)	3.8	1.7	4.5
PA1786	hypothetical protein (PA1786)	1.5	-1.3	2.1
PA2040	glutamine synthetase (PA2040)	1.3	-1.0	-1.6
PA2442	glycine cleavage system protein T2 (gcvT2)	1.2	1.3	-2.7
PA3459	glutamine amidotransferase (PA3459)	-1.3	-1.8	1.4
PA3876	nitrite extrusion protein 2 (narK2)	-3.2	-1.8	1.5
PA3877	nitrite extrusion protein 1 (narK1)	-4.5	-2.1	1.2
PA4588	glutamate dehydrogenase (gdhA)	-1.2	-1.2	1.7
PA4920	NAD synthetase (nadE)	-1.0	-1.5	2.9
PA5035	glutamate synthase subunit beta (gltD)	-1.6	1.0	1.7
PA5036	glutamate synthase subunit alpha (gltB)	-1.1	1.1	2.4
PA5119	glutamine synthetase (glnA)	-1.3	1.5	2.0
PA5173	carbamate kinase (arcC)	-1.4	-4.6	1.1

Alginate

PA0762	RNA polymerase sigma factor AlgU (algU)	1.0	-1.7	2.3
PA0763	anti-sigma factor MucA (mucA)	-1.0	-1.7	1.3
PA0764	negative regulator for alginate biosynthesis MucB (mucB)	1.1	-1.9	1.2
PA0766	serine protease MucD precursor (mucD)	1.0	1.0	-1.7
PA3385	alginate and motility regulator Z (amrZ)	-1.4	1.9	1.8
PA3541	alginate biosynthesis protein Alg8 (alg8)	-1.7	-1.3	1.2
PA3542	alginate biosynthesis protein Alg44 (alg44)	1.1	1.0	1.5
PA3545	alginate-c5-mannuronan-epimerase AlgG (algG)	-1.0	-1.1	1.8
PA3546	alginate biosynthesis protein AlgX (algX)	-1.5	-1.3	1.3
PA3547	poly(beta-D-mannuronate) lyase (algL)	1.1	-1.1	1.6
PA3548	alginate o-acetyltransferase AlgI (algI)	-1.7	-1.2	1.6
PA3549	alginate o-acetyltransferase AlgJ (algJ)	1.2	-1.6	1.4
PA3550	alginate o-acetyltransferase AlgF (algF)	-1.7	-1.0	1.4
PA3649	hypothetical protein (PA3649)	1.0	1.2	1.6
PA4033	hypothetical protein (PA4033)	-1.2	1.0	2.2
PA5483	two-component response regulator AlgB (algB)	-1.1	-1.7	1.2

Chemotaxis

PA0173	chemotaxis-specific methylesterase (PA0173)	-1.3	-2.2	-1.5
PA0175	putative chemotaxis protein methyltransferase (PA0175)	1.2	-1.6	1.1
PA0176	aerotaxis transducer Aer2 (aer2)	1.4	-1.6	1.0
PA0177	putative purine-binding chemotaxis protein (PA0177)	1.5	-1.9	1.2
PA0178	putative two-component sensor (PA0178)	1.8	-2.1	-1.0
PA0179	putative two-component response regulator (PA0179)	1.6	-1.2	1.8
PA1608	chemotaxis transducer (PA1608)	1.1	1.5	1.6
PA1646	chemotaxis transducer (PA1646)	-1.2	-1.8	1.0
PA1946	binding protein component precursor of ABC ribose transporter (rbs	-1.0	-1.9	2.0
PA2561	putative chemotaxis transducer (PA2561)	-1.8	3.9	2.0
PA2573	chemotaxis transducer (PA2573)	1.2	-1.2	1.6
PA2652	putative chemotaxis transducer (PA2652)	-1.4	1.9	1.5
PA2654	putative chemotaxis transducer (PA2654)	-1.3	1.7	1.5
PA2920	putative chemotaxis transducer (PA2920)	1.3	1.4	1.9
PA3348	putative chemotaxis protein methyltransferase (PA3348)	-1.1	1.0	1.5
PA4290	chemotaxis transducer (PA4290)	1.3	-1.1	5.3
PA4307	chemotactic transducer PctC (pctC)	-2.1	1.8	-1.7
PA4309	chemotactic transducer PctA (pctA)	-1.2	2.1	2.2
PA4310	chemotactic transducer PctB (pctB)	-1.1	1.8	-1.2
PA4502	binding protein component of ABC transporter (PA4502)	1.2	2.6	1.8
PA4520	putative chemotaxis transducer (PA4520)	-1.2	-1.1	1.6
PA4633	putative chemotaxis transducer (PA4633)	1.0	1.3	1.8
PA4915	chemotaxis transducer (PA4915)	1.1	-1.3	2.5
PA4954	flagellar motor protein MotA (motA)	1.0	1.1	2.1
PA5072	putative chemotaxis transducer (PA5072)	-1.5	1.7	1.1

Type IV Pili

PA3805	type 4 fimbrial biogenesis protein PilF (pilF)	-1.1	1.5	1.2
PA4525	type 4 fimbrial precursor PilA (pilA)	-1.4	-1.7	-1.0
PA4526	type 4 fimbrial biogenesis protein PilB (pilB)	-1.3	-2.0	1.6
PA4527	pseudo (pilC)	-1.0	1.1	2.0
PA4528	type 4 prepilin peptidase PilD (pilD)	-1.0	-1.2	2.0
PA4547	two-component response regulator PilR (pilR)	1.0	1.5	-1.1
PA4549	type 4 fimbrial biogenesis protein FimT (fimT)	-1.6	-2.5	1.2
PA4550	type 4 fimbrial biogenesis protein FimU (fimU)	-1.6	-1.1	-1.5
PA5040	Type 4 fimbrial biogenesis outer membrane protein PilQ precursor (	-1.0	1.0	1.7
PA5041	type 4 fimbrial biogenesis protein PilP (pilP)	-1.1	-1.2	2.0
PA5042	type 4 fimbrial biogenesis protein PilO (pilO)	-1.1	-1.3	1.6

Flagella

PA1077	flagellar basal body rod protein FlgB (flgB)	1.2	-1.4	1.9
PA1078	flagellar basal body rod protein FlgC (flgC)	1.2	-1.3	1.7
PA1081	flagellar basal body rod protein FlgF (flgF)	1.2	-1.6	2.0
PA1085	flagellar rod assembly protein/muramidase FlgJ (flgJ)	-1.0	-1.2	1.5
PA1095	flagellar protein FliS (fliS)	1.1	1.2	1.5
PA1446	flagellar biosynthesis protein FliP (fliP)	-1.1	-1.5	1.4
PA1449	flagellar biosynthesis protein FlhB (flhB)	1.5	1.2	1.2
PA1452	flagellar biosynthesis protein FlhA (flhA)	1.1	-1.5	1.3
PA3350	flagellar basal body P-ring biosynthesis protein FlgA (flgA)	-1.1	-1.3	1.7
PA3352	hypothetical protein (PA3352)	-1.1	1.5	2.0
PA3526	outer membrane protein precursor (PA3526)	-1.1	1.4	2.0
PA4954	flagellar motor protein MotA (motA)	1.0	1.1	2.1

Quorum Sensing

Locus Tag	General Description and Gene Name	*Δsmc*	*ΔmksB*	*ΔΔ*
PA0222	hypothetical protein (PA0222)	-1.1	-1.3	1.6
PA0295	periplasmic polyamine binding protein (PA0295)	-1.3	1.7	-1.3
PA0603	ABC transporter ATP-binding protein (PA0603)	1.9	1.7	1.2
PA0604	putative binding protein component of ABC transporter (PA0604)	2.0	1.9	1.4
PA0605	ABC transporter permease (PA0605)	1.8	1.5	1.5
PA0606	ABC transporter permease (PA0606)	1.5	2.0	1.5
PA0649	anthranilate synthase component II (trpG)	1.1	-1.2	1.6
PA0844	hemolytic phospholipase C precursor (plcH)	1.4	-1.6	1.3
PA0996	coenzyme A ligase (pqsA)	-1.1	1.3	2.9
PA0997	beta-keto-acyl-acyl-carrier protein synthase-like protein (pqsB)	-1.5	1.1	1.6
PA1000	quinolone signal response protein (pqsE)	-1.6	-1.6	-1.0
PA1001	anthranilate synthase component I (phnA)	1.1	-1.6	-1.6
PA1002	anthranilate synthase component II (phnB)	1.3	-1.2	1.7
PA1003	Transcriptional regulator MvfR (mvfR)	1.5	-1.5	2.0
PA1071	branched-chain amino acid transport protein BraF	1.4	1.0	1.6
PA1073	branched-chain amino acid transport protein BraD (braD)	1.3	-1.6	1.4
PA1303	signal peptidase (PA1303)	1.2	1.0	-2.2
PA1431	regulatory protein RsaL (rsaL)	1.4	-1.5	1.3
PA1432	autoinducer synthesis protein LasI (lasI)	1.1	-2.6	1.4
PA1871	LasA protease precursor (lasA)	-1.1	-1.6	1.2
PA1874	hypothetical protein (PA1874)	1.1	-1.8	1.2
PA1900	phenazine biosynthesis protein (phzB2)	1.7	-1.7	1.4
PA1902	phenazine biosynthesis protein PhzD (phzD2)	-1.4	-2.9	-1.9
PA1904	phenazine biosynthesis protein (phzF2)	2.7	1.5	3.8
PA2569	hypothetical protein (PA2569)	-1.1	-1.2	2.0
PA2843	aldolase (PA2843)	-1.1	1.5	1.1
PA3250	hypothetical protein (PA3250)	-1.1	1.2	1.8
PA3252	ABC transporter permease (PA3252)	1.2	-1.2	1.6
PA3253	ABC transporter permease (PA3253)	-2.0	-1.8	1.1
PA3254	ABC transporter ATP-binding protein (PA3254)	-1.2	1.4	2.0
PA3299	acyl-CoA synthetase (fadD1)	-1.3	1.7	1.0
PA3300	acyl-CoA synthetase (fadD2)	-1.1	1.2	1.9
PA3319	non-hemolytic phospholipase C precursor (plcN)	1.0	1.1	1.6
PA3320	hypothetical protein (PA3320)	1.1	2.3	3.1
PA3361	fucose-binding lectin PA-IIL (lecB)	-1.9	-1.3	1.7
PA3364	aliphatic amidase expression-regulating protein (amiC)	-1.1	1.1	2.6
PA3476	autoinducer synthesis protein RhlI (rhlI)	1.2	-1.3	1.7
PA3478	rhamnosyltransferase chain B (rhlB)	-1.1	-1.1	2.5
PA3479	rhamnosyltransferase chain A (rhlA)	-1.7	-1.6	-1.4
PA3649	hypothetical protein (PA3649)	1.0	1.2	1.6
PA3724	elastase LasB (lasB)	1.0	1.4	3.2
PA4205	hypothetical protein (mexG)	1.2	-1.3	-1.6
PA4206	RND efflux membrane fusion protein precursor (mexH)	1.1	-1.4	-1.9
PA4212	phenazine biosynthesis protein PhzC (phzC1)	1.0	1.2	1.8
PA4215	phenazine biosynthesis protein (phzF1)	-1.4	-2.7	1.3
PA4276	preprotein translocase subunit SecE (secE)	-1.2	1.4	1.6
PA4804	amino acid permease (PA4804)	1.1	-1.0	2.0
PA4909	ABC transporter ATP-binding protein (PA4909)	-1.0	-1.8	1.1
PA4910	branched chain amino acid ABC transporter ATP binding protein (PA4910	1.2	1.3	2.2
PA4913	putative binding protein component of ABC transporter (PA4913)	1.3	-1.1	2.6
PA5499	transcriptional regulator np20 (np20)	-1.2	-1.4	1.7

Fimbriae

PA0993	chaperone CupC2 (cupC2)	2.4	-2.3	3.0
PA2128	fimbrial subunit CupA1 (cupA1)	1.4	-1.2	-1.6
PA2129	chaperone CupA2 (cupA2)	1.3	-1.0	-1.6
PA2132	chaperone CupA5 (cupA5)	1.6	1.3	1.0
PA4081	fimbrial protein cupB6 (cupB6)	-1.1	-1.2	1.7
PA4083	chaperone CupB4 (cupB4)	1.1	1.2	1.6
PA4084	usher CupB3 (cupB3)	1.0	-1.1	3.1
PA4085	chaperone CupB2 (cupB2)	-1.5	-5.6	-1.0
PA4086	fimbrial subunit CupB1 (cupB1)	1.0	-1.3	1.7

Two-Component System

Locus Tag	General Description and Gene Name	*Δsmc*	*ΔmksB*	*ΔΔ*
PA0119	C4-dicarboxylate transporter DctA (PA0119)	-1.2	-1.5	2.3
PA0173	chemotaxis-specific methylesterase (PA0173)	-1.3	-2.2	-1.5
PA0175	putative chemotaxis protein methyltransferase (PA0175)	1.2	-1.6	1.1
PA0176	aerotaxis transducer Aer2 (aer2)	1.4	-1.6	1.0
PA0177	putative purine-binding chemotaxis protein (PA0177)	1.5	-1.9	1.2
PA0178	putative two-component sensor (PA0178)	1.8	-2.1	-1.0
PA0179	putative two-component response regulator (PA0179)	1.6	-1.2	1.8
PA0518	cytochrome c-551 precursor (nirM)	1.6	1.4	1.0
PA0749	hypothetical protein (PA0749)	1.6	-2.2	-1.5
PA0766	serine protease MucD precursor (mucD)	1.0	1.0	-1.7
PA0885	C4-dicarboxylate transporter (PA0885)	-1.5	-2.3	-1.5
PA0905	carbon storage regulator (rsmA)	1.3	-2.1	1.2
PA0929	two-component response regulator (PA0929)	7.1	-1.5	3.0
PA0931	outer membrane receptor FepA (pirA)	1.7	-1.3	-1.1
PA1157	two-component response regulator (PA1157)	-1.3	-1.1	-1.8
PA1158	two-component sensor (PA1158)	1.1	1.5	-1.0
PA1183	C4-dicarboxylate transporter DctA (dctA)	-1.1	-2.7	4.8
PA1339	amino acid ABC transporter ATP binding protein (PA1339)	1.4	-1.2	-1.5
PA1340	amino acid ABC transporter membrane protein (PA1340)	1.6	-1.4	-1.6
PA1341	amino acid ABC transporter membrane protein (PA1341)	1.6	-1.5	-1.3
PA1342	putative binding protein component of ABC transporter (PA1342)	1.6	1.0	-1.3
PA1438	putative two-component sensor (PA1438)	1.2	-1.5	1.0
PA1552	Cytochrome c oxidase, cbb3-type, CcoP subunit	1.4	1.3	-1.9
PA1552.1	Cytochrome c oxidase, cbb3-type, CcoQ subunit	1.2	1.7	-1.8
PA1553	Cytochrome c oxidase, cbb3-type, CcoO subunit	1.5	1.6	-1.8
PA1554	Cytochrome c oxidase, cbb3-type, CcoO subunit	1.4	1.4	-2.3
PA1555	Cytochrome c oxidase, cbb3-type, CcoO subunit	-1.2	-1.4	-1.8
PA1556	Cytochrome c oxidase, cbb3-type, CcoO subunit	-1.3	-1.3	-2.3
PA1557	Cytochrome c oxidase, cbb3-type, CcoO subunit	-1.3	-1.2	-3.1
PA1566	hypothetical protein (PA1566)	1.8	1.4	1.9
PA1608	chemotaxis transducer (PA1608)	1.1	1.5	1.6
PA1634	potassium-transporting ATPase subunit B (kdpB)	1.1	-1.7	1.4
PA1646	chemotaxis transducer (PA1646)	-1.2	-1.8	1.0
PA1736	acetyl-CoA acetyltransferase (PA1736)	1.2	-1.7	1.1
PA1799	two-component response regulator, ParR	1.1	-1.2	-1.5
PA1856	cytochrome oxidase subunit (PA1856)	1.4	1.5	1.3
PA1976	sensor histidine kinase	1.1	-1.6	-1.0
PA1980	response regulator EraR	-2.2	-1.9	-1.1
PA2040	glutamine synthetase (PA2040)	1.3	-1.0	-1.6
PA2523	putative two-component response regulator (PA2523)	-1.0	-1.1	1.8
PA2548	hypothetical protein (PA2548)	1.9	1.1	1.8
PA2553	putative acyl-CoA thiolase (PA2553)	1.6	1.6	1.7
PA2561	putative chemotaxis transducer (PA2561)	-1.8	3.9	2.0
PA2573	chemotaxis transducer (PA2573)	1.2	-1.2	1.6
PA2583	sensor/response regulator hybrid (PA2583)	1.1	-1.0	1.7
PA2586	response regulator GacA (gacA)	-1.0	1.3	2.0
PA2652	putative chemotaxis transducer (PA2652)	-1.4	1.9	1.5
PA2654	putative chemotaxis transducer (PA2654)	-1.3	1.7	1.5
PA2686	two-component response regulator PfeR (pfeR)	1.4	1.6	1.4
PA2687	two-component sensor PfeS (pfeS)	1.8	1.1	1.3
PA2824	sensor/response regulator hybrid (PA2824)	-1.1	1.1	1.6
PA2920	putative chemotaxis transducer (PA2920)	1.3	1.4	1.9
PA3045	putative two-component response regulator (PA3045)	-1.2	1.0	2.9
PA3296	alkaline phosphatase (phoA)	-1.2	-1.7	1.4
PA3345	hypothetical protein (PA3345)	-1.4	1.1	1.9
PA3346	putative two-component response regulator (PA3346)	-1.2	1.1	2.0
PA3347	hypothetical protein (PA3347)	-1.0	1.7	3.2
PA3348	putative chemotaxis protein methyltransferase (PA3348)	-1.1	1.0	1.5
PA3476	autoinducer synthesis protein RhlI (rhlI)	1.2	-1.3	1.7
PA3589	acetyl-CoA acetyltransferase (PA3589)	-2.0	1.1	-1.0
PA3658	PII uridylyl-transferase (glnD)	-1.1	1.1	1.8
PA3703	chemotaxis-specific methylesterase (wspF)	-1.0	1.4	1.9
PA3704	putative chemotaxis sensor/effector fusion protein (wspE)	-1.6	1.3	1.3
PA3706	putative methyltransferase (wspC)	-1.2	1.1	1.8
PA3707	hypothetical protein (wspB)	-1.2	1.2	1.8
PA3708	putative chemotaxis transducer (wspA)	-1.2	1.1	1.8

Two-Component System

Locus Tag	General Description and Gene Name	*Δsmc*	*ΔmksB*	*ΔΔ*
PA3714	putative two-component response regulator (PA3714)	1.1	-2.0	1.4
PA3872	respiratory nitrate reductase gamma chain (narI)	-1.1	-1.3	1.6
PA3873	respiratory nitrate reductase delta chain (narJ)	-1.2	-1.2	1.8
PA3874	respiratory nitrate reductase beta chain (narH)	-1.4	-1.3	1.8
PA3875	respiratory nitrate reductase alpha chain (narG)	-1.7	-1.5	2.0
PA3879	transcriptional regulator NarL (narL)	-1.5	-1.0	1.7
PA3910	extracelullar DNA degradation protein EddA	-1.1	1.3	2.2
PA3925	putative acyl-CoA thiolase (PA3925)	-1.0	1.5	-1.4
PA3929	cyanide insensitive terminal oxidase (cioB)	1.6	1.4	1.5
PA3930	cyanide insensitive terminal oxidase (cioA)	1.9	1.5	1.7
PA4080	putative response regulator (PA4080)	-1.0	-1.0	1.9
PA4144	outer membrane protein precursor (PA4144)	-2.5	-1.2	-1.1
PA4290	chemotaxis transducer (PA4290)	1.3	-1.1	5.3
PA4307	chemotactic transducer PctC (pctC)	-2.1	1.8	-1.7
PA4309	chemotactic transducer PctA (pctA)	-1.2	2.1	2.2
PA4310	chemotactic transducer PctB (pctB)	-1.1	1.8	-1.2
PA4429	putative cytochrome c1 precursor (PA4429)	-1.5	1.8	-2.4
PA4430	putative cytochrome b (PA4430)	-1.4	1.8	-2.8
PA4431	iron-sulfur protein (PA4431)	-1.4	1.9	-2.3
PA4520	putative chemotaxis transducer (PA4520)	-1.2	-1.1	1.6
PA4525	type 4 fimbrial precursor PilA (pilA)	-1.4	-1.7	-1.0
PA4547	two-component response regulator PilR (pilR)	1.0	1.5	-1.1
PA4633	putative chemotaxis transducer (PA4633)	1.0	1.3	1.8
PA4885	two-component response regulator (irlR)	-1.9	-1.5	-1.7
PA4915	chemotaxis transducer (PA4915)	1.1	-1.3	2.5
PA4954	flagellar motor protein MotA (motA)	1.0	1.1	2.1
PA5072	putative chemotaxis transducer (PA5072)	-1.5	1.7	1.1
PA5082	putative binding protein component of ABC transporter (PA5082)	-1.0	1.1	1.5
PA5119	glutamine synthetase (glnA)	-1.3	1.5	2.0
PA5124	two-component sensor NtrB (ntrB)	1.0	1.2	3.7
PA5125	two-component response regulator NtrC (ntrC)	1.0	-1.1	1.5
PA5167	c4-dicarboxylate-binding protein (PA5167)	1.3	-1.2	2.1
PA5168	dicarboxylate transporter (PA5168)	1.5	1.1	2.3
PA5169	C4-dicarboxylate transporter (PA5169)	1.2	-1.3	2.5
PA5483	two-component response regulator AlgB (algB)	-1.1	-1.7	1.2
PA5484	two-component sensor (PA5484)	-1.0	-1.6	1.2
PA5512	sensor histidine kinase MifS	1.1	-1.1	1.9